Molecular Basis of Plant Cell Death Suppression By The *Phytophthora infestans* effector AVR3a

Ángela Chaparro-García

Thesis submitted to the University of East Anglia

for the Degree of Doctor of Philosophy

September 2012

Abstract

Plants actively perceive pathogens and activate their immune system upon pathogen recognition. The first encounter with the pathogen relies on the recognition of highly conserved microbial molecules known as pathogen-associated molecular patterns (PAMPs) by cell surface receptors called pattern-recognition receptors (PPRs). Successful pathogens have evolved effectors to overcome plant defense and to colonize their host. INF1 is a *P. infestans* elicitin with features of PAMPs that requires the co-regulator receptor-like kinase SERK3/BAK1 to trigger cell death. AVR3a is an effector translocated by *P. infestans* that suppresses INF1-triggered cell death (ICD). However, the potato protein R3a can recognize AVR3a. The avirulence and suppression activities of this effector are conditioned by distinct amino acids but the precise series of events leading to ICD suppression by AVR3a, the nature of the INF1 receptor, and the composition of the receptor complex remain unknown.

This study investigates mechanisms underlying AVR3a interference with basal immunity and its importance for *P. infestans* pathogenicity. Homologs of SERK3/BAK1 in *N. benthamiana* were shown to be required for resistance against *P. infestans*. To further our understanding of the molecular events after INF1 elicitation, a receptor-like protein (RLP) implicated in ICD was characterized. Using a combination of fluorescence microscopy and biochemistry, I showed that this RLP localizes to the endoplasmic reticulum and plasma membrane and forms a complex with SERK3/BAK1. I assessed the extent to which AVR3a interferes with SERK3/BAK1-dependent signaling pathways and found that variants of AVR3a suppress defense responses elicited by diverse PAMPs to different degrees. Additional plant proteins interacting with AVR3a were searched using *in planta* complex purification and mass spectrometry analysis. A host GTPase (dynamin) protein involved in endocytosis was found. Dynamin was shown to be required for ICD suppression activity by AVR3a. Notably, dynamin accumulates around *P. infestans* (Pi) haustoria possibly pointing to its role in the plant-Pi interaction.

List of Contents

List of Tables

List of Figures

Acknowledgements

My biggest thanks go to God, for enlightening me and for giving me the strength and motivation to pursue a PhD in the first place, let alone the writing of it all!

Next, I would like to thank my supervisor Sophien Kamoun for teaching me that often there is more to it than meets the eye, not only scientifically but also when it comes to teamwork. Many thanks as well for giving me the opportunity to join your research team and for your generous support and for teaching me that focus is indispensable in science, and for critical suggestions of my work. I am very grateful to my mentor Sebastian Schornack taking the time to show how to become a researcher, for the hours of fruitful discussions, for sharing his knowledge and for critical comments of my work. I want to thank Cyril Zipfel for critical suggestions of my work throughout my course of study and for hosting me in his lab meetings for JC. I also want to thank my dear friend Liliana for her support and advice and for convincing me that England is not too bad of a place to move to.

Needless to say, I am in debt to all my fellow colleagues at the Kamoun group, I am thankful for everyone's support through the ups and downs of conducting this research. Special thanks to Tolga for taking my silly questions with patience and being such a good friend, always helpful and insightful. I want to thank my bench-mate Diane for coaching me in the art of being a PhD student. I also want to thank Vanesa for giving me a hand when needed and for making our house a very cozy place to live and write.

I want to express my sincere gratitude to all the researchers that make The Sainsbury Laboratory such a great place to learn and do science. I cannot think of another place hosting so many talented people who are always welcoming and enthusiastic about science; this made all the difference! Thank you fellow TSL students for all the shared activities undertaken to make us better researchers.

I did not get here all on my own and I want to thank my very first supervisors Adriana Bernal and Silvia Restrepo for their inspiring advice and careers. I also want to thank Lina Quesada and my first mentor ever Jorunn Bos who taught me serious pipetting, cloning, and infiltrations.

Finally, I want to give a big thank you to my mom without whom I would not be who I am, or have accomplished what I have. She has always supported me and given me the courage to go a step further against all odds. (Muchísimas gracias Elena por mostrarme como ser valiente y el valor del esfuerzo, por tu incondicional apoyo, amor y los regaños que de vez en cuando necesito! Dios te recompense todo lo que has invertido). I also want to thank my little sister for teaching me many life-long lessons I was overdue to learn. I also thank JS and family for their kindness and generosity and for providing me with an excuse to travel frequently. This kept me sane! I can truly say that I have the best friends in the world. Maria and Brian, I have no words to thank you for your constant support, for pushing me when needed, and for sitting next to me in silence when required. Thank you very much for helping me navigate through life with understanding and patience. I want to dedicate this work to my family and the siblings Chaparro-López.

One last thought. To my beloved Colombia: may we finally reach the understanding of peace and equal opportunities for all, so that we can all reach our potential and dreams!

Abbreviations

BAK1	BRI1 associated kinase 1
BR	Brassinosteroid
BRI1	Brassinosteroid insensitive
CaMV	Cauliflower mosaic virus
CC	Coiled-coil
CERK1	Chitin elicitor receptor kinase 1
Cf	*Cladosporium fulvum*
CLV	CLAVATA
DPI/dpi	Days post infiltration/infection
EFR	EF-Tu receptor
EF-Tu	Elongation factor TU
EH	Eps15 homology
EIX	Ethylene-inducing xylanase
eLRRs	Extracellular leucine-rich repeats
ER	Endoplasmic reticulum
ETI	Effector-triggered immunity
flg22	Peptide derived from *P. aeruginosa* flagellin
FLS2	Flagellin sensing 2
HR	Hypersensitive response
ICD	INF1-triggered cell death
INF1[Pi]	INF1 protein purified from *P. infestans* 88069
kDa	Kilodaltons
LysM	Lysin motif
MAPK	Mitogen associated protein kinase
NB	Nucleotide binding
OD	Optical density
PAMPs	Pathogen-associated molecular patterns
Pi	*Phytophthora infestans*
PM	Plasma membrane
PRRs	Pattern-recognition receptors

PTGS	Post-transcriptional gene silencing
PTI	PAMP-triggered immunity
PUB	Plant U-box
R	Resistance
RLK	Receptor-like kinase
RLP	Receptor-like protein
ROS	Reactive oxygen species
Rpm	Revolutions per minute
SERK	Somatic embryogenesis related kinase
SP	Signal peptide
TGN	Trans-Golgi network
TLR	Toll-like receptor
TM	Transmembrane
TMM	TOO MANY MOUTHS
WB	Western blot
ml	Millilitre
ng	Nanograms
nM	Nanomolar
µg	Microgram
µm	Micrometer

Chapter 1: General Introduction

Plants are sessile organisms that are constantly exposed to diverse microorganisms such as bacteria, fungi, nematodes, oomycetes, and insects and have the pressure to protect themselves against a potential pathogen attack. In order to achieve such protection, plants have evolved a sophisticated two-branched immune system that responds to external stimuli and even recognizes pathogen encoded molecules that have reached the cytoplasm (Dangl and Jones, 2001). The first line of defense involves the recognition of microbial molecules known as Pathogen-associated molecular pattern (PAMPs) at the cell periphery by pattern recognition receptors (PRR). This recognition is called PAMP-triggered immunity (PTI) and usually leads to broad-spectrum resistance. The second line of defense mediates the recognition of specific pathogen molecules that reach the host cell cytoplasm and are known as effector proteins. Plant proteins mediating the recognition of the secreted effectors are intracellular receptor proteins known as R proteins. This recognition leads to Effector-triggered immunity (ETI) and was first described by Flor (1955) as a "gene-for-gene" interaction given that the genetic variation giving resistance of host plants against virulent pathogens shows Mendelian inheritance.

The constant adaptation of pathogens to resistant plants, and the counter evolution of plants to develop new resistance is known as an "arms-race" (Stahl and Bishop, 2000). Since this process continues and the pressure to feed an ever-growing human population rises, conventional breeding and pesticides use alone are no longer sustainable strategies to keep cultivated plants at their maximum capacity for food production. Therefore, we need to get a solid understanding of the molecular mechanisms of the pathogen and host plant interaction to generate targeted strategies for crop improvement that builds on this knowledge.

1.1. PAMP-triggered immunity (PTI)

PAMPs are microbial derived signatures that are conserved across an entire class of microbes and contribute to the microbe's fitness. These exogenous molecules also occur in non-pathogenic microorganisms and are also known as microbe-associated molecular patterns (MAMPs). Examples of PAMPs encompass bacterial flagellin, fungal chitin, and peptidoglycans among others (Felix and Boller, 2003; Kunze et al., 2004). Recognition of such molecules is one layer of the plant immune system and is mediated by membrane-bound receptors so called pattern recognition receptors (PRRs) (Boller and Felix, 2009). PRRs allow the plant to discriminate between self and non-self molecules and can be classified in two classes: receptor-like kinases (RLKs) and receptor-like proteins (RLPs). So far the extracellular domains where recognition

of PAMPs takes place contain leucine-rich repeats (LRRs) or LysM-motifs (Win et al., 2012).

1.1.1. Receptor-like kinases and their elicitors

Well-studied PRR and PAMP pairs are FLS2 and flg22. FLS2 (flagellin sensing 2) is a leucine-rich repeat receptor kinase isolated by map-based cloning from *A. thaliana* (Gomez-Gomez and Boller, 2000). It directly binds the elicitor flg22 through its LRR domain and the high affinity binding sites are absent in an fls2 knockout demonstrating the true nature of FLS2 as the receptor for flg22 (Chinchilla et al., 2006). Homologs of FLS2 in tomato and *N. benthamiana* have been cloned as well (Hann and Rathjen, 2007; Robatzek et al., 2007). Flg22 is a conserved epitope derived from flagellin (Felix et al 1999), the main component of the bacterial flagellum and it triggers defense responses in a vast range of plants, angiosperm and gymnosperms alike, suggesting this recognition evolved early in plants (Albert et al., 2010). Although FLS2 homologs were found in all species investigated so far, the intensity of the flg22 response varies among species (Robatzek et al., 2007) probably due to some intrinsic characteristics of the receptor LRR domain.

EFR mediates the recognition of the bacterial PAMP elongation factor Tu (EF-Tu) (Zipfel et al., 2006). EFR has been found only in the *Brassicacea*e family (Kunze et al., 2004) and it belongs to the same family of receptor-like kinases (RLK) as FLS2 (Shiu and Bleecker, 2001). EFR requires ER-quality control components to be functional and given that FLS2 does not seem to require these components it was speculated that this could be linked to differential glycosylation status (Nekrasov et al., 2009). Interestingly, the glycosylation status influences the ability of EFR to recognize EF-Tu (Haweker et al., 2010). In the same manner as FLS2, EFR recognition of the epitope elf18 is mediated by its LRR domain (Albert et al., 2010). In rice, the RLK Xa21 mediates the recognition of the sulfated peptide Ax21 (Lee at el 2009) and triggering resistance to *Xanthomonas oryzae* pv. *oryzae* (Song et al., 1995). Interestingly, Xa21 is also sensitive to changes in the ER quality control mechanism (Park et al., 2010). Finally, the RLK AtPEPR1 was characterized as the true receptor of the damage-associated molecular pattern (DAMP) AtPep1, which induces defense responses after wounding and stress (Huffaker et al., 2006; Yamaguchi et al., 2006).

As mentioned above, the extracellular domain of the cell-surface receptors can also be of the LysM type. LysM (lysine motif) domains are carbohydrate-binding motifs and have been studied longer in the context of symbiosis (Monaghan and Zipfel, 2012). Chitin is a fungal PAMP that is formed by N-acetylglucosamine units and is perceived in rice by the LysM RLK CERK1 and LysM containing protein CEBiP which form a complex in a ligand dependent manner (Antolin-Llovera et al., 2012). In Arabidopsis,

the homologous AtCERK1 mediates the perception of chitin but additional interacting receptor-like proteins have not been identified (Antolin-Llovera et al., 2012).

1.1.2. Receptor-like proteins

Receptor-like proteins (RLPs) are transmembrane receptors like RLKs that can perceive external stimuli and process this information into intracellular signaling cascades. RLPs differ from RLKs in that they have a small cytoplasmic tail instead of a cytoplasmic kinase domain. How RLPs, lacking a kinase domain transduce a signal downstream recognition is still under study but it is possible that the short cytoplasmic tail interacts with other proteins with kinase activities or that they form heterodimers with RLKs (Wang et al., 2010) RLPs posses various distinctive domains: a signal peptide (SP), a cysteine rich domain, an eLRR or LysM domain, an acidic domain, a transmembrane domain, and a short cytoplasmic region (Jones and Jones, 1997) RLPs are involved in different cellular processes from plant development to innate immunity. Arabidopsis CLAVATA 2 (CLV 2) RLP is important to keep the homeostasis of undifferentiated stem cells and differentiated cells for organ initiation and formation (Jeong et al., 1999; Wang et al., 2010). Interestingly, CLV2 forms a complex with an RLK CLV1 upon perception of a secreted peptide known as CLV3 to limit the levels of undifferentiated cells in the shoot apical meristem (Wang et al., 2010). The RLP TOO MANY MOUTHS (TMM) is involved in the regulation of stomatal development probably controlling the divisions in the stomatal lineage (Bergmann and Sack, 2007). TMM was shown to associate with RLKs from the ERECTA family but does not form homodimers (Pillitteri and Torii, 2012). ERECTA has several family members that are involved in the early steps of stomatal development but also some of the family members act to orientate asymmetric spacing division at a later stage of stomatal development (Pillitteri and Torii, 2012).

An RLP involved in plant immunity is tomato Ve1 that mediates resistance to *V. dahliae* and recognizes multiple effectors from diverse fungal pathogens (Fradin et al., 2009; de Jonge et al., 2012). Ve1 is also functional when transferred to a different plant family indicating the conservation of downstream signaling components across tomato and Arabidopsis for this particular RLP (Fradin et al., 2011). The Cf proteins from tomato Cf-2, Cf-4, Cf-9 conferring resistance to *C. fulvum* are RLPs that are activated by small fungal pathogen derived peptides Avr4 and Avr9 respectively (Rivas and Thomas, 2005). Cf proteins are highly glycosylated and the glycosylation status impacts the activity of Cf-9 for instance (van der Hoorn et al., 2005). In addition, it might be possible that Cf-4 and Cf-9 undergo endocytosis given that both proteins carry the conserved endocytosis motif Yxxϕ (Robatzek, 2007) Therefore, receptor

endocytosis might be a common theme for membrane-bound receptors that is not limited to RLKs. Interestingly, this seems to be the case, as the RLP that mediates the recognition of xylanase LeEix2, which contains the Yxxϕ motif is processed by the endocytic machinery and this processing is required for triggering xylanase associated responses (Ron and Avni, 2004; Bar and Avni, 2009). Finally, there is emerging evidence demonstrating that the co-regulator SERK3/BAK1 of RLKs is also required for the function of some RLPs, namely LeEix2 and Ve1 (Fradin et al., 2009; Bar et al., 2010)

1.1.3. The Receptor-like kinase SERK3/BAK1

Regulation of the defense response initiated by LRR-RLKs and LRR-RLPs seems to be mediated by the RLK SERK3/BAK1. BAK1 is a member of the somatic-embryogenesis receptor kinase (SERK) family (Shiu et al., 2004; Zhang et al., 2006) that was first identified as a positive regulator of the brassinosteroid (BR) receptor BRI1, but that is also important in the plant immunity pathway. BAK1 forms a ligand-dependent complex with FLS2 and EFR (Chinchilla et al., 2007a; Heese et al., 2007; Roux et al., 2011) and it is required by the RLP Eix1 to exert is function as a negative regulator of the ethylene-induced xylanase response (Bar et al., 2010). *bak1* mutant alleles are compromised in flg22 and elf18 early responses and reduced expression of *NbSERK3* leads to enhanced susceptibility to *P. infestans* and *H. arabidopsidis* and loss of response to INF1 and CSP22 confirming the involvement of BAK1 in immune responses triggered by a diverse group of PAMPs (Chinchilla et al., 2007a; Heese et al., 2007; Chaparro-Garcia et al., 2011). However, LysM type receptors have not been shown to require BAK1 for signaling and do not form a complex with it after elicitation (Chinchilla et al., 2007a; Schulze et al., 2010; Roux et al., 2011). Heteromerization of BAK1 after elicitation has been demonstrated for several PRRs, namely FLS2, EFR, and AtPEPR1/2 (Chinchilla et al., 2007a; Heese et al., 2007; Postel and Kemmerling, 2009; Roux et al., 2011), and its role in BR signaling has been showed (Russinova et al., 2004). However, BAK1 is also important in cell death control, as evidenced by the spreading necrosis after infection with bacterial and fungal pathogens in *bak1* mutants (Chinchilla et al., 2009).

Interestingly, other RLKs besides BAK1 seem to be implicated in PTI signaling. BIK1 (Botrytis induced kinase 1), which was identified as being transcriptionally induced after infection with *B. cinerea*, is important for defense against *P. syringae* (Veronese et al., 2006) and it is phosphorylated after flg22 and elf18 elicitation. Moreover, BIK1 associates with FLS2 and EFR and later disassociates from the complex in a BAK1-dependent manner after elicitation (Lu et al., 2010).

1.1.4. Signaling events after elicitor perception

Upon detection of PAMPs a signal transduction cascade is activated that includes calcium influx, production of reactive oxygen species, activation of MAPK cascades and transcriptional reprogramming (Monaghan and Zipfel, 2012). Diffusible intracellular messengers such as Ca^{2+} or cAMP play an important role in activation and possible amplification of the signal (Aepfelbacher et al., 2003). Plants and mammals seem to share some of the intracellular regulatory components of this response like GTPases (Schwessinger and Zipfel, 2008).

There are also adaptor proteins, which mediate protein-protein interactions. In mammals these include the myeloid differentiation response gene 88 (MyD88) TIR domain protein, which recruits IL-1R-associated protein kinase (IRAK) (Han, 2006). After being phosphorylated, IRAK associates with an E3 ligase protein activating MAPK pathways. Interestingly, the tomato Pto kinase protein has similarities to the IRAK protein (Espinosa and Alfano, 2004) pointing to the conserved nature of the immune response.

1.1.5. Endosomal regulation of PTI

One of the first events after ligand binding is the formation of a hetero-complex with BAK1 (Roux et al., 2011). The internalization of plasma membrane receptors is a mechanism shared by mammals and plants to regulate signaling but also as a platform for signaling (Murphy et al., 2005). Ligand perception can also induce internalization of membrane-bound receptors into endosomes as revealed by co-localization studies with the endosomal markers ARA6 and ARA7, for FLS2 for example (Robatzek et al., 2006; Beck et al., 2012). BRI1 undergoes constitutive endocytosis and more strikingly, the co-regulator BAK1, which is also constantly internalized, accelerates BRI1 internalization (Russinova et al., 2004). Another receptor that has been reported to undergo endocytosis is LeEIX2 (Bar and Avni, 2009). The Arabidopsis homolog of Eps15-homology protein (EHD1/Rme1) AtEHD2 that regulates transport from the endosomal recycling compartment to the trans-Golgi network (TGN) and plasma membrane (PM), is involved in the correct signaling mediated by LeEIX2 and other RLPs Cf-4 and Cf-9 (Stergiopoulos and de Wit, 2009) but not FLS2 (Bar and Avni, 2009) suggesting distinct signaling requirements between RLPs and RLKs. Endosomal trafficking of receptors either to attenuate signaling or sustain it by recycling the receptor back to the PM results in a range of physiological responses as diverse as plant development to innate immunity (Murphy et al., 2009) making it a key cellular process that pathogens could potentially exploit to their advantage. Finally, PM-localized receptors sometimes contain an ubiquitination signal in their cytoplasmic domains that will usually target these receptors to the late endosomes (Murphy et al.,

2005). FLS2 is actually ubiquitinated by the Arabidopsis E3 ligases PUB12 and PUB 13 and sent for degradation most likely through the 26S proteasome, as treatment with the inhibitor of proteasome degradation MG132 also diminished FLS2 protein levels (Lu et al., 2011).

1.2. Pathogens deploy effectors to support infection

1.2.1. Effector definition

A common theme observed in pathogens ranging from bacteria, to fungi, oomycetes and nematodes is the occurrence of effector molecules deployed to different cellular compartments to facilitate colonization by means of manipulation and reprogramming of host immune responses

The term effector is rather flexible and does not dependent on the outcome of the interaction. As defined by Win et al. (2012), the term effector encompasses “microbial secreted molecules that influence host cell processes or structure to promote the microbe’s life style”. Effector functions are not limited to suppressing innate immunity but it is becoming evident that effectors also promote penetration or enhanced access to nutrients.

Effectors are secreted molecules produced by microbes to influence host cell processes and/or structure to promote the microbe’s life style. Effector activities are so diverse ranging from promoting penetration through enabling the microbe to access nutrients to suppressing immune responses. In recent years they have also been used as molecular probes to unravel novel components of the plant immune system and to “rewire” cellular processes (Bozkurt et al., 2011; Wei et al., 2012).

1.2.2. Effector delivery

The translocation of effectors inside the host cytoplasm is achieved by diverse mechanisms (Hogenhout et al., 2009). Gram-negative bacteria utilize the Type III Secretion System (TTSS) to deliver effectors inside host cells (Alfano and Collmer, 2004), whereas for fungi and oomycetes the mechanism to deliver effectors remains unknown. However, studies show that some effectors accumulate at the haustoria (Rafiqi et al., 2010; Bozkurt et al., 2012; Saunders et al., 2012) suggesting that haustorium-forming organisms might use this specialized structure to carry out the delivery function besides the uptake of nutrients.

1.2.3. Effector activities

Once inside the host cell, effectors are known to have differential activities: (1) alterations in protein turnover, (2) targeting host transcription or RNA stability, and (3) interference with the immune signal cascade by inhibition of kinases (Block et al.,

2008). For example, to interfere with host protein turnover, effectors can degrade or cleave host proteins, as exemplified by AvrRpt2, a cysteine protease that cleaves the negative PTI regulator RIN4 (Coaker et al., 2005).

Many effector activities aim at suppressing PTI. The Type III bacterial effector AvrPto is a strong suppressor of PTI in Arabidopsis and tomato (Deslandes and Rivas, 2012) probably by blocking receptor phosphorylation since its association with FLS2 does not affect heteromerization with BAK1 (Xiang et al., 2011; Deslandes and Rivas, 2012). AvrPtoB, another Type III bacterial effector suppresses flg22-elicited PTI by targeting FLS2 for degradation by ubiquitinating the receptor (Gohre et al., 2008). AvrRpt2 is activated by the cyclophilin ROC1 to process the plant protein RIN4 (Coaker et al., 2005) RIN4 is a negative regulator of PTI (Deslandes and Rivas, 2012) and cleavage of RIN4 should lead to higher defense responses, but it was shown that the fragments of RIN4 generated by AvrRpt2 processing are more efficient at suppressing PTI than the full length proteins (Afzal et al., 2011).

1.2.4. Effectors act in different cellular compartments

Besides PTI suppression, effector proteins can be targeted to other cellular compartments. The *P. syringae* effector HopG1 localizes to the host mitochondria and it has been shown to alter levels of ROS (Block and Alfano, 2011). The *Xanthomonas* TAL effectors accumulate in the nucleus where they activate plant gene expression (Szurek et al., 2001; Kay et al., 2007; Kay et al., 2009). Finally HopZ1 acetylates tubulin altering microtubule polymerization (Lee et al., 2012). Manipulation of the cytoskeleton is a widespread strategy to promote invasion of the host cell or to gain motility or to hijack intracellular transport (Bhavsar et al., 2007).

It has become apparent that endosomal and vesicle trafficking play an important role during infection as multiple components of these trafficking networks are recruited to the site of infection most likely to support invasion (Lu et al., 2012). Therefore, having effectors that manipulate this process would be beneficial to redirect cellular resources to where the pathogen needs it most.

1.2.4. Effector host interacting proteins

Identification of the plant targets of effectors has become a driving force to further our understanding of effector function. Those host proteins that are modified by the effector to manipulate host structure and function are thought of as targets. Examples encompass some effectors that have enzymatic activity like AvrPphB, which is a cysteine protease that cleaves PBS1 and BIK1 to induce ETI and suppress PTI respectively (Shao et al., 2003; Zhang et al., 2010). In addition to having targets, there is an emerging concept that effectors also need host proteins termed helpers to

achieve their function (Win et al., 2012). Effector helper proteins differ from targets in that they are not necessarily modified by the effector but are required by it maybe to be activated or to reach its final subcellular localization where the effector exerts its function. Effector helper proteins would be genetically upstream of the effector and might not impact the "cellular process that the effector is targeting" (Win et al., 2012). Importin α is an example of an effector helper. The bacterial effector AvrBs3 associates with importin α1 and importin α2 from pepper to reach the nucleus to activate gene expression (Szurek et al., 2001). AvrBs3 is an effector protein from *Xanthomonas camprestris* pv. *vesicatoria* with a central repeat region, functional nuclear localization signals (NLS) and an acidic activation domain (AAD) that are required for eliciting Bs3-mediated responses (Van den Ackerveken et al., 1996; Szurek et al., 2001). AvrBs3 is transported to the nucleus where it targets *upa* genes (up-regulated by AvrBs3) (Szurek et al., 2001; Marois et al., 2002). More exactly, AvrBs3 directly binds to plant DNA harboring a conserved promoter element known as the *UPA box*, hence acting as a eukaryotic transcription factor (Kay et al., 2007; Kay et al., 2009). Although AvrBs3 association with importin is important to reach the cellular compartment where it functions, the effector target is the *UPA box*. Another example is the *P. syringae* effector HopZ1a that is activated inside the host cell by phytic acid to become a functional acetyltrasnferase that acetylates the plant target of HopZ1a, tubulin (Lee et al., 2012). Acetylation of tubulin seems to dramatically compromise normal disposition of microtubule networks promoting *P. syringae* growth (Lee et al., 2012). However both effector target and helpers are susceptibility factors since they contribute to the accomplishment of the effector function favoring a state of effector triggered susceptibility, which is the suppression of innate immunity or enhancement of nutrient acquisition.

1.2.2. Host cellular pathways targeted by effectors

It is increasingly evident that pathogens often target cellular pathways at different levels to achieve disease. Often several effectors from the same pathogen target the same pathways probably to ensure success. The host ubiquitin-26S proteasome (UPS) is a vital cellular process and disruptions along the pathway result in severe effects (Marino et al., 2012). Ubiquitinylation is a sequential and hierarchical series of enzymatic reactions whereby ubiquitin, a 76-residue moiety, is attached to the protein targeted for degradation (Bhoj and Chen, 2009). Three enzymes mediate this process but it is the E3 ligase that determines the specificity of ubiquitination (Bhoj and Chen, 2009). In the *Arabidopsis thaliana* genome, there are >1200 genes that encode E3 ubiquitin ligases (whereas there are only two genes for E1 and 46 for E2s (Sullivan et al., 2003) reaffirming the importance of this class of proteins. Given that ubiquitination

is such a critical regulatory mechanism of different cellular processes including resistance to pathogens (Angot et al., 2007), it is not surprising that pathogens have evolved to target this pathway.

The pathogenic bacterium *Salmonella enterica* serovar Typhimurium uses the host UPS to degrade their own effectors and regulate the timing of their action (Angot et al., 2007). It has also been observed that some effector proteins contain E3 ligase domains, which likely imitate host E3 ubiquitin ligases. Such is the case of AvrPtoB (C-terminal E3 ligase domain) which ubiquitinates the tomato kinase Fen (a member of the Pto gene family, which shares homology with Pto but does not recognize AvrPtoB) promoting its degradation by UPS (Rosebrock et al., 2007). Effectors can also act indirectly by mediating the UPS-dependent elimination of a component of plant defense responses. For example, the *Pseudomonas syringae* effector HopM1, which lacks E3-ligase features, likely mediates the recognition of AtMIN7 (a plant protein involved in cell-wall host defense) by the plant UPS by acting as an adaptor protein (Rytkonen and Holden, 2007).

Other prevalent pathways that are manipulated by pathogens are the endocytic and secretory pathways. Internalization of PAMPs has been reported and some PAMPs from pathogenic oomycetes stimulate endocytosis. Moreover, cell surface receptors implicated in the recognition of such PAMPs carry a common motif (Yxxϕ) that signals for endocytosis pointing to a role of endocytosis in signaling in plant defense (Leborgne-Castel et al., 2008; Leborgne-Castel et al., 2010). In addition, the Arabidopsis protein AtEHD2 that has an EH-containing domain, binds the cytoplasmic region of the xylanase receptor LeEIX2 (Bar and Avni, 2009). The EH domain is found in an animal protein resident of coated vesicles, Eps15 adding to the growing evidence that endocytic mechanisms are put in motion upon elicitor treatment (Leborgne-Castel et al., 2010).

The secretory pathway which shuttles proteins from the ER through the Golgi apparatus to the PM, is presumably used to transport RLPs and RLKs but also important signaling lipids (Hilbi and Haas, 2012). Modulation of this pathway by intracellular pathogens is a clever mechanism to exploit the cellular machinery to create a pathogen friendly niche. For example, the bacterium *Legionella pneumophila* replicates in macrophages where the *Legionella*-containing vacuoles acquire endosomal small GTPases to communicate with the vesicle trafficking pathway (Hilbi and Haas, 2012). *Salmonella enterica* serovar Typhimurium also interacts with the secretory pathway besides interfering with the recycling one. It also replicates in a membrane-bound compartment that interacts in a dynamic manner with the early endosome protein Rab7 (Hilbi and Haas, 2012). Therefore it is possible that at

different stages of infection pathogens target different cellular compartments via one or multiple effectors to provide an ideal niche for the microbe.

1.3. Effector-triggered immunity (ETI)

Studying effector recognition in resistant plants also provides valuable information on their activities. Intracellular recognition of effectors occurs by the activation of host specific R proteins that mediated defense responses against a specific pathogen carrying the cognate pathogen molecule known as effector. This type of defense is known as effector-triggered immunity (ETI). The interaction between the appropriate R protein and the pathogen effector results in disease resistance. If one of these two critical components is missing, a state of disease results (Dangl and Jones, 2001). There are several classes of R proteins. The largest class is the polymorphic NB-LRR proteins (Nucleotide binding plus leucine-rich repeats) that can be subdivided into Toll Interleukin (IL)-1 receptors (TIR-NB-LRR) and coiled-coil N-terminal domain (CC-NB-LRR) (Dangl and Jones, 2001). R proteins contain a NB-ARC domain that is generally involved in ATP binding (Lukasik and Takken, 2009; Shirasu, 2009). The N terminal domain, CC or TIR seems to be important for receptor dimerization and specific recognition of the effectors (Lukasik and Takken, 2009; Dodds and Rathjen, 2010).

Several models of effector recognition have been proposed. One model proposes that recognition of the effector proteins by these receptors is direct (Dangl and Jones, 2001). For example the *R* genes L5, L6 and L7 from flax recognize different alleles of the gene *AvrL567*, which is an effector from *Melampsora line* that is expressed during infection (Dodds and Rathjen, 2010). Another model for recognition by R proteins, known as the “guard hypothesis”, postulates that the R protein monitors alterations of another plant protein which is the actual target of the effector and it is modified by it leading to ETI (Mackey et al., 2002; Axtell and Staskawicz, 2003; Rooney et al., 2005). Several effector/R protein pairs are consistent with the guard hypothesis, namely AvrB/RPM1, AvrRpt2/RPS2, and AvRpm1/RPM1; all of these effectors interact with RIN4 and perturbations of RIN4 are detected by the corresponding R protein (Mackey et al., 2002; Martin et al., 2003; Dodds and Rathjen, 2010).

Recently a different model of effector recognition was proposed (van der Hoorn and Kamoun, 2008). In this model, four players would be implicated in the interaction, namely: (1) **the effector**, (2) **the decoy** (effector target necessary for the function of the R protein but with no function in defense in its absence; the decoy doesn’t have any effect on pathogen’s fitness), **the operative target** (a host target that upon manipulation by the effector results in enhanced fitness for the pathogen), and (4) **the guardee** (effector target also necessary also for the function of the R protein but with a function in defense responses even in the absence of the R protein; the decoy would

contribute to a pathogen's fitness in susceptible plants). This model illustrates the following situation: an **R** protein would monitor a **decoy**, which would be mimicking the **operative target** in the perception of the effector but not in its function (in plant-defense responses). Decoys would compete with operative targets for binding the effector. Support for the decoy model is the interaction between the effector protein AvrPto and the R protein Prf. Upon translocation of AvrPto kinase inhibitor by *Pseudomonas syringae* pv. *tomato* JL1065 into the host cell, AvrPto (the effector) is localized to the plasma membrane (Shan et al., 2000) where it physically interacts with Pto (the decoy) kinase protein (Xiao et al., 2007). This interaction is recognized by Prf (R protein) leading to ETI (Block et al., 2008). AvrPto also inhibits the kinase activity of the receptor-like kinases FLS2 and EFR, which are important in PTI. In the absence of FLS2, AvrPto contributes to virulence (Xiang et al., 2008) reinforcing the idea that FLS2 could indeed be the operative target (van der Hoorn and Kamoun, 2008).

1.3.1. ETI signaling components

Recognition of the effectors leads to the activation of the ETI response. Some of the studied R proteins do not have an obvious trans-membrane motif although they seem to be associated with the membrane like RPM1 and RPS4 (Shirasu, 2009). For other R proteins, recognition of the effector re-directs the R protein to the nucleus for full signaling (Shirasu, 2009). Regardless of their subcellular localization, there are several components that are required for the function of these R proteins. One of these is the plant protein RAR1, a Zn^{2+} binding protein (Austin et al., 2002; Azevedo et al., 2002) whose role seems to be restricted to immunity as no other obvious phenotype besides loss of disease resistance has been reported (Shirasu, 2009). Interestingly, RAR1 is required by multiple R proteins from monocots (MLA, in barley) to dicots (RPS5, RPP5 in Arabidopsis) (Shirasu, 2009) T1 (Skyp1-cullin-F-box protein) interacts with RAR1 (Austin et al., 2002; Azevedo et al., 2002) and it is required by several R proteins such as MLA, N, Bs2, and R3a (Shirasu, 2009). Since the *sgt1a/b* (there are two copies in Arabidopsis) mutant in Arabidopsis is lethal, SGT1 is indispensable for growth and development. It has been reported that SGT1 interacts with the LRR domain of the R protein Bs2 (Azevedo et al., 2006). Another plant protein that associates with RAR1 and SGT1 is HSP90, which was reported as necessary for RPS2-mediated resistance (Takahashi et al., 2003). It has been proposed that SGT1 and RAR1 act as co-chaperones of HSP90 to stabilize/activate R proteins (Shirasu, 2009; Kadota et al., 2010).

In addition to the chaperones described above, some specific components of R signalling have been identified. The EDS1 protein (Enhanced disease susceptibility 1), PAD4 are specifically required for TIR-NB-LRRs R proteins but also have a role in

basal defense responses (Feys et al., 2005; Lipka et al., 2005). In a similar manner, the protein NDR1 (Non-race specific disease resistance 1) is localized to the PM (Coppinger et al., 2004) and is required for membrane-associated CC-NB-LRR R proteins signaling (Dodds and Rathjen, 2010).

1.4. *Phytophthora infestans*

Among eukaryotic plant pathogens the Stramenopiles form a particular group that causes significant damage in natural ecosystems and considerable economic losses for global agriculture (Kamoun and Goodwin, 2007). A historically notable member of the Stramenopiles for causing the Irish Famine of 1845, *Phytophthora infestans* is the causal agent of potato and tomato late blight and in recent years, several epidemics have been reported.

Phytophthora infestans was once associated with fungi due to its filamentous form of growth. Molecular phylogenies and biochemical studies have established that *Phytophthora infestans* is more closely related to brown algae than to true fungi (Kamoun and Smart, 2005). *Phytophthora infestans* is a hemibiotroph: in the first stage of infection it requires living cells; in the next stage, necrosis of the host tissue will spread establishing complete colonization and promoting sporulation. The infection process starts when motile zoospores swim on the leaf surface where they will encyst and germinate (Kamoun and Smart, 2005). *Phytophthora infestans* then penetrates the leaf surface through the formation of an appressorium and starts to colonize the intercellular spaces. Following colonization, the haustorium is formed: a structure that will allow the pathogen to feed and establish a close association with the host cell. During all infection stages, *P. infestans* will secrete a large number of effector proteins and other molecules to facilitate infection.

1.4.1. *Phytophthora infestans* effectors

P. infestans deploys two classes of effectors that target different host cellular sites and are named apoplastic or cytoplasmic. Apoplastic effectors are secreted into the plant extracellular space where they interact and inhibit plant pathogenesis-related (PR) proteins such as proteases, hydrolytic enzymes or glucanases. Cytoplasmic effectors are translocated inside the host cell through an unknown structure (most likely the haustoria) (Kamoun, 2007). An example of the former is EPI1 and EPI10, serine proteases of the kazal family that interact and inhibit the function of the plant protein P69B (Tian et al., 2004b). Cytoplasmic effectors are further classified depending on the presence of a conserved motif RXLR or LFLAK. The N-terminal RXLR motif is thought to be crucial for translocation of the effector into the cytoplasm of the host cell given its similarity to a target-signal from Plasmodium (Kamoun, 2006). RXLR containing

effectors are also found in other oomycetes. ATR1 and ATR13 from *H. arabidopsidis* (Hpa) and Avr1b and Avr3b from *P. sojae* all have the RXLR motif (Kamoun, 2006; Dong et al., 2011). Hpa ATR1 and ATR13 trigger resistance in Arabidopsis mediated by the R proteins RPP1 and RPP13 respectively (Allen et al., 2004; Rehmany et al., 2005). Heterologous expression demonstrated that these two effectors also suppress PTI (Sohn et al., 2007). In *P. sojae* Avr3b is recognized by the soybean R protein Rps3b but it also suppress accumulation of ROS and enhances susceptibility in *N. benathamiana*. Moreover, Avr3b has a Nudix hydrolase motif that is key for its enzymatic activity probably involved in Avr3b virulence but the avirulence activity is not altered by mutations in this motif (Dong et al., 2011) the N-terminal LFLAK motif is characteristic of the Crinkler (CRN) effector family. Intracellular expression of the C-terminal part of the CRN effectors results in cell death, supporting the proposed hypothesis that the LFLAK motif is also involved in translocation of the effector (Torto et al., 2003; Haas et al., 2009). CRN8 has recently been characterized as a secreted kinase that undergoes auto phosphorylation inside the host cell, and the interference with phosphorylation abolished the cell death induced by this effector (van Damme et al., 2012).

1.4.2. *Phytophthora infestans* effector AVR3a

AVR3a is probably the best-studied effector of *P. infestans*. This RXLR cytoplasmic effector was identified by searching ESTs for genes encoding secreted proteins such as Pex147 and using association genetics, (Armstrong et al., 2005). AVR3a has two alleles that showed 100% correlation with the recognition by the potato R3a protein. The allele *Avr3a* ($C^{19}K^{80}I^{103}$) associates with avirulence whereas the allele *avr3a* ($S^{19}E^{80}M^{103}$) associates with virulence (Armstrong et al., 2005). The *Avr3a* gene is expressed in sporangia, zoospores, germinating cyst but it reaches its highest expression at 48 hours of infection. Interestingly, within the same genetic region and flanking *Avr3a* there are two paralogs *Pex147-2* and *Pex147-3* but neither of them are recognized by R3a or expressed (Bos, 2007). As mentioned above, the RXLR motif is similar to the leader sequence containing a host-targeting (HT) motif in *Plasmodium falciparum* (the malaria causing pathogen) that is necessary for exporting parasite proteins to the erythrocyte (Bhattacharjee et al., 2006). Remarkably, Bhattacharjee et al., (2006) demonstrated that the first 50 amino acids of AVR3a fused to an ER-type signal sequence (pathogen proteins containing this signal are recruited to the parasite secretory pathway) was in fact exported to the host erythrocyte demonstrating that RXLR is able to function as a translocated signal and that this function is conserved across species.

AVR3a polymorphisms in the mature protein $K^{80}I^{103}$ (KI) or $E^{80}M^{103}$ (EM) are responsible for the dual activities in pathogenesis that AVR3a has. Only co-expression of $AVR3a^{KI}$ with R3a in *Nicotiana benthamiana* leads to HR while the $AVR3a^{EM}$ protein does not elicit an HR (Armstrong et al., 2005). Consequently, R3a confers resistance to *Phytophthora infestans* strains carrying $AVR3a^{KI}$. R3a was identified by comparative genomics taking advantage of the high degree of colinearity in the Solanaceae family. It was shown that *R3a,* a member of the *R3* locus on chromosome 11 is constitutively expressed (Huang et al., 2005). The events downstream of recognition are mostly unknown but the recognition of AVR3a by R3a is dependent on SGT1, an ubiquitin ligase-associate protein and HSP90, a molecular chaperone involved in protein folding, stress responses, signal transduction and transcriptional regulation (Liu et al., 2004) NbSGT1 plays an important role in the R-mediated HR (See ETI section) and also in cell death elicited by *Phytophthora infestans* INF1 (Peart et al., 2002) suggesting an overlapping signaling transduction cascade for resistance induced by intracellular or extracellular effectors. Besides interacting with HSP90, SGT1 interacts with the SCF (Skp1/Culli/F-box protein) E3 ligase complex (Liu et al., 2004). Interestingly HSP90 is also involved with SIPK, a MAPK of *Nicotiana benthamiana*. MAPKs are activated downstream of receptors and initiate signaling cascades capable of transducing extracellular stimuli into intracellular response (Kanzaki et al., 2003).

In addition to its avirulence activity, AVR3a also has a virulence activity and these activities required distinct amino acids uncoupling them at the structural level (Bos et al., 2006; Bos et al., 2009). In plats lacking R3a, $Avr3a^{KI}$ suppresses the cell death induced by the *Phytophthora infestans* elicitin INF1 (Bos et al., 2006). INF1 is an oomycete PAMP, a small cysteine-rich protein from *Phytophthora infestans* (Kamoun, 2006) that induces cell death and systemic acquired resistance in *Nicotiana* benthamiana. This elicitin is ubiquitous in all *Phytophthora* species (Kamoun et al., 1994) and it is highly expressed during the necrotrophic stage of *Phytophthora* infection (Kamoun et al., 1997c) and when silenced, it confers enhanced virulence on *Nicotiana benthamiana (Kamoun et al., 1998b)*. INF1 activates defense responses in several *Solanum* plants (Vleeshouwers et al., 2006) and INF1 signaling requires SERK3/BAK1 (Heese et al., 2007; Chaparro-Garcia et al., 2011). Interestingly, bacterial effectors AvrPto and AvrPtoB, known to suppress PTI, also suppress INF1 cell death (Hann and Rathjen, 2007). It is probable that AVR3a also shows a global suppression of PAMP-triggered responses.

A saturated high-throughput screen of AVR3a mutants demonstrated that R3a-loss of function (LOF) mutations affect protein stability resulting in inactive mutant proteins. The majority of the mutations at the polymorphic position 80 resulted in gain of function

(GOF) for AVR3a^{EM} confirming its importance for R3a recognition. Fifteen other mutations spread along the protein also generated GOF. The majority of these mutations affected exposed and charged residues suggesting that recognition by R3a involves key protein-protein interactions instead of enzymatic activities being exerted by AVR3a (Bos et al., 2009). Interestingly, none of the GOF changes suppressed INF1 cell death (ICD) like the wild type allele- Avr3a^{KI} except for Avr3a^{K80R} and the last amino acid at position 147 was identified as indispensible for ICD suppression activity but not for R3a-mediated HR confirming the functional separation of these two AVR3a^{KI} activities (Bos et al., 2009).

The search for effector interactors is one of the principal goals in trying to elucidate effector function. In yeast-two hybrid screen for AVR3a interactors CMPG1 an E3 ligase were identified (Bos et al., 2010). CMPG1 is a known positive regulator of plant-defense responses mediated by the surface-resident receptor Cf-9 and it is rapidly induced after Avr9 elicitation (Durrant et al., 2000; Gonzalez-Lamothe et al., 2006). Moreover, CMPG1 is required for ICD (Gonzalez-Lamothe et al., 2006). Given that CMPG1 is also involved in AvrPto/Pto cell death it is possible that CMPG1 is an important regulator of membrane-bound receptors signaling. Bos and colleagues (2010) demonstrated that both alleles of AVR3a (AVR3a^{KI} and AVR3a^{EM}) interact and stabilize CMPG1 whereas the mutants AVR3a$^{KI\text{-}Y147del}$ failed to interact with CMPG1, strongly suggesting that AVR3a targets CMPG1 to prevent INF1-induced cell death.

The process of ubiquitination is important in post-translation modification that allows the cell to regulate signaling and regulatory networks by adjusting the levels of the proteins involved in these processes through the ubiquitin/26S proteasome system (UPS) or by altering their localization and activities of those proteins (Sullivan et al., 2003; Angot et al., 2007; Rytkonen and Holden, 2007). Durrant and colleagues (2000) characterized the early defense responses upon Cf-9 (R protein of tomato) recognition of AVR9 (*Cladosporium fulvum* effector protein) and they identified several **A**VR9/**C**f-9 **R**apidly **E**licited (ACRE) genes in *Nicotiana tabacum* (Nt). Most of these genes were signaling components and out of the *ACRE* essential genes, two were putative E3 ligases (Gonzalez-Lamothe et al., 2006). One of them, ACRE 74 is a homolog to Parsley E3 ligase CMPG1 and it also has similarity to PUB20, a U-box E3 ligase as well (Gonzalez-Lamothe et al., 2006). NtCMPG1 is clearly induced after AVR9 recognition and when silenced, the hypersensitive response induced by Cf9/AVR9 is not visible. Furthermore, it seems that NtCMPG1 does not only play a role in R-mediated HR but also in general-elicitor-HR as demonstrated through silenced tobacco CMPG1 plants by reduced INF1-dependent HR.

1.5. Aims of this thesis

A comprehensive understanding of effector function includes the study of the molecular mechanisms by which effectors exert their activities inside the host cell. Unravelling effector contribution to pathogen virulence entails examining the host cellular proteins and processes that are targeted by effectors. This can be achieved by a combination of several experimental approaches, from cell microscopy, through genetic screens to uncover novel components of innate immunity, to biochemical analysis of protein-protein interactions.

The primary aim of this thesis was to determine the molecular mechanisms underlying the ability of the *P. infestans* effector AVR3a to supress ICD. The starting point was the finding by Heese et al (2007) that the co-regulator of PTI SERK3/BAK1 is required by INF1 to trigger cell death. Therefore, the first objective was to address the contribution of basal defense responses mediated by NbSERK3 to resistance to *P. infestans* in *N. benthamiana* (Chapter 3). INF1 is presumably recognized at the cell periphery and recently a candidate INF1 receptor was cloned (Verzaux, 2010). Hence, a pressing objective was to characterize this putative receptor at the molecular level by describing its subcellular distribution and possible association with the co-regulator SERK3/BAK1 (Chapter 4). The next question was to evaluate the extent and specificity to which AVR3a suppresses canonical outputs of PTI signaling activated by different PAMPs in *N. benthamiana*. Given that AVR3a interacts with and stabilizes the PRRs signaling component CMPG1, the role of CMPG1 in early defense responses was also evaluated (Chapter 5). As mentioned above, effector biology is ultimately linked to the host cell targets/pathways. In light of the evidence presented in Chapter 5, the last objective was to search for additional plant targets of AVR3a and given that dynamin was found, to investigate the impact of AVR3a on the plant endocytic pathway (Chapter 6).

CHAPTER 2: Materials and Methods

2.1. *Phytophthora* and bacterial strains

Infection assays were generally performed with *Phytophthora infestans* isolate *88069* and a transformed strain expressing a cytosolic tandem DsRed protein (88069td) (Bozkurt et al., 2011). Other *P. infestans* strains used in this study included T30-4 (Haas et al., 2009) and EC1 (Pel, 2010).

Agrobacterium tumefaciens strain GV3101 was used for transient transformation of *Nicotiana benthamiana*. *A. tumefaciens* Agl1 was used for transient transformation of *Solanum tuberosum* cv. Désirée and *Solanum hjetingii*.

2.2. *Phytophthora* infection assays

N. benthamiana plants (4 to 5 weeks-old) were transiently transformed with *A. tumefaciens* expressing the construct of interest and one day post-infiltration leaves were detached and placed on a clear tray under high humidity conditions. *P. infestans* strains were grown on rye sucrose agar (RSA) for 2 weeks at 18°C in the dark before the assay and zoospores suspensions were collected by flooding the agar plates with chilled water and incubated for 3 hours at 4°C. Zoospores concentration was measured with a hemacytometer and adjusted to 100 zoospores/µl. Leaves were droplet (10 µl, 6 spots per leave) inoculated with the zoospore suspension on the abaxial side and incubated at 16-18°C. Stable transgenic plants (AVR3a) were directly inoculated with zoospores at the same stage stated above. Disease lesions were measured (in mm) starting at 2 days post inoculation (dpi) until 6 or 7 dpi. Lesion area was calculated based on the width and length of the lesion. Disease scoring data was subjected to statistical analysis using one-way ANOVA and T-test with R package.

For infections with *P. infestans* 88069td, the procedure was the same as described above except that for scoring disease phenotype, lesions were scored using a Leica Stereomicroscope (Leica Microsystems CMS GmbH) mounted with a CCD camera under UV LED illumination and filter settings for DsRed. Images were processed as below (In collaboration with Dr. Ji Zhou, at The Sainsbury Laboratory, TSL).

2.2.1. InfectMeasure analysis (by Dr. Ji Zhou)

The algorithm reads a series of TIFF files into the Acapella™ image analysis platform. TIFF images are split into three planes – hue, saturation, and intensity value. Only intensity plane is used in the image analysis. Whilst splitting the image, a convolution method is used to harmonise intensity values. Image masks are applied to identify

regions with high intensity/contrast values – generated masks are randomly coloured and treated as a set of image objects. A filtering system is used to detect the scale (pixel to µm) according to its unique intensity, contrast, and width/length ratio. Another filtering system is used to filter out objects such as letters and experiment errors (inappropriate intensity, size, contrast, and location (attached to the image border). After screening, only genuine infected areas are retained.

Since the aim was to measure the area and the perimeter of the infected area, which contains many dark regions, we could not rely on measurement based on bright pixels. Hence, to perform the calculation, the algorithm firstly splits the detected infected areas into many smaller objects. Based on the split objects, the algorithm detects the centre as well as finds the most left/top/bottom/right pixels of the infection areas. Based on coordinates of those most left/top/bottom/right pixels, minor radius and major radius of the infection areas are calculated and refined. To calculate the area and the perimeter of the infected regions a calculation is based on the calculated minor radius and major radius. For example, the formula used for computing area is:

$Area=\pi ab$ (a, major radius; b, minor radius)

The formula used for computing perimeter is:

(a, major radius; b, minor radius) $C \approx \pi \left[3(a+b) - \sqrt{(3a+b)(a+3b)}\right] = \pi \left[3(a+b) - \sqrt{10ab + 3(a^2+b^2)}\right]$

For hyphal growth microscopy, infections with *P. infestans* 88069td were monitored at 2-4 days post inoculation (dpi) and subjected to confocal microscopy.

Infections assays on silenced plants: *N. benthamiana* plants were silenced using tobacco rattle virus vectors harboring an empty cloning site (*TRV::GFP*) or a partial NbSERK3 sequence (*TRV::NbSERK3*) (see chapter 3). Two weeks later leaves were detached and subjected to drop-inoculation as described above.

2.3. Plant material

2.3.1. *Nicotiana benthamiana*

N. benthamiana plants were grown under controlled environmental conditions at an average temperature of 23°C, with 45-65% humidity in long day conditions (16 hrs of light).

2.3.1.1. Transgenic *N. benthamiana* plants

N. benthamiana WT was transformed with GV3101-pBinplus:FLAG-AVR3a (different variants, see Table 2.4.1). Primary transformed plants (T1) were selected on

Murashige-Skoog salts (MS) media containing selective antibiotic (kanamycin). Plates showing a segregation of 3:1 were selected for protein expression confirmation by Western blots (WB). Total protein was extracted by bulking a small portion of the tissue for all the positives in one plate and subjected to immunoblotting with antiFLAG antibodies. If expression of the FLAG-AVR3a protein was confirmed, 10 plants from the selected segregating plates were transplanted for seed collection. Progeny (T2) were again selected on MS-kanamycin plates and segregation was checked. Plates showing 3:1 segregation ratio were selected for transplanting to soil. More or less 15 individuals per genotype were selected and protein expression was checked for each individual plant once the plants reached the 4-week-old stage. Lines with different expression profiles were selected for seed collection. This procedure was repeated two more times until T4 progeny were obtained.

Table 2.3.1. List of *Nicotiana benthamiana* lines used in this study

Lines	**Description**	**Comments**
N. benthamiana	Wild type	
SLSK1-NbAVR3a^{KI} J2	Over expression line of AVR3a^{KI} under constitutive promoter	It has a degree of developmental phenotype resembling mutants affected in Brassinosteroid perception. Leaves are thick and the plants are stunted. These plants show high expression of AVR3a^{KI}.
SLSK1-NbAVR3a^{KI} O5	Over expression line of AVR3a^{KI} under constitutive promoter	WT phenotype, Protein expression checked by WB with anti FLAG antibodies.
SLSK2-NbAVR3a^{EM} B4	Over expression line of AVR3a^{EM} under constitutive promoter	Protein expression checked by WB with anti FLAG antibodies
SLSK2-NbAVR3a^{EM} O2	Over expression line of AVR3a^{EM} under constitutive promoter	Protein expression checked by WB with anti FLAG antibodies
SLSK3-NbVector M	Transformed with empty vector used for developing the over expression lines of AVR3a, pBinplus	-
SLSK3-NbVector V	Transformed with empty vector used for developing the over expression lines of AVR3a, (pBinplus)	-
SLSK4-NbAVR3a$^{KI\text{-}Y147del}$ 11-6	Over expression line of AVR3a$^{KI\text{-}Y147del}$ under constitutive promoter	Protein expression checked by WB with anti FLAG antibodies
SLSK4-NbAVR3a$^{KI\text{-}Y147del}$ 6-2	Over expression line	Protein expression checked

	of AVR3a$^{KI\text{-}Y147del}$ under constitutive promoter	by WB with anti FLAG antibodies

2.3.2. *Arabidopsis thaliana*

A. thaliana plants were grown under controlled conditions in a long day photoperiod (16 hrs) at 22°C and 65% humidity.

2.3.2.1. Transgenic *A. thaliana* plants

Arabidopsis thaliana plants were generated by the floral dip method (Clough and Bent, 1998). *A. tumefaciens* Agl1 carrying the gene of interest was used. Primary transformants (T1) were selected in MS media containing the appropriate antibiotic for selection (kanamycin). The same procedure was used in *N. benthamiana* and applied for selecting the final T3 lines.

Table 2.3.2. List of *Arabidopsis thaliana* lines used in this study

Lines	**Description**
Col-0	Wild type line
SLSK5-AtAVR3a^{KI} # 5-3*	Over expression line of AVR3a^{KI} under constitutive promoter
SLSK5-AtAVR3a^{KI} # 6-1*	Over expression line of AVR3a^{KI} under constitutive promoter
SLSK6-AtAVR3a^{EM} # 4*	Over expression line of AVR3a^{EM} under constitutive promoter
SLSK6-NbAVR3a^{EM} # 13*	Over expression line of AVR3a^{EM} under constitutive promoter
SLSK8-NbVector # 1-3*	Transformed with empty vector used for developing the over expression lines of AVR3a, (pBinplus)
SLSK8-NbVector # 3-2*	Transformed with empty vector used for developing the over expression lines of AVR3a, (pBinplus)
SLSK7-NbAVR3a$^{KI\text{-}Y147del}$ # 9-2*	Over expression line of AVR3a$^{KI\text{-}Y147del}$ under constitutive promoter
SLSK7-NbAVR3a$^{KI\text{-}Y147del}$ # 22-1*	Over expression line of AVR3a$^{KI\text{-}Y147del}$ under constitutive promoter

* In Col-0 background

2.3.3. Seed sterilization

Seeds of either *N. benthamiana* or *A. thaliana* were sterilized before plating them on kanamycin MS plates for segregation analysis. Between 60 to 150 seeds were put into

a small paper bag and closed with a plastic clip. A small beaker containing 100 ml of 12% v/v chlorine bleach was put inside a seed desiccator and 10 ml of 37% w/v HCl was directly poured into the hypochlorite solution to release vapors. The seeds were placed on top of a small mesh and the desiccator lid was closed immediately and sealed with parafilm. Seeds were recovered after 8 to 12 hours and plated on MS+selection antibiotic. All the procedure was done in a fume hood.

2.4. *Agrobacterium*-mediated transient expression

Agrobacterium cells carrying the desired insert were grown over night at 28°C in Luria-Bertani (LB) medium with the appropriate antibiotics. Cells were harvested by centrifugation at 4500 rpm and resuspended in MES + $MgCl_2$ medium to a final OD_{600mm} of 0.3 or 0.5 (depending on the experiment). Acetosyringone was added to the resuspended cultures at a final concentration of 150 μM and left at room temperature for 2 hrs before infiltration. Infiltrations on *N. benthamiana* were mostly carried out using 4 to 5-week old plants on the abaxial side of the plant using a 1 ml syringe without needle.

2.5. AVR3a-related transient expression assays

2.5.1. Hypersensitive response (HR)

Co-expression of *A. tumefaciens* strains carrying pBinplus::R3a and pBinplus:FLAG-AVR3a^{KI} or pBinplus:FLAG-AVR3a^{EM} or pBinplus:FLAG-AVR3a$^{KI\text{-}Y147del}$ or pBinplus ΔGFP were mixed in a 2:1 ratio in MES + MgCl2 buffer to a final OD_{600} of 0.4. Symptoms were monitored from 2-6 days post inoculation (dpi).

2.5.2. INF1 cell death suppression

Constructs of AVR3a pBinplus:FLAG-AVR3a^{KI} or pBinplus:FLAG-AVR3a^{EM} or pBinplus:FLAG-AVR3a$^{KI\text{-}Y147del}$ or pBinplus ΔGFP were infiltrated using *A. tumefaciens* GV3101 to a final OD_{600} of 0.3. The following day, the infiltration sites were challenged with recombinant *A. tumefaciens* carrying pCB302:INF1 at a final OD_{600} of 0.3. Symptoms were followed from 3 to 7 days post inoculation (dpi).

2.6. PAMP triggered immunity related assays

2.6.1. Elicitors

Chitin (crab shell chitin) and flg22 (QRLSTGSRINSAKDDAAGLQIA) peptide were purchased from Sigma, UK and EzBiolab, US respectively. INF1 was purified from *P. infestans* 88069 by chromatography (Kamoun et al., 1998b; Chaparro-Garcia et al., 2011). See protocol in the protein section.

2.6.2. Reactive oxygen species

Generation of reactive oxygen species (ROS) was measured as previously described (Gimenez-Ibanez et al., 2009a). Briefly 16 to 24 4 mm leaf discs per treatment from 4 week-old wild type *N. benthamiana* leaves were floated for 16 h in 200 µl of water in a 96-well plate. The solution was replaced by a luminol/peroxidase mix (17 mg/ml (w/v) luminol (Sigma); 10 mg/ml horseradish peroxidase (Sigma)) supplied with either 10 µg/ml INF1 purified protein, or 5 µg/ml chitin, or 100 nM flg22 peptide or water. To confirm that the buffer in which INF1 was dissolved did not interfere with the ROS measurement, an additional control was included in which flg22 containing solution also had 10% of the buffer used to store INF1. Luminescence was measured over time (up to 1320 min) using an ICCD photon-counting camera (Photek) and analyzed using company software and Microsoft Excel.

2.6.7. Quantification of gene induction

Five *N. benthamiana* leaves per genotype (transgenic AVR3a variants and vector control) were treated for 0 and 180 minutes with flg22 (100 nM) or INF1[Pi] (10 µg/ml) on the left side of the leaf and on the right side of the leaf MilliQ water was used as an elicitor control. Two 8 mm leaf-discs were sampled per each side of the leaf and pooled for RNA extraction. Total RNA was extracted using TRI reagent (Invitrogen) (see section 2.7.2) and quantified with a Nanodrop spectrophotometer. DNAse treatment was performed and 1.5 µg of total RNA was used for cDNA synthesis using SuperScript II reverse transcriptase (Invitrogen). qRT-PCR was set using SybrGeen master mix (Sigma) in triplicate per sample per gene.

Gene induction of the *NbEF1*α was analyzed as a control and used to normalize values of transcript abundance for the marker genes *NbACRE132*, *NbCYP71D20* and *NbACRE31*. The marker genes monitored are known to be induced by PAMP treatment in *N. benthamiana* (Segonzac et al., 2011).

2.7. DNA, RNA, and cloning methods

2.7.1. DNA methods

2.7.1.1. Colony PCR

A PCR mix contained 1X buffer (Fermentas), DNA template, 0.4 µM primers, 0.2 mM dNTPs, 1 unit Taq polymerase (Fermentas) in a total reaction volume of 25 µl. Picked colonies with a 10 µl sterile tip (DNA template). PCR cycling conditions were as follows: Initial heating at 94°C for 5 minutes, then the initial denaturation, at 94°C for 3 min (cycle 1x), denaturation at 94°C for 15 seconds, annealing at 55°C for 15 seconds

(25-30X cycles), extension at 72°C for 1 minute per kb, and a final extension at 72°C for 10 minutes (1x cycle).

2.7.1.2. Proofreading PCR reaction (for cloning)

When high fidelity was required the reaction conditions were as follows; PCR mix contained 1X phusion buffer (Finnzyme), cDNA template (5 µl), 3% DMSO, 0.2 mM dNTPs mix, 0.4 µM primers, 1 unit Phusion polymerase (Finnzyme) in a total reaction volume of 50 µl.

PCR cycling conditions were as follows: Initial denaturation, at 98°C for 30 seconds (cycle 1x), denaturation at 98°C for 10 seconds, annealing at 62-70°C for 15 seconds (20-30X cycles), extension at 72°C for 30 seconds per kb, and a final extension at 72°C for 5 minutes (1x cycle).

For targeted mutagenesis the previous reaction conditions were used except that 1 µl of plasmid was used as a template. The PCR product was digested with 2 units of DpnI in 1X buffer. Reactions were incubated at 37°C O/N and 5 µl were transformed into *E. coli* chemical competent cells TOP10 (Invitrogen).

2.7.1.3. Sequencing reaction

[Plasmid up to 5 kb]: 200-400 ng/ µl, minimum volume per reaction: 5 µl.

4 µl Miniprep, 2 µl Primer (10 µM), 1.5 µl Buffer 5X (stored at 4°C), 1.5 µl H_2O, (change accordingly if you need to dilute plasmid concentration), 1 µl enzyme mix (Big Dye 3.1).

Program run: 96°C for 1 minute, 96°C for 10 seconds, 50°C for 10 seconds, 60°C for 3 minutes, (25 X cycles), 15°C forever.

2.7.1.4. Gel electrophoresis

Electrophoresis in a horizontal agarose gel was used to analyze PCR products. Gels contained 1X TAE (40 mM Tris, 20 mM NaAc, 1 mM EDTA, pH 7.9) plus 1 µg/ml ethidium bromide (SIGMA) for visualization purposes. Concentration of agarose was 1-1.2% (w/v). DNA samples had 0.1 vol of 6x loading buffer (Fermentas). Gels were run in 1X TAE at 100 V for 20 to 40 minutes and visualized on a short wavelength UV transilluminator (BioRad).

2.7.1.5. DNA gel purification

DNA was visualized on a long wavelength UV transilluminator and the DNA fragment was excised using a razor blade and purified using the QIAquick spin columns.

2.7.1.6. Miniprep preparation

Liquid cultures of positive individual colonies (identified by PCR) were started and incubated over night in 10 ml of LB plus the appropriate selective antibiotics. The O/N cultures were spun down at 4500 rpm for 10 minutes and the plasmid was extracted from the bacterial pellet using QIAgen spin miniprep kit (Qiagen).

2.7.1.7. Blunt cloning

The DNA fragment (cloned using proofreading PCR) was ligated into pCR-Blunt-II-TOPO (Invitrogen) according to the manufacturer's recommendations. The reaction was transformed into *E. coli* chemical competent cells TOP10 (Invitrogen).

2.7.1.8. Generation of the pENTR clone for Gateway cloning

The DNA fragment was amplified using primers containing CACC and ligated pENTR-TOPO vector (Invitrogen). Reaction proceeded for 30 minutes at room temperature. The reaction was transformed into *Escherichia coli* chemical competent cells TOP10 (Invitrogen).

2.7.1.9. Cloning using Gateway LR reaction

The LR reaction was set up using the destination vectors pGWB series (Nakagawa et al., 2007), Gateway (Karimi et al., 2002) and pHellsgate (Helliwell and Waterhouse, 2003). The reaction mix had 100 ng of the pENTR vector and 300 ng of the destination vector, $T_{10}E_1$ buffer pH 8.0 to a final volume of 4 µl, 2 µl LR Clonase II mix (Invitrogen) and incubated at 25°C for 2 hours. The reaction was stopped by adding 1 µl of proteinase K (Invitrogen) and incubated for 10 minutes at 37°C. The reaction was transformed into *E. coli* chemical competent cells TOP10 (Invitrogen).

2.7.1.10. Conventional cloning

Destination vector was digested with the appropriate restriction enzymes. If enzymes required different buffers, step-wise digestion was performed and the digestion products were clean in between cleavage events. Proofreading PCR was set up using primers containing the same restriction sites as the destination vector. Either gDNA or cDNA were used as template. PCR product was cleaned using QIAgen columns and eluted in 43 µl or 50 µl of MilliQ water.

2.7.1.10.1. Digestion reaction

Clean PCR product (35 µl) was mixed with 2 units of enzyme, 8 µl MilliQ water and 1X of the appropriate buffer and incubated at 37C for 2-3 hours. Digestion product was cleaned using the QIAgen columns and eluted in 30 µl MilliQ water.

2.7.1.10.2. Ligation reaction

Digested PCR product was mixed with digested destination vector as follows. 1 µl vector, 7 µl insert, 1X ligase buffer and 1 unit ligase (T4) (Promega). The reaction was left overnight at room temperature. The following day ligation product was transformed into GV3101 and DH5α for sequencing.

2.7.1.11. Chemically competent cells transformation

Ligation product (6 µl) was transferred into 50 µl TOP 10 (Invitrogen) *E. coli* cells (thaw on ice) and left 15 minutes on ice. Cells were subjected to a heat shock cells for 45 seconds at 42°C (water bath or dry block) and left 2 more minutes on ice. 250 µl SOC was added and transformed cell were incubated for 1 hr at 37°C. Transformed cells were plated on LB plates containing the appropriate antibiotic for selection. The following day, recombinants were analyzed by colony PCR using M13F primer and the reverse primer specific to the cloned fragment.

2.7.1.12. Electro-competent cells transformation

The desired plasmid was added to thaw GV3101 cells (50 µl) and the cells were transferred to an electroporation cuvette having 1 mm width and used an electroporator (Biorad) with the following settings: 1800 V with a capacity of 25 µF over 200 Ω resistance. Immediately 400 µl SOC were added to the electroporated cells and incubated for 1hr at 28C shaking at 300 rpm. Transformed cells were plated on LB plates containing the appropriate antibiotics for selection.

2.7.1.13. Virus induced gene silencing (VIGS)

Fragments for silencing were cloned into pTRV (RNA2) and were mixed with the TRV RNA1 construct, pTRV1 in a 2:1 ratio (RNA1:RNA2) in infiltration buffer medium (10mM MgCl2, 5mM 2-N-morpholino ethanesulfonic acid (pH 5.3), and 150 µM acetosyringone) to a final OD600 of 0.6. Two week old *N. benthamiana* plants were infiltrated with the Agrobacteria and systemic spread of the virus and system silencing was monitored by RT-PCR or morphological changes attributable to the silencing and by silencing of two additional plants with TRV::SU that reduced chlorophyll content of silenced leaves.

2.7.1.14. Primers used in this study

All primers were designed using Primer 3 (http://frodo.wi.mit.edu/) and tested *in silico* in Amplify 3X.

Table 2.7.1. Plasmids used in this study

Primer ID	Sequence (5' to 3')
AVR3a_ENF	CACCATGGACCAAACCAAGGTCCTGG
AVR3a_R	CTAATATCCAGTGAGCCCCAGGTG
AVR3a_del147R	CTATCCAGTGAGCCCCAGGTG
PcAVR3a_ENTF	CACCATGAATGTGGACTCGAACC
PcAVR3a_11_R	TTACACATAATCCCTATAGGTCATGTA
PcAVR3a4R	TCAATAATCCAGGTGGATCAC
Dyn_F1ENTR	CAC CAT GGA AGC AAT CGA GGA ATT GGA GCA GCT GTC
Dyn_F2ENTR	CAC CAT GGA AGC AAT CGA GGA ATT GGA GCA G
DynF3ENTR_Nt	CAC CAT GGA GGC GAT CGA GGA ATT GGC
DynR1_Pot	TTA AGA TCT ATA ACC GGA TCC AGA CTG TGG
Dyn_R2_Nb	ATT TAT GAT CTA TAA CCA GAT CCA GAC TGC GG
Dyn_R3Tom	TTA AGA TCT ATA ACC GGA TCC AGA AGC TGG
Nb_Dyn_wSTOP	TTATGATCTATAACCAGATCCAGACTGTGGTGG
Nb_Dyn_NStPR	TGATCTATAACCAGATCCAGACTGTGGTGG
Nb_Dyn_SEQF1	TTGCTGGTCGTAATATCTGCTGC
Nb_Dyn_SEQR1	GCTCAAGTGCCAAGGCTTTGGTACCTTC
Nb_Dyn_SEQ1RevCom	GCAGCAGATATTACGACCAGCAA
Nb_Dyn_SEQF2	GGTAGGTTAGCATTGGTCGAGACC
Nb_Dyn_SEQR2	GATTTCAAGCTTCCTCCACCTTGCT
Nb_Dyn_SEQF3	CTGCTGCATTGGATGGGTTTAAAAC
Nb_Dyn_SEQR3	CCATCTGAAAGACTATGTCG
Nb_Dyn_SEQF4	GTTCCATATAAAACAGTTTTAAAGG
Nb_Dyn_SEQR4	CCCATACCTAGAGAGACTAGAAG
Nb_Dyn_SEQF5	CCAGTTACACAAATGGTGAAGCAGAAAATAGCCC
IRinf1_1_F	TGC TTT TCT TCA TCC TTT GAT CAT CAT CTT TGC TC
IRinf1_2_R	GGC CAA TGT TAT GTG AGA TTG AAG AAG TTG AAA AG
IIRinf2_1_F	TAC AAA TCT GGA GGT ACT AGC TCT CTT TCT TGG
IIRinf2_2_R	AAC AGA GTG TTG CTC CAG TGG ATC TTT GG
IIIRinf3_1_F	ATC TTT CTC GTA ATG ATT TCA GTG GCT CAC TTC C
IIIRinf3_2_R	AGT CCT TCG TCT CTG AGC TCT CTT CTT TG
IV_Rinf1_F	AGA ACT TTT TCC TTC TGC CAA AC
IV_Rinf1_R	CAT TCC CTC ATC AAT GGT GAT G
V_Rinf1_F	AAC TGT ATT TAA GCA ATA ATC AAC
V_Rinf1_R	ATAAGGACCTGCAGCTCTTGAAG
VI_Rinf1_F	CTACCACAATTTCGTTACGAT
VI_Rinf1_R	CAA TTG CCC CAA TTC CAT TGG
NbSerk3_F	TCCTGACGGACCATCTCCTCTTT
NbSerk3_R	GCTCATAACTGGGCAAAGGGCTT
NbEF1α_F	AAGGTCCAGTATGCCTGGGTGCTTGAC
NbEF1α_R	AAGAATTCACAGGGACAGTTCCAATACCA
NbACRE31 F1	AAG GTC CCG TCT TCG TCG GAT CTT CG
NbACRE31 R1	AAG AAT TCG GCC ATC GTG ATC TTG GTC
NbCYP71D20-F2	AAG GTC CAC CGC ACC ATG TCC TTA GAG
NbCYP71-D20-R	AAG AAT TCC TTG CCC CTT GAG TAC TTG C
NbACRE132-F1	AAG GTC CAG CGA AGT CTC TGA GGG TGA
NbACRE132-R1	AAG AAT TCC AAT CCT AGC TCT GGC TCC TG
I_EcRI_Dyn_F	AAAAGAATTCCGATCGAGGAATTGACACAA
I_KpnI_Dyn_R	AAAAGGTACCCAAGGTTTCCCTTGTCAACC
I_BmHI_Dyn_F	AAAAGGATCCCGATCGAGGAATTGACACAA

II_EcRI_Dyn_F	AAAAGAATTCATCAGCTCTAAAGGCGGTCA
II_SpeIDyn_F	GCGACTAGTATCAGCTCTAAAGGCGGTCA
II_KpnI_Dyn_R	AAAAGGTACCGCTGTTGGGCTACTTTCTGC
R_SmaIDynII	GCGCCCGGGGCTGTTGGGCTACTTTCTGC
F_EcRI_Dyn_III	AAAAGAATTCTAGAGAAGGCCAAAGAAGAC
III_BhI_DynF	GCGGGATCCTAGAGAAGGCCAAAGAAGAC
III_KpnI_DynR	AAAAGGTACCGTATAACATGCTCGAAATC
R_SmaIDynII	GCGCCCGGGGTATAACATGCTCGAAATC
F_36_500_St	TATCCCTCCCTCATTGGGCAAGCTTCAG
F-24_730_tom	TTACTCCTATAAGTTTTGC
F_33_900_Std	TGGAGCTATCGCTGGAGGAGTTGC
F_36_2000St	CTTCTTTTTTTTGGGTTAATTGGTATATG
R_33_1270_St	CATGTACGGATAAACAAGCAC
R_36_1440_St	CCAACAACTGCTTCAAACTCCTC
R_33_2250_St	CATGCTCGAGCGGCCGCC
St_S3_ENTF	CACCATGGATCAGTCGGTGTTGGCGATC
Std_S3_NSTPR	TCTTGGCCCTGACAACTCATCCG
NtDyn_K50E_F	GGCACTGGTGCAGGTGAGTCAGCTGTACTGAAC
R_NtDyn_K50E	ACCGATAGCAACGACATTGAGAAAAGTGGA
NtDyn_del344_F	TAAAAGGGTGGGCGCGCCGACCCAGCTTTCTTG
R_NtDyn_del344	TCCCTCAGGCCCTGCTGTTTTCAAAGCCGAGCC
AVR3a-PacI-FLAG-F	GGATTAATTAAATGGACTACAAGGACGACGATGACAAAG TCAAGCTTCTCGAGAATTCCATCGACCAAACAAAGGTC
CMPG1-intF	GGTTCTTGAAGAATGGGAGTTTATC
CMPG1-IntR	GATAAACTCCCATTCTCCAAGAACC
CMPG1-INtR2	CTGTTGATAAAGTCACTGGATCTTTC
Le74RNAi5	ACCGTCGACAGTGACTTTATCAACAGGGATT
Le74RNAi3	ACCCTCGAGGCATTTTTCGCGTTTTTCCC
NtCMPGF8	ACCGTCGACAGTGACCTTGTCAACAGGGATC
NtCMPGR8	ACCCTCGAGCGATTTCTCATATTATTTCC
NtCMPG1_silF	CAGTGACCTTGTCAACAGGGATC
NtCMPG1_sil_R	TGAAAATGCAACAAATGCAGCTG
ELR1_SP_Rv	AGAAAAGCATCCACTTATTAAAAACAC
ELR1_mature_F	TCATCCTTTGATCATCATCTTTGCTCTCCC
ELR1SPR_X3aa	AAAGGATGAAGAAAAGCATCCACTTATTAAAAACAC
FwmELR1Phosp	TCATCCTTTGATCATCATCTTTGCTCTCCCACTG

2.7.2. RNA methods

2.7.2.1. RNA extraction

RNA extraction was done under the flow hood. Leaf-discs were collected and froze and ground immediately in liquid nitrogen. To the ground powder, 1 ml of TRI reagent (SIGMA) was added and the samples were vortex briefly to homogenize, and incubated at room temperature (RT) for 5 minutes. Chloroform was added to each sample (200 µl) and samples were shaked by hand for 15 seconds and incubated at RT for 5 minutes. Centrifugation was carried out at 9000 × *g* for 20 min at 4°C. The upper phase was removed (more or less 400-500 µl) into a new eppendorf tube. The same volume of isopropanol was added and samples were incubated at RT for 10 min.

A new centrifugation was carried out at 11000 × *g* for 20 min at 4°C. SN was discarded by pipetting, and 400 µl cold (4°C) EtOH 70% was added. Additional centrifugation was carried out at 11000 × *g* for 5 minutes at 4°C. The pellet was dried at RT for 5 -10 min. RNA was re-suspended in 30-50 µl of RNAse-free water (to help dissolve RNA, samples were incubated 5 min at 53°C).

2.7.2.2. DNAse treatment for RNA purification

TURBO DNA-free Kit (AMBION) was used and manufacturer's instructions were followed. Treated RNA was loaded (1 µg l of RNA) on 1.5 - 2% agarose gel to check integrity.

2.7.2.3. cDNA synthesis

Starting with 1.5 to 5 µg of RNA in a 20 µl reaction following manufacturer guidelines (Invitrogen) cDNA was synthesized as follows; 1 µl oligo $(dT)_{15}$, 1 µl dNTPs (10 mM each) and 12 µl of DEPC water. The reaction was incubated at 65°C for 5 minutes and chilled on ice immediately. The content of the tube was collected by centrifugation and 8 µl of a mix containing 4 µl First-strand buffer (5X), 2 µl DTT (0.1 M), 1 µl RNaseOut, 1 µl SuperScript II Reverse Transcriptase (Invitrogen) was added. The reaction was incubated at 42°C for 1 hour. Inactivation of the reaction was done by heating at 70°C for 15 min. Samples were kept at -20°C for storage.

2.8. Protein methods

2.8.1. SDS-polyacrylamide gel electrophoresis

Gels were run in Tris-glycine buffer (25 mM Tris, 250 mM glycine pH 8.3, 0.1% (w/v) SDS) for 1.5 hours at 150 V. All gels were run with a protein size marker 10-250 kDa (PageRuler Plus, Fermentas).

2.8.2. Western Blotting

Two sponges and two Whatman papers were equilibrated for 10 minutes in cold (4°C) transfer buffer (25 mM Tris, 192 mM glycin, 20% (v/v) methanol, pH 8.3). The PVDF membrane (BioRad) was activated for several minutes in 100% methanol. The device was assembled following the manufacturer's instructions (BioRad). The membrane was facing the anode and the gel the cathode. Transfer was carried out at 4°C overnight at 30 V or for 2 hours at 95 V.

2.8.3. Immunoblotting

PVDF membrane containing the immobilized, denatured proteins were blocked for 1 hour in 0.1% TBS-T buffer (0.5 M NaCl, 200 mM Tris-HCl, 0.05% (v/v) Tween-20, 0.2% (v/v) Triton X-100, pH 7.5) plus 3% (w/v) BSA with gentle agitation on a platform

shaker. The membrane was washed for 5 minutes in TBS-T buffer. The membrane was incubated with the primary antibody directed to the target protein in TBS-T + 3% BSA for 1 hour at RT. Then the membrane was washed for 30 minutes in TBS-T buffer changing the buffer every 10 minutes. Secondary antibodies covalently coupled to horseradish peroxidase (HRP) were then added. Finally the membrane was washed for 30 minutes in TBS-T buffer changing the buffer every 10 minutes. Detection of the peroxidase signal of the secondary antibody-HRP conjugate was performed with ECL (Amersham Biosciences) or SuperSignal West Femto (Pierce). Film exposure ranged from 30 seconds to 24 hours. The film was aligned to the membrane and the protein marker was marked on the film.

The primary antibodies were diluted in TBS-T + 3% BSA to the following concentration: anti-HA (1:2000, Santa Cruz), anti-GFP (1:5000, Santa Cruz), anti-myc (1:2000, Santa Cruz), anti-FLAG (1:8000, Sigma or Santa Cruz). Secondary antibodies: anti-rabbit-HRP (1:5000, Sigma), anti-rat-HRP (1:5000, Sigma).

2.8.4. FPLC for INF1 purification

INF1 protein was purified as described by Kamoun (1993) with modifications. Briefly, *P. infestans* 88069 was grown for 3-4 weeks in plich medium. The culture medium was harvested by filtration and the plich medium was exchanged for 10 mM NaCl with 10 mM Tris HCl (pH 7.4) by dialysis at 4ºC. The resulting solution containing INF1 was loaded onto a Fast-Flow Sepharose Q (GE Healthcare) equilibrated column with 10 mM Tris HCl (pH 7.4). Subsequently, the column was eluted with a linear gradient of 0-500 mM NaCl in 10 mM Tris HCl (pH 7.4). The presence of INF1 throughout purification was established by silver staining of 15% SDS-PAGE gels. Further analysis of the final pooled fractions by mass spectrometry (data not shown) confirmed the purity of the sample. Concentration was determined using BCA Protein Assay Kit (Thermo Scientific). The protein was further diluted in water before carrying out experiments.

2.8.5. FLAG-Immunoprecipitation from plant tissue

Harvested leaves were frozen and ground to powder in liquid N_2. Leaf tissue was weighed and 2.5X volume of ice-cold extraction buffer GTEN was added to the ground tissue. Vortex. Once the powdered was completely thawed on ice, centrifugation was carried out at 3000 × *g* for 10 min at 4°C and the supernatant was transferred to a 2 ml eppendorf tube. Spun at full speed for 10 minutes. Transferred the supernatant to a new tube. Anti-FLAG (SIGMA) resin was added (50 µl) to 2 ml of protein extract. Samples were incubated for 3 hours at 4°C, spun at 800 × *g* for 30 s. Discarded supernatant and added 1ml of fresh IP buffer. Repeated four more times. After the last

wash, samples were spun again and the remaining liquid was aspirated with a 1 ml syringe fitted with a very fine (25G) needle.

2.8.5.1. Preparation of Anti-FLAG resin

The FLAG resin was resuspended in 5X volumes of IP buffer [GTEN + 0.15% (v/v) NP-40 or GTEN + 0.1% (v/v) Tween 20] and spun at 800 × *g* for 1 min discarding the supernatant as above. Repeated twice. The resin was resuspended in the original volume with the IP buffer.

2.8.5.2. Elution of the FLAG-tagged proteins

The FLAG-bound protein was eluted by adding 100 µl IP buffer containing 150 ng μl^{-1} 3X FLAG peptide (3 µl of 5 µg μl^{-1} 3X FLAG to 97 µl IP buffer) and incubating with gentle shaking for 30 min at 4°C. The supernatant containing the eluted proteins was transferred to a fresh tube using a syringe and needle. 10-20 µl of the sample was loaded onto an SDS-PAGE gel for western blot analysis and/or colloidal coomassie blue staining for Mass Spec.

2.8.6. GFP-immunoprecipitation

This follows the protein extraction method from section 2.8.5 but with a modified extraction buffer. Centrifugation was carried out at 4°C at 3500 × *g* for 15 minutes and the extracts were passed through a 0.45 µm filter. GFP-affinity matrix (20 µl) was added (Chromotek) in a 1.5 ml low-bind eppendorf. Incubation was done on roller mixer for 4 hours at 4°C. After incubation with the GFP beads, centrifugation was carried out at 0.5 × *g* to pellet beads for 30 seconds. Supernatant was discarded. IP was washed with washing buffer (TBS + 0.5 % (v/v) NP40) and inverted several times to rinse beads; this was repeated 4 times. For the last wash, a syringe fitted with a needle was used. Finally, 40 µl of 1X SDS buffer (10 µl 4x (w/v) SDS, 4 µl DTT (1 M), 26 µl dH2O) was added and the samples were heated at 70°C for 10 minutes before loading in a gel.

2.8.7. Samples for mass spectrometry (MS)

Immunoprecipitation samples were loaded on a SDS gel (20 µl sample/well) and the gels were run at 80-100 V for 1-2 hours. Gels were stained with coomassie staining (0.5% (w/v) bromophenol blue R-250, 50% (v/v) methanol, and 7.5% (v/v) glacial acetic acid) at RT for 1 hour. Next, gels were de-stained three times under agitation for 30 minutes with coomassie de-stain solution (20% (v/v) methanol, 5% (v/v) acetic acid). Slices from the gel were transferred to individual eppendorf tubes (low-binding). Trypsin digestion was performed followed by LC-MS/MS analysis using LTQ-Orbitrap mass spectrometer and a nanoflow HPLC system.

2.9. Confocal microscopy methods

Cut leaf patches were mounted in water, after transient *A. tumefaciens* mediated expression of the fluorescent proteins. Pictures were acquired on a Leica DM6000B/TCS SP5 microscope (Leica Microsystems CMS GmbH) with laser settings for eYFP (488 nm), GFP (858 nm) and RFP (561 nm).

2.10. Media and buffer recipes

2.10.1. Protein extraction buffer

GTEN (10% glycerol, 25 mM Tris (pH 7.5), 1 mM EDTA, 150 mM NaCl) + 10 mM DTT + 2% (w/v) PVPP (polyvinylpolypyrolidone; not to be subsitituted with PVP (polyvinylpyrolidone) + 1% (v/v) protease inhibitor cocktail (Sigma) + 0.1% (v/v) Tween 20 or 0.15% (v/v) NP-40.

2.10.2. Modified protein extraction buffer

Add 150 mM Tris-HCl (pH 7.5); 150 mM NaCl; 10 % (v/v) glycerol; 10 mM EDTA; Add fresh: 10 mM DTT; 0.5% (w/v) PVPP; 1% (v/v) protease inhibitor cocktail (Sigma); 1% (v/v) NP-40.

2.10.3. Orange dye 6X (for DNA loading of gels)

Add Orange G 0.3% (w/v), Ficoll PM 400 15% (w/v), Tris HCl (pH 7.5) 10 mM, EDTA (pH 8) 50 mM.

2.10.4. SDS-PAGE buffer (for protein loading)

For a 5X final concentration, add bromophenol blue 0.2% (w/v), Tris HCl (pH 6.8) 200 mM, Glycerol 2.5% (v/v), and SDS 4% (w/v).

2.10.5. Agroinfiltration buffer

Add 10 mM of $MgCl_2$, 10 mM of MES, and 150 μM acetosyringone to 1 liter of MilliQ water. Adjust to pH5.6.

Acetosyringone: dissolve powder in either DMSO or Ethanol for a stock solution of 100 mM. Store at -20°C.

2.10.6. LB

Add 10 g of tryptone, 5 g of yeast extract, 10 g of NaCl to 1 liter of MilliQ water. Adjust to pH 7.0. For solid media add 10 g of agar.

2.10.7. SOC

Add 2 g of tryptone, 0.5 g of yeast extract, 1 ml of a solution of NaCl (1 M), 1 ml of a solution of $MgSO_4$ (1 M) and 1 ml of a solution of $MgCl_2$ (1 M), and 97 ml of water.

2.10.8. Murashige-Skoog salts MS

Add 4.3 g of MS salts, 0.59 g of MES, 0.1 g of myo-inositol, 1 ml of 100X MS vitamin stock, 10 g of sucrose, and 1 liter of MilliQ water. Adjust to pH 5.7 with KOH. For solid media add 8 g of agar.

2.10.9. Antibiotics

For bacterial cultures kanamycin was used at a final concentration of 50 µg/ml, gentamycin 25 µg/ml, carbenicillin 100 µg/ml, rifampicin 100 µg/ml, and Spectinomycin 50 µg/ml. For selection of transgenic plants, kanamycin was used at a final concentration of 50 µg/ml. All antibiotic solutions were sterilized with a 22 µm filter.

CHAPTER 3: The receptor-like kinase SERK3/BAK1 is required for basal resistance against the late blight pathogen *Phytophthora infestans* in *Nicotiana benthamiana*

3.1. Introduction

The first line of active host defences against pathogenic organisms consists of surface-exposed pattern-recognition receptors that mediate the recognition of highly conserved microbial molecules termed pathogen-associated molecular patterns (PAMPs) (Medzhitov and Janeway, 1997; Chisholm et al., 2006). Examples of PAMPs recognised in plants are peptides derived from the bacterial flagellin and elongation factor Tu (EF-Tu), as well as several conserved secreted proteins from bacteria, fungi and oomycetes, and the polysaccharides chitin and beta-glucans (Postel and Kemmerling, 2009).

PAMP triggered immunity (PTI) in plants is thought to be the main mediator of basal immunity (Jones and Dangl, 2006). PTI is mediated by peripherally located receptor-like proteins (RLPs) or receptor-like kinases (RLKs) which consist of extracellular domains that are linked by a transmembrane domain to either an intracellular adapter domain (RLPs) or a kinase domain (RLKs) (Zipfel, 2008). In Arabidopsis plants, the leucine-rich repeat (LRR)-RLK FLS2 (Flagellin Sensing 2) was shown to heterodimerize with the regulatory LRR-RLK Brassinosteroid-insensitive associated kinase 1 (BAK1) upon binding of the cognate PAMP leading to activation of signal transduction (Chinchilla et al., 2007a; Heese et al., 2007). BAK1 is also required for responses to other PAMPs (Heese et al., 2007; Shan et al., 2008; Zipfel, 2008). Arabidopsis BAK1 (also called SERK3) is a member of a family of five somatic embryogenesis receptor kinases (SERKs) (Hecht et al., 2001), which are important regulators for RLKs involved both in immune responses and in various developmental processes. SERKs consist of five extracytoplasmic LRRs, a family specific serine-proline-rich hinge region, a transmembrane domain, a cytoplasmic Ser/Thr kinase and a C-terminal tail (Chinchilla et al., 2009). BAK1/SERK3 function appears to be conserved in solanaceous plants, such as tobacco and tomato (Heese et al., 2007; Fradin et al., 2009; Bar et al., 2010), however, no corresponding full-length coding sequences have been described to date.

Plants of the nightshade family (Solanaceae), particularly the crop plants potato and tomato, are infected by the economically important filamentous pathogen *Phytophthora infestans*, the causal agent of late blight disease. *P. infestans* causes disease on a range of solanaceous species including, but not limited to, tomato, potato and the wild

tobacco-relative *Nicotiana benthamiana* (Becktell et al., 2006; Shibata et al., 2010). Similar to other plant pathogens, *P. infestans* is thought to colonize these host plants by suppressing basal immunity through the production of a wide array of effector proteins (Dou et al., 2008; Bos et al., 2009). However, some plants such as tobacco (*Nicotiana tabacum*) are resistant to *P. infestans* (Kamoun et al., 1998a), possibly because of the recognition of PAMPs such as the secreted protein INF1, and/or the inability of *P. infestans* to suppress immunity on this plant. INF1 recognition results in a localized plant cell death (hypersensitive response) and prevents pathogen growth (Kamoun et al., 1998a). Heese and co-authors (2007) showed that INF1 also elicits a cell death response and triggers accumulation of reactive oxygen species (ROS) in *N. benthamiana*. This cell death was abrogated upon knockdown of *Serk3*-like sequences (Heese et al., 2007). INF1 has, therefore, emerged as a typical PAMP given that it is widely conserved in *Phytophthora* and *Pythium*, and triggers defense responses dependent on a conserved immune regulator which is suppressed by the effector AVR3a and two other RXLR-type effectors of *P. infestans* (Kamoun et al., 1997b; Bos et al., 2006; Heese et al., 2007; Oh et al., 2009; Bos et al., 2010). Nevertheless, the nature of the INF1 receptor and the composition of the receptor complex remain unknown, although INF1-interacting plant membrane proteins have been identified (Kanzaki et al., 2008).

Nicotiana benthamiana is a model plant for studies of host-pathogen interactions (Goodin et al., 2008). Initially, it was used extensively in virus research because it is unusually susceptible to many virus species. More recently, *N. benthamiana* has also emerged as a popular model for the study of bacterial plant pathogens and filamentous pathogens such as fungi and oomycetes. In the oomycete community, *N. benthamiana* is utilised as a model system to study *P. infestans* pathogenicity and host-interactions at both functional and cellular levels (Becktell et al., 2006; Bos et al., 2006; Bos et al., 2010; Shibata et al., 2010). *Nicotiana benthamiana* has several advantages over potato and tomato as an experimental system to study *P. infestans* pathogenicity and particularly the facile application of transient gene expression and gene silencing assays (Goodin et al., 2008). Moreover, *N. benthamiana* is also emerging as an excellent system for microscopic studies of infections caused by filamentous plant pathogens, such as *Phytophthora* spp., given that tissues can be mounted and analysed without prior treatment (Tanaka et al., 2009; Schornack et al., 2010).

The aim of the present study was to address the extent to which defence responses mediated by NbSERK3 contribute to resistance to *P. infestans* in *N. benthamiana*. We found that four species of *Phytophthora* have different degrees of virulence on *N. benthamiana* ranging from avirulent *P. mirabilis* to moderately virulent *P. infestans* through to full aggressive *P. capsici*. We identified and silenced the expression of two

N. benthamiana orthologs of the *Arabidopsis thaliana* gene *BAK1/SERK3*. Remarkably, *NbSerk3* silencing resulted in significantly enhanced susceptibility to *P. infestans* but did not affect resistance to *Phytophthora mirabilis*, a sister species of *P. infestans*. NbSERK3A and NbSERK3B were also shown to regulate plant responses triggered by the *P. infestans* PAMP protein INF1. Most of the results presented in this chapter have been published[1].

3.2. Results

3.2.1. *N. benthamiana* shows varying degrees of susceptibility to *Phytophthora* species and *P. infestans* isolates

We wanted to compare different *Phytophthora* species and isolates of *P. infestans* for their ability to colonize *N. benthamiana* leaves. We infected 25-day-old detached *N. benthamiana* leaves with zoospore suspensions of isolates representing four different species and monitored infection using ultraviolet (UV) illumination. We could discriminate two circular zones of infection; a central necrotic area around the inoculation site, which fluoresced green under UV, and a ring of yellow fluorescent tissue that did not show macroscopic, cell death and corresponds to the biotrophic phase of the disease (Fig. 3.1.A,B). Zone diameters indicate that the tested *P. capsici* and *P. palmivora* isolates are highly virulent with large infection site diameters, while *P. infestans* isolate 88069 showed smaller infection zones (Fig. 3.1.A). On the other hand, *P. mirabilis* did not cause spreading lesions on *N. benthamiana,* instead triggering a localized cell death response typical of the hypersensitive response (HR) (Fig. 3.1.A). We consistently observed a larger autofluorescent ring with *P. palmivora* and *P. infestans* infections compared to *P. capsici* infections, suggesting differences in the extent of the biotrophic phase between these pathogens. In summary we found varying degrees of infection phenotypes ranging from complete HR-based resistance (*P. mirabilis*) to very susceptible (*P. capsici*).

To determine to what extent moderate colonization of *N. benthamiana* by *P. infestans* is isolate-specific, we tested two additional isolates (T30-4 and EC1). At three days post-inoculation (dpi), spreading infections of *P. capsici* and to a lesser extent *P. infestans* 88069 were observed (Fig. 3.1.A-C). However, no watersoaking or enlarging necrotic regions was observed with the isolates EC1 and T30-4. Instead, strong UV autofluorescent accumulation of defence compounds was observed in the proximity of the spore droplet (Fig. 3.1.B), suggesting a defence response that limits infection as reported earlier (Kamoun et al., 1998a). At later stages sporangia formed by strain

[1] **Chaparro-Garcia, A., Wilkinson, R.C., Gimenez-Ibanez, S., Findlay, K., Coffey, M.D., Zipfel, C., Rathjen, J.P., Kamoun, S., and Schornack, S.** (2011). The Receptor-Like Kinase SERK3/BAK1 Is Required for Basal Resistance against the Late Blight Pathogen Phytophthora infestans in Nicotiana benthamiana. Plos One **6**.

88069 were observed (Fig. 3.1.C) and viable, infectious zoospores could be obtained from them (data not shown). Furthermore, confocal fluorescence microscopy and electron microscopy revealed haustorial structures between 2-5 dpi upon infection with *P. infestans* 88069 or the derived strain 88069 (tdtomato) that expresses a red fluorescent protein (Fig. 3.1.D,E). Notably, EC1 and T30-4 isolates showed few intercellular hyphae upon microscopical inspection, but only at 4-5 dpi (data not shown).

These data suggest that of all tested *P. infestans* isolates, 88069 most successfully infects and completes its asexual life cycle on *N. benthamiana*, while the other isolates are less aggressive and trigger a stronger defence response. We hypothesized that varying degrees of suppression of PTI drives some of the observed isolate variation in infection efficiency.

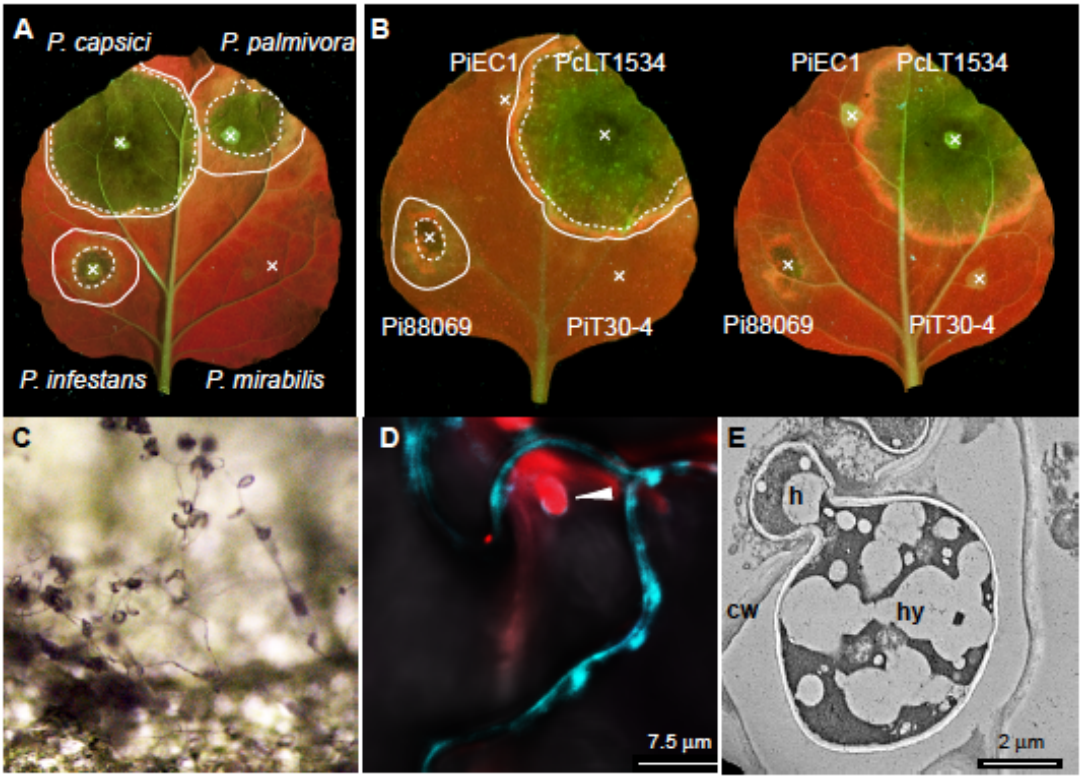

Fig. 3.1. *N. benthamiana* shows varying degrees of susceptibility to *Phytophthora* species and *P. infestans* isolates.

Detached leaves of *N. benthamiana* were infected with spore solution droplets (marked as X) of *Phytophthora capsici* LT1534, *P. palmivora* 16830, *P. infestans* 88069 and *P. mirabilis* PIC99114. (A) or *P. infestans* isolates (B) and using *P. capsici* as a reference. Photographs were taken 3 days post inoculation under UV illumination. Lines mark infected areas, dotted lines mark the border between necrotic tissue and living tissue. *P. infestans* is able to produce sporangia on *N. benthamiana* 8 days post infection (C*). P. infestans* isolate 88069td (expressing tdTomato red fluorescent protein) formed digit like haustoria (arrowhead) that invaginated the *N. benthamiana* cell membrane labelled by transient *Agrobacterium tumefaciens* mediated

expression of a membrane localised cyan fluorescent protein at 3 dpi (D). Haustoria were also observed by electron microscopy (E). h, haustorium; cw, cell wall; hy, hypha.

3.2.2. Identification of *Nicotiana benthamiana* homologs of Arabidopsis BAK1

SERK3 (also termed BAK1) is a member of the family of five SERK proteins in Arabidopsis. Previous work points to a role for *N. benthamiana* SERK3 homologs in immune responses towards the oomycete pathogen *Hyaloperonospora arabidopsidis (Heese et al., 2007)*. Heese and colleagues also showed that expression of *SERK3* homologs is required for multiple PAMP-mediated responses in *N. benthamiana,* thereby suggesting functional and sequence conservation of SERK3.

We thus wanted to address whether knockdown of NbSERK3 expression enhances *N. benthamiana* susceptibility to *P. infestans*. Searches in the TIGR expressed sequence tag (EST) databases of *Nicotiana* and potato species revealed four ESTs with similarity to AtBAK1 extending over the kinase domain (potato|TC194641, tobacco|TC102165, tobacco|TC84094, and potato|TC201428). However, only a partial *Serk3*-like sequence from tobacco identified Arabidopsis SERK3 in reciprocal BLAST analyses. The others are most likely not functional homologs of SERK3. Additional ESTs were identified in potato that appeared orthologous to Arabidopsis *SERK2*.

To facilitate the cloning of *Serk3* homologs from *N. benthamiana* using conserved sequences, we screened the genomes of the related solanaceous species, tomato and wild potato (*Solanum phureja*), which identified two *Serk3* homologs from tomato (*SlSerk3A, SlSerk3B*) and one from *S. phureja* (*SpSerk3A*). Based on these sequences we then cloned two *NbSerk3* homologs (*NbSerk3A, NbSerk3B*) from *N. benthamiana* cDNA using conserved primers. Reciprocal BLAST with *NbSerk3A* and *NbSerk3B* against Arabidopsis identified BAK1/SERK3 as the top hit, suggesting that the identified sequences were the most similar homologs. The coding sequences of *NbSerk3A* and *NbSerk3B* differ in 22 single nucleotide polymorphisms (98.8% identical). Both derived NbSERK3 proteins follow the conserved structure consisting of an N-terminal signal peptide, followed by four equally spaced leucines that could form a leucine zipper (LZ), five extracellular leucine rich repeats (LRR), a proline/serine rich hinge domain, a transmembrane domain and an intracellular serine/threonine kinase domain (Fig. 3.2.). Notably, 12 of 14 amino acid polymorphisms between NbSERK3A and NbSERK3B are located in extracytoplasmic domains. In summary, we identified two close *N. benthamiana* SERK3 paralogs, highly homologous to Arabidopsis BAK1/SERK3, which are conserved in sequence and domain structure.

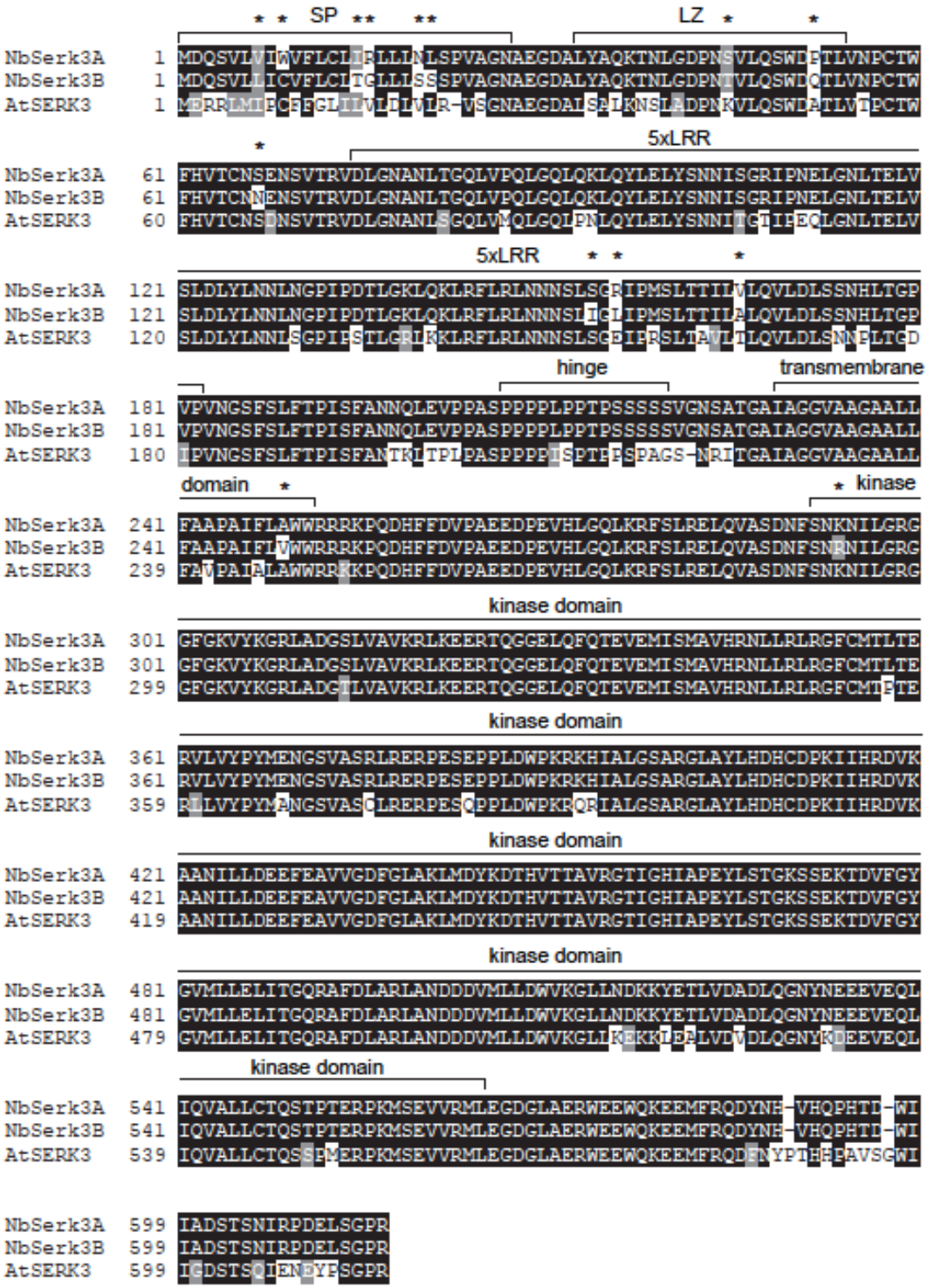

Fig. 3.2. *N. benthamiana* homologs of AtBAK1

ClustalW alignment of SERK3 homologs from Arabidopsis and *Nicotiana benthamiana*. Amino acid residues are shaded black if identical or grey if similar. The signal peptide was predicted using the SignalP3 web prediction tool. Domain identities are labelled above sequences. Asterisks indicate difference between NbSERK3A and NbSERK3B.

3.2.3. *NbSerk3* silencing in *N. benthamiana* results in enhanced susceptibility to *P. infestans*

We next asked whether silencing of *NbSerk3* variants affects colonization of *N. benthamiana* by *P. infestans*. Plants were silenced using virus-induced gene silencing (VIGS) and the constructs TRV::*GFP* or TRV::*NbSerk3* (Heese et al., 2007). Silencing was confirmed by RT-PCR using a primer combination that annealed to both *NbSerk3* transcripts, upstream of the region targeted by the TRV::*NbSerk3* silencing construct (Fig. 3.3.). Detached leaves of silenced plants were challenged 19 days after silencing by drop inoculation with *P. infestans* zoospore solutions of strains 88069 or the red fluorescent 88069td. Better infection was repeatedly observed during infection and faster progression at the infection sites to the stage of sporulating hyphae in several independently *NbSerk3*-silenced leaves, alongside extended hyphal growth (Fig. 3.4.). By 4-5 days whole leaves were infected and sporulating, while no sporulation was observed on the control silenced leaves (Fig. 3.4.E). Similar results were obtained with two other *P. infestans* isolates (Fig. 3.5.), indicating that *NbSerk3* silencing enhanced the susceptibility of *N. benthamiana* to *P. infestans* infection.

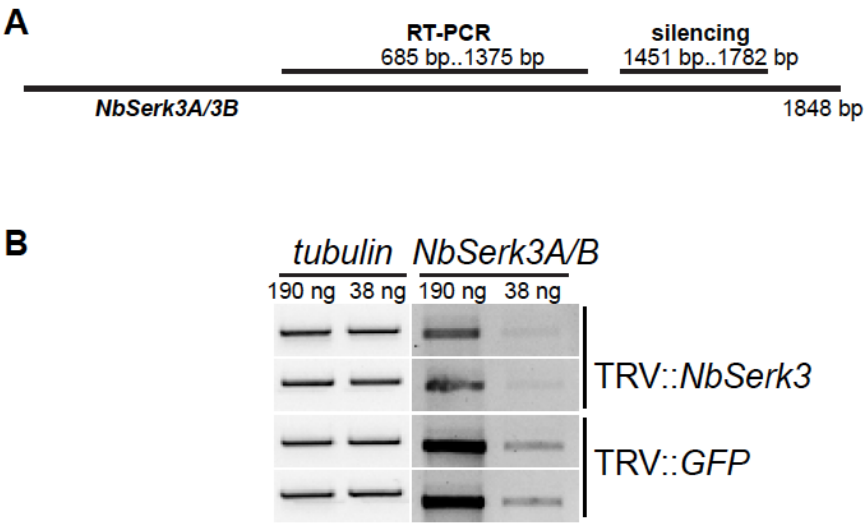

Fig. 3.3. *NbSerk3* variants are silenced by TRV::*NbSerk3* silencing construct

RT-PCRs were carried out on *NbSerk3*- or control silenced leaf discs using primers that amplify a region that does not overlap with the silencing target sequence (A). Different amounts of total cDNA were subjected to PCR using control *tubulin* primers or *NbSerk3* specific primers and visualized in an ethidium bromide stained gel (B).

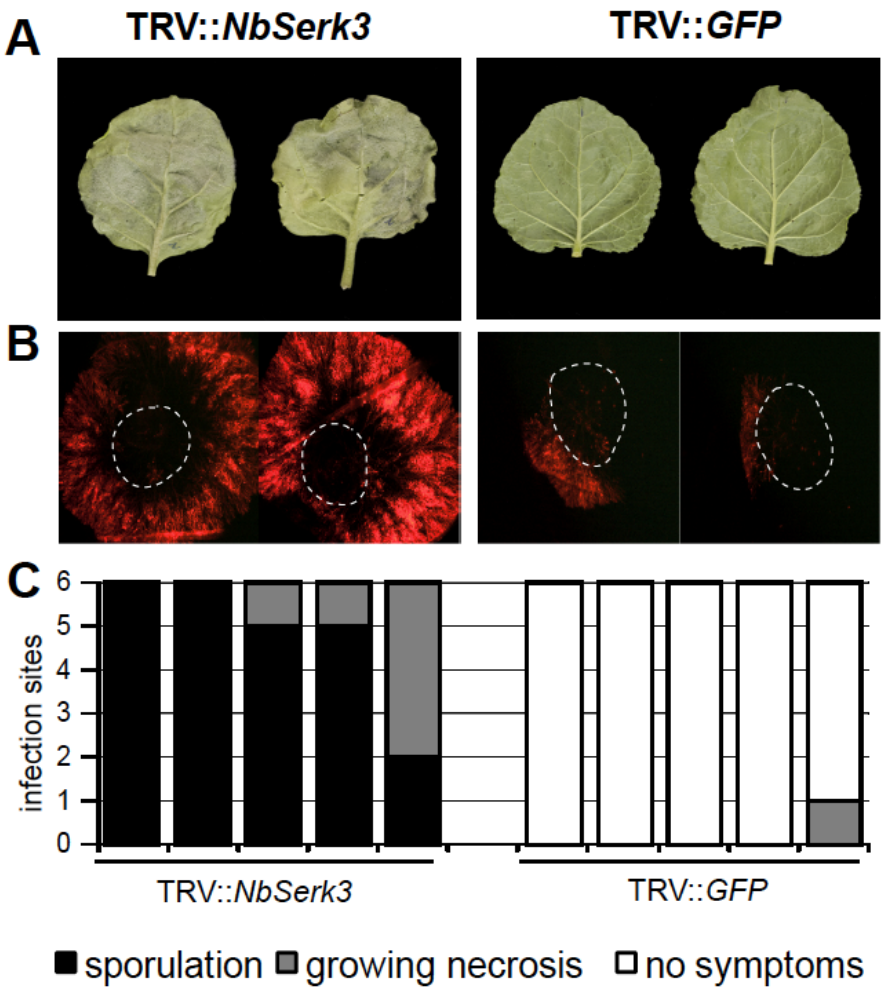

Fig. 3.4. *NbSerk3* silenced *N. benthamiana* leads to enhanced susceptibility to *P. infestans* infection

N. benthamiana plants were silenced using tobacco rattle virus vectors harbouring an empty cloning site (TRV::*GFP*) or a partial *NbSerk3* sequence (TRV::*NbSerk3*). Nineteen days later, leaves were detached and spore droplet inoculated within the dotted lines with *P. infestans* 88069 (A) or 88069td (B). Pictures were taken 6 dpi (A) and 3 dpi (B). Infection stages of at least 5 independent plants of each silencing construct were scored at 4 dpi (C).

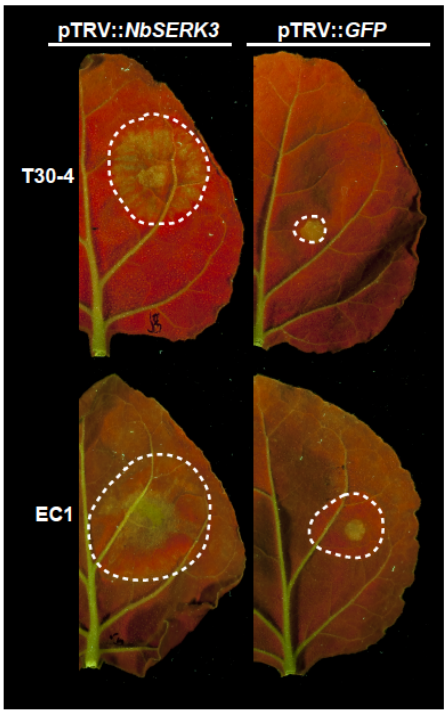

Fig. 3.5. *NbSerk3* silenced *N. benthamiana* shows enhanced susceptibility to infection by *P. infestans* T30-4 and EC1 isolates

N. benthamiana plants were silenced using tobacco rattle virus vectors harbouring green fluorescent protein gene that is not present in *N. benthamiana* (TRV::*GFP*) or a partial *NbSerk3* sequence (TRV::*NbSerk3*). Nineteen days later, leaves were detached and spore droplet inoculated within the dotted lines with *P. infestans* T30-4 (upper row) or EC1 (lower row). Images were taken 6 dpi with UV illumination. Dotted lines represent infected areas.

3.2.4. Silencing of *NbSerk3* in *N. benthamiana* does not alter resistance to *P. mirabilis*

To study whether NbSERK3A and NbSERK3B are also required for resistance towards *P. mirabilis* we carried out zoospore drop inoculations of *NbSerk3*- or control silenced leaves as described above. No difference was observed in infections with *P. mirabilis* between *NbSerk3*-silenced and control leaves, while *P. infestans* infections were enhanced (Fig. 3.6.). UV auto fluorescence within the leaf area under the droplet suggested a localized defence response (Fig. 3.6.). Drop inoculations on the host plant *Mirabilis jalapa* showed sporulating infections 3-4 days post spore inoculation and confirmed viability of the *P. mirabilis* zoospores (data not shown). This data suggest that other mechanisms besides NbSERK3-mediated defence response contribute to resistance towards *P. mirabilis* infection.

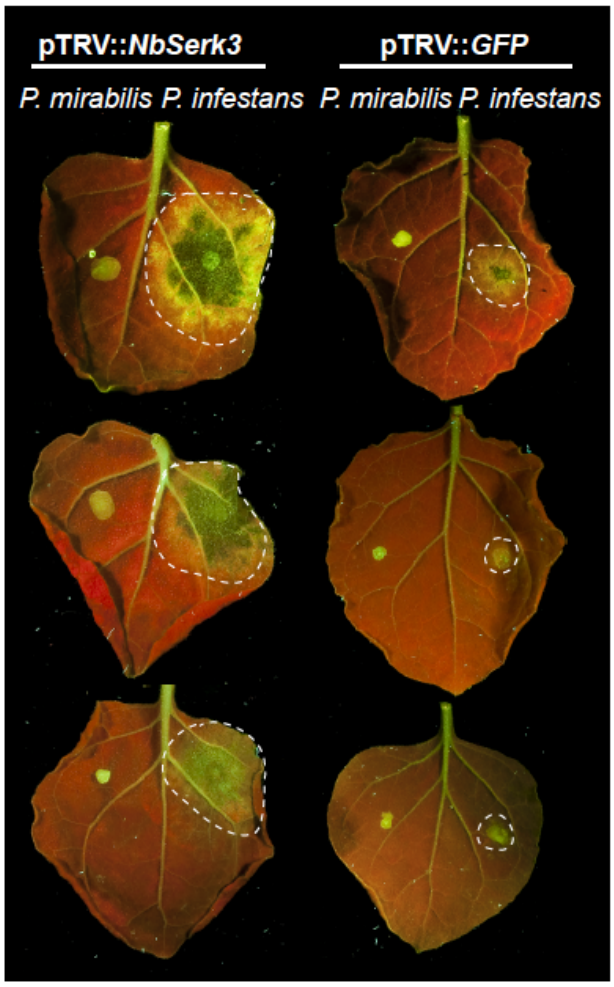

Fig. 3.6. *NbSerk3* silenced *N. benthamiana* leaves are not infected by the non-host pathogen *P. mirabilis*

NbSerk3 -silenced (left) or control silenced plants (right) were inoculated with *P. mirabilis* (left leaf halves) or *P. infestans* 88069 (right leaf halves). Images were taken three dpi with UV illumination. Dotted lines represent infected areas. Note the occurrence of autofluorescent spots at *P. mirabilis* infection sites.

3.2.5. INF1 purified from *P. infestans* triggers cell death and a late ROS burst in *N. benthamiana*

A well-studied elicitor of *P. infestans* that is recognized by *N. benthamiana* is the INF1 protein, which is secreted by the pathogen into the extracellular space. Heese and colleagues (2007) established a link between INF1 responses (cell death, ROS burst) and *NbSerk3* mainly using recombinant INF1 protein produced in *E.coli* (INF1[Ec]).

To expand these results and to exclude modulation of PAMP responses by residual *E. coli* PAMPs that induce SERK3-dependent responses, INF1 purified from *P. infestans* (INF1[Pi]) was used. To that end, I purified INF1[Pi] from *P. infestans* strain 88069 culture supernatant using anion exchange and size exclusion chromatography. INF1 elution fractions did not show additional protein bands in silver-stained protein gels

(Fig. 3.7.A). Purity was also confirmed by mass spectrometry analysis (data not shown). Similar to the data obtained with INF1[Ec] it was found that INF1[Pi] protein infiltration into *N. benthamiana* induced cell death, suggesting that the purification process did not affect its known activity (Fig. 3.7.B).

Then 10 µg/ml of purified INF1[Pi] were tested for its ability to trigger a temporal accumulation of ROS. Significant ROS production was observed peaking at 50 min post-application of INF1. Notably, the burst was lower and delayed compared to flg22-triggered ROS burst peaks in *N. benthamiana* (Fig. 3.7.C). However total photon counts were comparable between flg22 and INF1 response (Fig. 3.7.D). This indicates that the INF1-triggered ROS response differs in kinetics and amplitude from the flg22-triggered response without affecting the total amount of ROS produced.

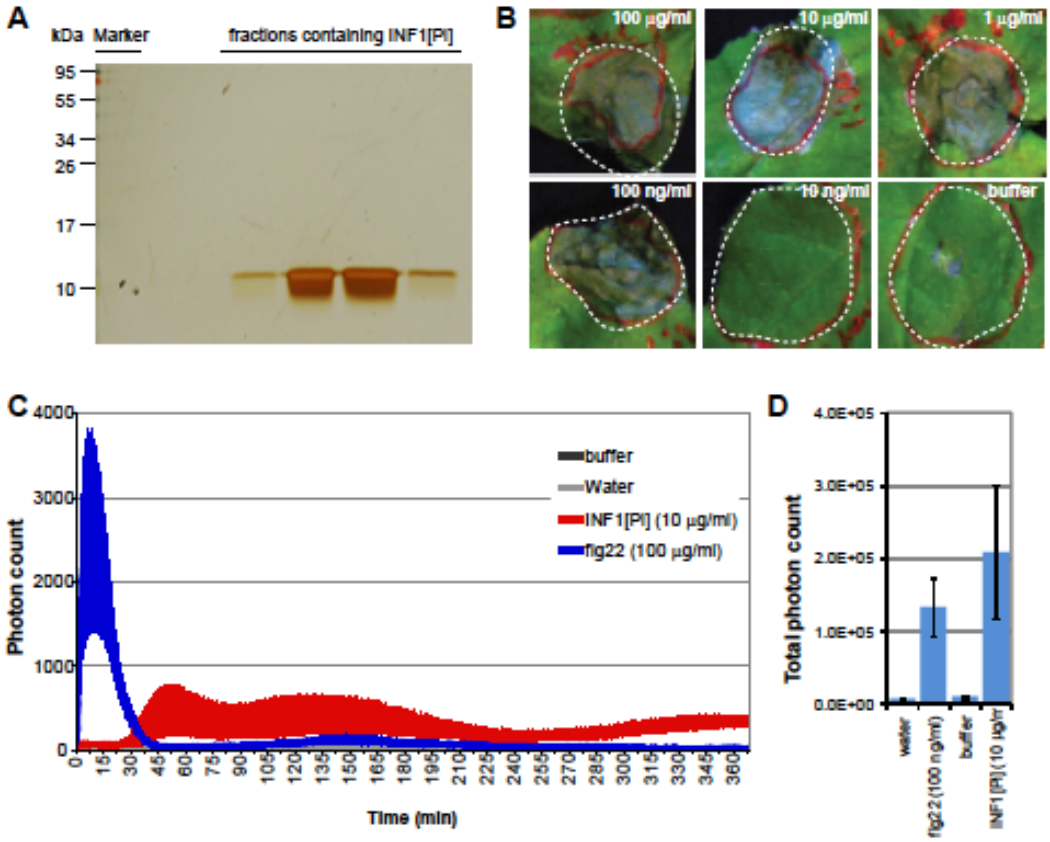

Fig. 3.7. INF1 purified from *P. infestans* triggers cell death and a delayed ROS burst in *N. benthamiana*

INF1[Pi] was purified from *P. infestans* 88069 culture supernatant and fractions loaded on a silver stained gel to confirm absence of contaminating proteins (A). Cell death inducing activity in *N. benthamiana* was tested by infiltration of stepwise diluted INF1[Pi] protein solution or buffer into the plant apoplast and pictures were taken 6 dpi (B). Incubation of leaf discs in INF1 or flg22-containing buffer triggered accumulation of ROS, measured in a peroxidase assay as emitted photons. Accumulation of ROS is shown over time (C) or as total count (D).

3.2.6. Cell death triggered by INF1 protein purified from *P. infestans* requires NbSERK3

To address whether NbSerk3 variants are required for INF1[Pi]-triggered responses, we silenced *NbSerk3A*/*B* using VIGS. Plants were either infected with TRV::*GFP* (negative control) or TRV::*NbSerk3*. Nineteen days later, leaves were infiltrated with *A. tumefaciens* harbouring *INF1*-expressing T-DNA constructs, or with purified INF1[Pi]. We observed a cell death response with *in planta* expressed INF1 and 10 µg/ml INF1[Pi] in control plants. Interestingly, plants silenced for *NbSerk3*A and *NbSerk3B* showed a significantly reduced cell death response to *35S-INF1* and injected INF1[Pi] (Fig. 3.8.). We conclude that *NbSerk3A* and *NbSerk3B* are required for cell death triggered by the secreted protein INF1 from *P. infestans*.

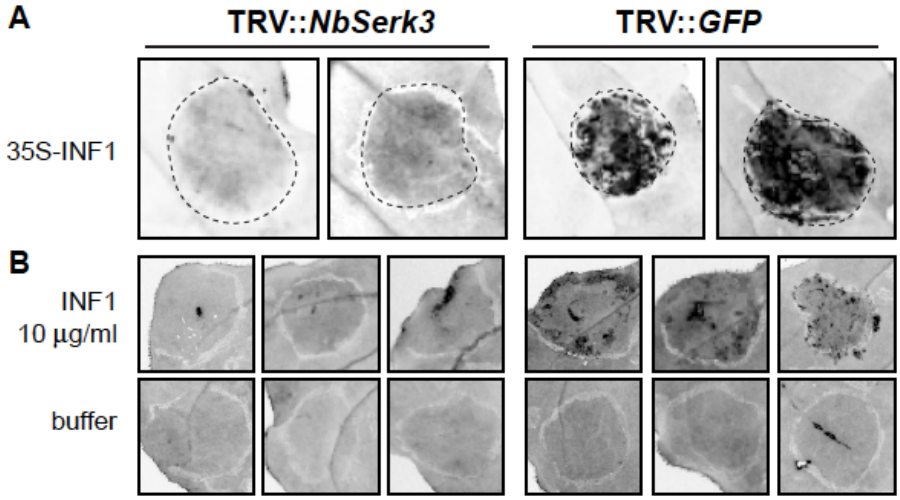

Fig. 3.8. Cell death triggered by INF1 in *N. benthamiana* requires NbSERK3 variants
Leaves of *NbSerk3* or control silenced plants were infiltrated with *A. tumefaciens* harbouring 35S-INF1 for transient *in planta* expression (A) or with *P. infestans* purified INF1 (B). Phenotypes were scored 6 dpi by visualizing cell death (dark areas) using UV trans-illumination.

3.2.7. INF1 purified from *P. infestans* does not activate early defense responses in *Arabidopsis thaliana*

To determine conclusively whether there is a response to INF1 in *Arabidopsis thaliana*, five-week-old *Arabidopsis* Col-0 plants were tested for their early defense responses to different batches of purified INF1 from *P. infestans* 88069. I measured the accumulation of reactive oxygen species upon elicitor treatment. Leaf-discs from either *A. thaliana* or *N. benthamiana* were collected and floated overnight in water. Then the water was replaced by a solution containing either flg22 (100 nM) or INF1[Pi] (10 µg/ml) and luminescence was measured over time. As a control, ROS accumulation was also followed upon flg22 treatment. For both plant species, flg22-elicited ROS

started within 10 minutes of elicitation peaking around 12 minutes for *A. thaliana* and 30 minutes for *N. benthamiana* (Fig. 3.9.A). It was evident that *N. benthamiana* displays higher amplitude in ROS accumulation upon flg22 treatment compared to *A. thaliana*. The difference might be attributable to intrinsic physiological properties of the system. Another explanation could be that the affinity of the homolog of AtFLS2 in *N. benthamiana* is higher to flg22 and perhaps nonreversible as it is the case for the homolog in *S. lycopersicum* (Mueller et al., 2012) hence amplifying the signal over time.

Then ROS production after INF1[Pi] elicitation was measured. Luminescence reflecting the ROS burst was detected over a relatively long period of time in *N. benthamiana* peaking around 7 hours post elicitation (Fig. 3.9.B, blue) but ROS production was not detected in *A. thaliana* (Fig. 3.9.B, green). Two different batches of INF1[Pi] stored in water were tested in both plant species to ensure that lack of response was not due to faulty purified protein. Although previous batches of INF1[Pi] showed faster kinetics of ROS production (Fig. 3.7.C), the two new batches still triggered ROS and cell death (data not shown) in *N. benthamiana*. Differences in kinetics between INF1[Pi] batches are most likely the result of the different buffers in which the purified protein was stored. Although I confirmed that the buffer does not elicit any defense response (data not shown), it is possible that INF1 protein is more stable in buffer than in water hence the protein would be more active leading to a faster response.

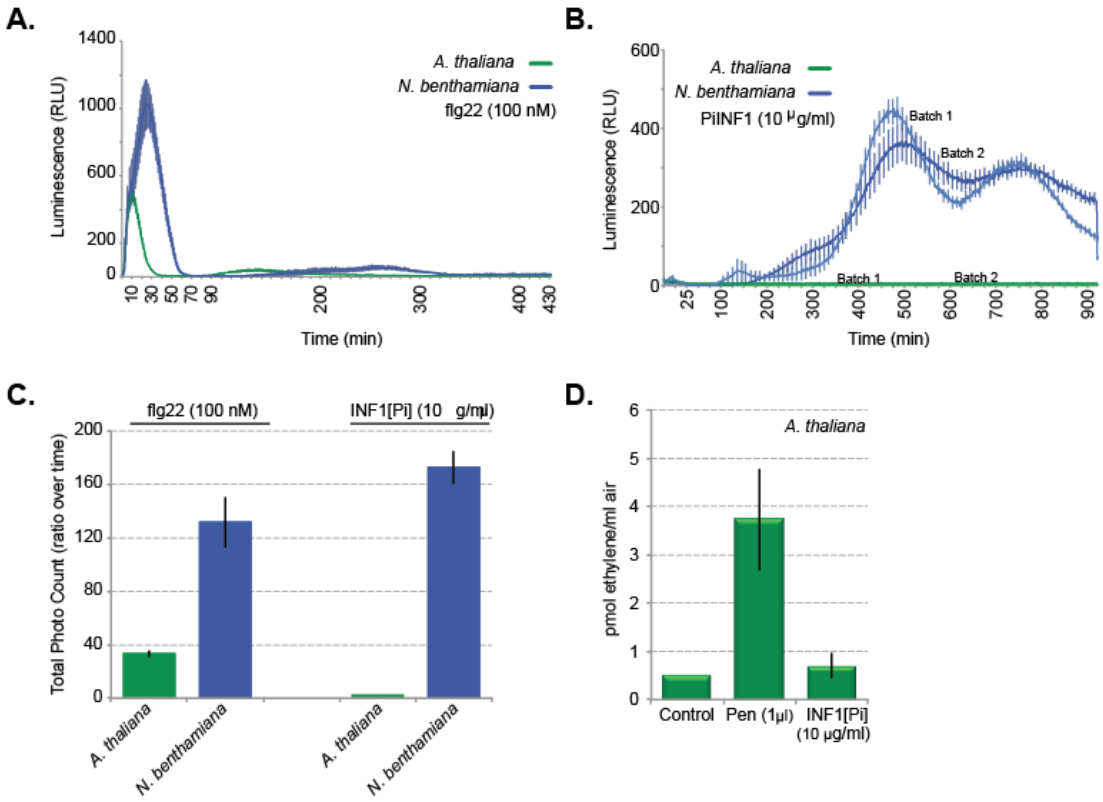

Fig. 3.9. INF1 purified from *P. infestans* does not activate early defense responses in *Arabidopsis thaliana*

Leaf-discs of *Arabidopsis thaliana* (green) or *Nicotiana benthamiana* (blue) were incubated with either (A) flg22 (100 nM) or (B) INF1[Pi] (10 µg/ml) and the accumulation of ROS was measured over time as emitted photons. The total photo count for flg22 or INF1[Pi] ROS in *A. thaliana* and *N. benthamiana* was calculated as the ratio of emitted photons over the total time (C). Ethylene production measured by gas chromatography after elicitation with Pen or INF1[Pi] in leaf discs of *A. thaliana* is showed in (D). The experiment depicted in (D) was done in collaboration with the laboratory of Professor Georg Felix.

Given that the same batch of plants and experimental conditions were used for testing flg22, lack of INF1[Pi] response in *A. thaliana* is likely due to absence of required genetic elements. Additional evidence for this hypothesis comes from another set of experiments in which either *A. thaliana* leaf discs were tested for ethylene production (induction of C_2H_4) or *A. thaliana* cell cultures were used to monitor changes in the growth medium pH due to ion fluxes across the membrane using the same purified INF1[Pi] used for the ROS assays. An extract from the mycelium of *Penicillium chrysogenum* refered here as "Pen" was used as a positive control since it elicits early defense responses in Arabidopsis (Thuerig et al., 2006). In those experiments, no induction of either C_2H_4 (Fig. 3.9.D) or medium alkalinization was observed upon INF1[Pi] treatment in Arabidopsis whereas tobacco cell cultures did show good alkalinization response (Georg Felix, personal communication). In summary, INF1[Pi] triggers strong defense responses in *N. benthamiana* but not *A. thaliana*, making *N.*

benthamiana a suitable plant model for studying downstream signaling upon INF1 recognition.

3.3. Discussion

In this study we show that different species of *Phytophthora* have varying degrees of virulence on *N. benthamiana* ranging from incompatible to moderate virulence to full virulence. Three of the tested species, *P. infestans*, *P. palmivora*, and *P. capsici*, can colonize *N. benthamiana*, while a fourth species *P. mirabilis* was avirulent. This suggests that this model plant can be used to study a wide range of *Phytophthora*-host interactions. We further characterized the moderate virulence of *P. infestans* by testing the hypothesis that PTI is implicated. To this purpose, we identified two *NbSerk3* genes from *N. benthamiana* that are similar to the key regulator of surface immune receptors BAK1 of Arabidopsis. *NbSerk3* silencing in *N. benthamiana* resulted in markedly enhanced susceptibility to *P. infestans* but did not alter resistance to *P. mirabilis*. Silencing of *NbSerk3* also reduced the cell death response triggered by INF1 protein purified from *P. infestans*. We conclude that *N. benthamiana* exhibits an effective basal resistance against *P. infestans*, probably via recognition of the INF1 protein, resulting in a relatively moderate degree of compatibility. Overall, these results further confirm the general importance of PTI in plant-pathogen interactions and suggest that the concepts developed for bacterial pathogens can be extended to oomycetes (Dodds and Rathjen, 2010).

There are seemingly conflicting reports in the literature on the extent to which *N. benthamiana* is susceptible to *P. infestans*. An early report by Kamoun (1997a) concluded that *P. infestans* is avirulent on *N. benthamiana*, and that resistance is partially due to recognition of the elicitin protein INF1. However, the authors noted the occurrence of secondary hyphae and haustoria on *N. benthamiana* although they were limited to the initial infection zone (Kamoun et al., 1997a). Later reports, including field and greenhouse trials with *N. benthamiana*, concluded that this plant is susceptible to several *P. infestans* isolates and that compatible interactions can be established (Kamoun, 2001; Becktell et al., 2006; Asai et al., 2008). More recently, Shibata and colleagues (2010) confirmed that *N. benthamiana* is susceptible but that the age of the host plant affects the ability of *P. infestans* to infect. In this study, we confirmed that *P. infestans* can establish spreading infections on *N. benthamiana* that are not limited to the initial inoculation site (Fig. 3.1. and 3.4.). We conclude that many *P. infestans* isolates, including 88069, can colonize *N. benthamiana*. However, *P. infestans* shows clearly reduced levels of virulence relative to *P. palmivora* and *P. capsici*.

We found that the aggressiveness of *P. infestans* was dramatically enhanced upon silencing of *NbSerk3* in *N. benthamiana* (Fig. 3.4.), suggesting that variation in

virulence between isolates of *P. infestans* may depend on suppression of NbSERK3-mediated immunity, possibly by host translocated RXLR effectors such as AVR3a, PEXRD8, and PEXRD36 which were shown to suppress INF1-triggered cell death (Bos et al., 2006; Oh et al., 2009). Conversely, NbSERK3-mediated immunity is not required for the effective resistance of *N. benthamiana* to *P. mirabilis* (Fig. 3.6.). This NbSERK3-independent resistance could be due to the recognition by *N. benthamiana* of specific effector proteins by host disease resistance proteins. Indeed, Wei et al. (2007)showed that recognition of a single effector protein, HopQ1-1, was sufficient to define host-specificity in the interaction between *P. syringae* DC3000 and *N. benthamiana* (Wei et al., 2007).

How does *P. infestans* suppress immunity to successfully colonize *N. benthamiana*? Most likely this involves host-translocated effectors, such as members of the RXLR family (Schornack et al., 2009b; Tyler, 2009). For instance, the RXLR effector AVR3a targets the E3 ubiquitin ligase CMPG1 to suppress defence during the biotrophic stage of the late blight disease (Bos et al., 2010). CMPG1 is a component of membrane receptor-mediated immunity to several pathogens (Gonzalez-Lamothe et al., 2006; Heese et al., 2007; Bos et al., 2010). Interestingly, both NbSERK3 (Fig. 3.8.) and CMPG1 are required for responses to INF1, when this protein is delivered by infiltration into the apoplast of *N. benthamiana* (Gonzalez-Lamothe et al., 2006; Heese et al., 2007). In the future, identification of a membrane receptor for INF1 and unravelling its interplay with the genetic elements *CMPG1*, *NbSerk3A* and *NbSerk3B* will help in understanding how *P. infestans* suppresses surface immunity and whether these elements are targeted by dedicated *P. infestans* effectors.

We discovered that *N. benthamiana* carries two *NbSerk3* variants unlike Arabidopsis, which only harbours a single *BAK1/SERK3* gene. Most likely, this can be attributed to the allopolyploidic nature of *N. benthamiana* (Goodin et al., 2008). It remains to be determined whether both *NbSerk3* homologs contribute to the same extent to basal resistance to *P. infestans*. The two *NbSerk3* genes are too similar to enable specific silencing of individual copies and in our experiments transcript level reduction was observed for both *NbSerk3* variants (Fig. 3.3.). Interestingly, we also identified two sequences similar to *BAK1/SERK3* in the recently sequenced genome of tomato while only one copy was detected in the genome of wild potato *Solanum phureja* (see Material and Methods Chapter 2). It remains to be determined whether the copy number variation of the *Serk3* genes in solanacaeous plants is biologically relevant. However, knockdown experiments suggest that the SERK3 proteins are important elements of surface immunity in the Solanaceae (Heese et al., 2007; Fradin et al., 2009; Bar et al., 2010).

Differences between the NbSERK3 variants almost exclusively reside in the extra cytoplasmic domains (Fig. 3.2.). By analogy with BAK1, NbSERK3 hetero-oligomerization with other RLKs might not require its kinase activity and downstream signalling is probably mediated by the trans-interacting partner RLK (Chinchilla et al., 2009; Kim and Wang, 2010; Schwessinger et al., 2011). Less is known about the role of the extra cytoplasmic domains of BAK1/SERK3 in interaction with the ligand-binding RLK or signalling. Mutations of Arabidopsis BAK1 LZ domain residues L32E and L46E, which are conserved in the NbSERK3 variants, affects heteromerization with BRI1 in yeast two-hybrid assays but alterations in the subcellular localisation or stability of the mutant BAK1 were not addressed (Yun et al., 2009; Kim and Wang, 2010). However, recent reports show that the extra cytopasmic domain of BAK1/SERK3 also plays a crucial role in heterodimerization probably by bringing together the receptor and coreceptor pair in perfect spatial orientation for further activation and signaling (Jaillais et al., 2011). Hence differences in the N-terminal region can still determine specificity and perhaps amplitude of the response.

Further comparison of the NbSERK3 proteins to Arabidopsis BAK1 revealed significant divergence within the signal peptide, the proline/serine-rich hinge region and the non-kinase C-terminus (Fig. 3.2.). Remarkably, the region between the transmembrane and kinase domains, which is often highly variable in LRR-RLKs, is conserved between all three proteins with only one conservative lysine/arginine substitution. By analogy with the mammalian receptor EGFR, this juxta-membrane region may contribute to heteromerization with other RLKs (Ubersax and Ferrell, 2007). Inspection of known BAK1/SERK3 phosphorylated residues (Kim and Wang, 2010) showed that both activating and suppressor phosphorylation sites are conserved between BAK1 and NbSERK3. A threonine to serine exchange at position 312 (based on BAK1 sequence) should not affect the phosphorylation of this residue. The extent to which other identified polymorphisms affect the activities of SERK3 remains to be addressed. Such analyses could include the effect on downstream signalling or interactions with *Nicotiana*-specific RLKs or RLPs. BAK1/NbSERK3 chimeric constructs might help to dissect the contribution of specific domains as performed previously with FLS2, EFR and the wall-associated kinase WAK1 (He et al., 2000; Albert et al., 2010; Brutus et al., 2010).

Similar to previous reports, this study confirms the role of SERK3 in INF1-mediated cell death and production of reactive oxygen species when using *P. infestans* produced INF1 protein (Fig. 3.7.C). Interestingly, the amplitude and kinetics of the response was very different from the flg22-induced response, pointing to intrinsic characteristics at the detection or signaling level. Whether a more sustained response is biologically relevant for full signaling remains unknown. A different response is also seen when

comparing the flg22-ROS between *N. benthamiana* and Arabidopsis (Fig 3.9.A). This probably reflects essential differences within each species FLS2 receptors extracellular ligand-binding region (Mueller et al., 2012).

Even though *P. infestans* does not infect *A. thaliana*, there was the need to address whether INF1 is capable of eliciting any defense response in Arabidopsis. In such case, we would be able to explore this system to identify the membrane bound-receptor that mediates INF1 recognition. However, several experiments lead me to conclude that INF1[Pi] does not trigger immune responses in Arabidopsis (Fig. 3.9.). Most likely, the receptor or even other signaling components are missing in this plant species, which clearly lacks the selective pressure to have immune components towards recognition of *P. infestans* proteins. In this line of thought, it makes sense that INF1[Pi] triggers strong defense responses in *N. benthamiana* probably reflecting the fact *P. infestans* evolved to infect members of the Solanaceae.

In summary, the availability of the NbSERK3 proteins enables additional structure/function studies of this important immune regulator and may also lead to the identification of additional PAMP receptors recognizing oomycete pathogens. This work also points to the importance of identifying immune elements from plant species that are relevant for the pathogen under study knowing that the final outcome of the immune response requires the proper synchronization of multiple plant components. The fact that some elicitors are widely recognized across kingdoms while others are more specific, suggests that plants have evolved a specific set of receptors to secure the recognition of more specialized pathogens. Once perception is accomplished similar signal transduction cascades seem to occur.

3.4. Conclusion

We demonstrated that *N. benthamiana* NbSERK3 contributes to resistance to *P. infestans* and regulates the immune responses triggered by the *P. infestans* PAMP protein INF1. In the future, the identification of novel surface receptors that associate with NbSERK3A and/or NbSERK3B should lead to the identification of new receptors that mediate recognition of oomycete PAMPs, such as INF1.

CHAPTER 4: Characterization of a receptor-like protein (RLP) from *Solanum microdontum* that mediates the response to *P. infestans* elicitin INF1

4.1. Introduction

The perception of external signals is crucial for plants to sense possible pathogen threats. Since plants do not have an adaptive immune system like mammals, each cell must achieve interaction with its extracellular environment and does so through an array of cell surface receptors known as Pattern Recognition Receptors (PRRs). PRRs recognize conserved molecules from microbes or potential pathogens known as microbe-associated molecular patterns (MAMPs) or pathogen-associated molecular patterns (PAMPs). Examples of such molecules include bacterial flagellin, the fungal cell-wall component chitin, and quorum sensing signals (Boller and Felix, 2009). Receptors interpret the extracellular signals into intracellular responses leading to a form of defense called PAMP- triggered immunity (PTI).

Plant-PRRs, which are membrane-bound, fall in two major groups. The first group harbors the receptor-like kinases (RLKs) that consist of an eLRR, a transmembrane domain (TM) and a non-RD kinase domain (Schwessinger and Ronald, 2012). In *Arabidopsis thaliana* well-characterized members of this group are flagellin sensing 2 (FLS2) and EF-Tu Receptor (EFR) that specifically recognize peptides derived from bacterial flagellin and elongation factor Tu respectively (Gomez-Gomez and Boller, 2000; Chinchilla et al., 2006; Zipfel et al., 2006). The second group comprises the receptor-like proteins (RLP), which have an eLRR, a TM domain and a short cytoplasmic tail (Wang et al., 2008). One characteristic of most PRRs is their extracellular leucine-rich repeats (eLRRs) that are involved in protein-protein interaction and are thought to mediate complex formation upon ligand binding (Jaillais et al., 2011).

RLPs important for mediating disease resistance include the tomato Cf-9, Cf-4 and Ve1/2 proteins, which mediate defense signaling against the fungi *Cladosporium fulvum* and *Verticullium* spp., respectively (Wang et al., 2010). In addition, the tomato genes *LeEIX* encode RLPs that recognize the ethylene-inducible xylanase to trigger plant defense responses (Ron and Avni, 2004). Although these RLPs have different numbers of eLRRs, in general they share the same domain organization: domain A at the N-terminus, harbors the signal peptide (SP); domain B containing several cysteines; domain C consists of the LRRs and a loop; domain D with no obvious characteristics; domain E is the acidic domain; domain F is the transmembrane

domain; and domain G, which is very basic and corresponds to the short cytoplasmic tail (Jones et al., 1994; Kawchuk et al., 2001; Ron and Avni, 2004). Interestingly, these membrane-bound proteins all harbor an endocytosis signal Yxxϕ (where Y stands for the tyrosine residue, x for any amino acid residue, and ϕ for any bulky hydrophobic residue) in domain G, although its relevance in defense responses has only been shown for LeEIX (Ron and Avni, 2004; Bar and Avni, 2009). In Arabidopsis well-studied RLPs have been mostly implicated in organ and stomata development and only few have been demonstrated to have a role in plant defense (Wang et al., 2010).

Phytophthora species secrete small 10 kDa proteins that are termed elicitins. These molecules are highly conserved (Kamoun et al., 1997a) and induce cell death in a genus specific manner (Kamoun et al., 1994). The *P. infestans* protein INF1 is a cysteine-rich elicitin thought initially to be an avirulence factor (Kamoun et al., 1998a) in the *N. benthamiana – P. infestans* interaction as *Nicotiana* plants that recognize INF1 are also resistant to *P. infestans*. However, in some species of *Solanum* INF1 triggers cell death but this recognition is not correlated with resistance to *P. infestans* (Vleeshouwers et al., 2006). More recently, INF1 has emerged as a typical PAMP as it is widely conserved in *Phytophthora* and *Pythium*, and triggers defense responses that require the immune regulator of PTI SERK3/BAK1 (Heese et al., 2007) (see also chapter 3) and *P. infestans* effectors suppress its activity (Bos et al., 2006). The identification of high-affinity binding sites for cryptogein, an elicitin from *P. cryptogea*, to the plasma membrane of tobacco leaves (Wendehenne et al., 1995), suggest that elicitins are presumably recognized by membrane-bound receptors. Additionally, INF1 triggers a similar set of responses that are common for canonical BAK1-dependent PAMPs such as flagellin or EF-Tu, (Heese et al., 2007; Chaparro-Garcia et al., 2011). Based on these factors a plausible hypothesis is that INF1 is perceived by plasma membrane resident PRR receptors.

This chapter describes the subcellular distribution of a novel RLP implicated in INF1-mediated cell death termed ELR1 and its association with the co-regulator SERK3. I show that ELR1 localizes to the plasma membrane (PM) and the endoplasmic reticulum (ER) and demonstrate that the addition of C-terminal tags on ELR1 impairs its ability to complement INF1 cell death in a heterologous plant system whereas a tag at the N-terminal region has a weaker impact on this phenotype. In addition, this work reveals that the PTI co-regulatory receptor SERK3 constitutively heterodimerizes with ELR1 in vivo and that this complex is enhanced upon elicitor treatment. These findings cast light on the molecular events following INF1 perception and will further our understanding of the contribution of RLPs to innate immunity.

4.2. Results

4.2.1. The INF1 candidate receptor ELR1 is a Receptor like protein (RLP) that localizes to the endoplasmic reticulum (ER) and the plasma membrane (PM)

Verzaux and colleagues (2010) cloned a candidate INF1 receptor by conventional map-based cloning from the INF1 responding *Solanum microdontum* (Vleeshouwers et al., 2006). We have established collaboration with the group of Dr. Vivianne Vleeshouwers (Wageningen UR Plant Breeding, Wageningen, The Netherlands) on the characterization of this putative receptor called ELR1 herein. Based on sequence similarity, ELR1 belongs to the receptor like protein (RLP) class of membrane-bound receptors with extracytoplasmic highly glycosylated LRR domains. ELR1 has 43% identity with the tomato RLP Cf-9 and 35% with Cf-2 and shares a similar domain structure: it has 36 imperfect eLRRs, a transmembrane domain flanked by an acidic region on the extracytoplasmic side and a basic region towards the cytoplasmic side. The LRR motif is LxxLxxLxxLDLSSNNLxGxIPxx (Jones et al., 1994; Verzaux, 2010).

In order to assess ELR1 function, I generated C-terminal epitope-tagged variants of the *Solanum microdontum* ELR1. The ELR1-GFP (Fig. 4.1A) fusion protein was used for localization studies in transient expression assays in *N. benthamiana*. It is known that some RLPs can accumulate only at very early time points without triggering the post-transcriptional gene silencing (PTGS) machinery (Van Der Hoorn et al., 2003). ELR1-GFP was visible at one-day post infiltration (DPI) using confocal fluorescence microscopy but was not detectable by western blot analysis (data not shown). Starting at two DPI until four DPI, ELR1-GFP protein did not accumulate at detectable levels (Fig. 4.1C). However, this tendency, low detection/expression levels under constitutive expression control has been reported for other RLPs such as Cf-9 and Cf-4 (Rivas et al., 2002b; Rivas et al., 2002a; Voinnet et al., 2003). To assess the influence of PTGS on levels of ELR1-GFP, I co-expressed it with p19, a known inhibitor of PTGS (Voinnet et al., 2003). A time course experiment revealed that the protein accumulation and localization of ELR1-GFP changed over time (Fig. 4.1B). ELR1-GFP localized at the periphery of the cell but was predominantly associated with the endoplasmic reticulum (ER) at all time points (Fig. 4.1B). Western blots showed protein accumulation of ELR1-GFP only when expressed with p19, suggesting that its levels are post-transcriptionally regulated probably to prevent inadvertent signaling (Fig. 4.1 C).

FLS2-GFP (Arabidopsis) was used as a control and given that FLS2 seemed to be present at the ER as well after 3 DPI (Fig. 4.1B), I tested whether the detected occurrence of ELR1 in the ER was due to the enhancement of expression and might be attributed to experimental reasons. Therefore, I co-expressed ELR1-GFP with a red

fluorescent chromobody protein (CB) that binds, labels and stabilizes GFP protein complexes (Schornack et al., 2009a) at two DPI, which was the day that showed a more pronounced ER accumulation (Fig. 4.1B). ELR1 accumulated mainly at the cell periphery and was rarely seen at the ER (Fig. 4.1D). FLS2-GFP was only seen at the PM (Fig. 4.1D). These dissimilar results might reflect that ELR1-GFP enhanced expression leads to more ELR1 in the secretory system/ER as a byproduct of PTGS interference by p19. Alternately the chromobody might stabilize the levels of ELR1-GFP post-transcriptionally by sequestering it into an antibody complex at the PM. If there is an ER fraction of ELR1-GFP it could not be seen with the chromobody (CB) since the CB is unable to enter the ER (Schornack et al., 2009a).

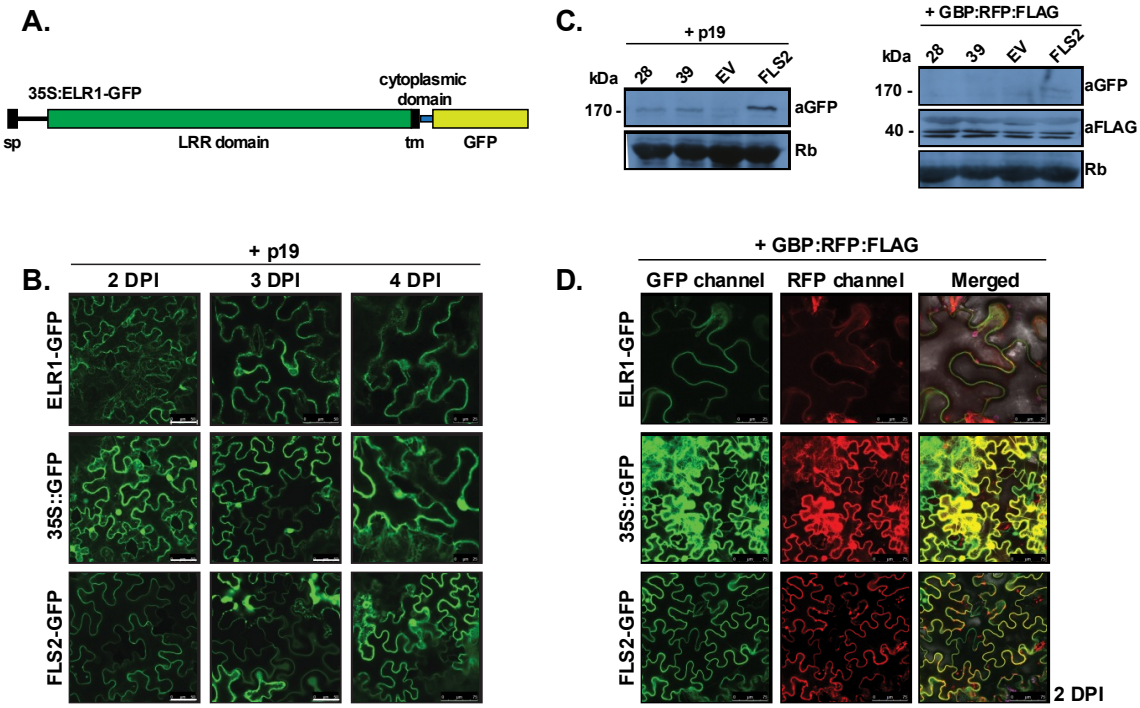

Fig. 4.1. The INF1 candidate receptor ELR1 is a Receptor like protein (RLP) that localizes to the endoplasmic reticulum (ER) and the plasma membrane (PM)

(A) Schematic representation of ELR1 fused to GFP at the C-terminus, (sp signal peptide, tm transmembrane domain). (B) *A. tumefaciens*-mediated expression of pK7FWG2:ELR1-GFP, pK7FGW2:FLS2-GFP or 35S:GFP plus p19 at two, three, and four days post infiltration (DPI) in *N. benthamiana*. Fusion proteins revealed peripheral and ER localization. The control fusion protein FLS2-GFP localization is mainly at the plasma membrane, although at later time points it was also present at the ER most likely due to enhanced over expression with p19. (C) Western blots showing protein accumulation of all constructs used in (B) and (D) at 2 DPI. Only in the presence of p19 detectable levels of protein were observed. Two identical clones of ELR1-GFP labelled 28 and 39 are shown. The red fluorescent chromobody (CB) expression corresponding to panel (D) is shown in the anti FLAG blot. Rb stands for rubisco to indicate protein loading. (D) ELR1-GFP, FLS2-GFP or 35S:GFP co-expressed with red fluorescent chromobody

(GBP:RFP:FLAG; see text for further details. GBP stands for Green fluorescent protein-binding protein and is also referred as chromobody (CB) in the text) showed the peripheral localization of ELR1-GFP. FLS2-GFP control was always found at the PM. Each image has the corresponding scale bar. Same confocal settings were used for each panel but differ between panels (B) and (D).

Accessions of *Nicotiana simulans* that do not respond to INF1 and that are less affected by environmental conditions were used as an independent heterologous system to test the tagged fusions of ELR1. However, as seen in *Solanum* species no complementation of the INF1 cell death response was observed (Data not shown). Overall, these results are in line with previous reports of a well-studied RLP Cf-9, which has been tagged at the C-terminus and its functionality was compromised (Piedras et al., 2000; Van Der Hoorn et al., 2003). Protein activity *in planta* is highly affected by the addition of labeling tags for biochemical studies and it often depends on the plant process under study and intrinsic characteristics of the system (Ntoukakis et al., 2011).

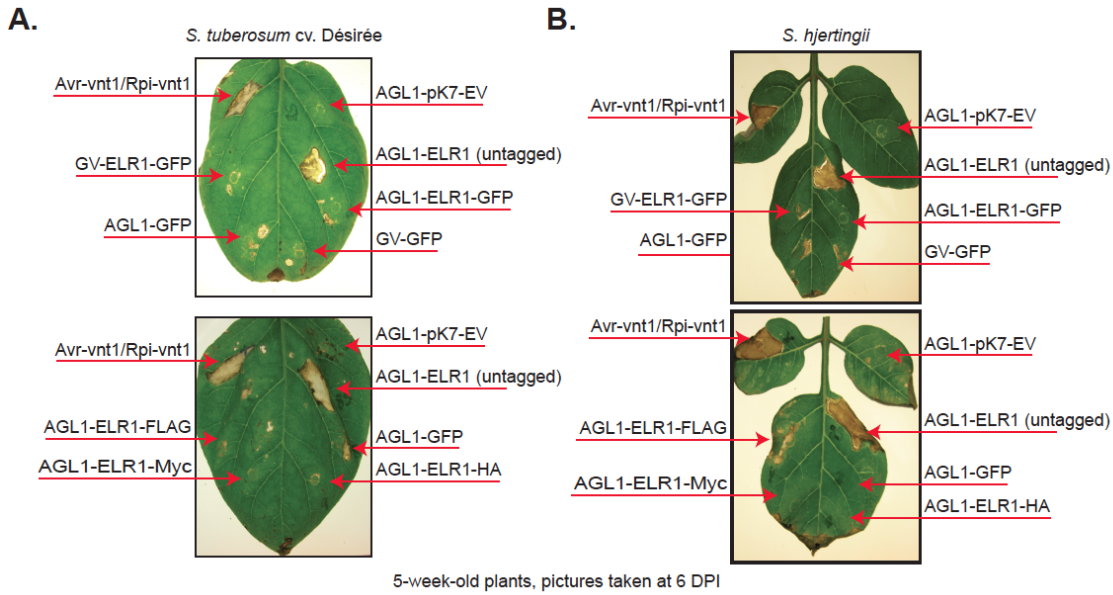

Fig. 4.2. C-terminal tags on ELR1 render the protein non-functional

Complementation assays in INF1 non-responsive *Solanum tuberosum* cv. Désirée (A) or *Solanum hjertingii* (B) showing that any C-terminal tag on ELR1 abolishes its function *in planta*. 5-week-old plants were transiently infiltrated with either *A. tumefaciens* Agl1 (AGL1) or GV3101 (GV) harbouring ELR1-C-terminal tags or untagged ELR1and co-expressed with Agl1-pK7WG2-SP-INF1 at 1:1 ratio. Cell death positive control is at the left upper side of each picture and is the transient expression of Agl1-pK7WG2-Avr-vnt1 + Agl1-pCB302-Rpi-vnt1 (1:1 ratio). ELR1

fusion proteins are in the following Gateway compatible vectors: pK7FWG2 (GFP), pGWB11 (FLAG), pGWB14 (3xHA), and pGWB17 (4xMyc). The untagged control ELR1 is in pK7WG2.

4.2.3. ELR1 N-terminal tagged localizes to the endoplasmic reticulum and plasma membrane

Given that any tested epitope tag at the C-terminus of ELR1 renders the protein non-functional, I explored a different approach to introduce a fluorescent tag between the signal peptide and the leucine-rich repeats (LRRs). A fluorescent tag is highly desirable for live-cell imaging assays and can also be used for established biochemical methods required for ELR characterization. GFP is unable to efficiently fluoresce at the low apoplastic pH and the available RFP results in low expression levels. Therefore, I chose an improved mutant of YFP, citrine, which is brighter, more stable, and less sensitive to pH fluctuation (Griesbeck et al., 2001). The latter characteristic made citrine a prime candidate to explore protein localization to more acidic subcellular compartments like the ER (Tian et al., 2004a). To generate SP-citrine-ELR1, I first PCR-amplified a pENTR clone containing ELR1 with stop codon. In parallel, citrine was amplified from a different vector with phosphorylated primers. After digestion of the parental strands, both PCR products were ligated and transformed into *E. coli* (TOP 10 competent cells). The resulting pENTR was recombined into pK7WG2 for final expression *in planta* mediated by *A. tumefaciens* GV3101 or Agl1 (for assays in *S. tuberosum* cv. Désirée).

SP-citrine-ELR1 (Cit-ELR1 herein) was transiently expressed in *N. benthamiana* with and without p19 (Fig. 4.3A). A time course experiment revealed that at one DPI ELR1-GFP expression was low and Citrine-ELR1 was not detected with or without p19 (data not shown). After two DPI Cit-ELR1 (both constructs tested #4 and #15) expression without p19 was low but detectable whereas ELR1-GFP was barely expressed (Fig. 4.3A). As expected, p19 enhanced the expression of both fluorescent versions of ELR1 (Fig. 4.3A, B). Confocal imaging (Z-stack and a close-up) revealed that Citrine-ELR1 subcellular localization was preferentially at the ER and a fraction of it at the PM (Fig. 4.3A, B- upon dehydration stress). However to conclusively demonstrate PM distribution besides ER, a set of known markers like BiP for the ER and PMA2 for PM, should be co-localized with ELR1. Alternatively, one could use the enzyme endoglycosidase H (Endo H) to resolve the amount of glycosylated protein only present in the PM (Nekrasov et al., 2009). Surprisingly, protein levels without p19 were not detectable by western blot (WB) at any time point suggesting a rapid post-transcriptional regulation of the ELR1 transcript that was circumvented with p19 (Fig. 4.3D). In addition, it seemed that ELR1-GFP tag was more stable than Cit-ELR1 or perhaps the GFP antibody reacts differently with citrine. However, both versions seem

to undergo some degree of processing and cleavage of the fluorescent tag as seen by multiple bands below the full-length expected size (ELR1-GFP is ~150 kDa theoretically and runs at 170 kDa most likely due to glycosylation events) and at the expected size for GFP (26 kDa) (Fig. A1.1.; Fig. 4.3D). Still given that different tagged-versions of ELR1 (Fig. 4.3C) localize to the ER and to a lesser extent PM it is necessary to evaluate the functionality of these new constructs. It remains to be tested whether the ER localization is important for signaling or only as part of the biogenesis of the receptor.

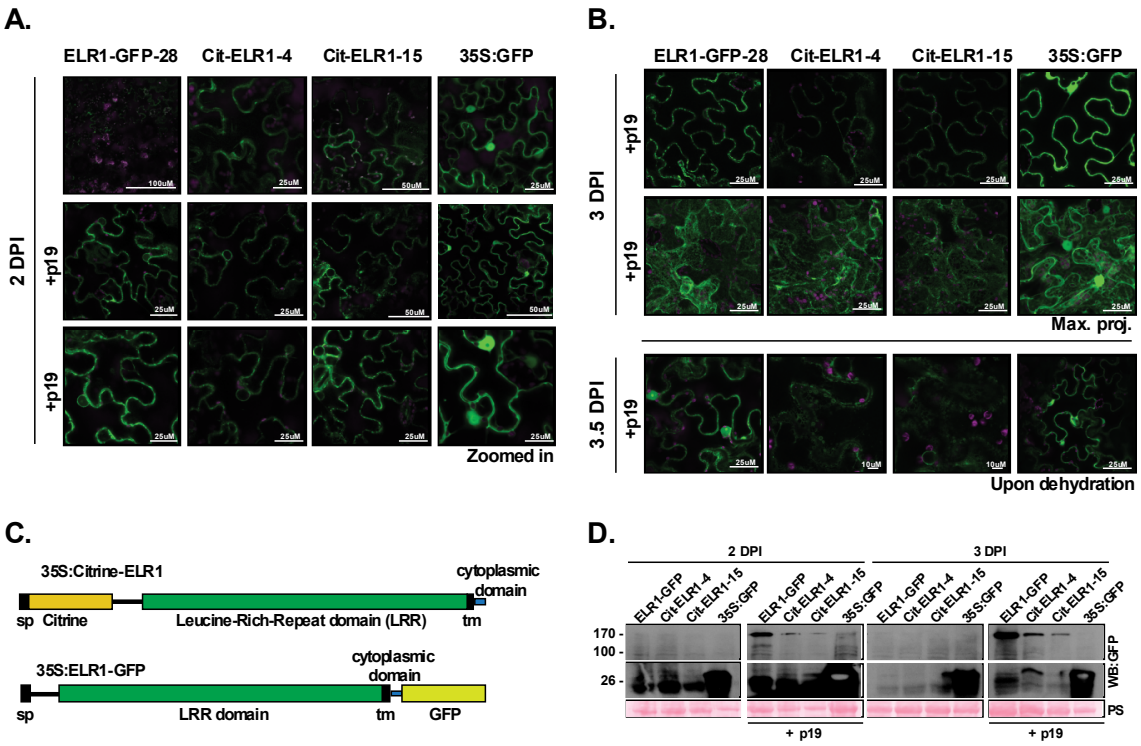

Fig. 4.3. N-terminal tagged ELR1 also localizes to the endoplasmic reticulum and plasma membrane

(A) Representative confocal images of 35S:Citrine-ELR1 or 35S:ELR1-GFP fusion proteins in *N. benthamiana* at 2 days post infiltration (DPI) with and without p19 as indicated. Bottom set of images was zoomed in 3.5 times. Expression of two fluorescent ELR1 proteins tagged at the N-terminus labelled Citr-ELR1-4 or Cit-ELR-15 showed similar subcellular distribution confirming that ELR1 mainly resides at the ER and a small fraction might reside at the plasma membrane. (B) Images taken at 3 DPI showed clear ER localization; bottom row is a maximum projection of 20-25 slices taken at 10 µm step-size. The same confocal settings were used in panel (A) and (B). Each image has the corresponding scale bar. This experiment was done twice. (C) Schematic representation of ELR1 fused to either citrine at the N-terminus or GFP at the C-terminus, (sp signal peptide, tm transmembrane domain). (D) Immuno blots showing the stability of the fusion proteins in panel (A) and (B). Tags at either side of the protein showed the same pattern of processing and cleavage, although the C-terminal tagged version accumulated to higher concentrations.

4.2.4. ELR1 constitutively associates with AtBAK1 *in planta*

BAK1 is an important regulator of membrane-bound receptors signaling and interacts with LRR containing PRRs such as FLS2 and EFR (Chinchilla et al., 2007a; Heese et al., 2007; Roux et al., 2011). Homologs of AtBAK1/SERK3 in *N. benthamiana* are required for INF1 cell death (Chaparro-Garcia et al., 2011). Therefore another aspect of ELR1 activity is its potential association with SERK3/BAK1 and the potential functional relevance of the complex. To test whether ELR1 heteromerizes with AtBAK1/SERK3, I used previously characterized immuno-tagged BAK1 constructs that are suitable for transient expression in *N. benthamiana* (Roux et al., 2011; Schwessinger et al., 2011). I first tested the C-terminal GFP epitope-tagged ELR1 (ELR1-GFP) given its higher protein stability, and coexpressed it with an HA epitope-tagged BAK1 (BAK1-HA). Ntoukakis and colleagues (2011) warned that BAK1 containing C-terminal tags were impaired in their ability to complement *bak1* null mutants responsiveness to flagellin and elongation factor EF-Tu. However, BAK1 C-terminal fusions are still capable of association with FLS2 in a ligand-dependent manner (Ntoukakis et al., 2011) and thus the use of immunotagged BAK1 in these experiments might be justified.

In the absence of p19, immunoprecipitated ELR1-GFP was below the threshold for detection by anti-GFP antibody. However, the specific Co-IP of BAK1 with samples containing ELR1 suggests that BAK1 associates with ELR1 (Fig. 4.4A). Strikingly, BAK1-HA was visible with or without treatment with INF1 (Fig. 4.4A). This suggests that heteromerization does occur and it is only dependent on the presence of the membrane-bound receptor. As reported in previous paragraphs, ELR1 protein levels tend to diminish after one DPI most likely reflecting a rapid protein turnover and the remaining protein might not be enough for detection by western blot. The fact that BAK1 is still recovered could be indicative of a strong association and/or a nonsymmetrical stoichiometry. It has been proposed that a membrane bound receptor BRI1 could form heterodimers with BAK1 in a ligand independent manner but that this complex would be inactive and that only after ligand complex induction signaling would take place by recruitment of additional heterodimers (Nam and Li, 2002). Consistent with previous reports (Chinchilla et al., 2007b; Heese et al., 2007), FLS2-BAK1 association was induced after elicitation with flg22 although a weak signal was seen in the absence of flg22 (Fig. 4.4A).

To test whether the biased accumulation of ELR1 at the ER (due to overexpression with p19 (Fig. 4.1B, Fig. 4.3A,B) had an effect on the ability of ELR1 to form a complex with BAK1, I coexpressed ELR1-GFP and BAK1-HA with p19. The association of ELR1-GFP and BAK1-HA remained the same, INF1-independent and stronger on

account of the overexpression (Fig. 4.4B). In the same manner, FLS2 and BAK1 interaction was not impaired by overexpression although a much higher constitutive association was seen (Fig. 4.4B). These results suggest that the higher expression of the receptors achieved by using p19 does not interfere with their ability to associate. Moreover, the fact that there is some constitutive association of FLS2 and BAK1 that is nonetheless enhanced upon flg22 might indicate that constitutive association might not be detrimental to initiate signaling and that elicitor-mediated recruitment of BAK1 into the FLS2 complex is still possible. However, the constitutive association might only be an artifact of over production of the involved proteins. The lack of PAMP-triggered association of ELR1 and AtBAK1 could also be attributed to limited molecular compatibility. BAK1 is an Arabidopsis protein and did not co-evolve with *Solanum* ELR1.

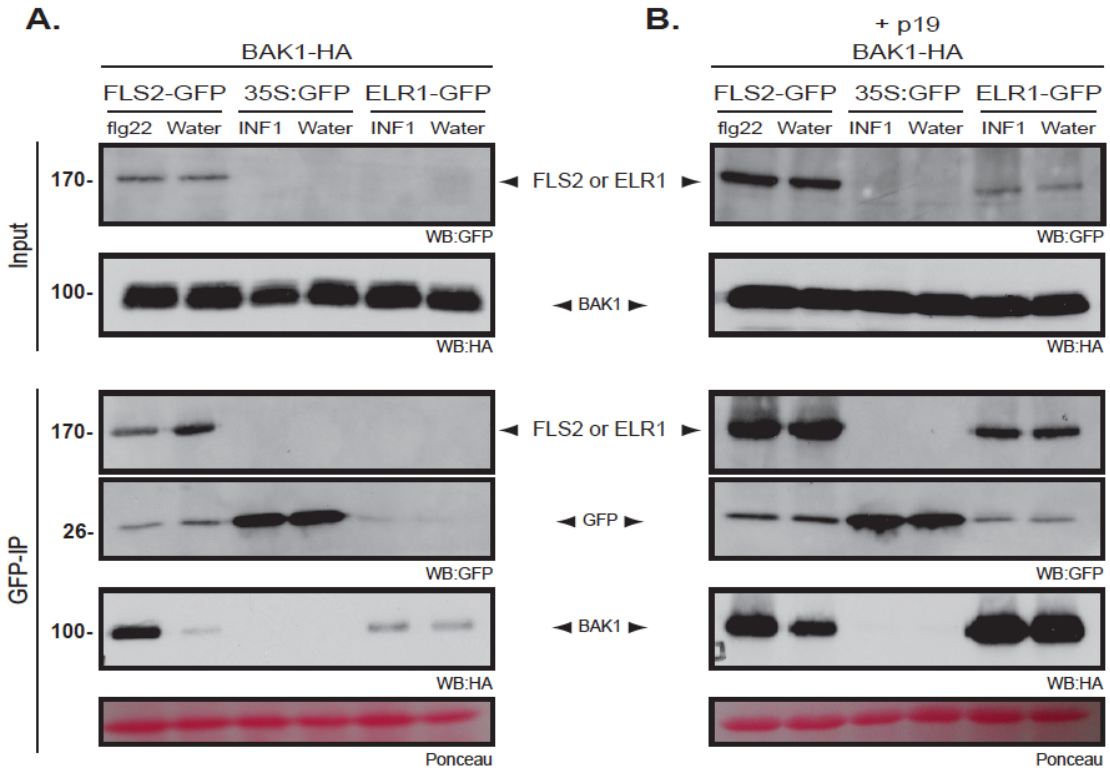

Fig. 4.4. ELR1 constitutively associates with AtBAK1 *in planta*

ELR1 co-immunoprecipitates with AtBAK1 in an INF1 independent manner. ELR1-GFP was transiently co-expressed with AtBAK1-HA in the absence (A) or presence (B) of p19 and challenged with INF1[Pi] (10 µg/ml) or water for 15 minutes. Immunoprecipitation (IP) was carried out with GFP beads and total protein extracts and IP were blotted with the appropriate antisera as indicated. As negative control AtBAK1-HA was also co-expressed with 35S:GFP and subjected to the same treatment as described above. FLS2-GFP and AtBAK1-HA treated with flg22 (100nM) or water for 15 minutes is shown on the left side of each panel as a positive control. Ponceau stain of the total extract blot indicates equal loading (bottom).

4.2.5. *Solanum tuberosum* cv. Désirée has two homologs of AtBAK1

To test the hypothesis that the constitutive association of ELR1 and SERK3/BAK1 can be enhanced upon PAMP treatment only when all components of the complex are from the same plant species, I cloned a close homolog of AtBAK1 from *S. tuberosum* cv. Désirée (Std). An initial screen of the available *Solanum* genomes data (solgenomics.net; solanaceae.plantbiology.msu.edu/index) identified a single homolog in accordance with previous reports (Chaparro-Garcia et al., 2011). Using the same conserved primers developed for NbSERK3/BAK1 (Chaparro-Garcia et al., 2011), I cloned one *StdSERK3* homolog from *S. tuberosum* cv. Désirée cDNA. Reciprocal BLAST with *StdSERK3* against the *Arabidopsis* genome identified SERK3/BAK1 as the top hit, suggesting this sequence is probably most similar to BAK1 in *S. tuberosum* cv. Désirée. The StdSERK3/BAK1 protein has the same conserved domain structure of the well-characterized AtSERK3/BAK1. Nevertheless StdSERK3/BAK1 is more similar to NbSERK3A (91%) and NbSERK3B (89%) than to AtSERK3/BAK1 (77%).

A more recent search in the latest release of the potato genome (PGSC DMv3.4) revealed an additional copy in the genome *of S. tuberosum* Group Phureja Clone DM1-3516R44. TBLASTN using AtBAK1 as query had two major hits annotated as *StSERK3A* (PGSC0003DMG40001769, Sotub10g013940) and *StSERK3B* (PGSC0003DMG400012594, Sotub01g042020). A closer inspection of the sequences showed that the one I cloned corresponds to StdSERK3A (Fig. A1.2.) so the clone was renamed accordingly. As seen in Table 4.2 StdSERK3A and StdSERK3B are very similar to AtBAK1 (84% and 83% respectively) (Fig. 4.5A). However, StdSERK3A shares the highest identity to NbSERK3A/B (95%) (Fig. 4.5B) and has the closest genetic distance to NbSERK3A/B and AtBAK1 (Fig. 4.5C). StdSERK3A and StdSERK3B differ in 59 amino acids particularly in the LRR domain and the kinase domain whereas NbSERK3A and NbSERK3B differ only in 30 amino acids (Fig. 4.5D). Notably, it is not known whether NbSERK3A/B have identical functionality. Since the majority of the polymorphisms are non-conservative amino acid changes that could potentially change the specificity and/or activity of the protein for down stream signaling. Although a reciprocal tblastn against the Arabidopsis genome using StdSERK3B also had AtBAK1 as top hit, as mentioned above, StdSERK3A has the closest homology and genetic distance to AtBAK1 and NbSERK3A/B (Fig. 4.5B,C) and hence was used for all further experiments.

Table 4.2. Similarity of *N. benthamiana* and *S. tuberosum* SERK3 to At BAK1

% Similarity	**NbSERK3A**	**NbSERK3B**	**StdSERK3A (Sotub10g013940)**	**StdSERK3B Sotub01g042020**
AtBAK1	84	83	84	83
NbSERK3A	------	98	95	88
NbSERK3B	------	------	95	88
StdSERK3A	------	------	------	88

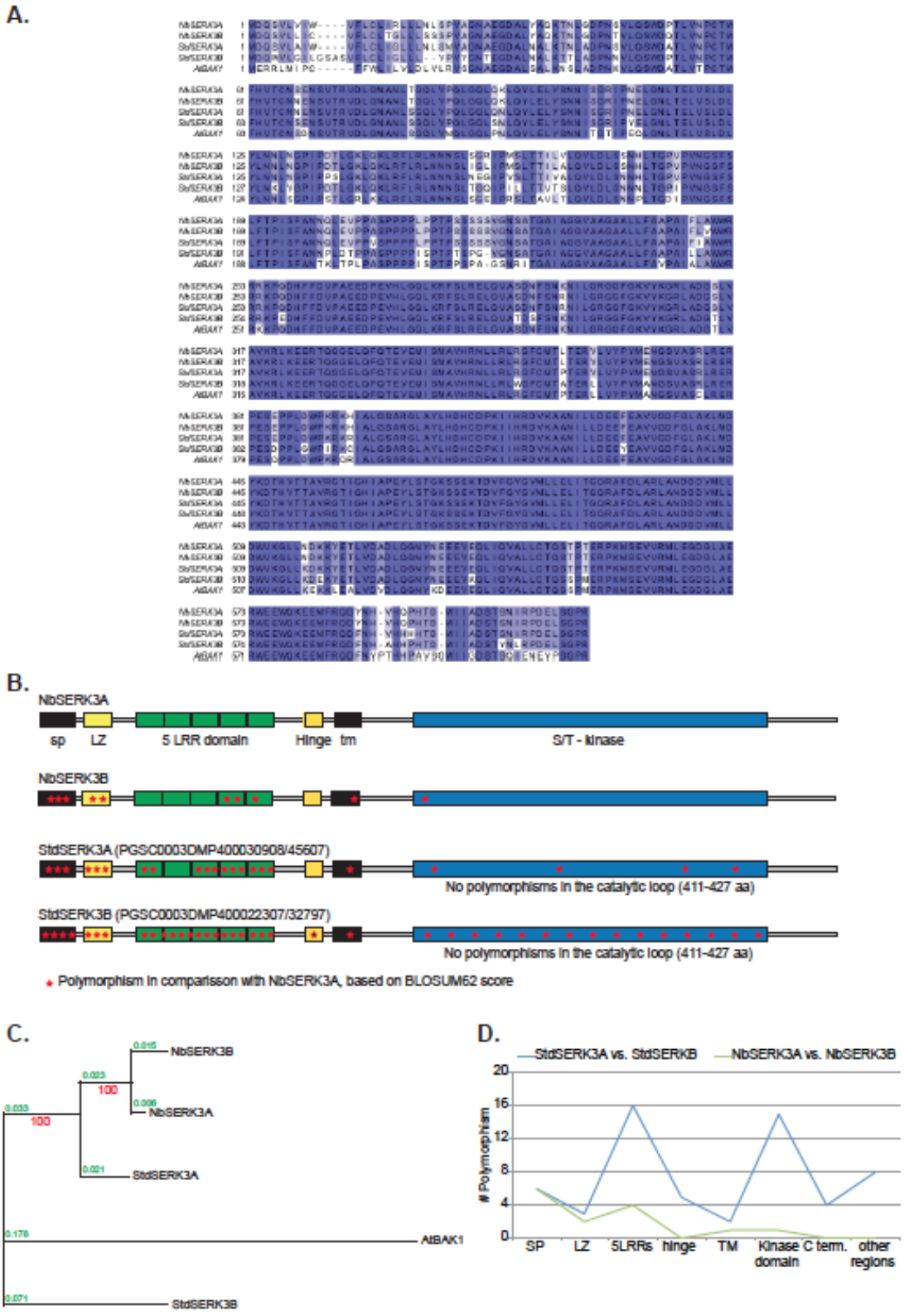

Fig. 4.5. *Solanum tuberosum* cv. Désirée has two homologs of AtBAK1

(A) ClustalW alignment showing homologs of AtBAK1 in *N. benthamiana* and *S. tuberosum* cv. Désirée. Amino acid residues are shaded dark blue if identical and a lighter shade of blue if similar. Sequences were viewed in Jalview. (B) Schematic domain representation of *N. benthamiana* (NbSERK3A, NbSERK3B) and *S. tuberosum* cv. Désirée (StdSERK3A, StdSERK3B) homologs of AtBAK1; red stars indicate amino acid polymorphism of each

sequence compared to NbSERK3A. (C) Phylogenetic tree of SERK3 sequences from Arabidopsis, *N. benthamiana* and *S. tuberosum* cv. Désirée. The unrooted tree was constructed using maximum likelihood method (PhyML at Phylogeny.fr, Dereeper et al., 2008) with full-length amino acid sequences. Branch length (green values) represents the estimated genetic distance. Bootstrap (100) support values are in red. (D) Paralogs of SERK3 in *S. tuberosum* cv. Désirée show a higher ratio of polymorphism across all domains compared to paralogs in *N. benthamiana*.

4.2.6. StdSERK3A localizes to the plasma membrane and its constitutive association with ELR1 is enhanced upon INF1 treatment *in planta*

CITRINE-ELR and ELR-GFP both were predominantly detected in the ER. However, they associate with PM localized AtBAK1. To determine whether StdSERK3A is like AtBAK1 (PM-localized) or has additional ER localization, transient expression of a C-terminal tag GFP fusion of StdSERK3A under the 35S (CaMV) promoter in *N. benthamiana* was performed. Localization of the fusion protein was followed over time using confocal laser scanning microscopy. Figure 6A shows representative images of StdSERK3A-GFP, AtBAK1-YFP and 35S:GFP at 2.5 DPI. StdSERK3A-GFP localizes at the plasma membrane and the tonoplast indicated by the smooth fluorescence surrounding the nucleus (Fig. 4.6A close-up, white arrows). AtBAK1-YFP expression was low and intensification of the excitation laser intensity was necessary, which lead to bleed-through of plastid auto-fluorescence in the YFP channel (Fig. 4.6A) however it is clear that AtBAK1 localizes to the membrane as previously reported (Russinova et al., 2004). In addition, both constructs showed a degree of cell death (data not shown) starting at 3.5 DPI, which led to perform subsequent experiments at 3 DPI.

To check whether StdSERK3A localization at the PM *in planta* is predictive of heteromerization with FLS2, I tested StdSERK3A for heteromerization with FLS2 upon flg22 elicitation (Fig. A1.4). Using co-immunoprecipitation experiments, I showed that after co-expression of FLS2-GFP and AtBAK1-HA or StdSERK3A-HA (without p19), FLS2 is also able to form a complex with StdSERK3A upon flg22 treatment after 15 minutes of elicitation. Although the amount of StdSERK3A protein was lower than that of AtBAK1 after the GFP-IP, this does not necessarily indicate that FLS2 has a higher affinity for AtBAK1 since the starting protein amounts of StdSERK3A were much lower than that of AtBAK1 in all replicates of the experiment (3 times). This seems counterintuitive, as every time I did microscopy it appeared that AtBAK1 expression was always lower compared to StdSERK3A. However in some cases, microscopy impressions about protein levels do not match what it is found by biochemical methods.

Next ELR1-StdSERK3A association was assessed *in planta* by co-immunoprecipitation. Transient *Agrobacterium*–mediated expression of ELR1-GFP

and StdSERK3A-HA in the absence of p19 showed that the protein levels of ELR1-GFP and StdSERK3A were so low that the detection of the complex was not possible. This was seen in the two experiments done. Therefore, I transiently co-expressed ELR1-GFP, StdSERK3A-HA and p19 in *N. benthamiana*. FLS2 or ELR1 was pulled down using GFP trap beads (Chromotek) and probed with anti HA to check for the presence of StdSERK3A. This revealed that ELR1 and StdSERK3A were constitutively associated. However, a clear enhancement of heterodimerization between ELR1 and StdSERK3A was seen 15 minutes after elicitation with INF1[Pi] (10 µg/ml) (Fig. 4.6B). Hence similar to FLS2, it seems that ELR1 might associate in an activated receptor complex for signaling after the perception of ligand. The fact that an induced enhancement of heteromeric complexes was seen only when using StdSERK3A but not AtBAK1 supports the hypothesis that proper signaling might require that all complex components belong to the same plant species.

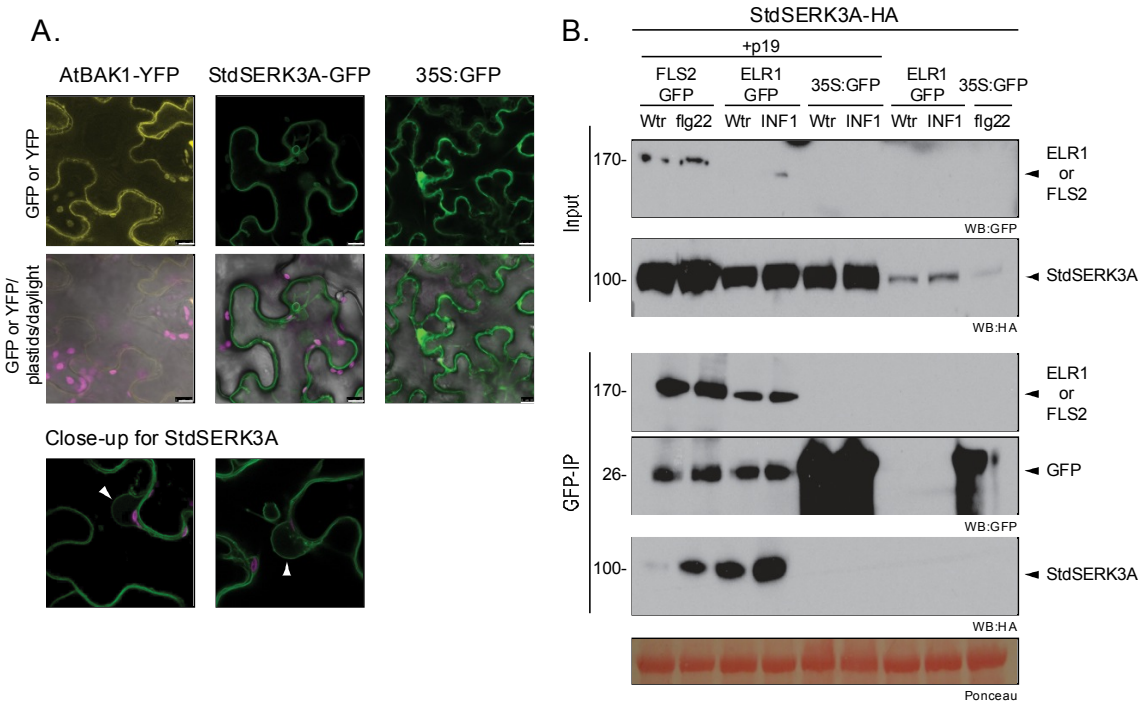

Fig. 4.6. StdSERK3A localizes to the plasma membrane and its constitutive association with ELR1 is enhanced upon INF1 treatment *in planta*

(A) *Agrobacterium*-mediated transient expression of StdSERK3A-GFP or AtBAK1-YFP in *N. benthamiana* 3 DPI showing that StdSERK3A localizes to the plasma membrane and the tonoplast. Magenta corresponds to plastid fluorescence. (Scale bars = 10 µm). (B) ELR1-GFP or FLS2-GFP was transiently co-expressed with StdSERK3A-HA in *N. benthamiana* along with p19 when indicated. Leaves were treated with water (Wtr), flg22 (100nM) or INF1[Pi] (10 µg/ml) for 15 minutes. Proteins were extracted enriching for membrane proteins and subjected to immunoprecipitation (IP) with anti GFP. Western blot analysis shows that ELR1 and FLS2 can

be co-immunoprecipitated with StdSERK3A and that the association is enhanced upon elicitor treatment. Ponceau stain of the total extract blot indicates equal loading (bottom).

4.2.7. Expression of ELR1 reduces the growth of *P. infestans* in *S. tuberosum* cv. Désirée

To test whether ELR1 contributes to disease resistance against *P. infestans*, *S. tuberousm* cv. Désirée plants were stably transformed (Vleeshouwers V, unpublished) with untagged ELR1. Five week-old detached leaves of the transgenic plants (expressing ELR1 under the 35S promoter) or wild type plants were droplet inoculated with *P. infestans* 88069td zoospores (Chaparro-Garcia et al., 2011) and the infection was followed starting 2 days post infection (DPI). Expression of the transgene was assessed by infiltrating INF1[Pi] protein (10 µg/ml) and checking for cell death at 2 and 4 DPI (Fig. 4.7A). INF1 triggered cell death response was also checked in *N. benthamiana* where INF1 is recognized by an endogenous mechanism (Fig. 7A).

Infection of ELR1 transgenic and control potato plants with *P. infestans* did not show any visible symptoms at 2 DPI but at 3 DPI wild type (WT) plants had a faster progression of the infection than plants expressing ELR1 (both lines 34 and 61) (Fig. 4.7B). At 4 DPI the difference in growth had been overcome and infected leaves started to show signs of sporulation (not shown). This clearly illustrates that the advantage that ELR1 confers to the plants is transient and even though the plants are now able to recognize INF1 that does not correlate with complete resistance to *P. infestans* as it is the case for other elicitin responses in other *Solanum* accessions (Vleeshouwers et al., 2006). As a control, plants transformed with a paralog of ELR1 named RLP-207 was used. *RLP-207* was cloned as one of the two candidate genes for the gene mediating INF1 cell death response (Verzaux, 2010). The RLP-207 protein sequence is 85% similar to ELR1 (Fig. A1.5). Although RLP-207 does not complement INF1 cell death in *S. tuberosum* (Verzaux, 2010), it slowed down the growth of *P. infestans* to the same extent as ELR1 (Fig. 4.7B). This result could indicate that its mere expression is constitutively activating some defense components that are also activated by INF1 perception at the membrane by ELR1. It is also possible that even though there is no macroscopic cell death, RLP-207 is capable of perceiving INF1 as well and initiate signaling. This result might indicate that RLP-207 is also a genetic component that the plant uses for recognition of *P. infestans* PAMPs that do not result in visible cell death.

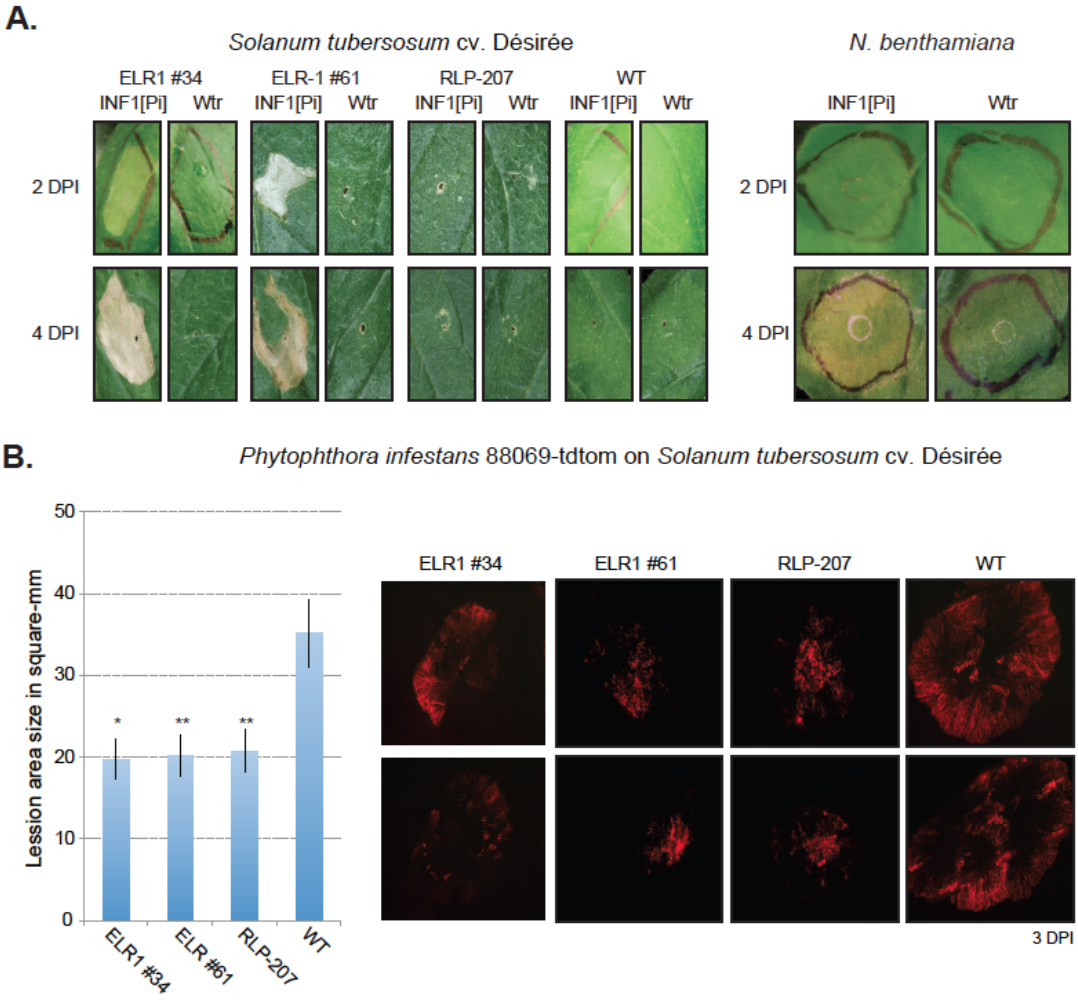

Fig. 4.7. ELR1 reduces the growth of *P. infestans* in *S. tuberosum* cv. Désirée

S. tuberosum cv. Désirée plants were stably transformed with untagged ELR1 or a similar RLP, RLP-207 under the 35S (CaMV) promoter. (A) Four-week-old plants were infiltrated with INF1[Pi] (10 µg/ml) or water to confirm the expression of the transgene. Non-transgenic *N. benthamiana* was also infiltrated with the same aliquot of INF[Pi] to confirm its cell death inducing activity. Plants giving localized cell death were selected for infection assays. (B) Leaves from five-week-old plants were detached and spore droplet inoculated with *P. infestans* 88069 tdtom. Infection was followed in 6 leaves per genotype and 4 droplets per leaf at 2, 3, and 4 DPI. The histogram represents the average infection area in mm^2 at 3 DPI measured from the pictures (see methods). Values are average ± SE (n = 24). Asterisks represent statistically significant difference at $P < 0.05$ (*) and $P < 0.01$ (**) (ANOVA, HSD post-test). Two different lines of ELR1 were tested (ELR1 # 34 and ELR1 #61). All experiments were repeated three times with similar results.

4.3. Discussion

Processing external cues into internal cellular responses is one of the major processes that plants must execute with precision and speed. To achieve this plants rely on cell-surface ligand binding receptors such as RLKs or RLPs. In recent years it has become evident that components of PTI such as the RLK SERK3/BAK1 play a role in defense against *Phytophthora* (Chaparro-Garcia et al., 2011). The identification by Verzaux and colleagues (2010) of a novel receptor like protein (RLP) ELR1 involved in the perception of the *P. infestans* elicitin INF1 in *Solanum microdontum* emphasized the importance to study basal defense responses towards *P. infestans*.

4.3.1. Heterologous expression of ELR1 contributes to *P. infestans* resistance

Transferring pattern recognition receptors (PRRs) between different plant-families has already been successfully achieved (Lacombe et al., 2010; Fradin et al., 2011). Potentially one of the advantages of this approach would be to confer broader-spectrum resistance, since PRRs recognize conserved microbe's molecules that are harder to change without affecting the microbe's fitness. The observable overlap in downstream signaling components for various PRRs recognizing different PAMPs, suggests that plants have possibly evolved a conserved first layer of defense across species. Hence, introduction of one of the signaling components might be sufficient to activate plant defences. However, given the constant evolutionary pressure exerted by emerging pathogens, it is plausible that pathogens evolved mechanisms for suppressing this defense layer.

Two candidate genes from *S. microdontum* were linked to INF1 cell death responses by map-based cloning. Both ELR1 and RLP-207 belong to the receptor like protein (RLP) family but only ELR1 confers INF1 cell death upon expression in plants previously not responding to INF1 (Verzaux, 2010). Transfer of the putative PAMP receptor to *S. tuberosum* cv. Désirée reduced the severity of *P. infestans* infections but did not confer full resistance. Besides INF1 cell death no other previously reported INF1-induced response was assessed in potato plants expressing these RLPs. Notably, ELR1 plants did not show reduced growth or any other obvious detrimental phenotype. Since the receptor originates from a closely related species, it is likely that most signaling components are conserved and less susceptibility to *P. infestans* was expected. However a slight improvement is significant and similar results have been reported for EFR (Lacombe et al., 2010). One surprising observation is that RLP-207, which does not lead to INF1 cell death, showed a similar degree of reduction in infection severity as ELR1 when transgenically expressed in potato. One possible

explanation is that potentially both paralogs are able to perceive INF1 but perhaps their downstream signaling responses diverge or have different strengths. It is also possible that RLP-207 acts as a regulator of ELR1 responses in the same manner as LeEIX1 down regulates EIX responses mediated by LeEIX2 (Bar et al., 2010). Another possibility could be that the decreased susceptibility conferred by RLP-207 is indirect due to the fact that RLP-207 transgenic plants have a slightly different phenotype than wild-type plants. It is possible that transfer of only one signaling component is not sufficient to confer full resistance as *P. infestans* has evolved an arsenal of effectors that keeps the initial defense responses at bay.

4.3.2. ELR1 subcellular distribution and dynamics

ELR1 localization studies showed that it mainly resides at the ER and a small fraction was also seen at the PM. According to Benghezal et al, (2000) Cf-9 localizes exclusively in the ER. Although in that study neither the N-terminal GFP Cf-9 fusion (containing the acidic, the TM and the basic domain) nor the full-length N-terminal HA Cf-9 fusion proteins were tested for functionality, it is known from other studies that N-terminal tags of Cf-9 remain functional (Van Der Hoorn et al., 2003). However, it was also shown that Cf-9 actually localizes to the PM raising the possibility that the ER localization is not required for the AVR9/Cf-9 HR (van der Hoorn et al., 2001), suggesting that the ER localized receptor is not active. LeEIX2 is also localized at the PM and lacks any obvious ER retention motif (Bar and Avni, 2009). ELR1 contains a candidate ER-retention signal RXR at the C-terminus. This motif is important for the regulation of assembly of protein complexes by limiting abundance outside the ER until properly assembled and its functionality was shown for $GABA_B$ receptors (Couve et al., 1998; Gassmann et al., 2005). In mammals, localization at two independent compartments is seen for the receptor TLR8, although their biological relevance has not been fully studied (Nishiya et al., 2005). It is plausible that a fraction of ELR1 resides in the ER until the elicitor activates the fraction at the PM and further signaling is needed. Another mammalian receptor, TLR9 actually reaches its final destination after elicitor activation and the ER localization is essential for its activity (Leifer et al., 2004; Brinkmann et al., 2007). Another explanation for ELR1 ER localization would be that the ER distribution is an artifact of transient overexpression and the presence of *Agrobacterium.* It is possible that ELR1 over expression is overloading the plant folding and glycosylation machinery, and thus it is kept in its route to the membrane at the ER in order to prevent unnecessary signaling as a quality control mechanism. In this case stable transgenic plants with fluorescent ELR1 would be more sensible to study its proper localization.

It is also possible that ELR1 localization at the ER is required for its activity and subsequent signal transduction. In mammals some Toll-like receptors trigger signaling

from different cellular compartments (Ahmad-Nejad et al., 2002). For example, TLR9 requires endosomal localization and activation by endosomal proteases to distinguish non-self from self-signals to mount immune responses (Li et al., 2012). It remains to be tested whether ELR1 localization is changed by INF1 treatment and whether or not the RXR motif is actually needed for ELR1 to be at the ER and whether ER localization is part of the signaling mechanism or only a receptor maturation process.

It has been shown that ligand-binding receptors undergo endocytosis most likely to attenuate signaling and/or transduce the signal (Ron and Avni, 2004; Russinova et al., 2004; Robatzek et al., 2006). ELR1 shows homology to known RLPs implicated in disease resistance that contain an endocytosis motif (Jones et al., 1994; Kawchuk et al., 2001; Ron and Avni, 2004) but ELR1 itself does not contain a canonical endocytosis YxxΦ motif like LeEIX1 and LeEIX2 (Ron and Avni, 2004) or Cf-9 (Jones and Jones, 1997). It is possible though that ELR1 has a non-canonical endocytosis motif. Royle and colleagues (2005) demonstrated that the motif YxxxGΦ also mediates endocytosis and ELR1 has such sequence except that it resides in the predicted TM domain. The length of a transmembrane helix has not been fully determined (von Heijne, 2006) and it could be that the TM is shorter than previously thought. However whether ELR1 does undergo endocytosis was not tested due to experimental limitations and low levels of detectable protein. Nevertheless the proposed endocytosis motif could be mutated and asses its effect in ELR1 localization and function.

4.3.3. ELR1 association with the regulatory receptor kinase SERK3/BAK1

One of the early key events in PTI signaling is the rapid ligand-induced heterodimerization of SERK3/BAK1 with PRRs. Upon perception of their respective elicitors flagellin and elongation factor EF-Tu RLK receptors such as FLS2 and EFR associate with SERK3/BAK1 (Chinchilla et al., 2007b; Heese et al., 2007; Roux et al., 2011). The role of SERK3/BAK1 in RLK signaling has been widely studied and precise molecular events after complex formation have been described (Lu et al., 2010; Schwessinger et al., 2011). However, the role of SERK3/BAK1 in RLP signaling has not been investigated throughout. There is genetic evidence linking SERK3/BAK1 to RLP signaling as when SERK3/BAK1 is silenced in tomato, susceptibility to *Verticillium* (Fradin et al., 2009) is enhanced and the main resistance locus is Ve1, which encodes a receptor like protein (Fradin et al., 2009). Moreover, Bar and colleagues (2010) showed that BAK1 binds the RLP LeEIX1 and not LeEIX2, to down regulate the activity of LeEIX2. Since INF1 cell death requires SERK3/BAK1, ELR1 and SERK3/BAK1 heteromerization was tested. Using co-immunoprecipitation experiments in *N. benthamiana*, I demonstrated that indeed ELR1 and SERK3/BAK1 form a complex. However heteromerization with the Arabidopsis SERK3/BAK1 was constitutive and it

was not altered by elicitation with INF1. This phenomenon has not been reported for RLKs such as FLS2, EFR and BRI1 beyond background levels (Nam and Li, 2002; Chinchilla et al., 2007b; Heese et al., 2007; Roux et al., 2011). One possibility is that overexpression leads to constitutive dimerization, as it is the case when FLS2 and SERK3/BAK1 are co infiltrated in the presence of p19 although to a much lesser extent. Another possibility is that these proteins can exist at the membrane as a heterodimer but are non-functional (Nam and Li, 2002) and once the elicitor is perceived, then enhanced recruitment of the regulator activates signaling. However, this is not probably the case, as INF1 treatment did not produce any change in the amount of SERK3/BAK1. Nevertheless, where the interaction between ELR1 and SERK3/BAK1 occurs was not addressed and it might be that the detected association takes place in another cellular compartment that both proteins have to pass before reaching the PM.

Altogether, this led to another hypothesis in which failure to see enhanced SERK3/BAK1 recruitment upon INF1 elicitation was due to the intrinsic nature of the regulatory RLK SERK3/BAK1. That is, that regulation and overall initiation of PTI may require species-specific components to result in a coordinated cellular response. It is known that PTI signaling cascades mediated by different membrane-bound receptors overlap greatly (Roux et al., 2011). Moreover, PTI signaling seems to be conserved across plant species as demonstrated by Lacombe and colleagues (2010) by the heterologous expression of EFR in *N. benthamiana* and tomato giving recognition to EF-Tu and enhanced resistance. Fradin et al. (2011) also demonstrated this principle by transferring Ve1 to Arabidopsis and gaining resistance to race 1 strains of *V. dahliae*. Nevertheless it is plausible that fine-tuning relies on species-specific components. After cloning a homolog of SERK3/BAK1 from *S. tuberosum*, it was possible to determine that StdSERK3A is able to form a complex with ELR1 and that this association is indeed enhanced upon INF1 treatment. This supports the proposed hypothesis. Surprisingly, heterodimerization was still perceptible without elicitor treatment. If this is due only to overexpression is unavoidable since the protein levels of ELR1 without p19 are not detectable in most of the cases. Moreover, StdSERK3A accumulated to lower levels than its homolog from Arabidopsis (Fig. A1.4) and it was not possible to get similar results as those in Figure 4.5 (without p19 panel).

ELR1 association with SERK3 was differential when using the protein from potato and not differential if using the homolog from Arabidopsis. However, the reverse situation was not relevant for FLS2 heterodimerization. FLS2 interacted with StdSERK3A in a similar fashion as with SERK3/BAK1 (Fig. A1.4) and constitutive association was not present, not even when co-infiltrated with p19 (Fig. 4.6). What could be the reason for such a discrepancy? It might be that RLKs can accommodate more polymorphisms in

the signaling enhancer protein for forming a dimer or even for regulation by phosphorylation. It is known that the eLRRs of SERK3/BAK1 are critical for establishing the complex with the ligand-binding receptor (Jaillais et al., 2011).

Therefore, since RLPs lack a kinase domain and most likely rely mainly on their eLRRs for interaction specificity, having the proper signaling partner may guarantee conformational changes to possibly accommodate additional signaling proteins besides SERK3. Although heterodimerization is a necessary step for signaling it is definitely not sufficient and still it is important to establish whether StdSERK3A actually has the same function as SERK3/BAK1 by complementation of the null *bak1* mutant. If that is the case, there may be an intrinsic differential regulation property between RLKs and RLPs at the complex formation level. Differential regulatory properties are already seen in RLKs, depending whether they are RD or non-RD kinases (Schwessinger et al., 2011). This would be in line with the fact that SERK3/BAK1 is involved in many different signaling pathways.

4.3.4. Homologs of SERK3A/BAK1 in *S. tuberosum* cv. Désirée

S. tuberosum cv. Désirée seems to carry two homologs of SERK3/BAK1 and they reside on different chromosomes in potato whereas Arabidopsis carries only one. Relatives of *S. tuberosum* from the *Solanaceae* family like *N. benthamiana* and tomato (Chaparro-Garcia et al., 2011) also carry at least two SERK3 homologs. The two potato homologs are not as similar to each other as their counterparts in *N. benthamiana*. Genetic analysis such as targeted silencing of each individual homolog or Arabidopsis *bak1* mutant complementation assays would help to resolve their individual roles in PTI and their individual contribution to INF1 responses. Nevertheless one can hypothesize that StdSERK3A, which has fewer polymorphisms overall compared to NbSERK3A/B and even to AtBAK1, and shares conserved UTR regions, is the one most likely to be functionally similar.

StdSERK3A subcellular localization is the same as the one reported for SERK3/BAK1 (Russinova et al., 2004). One interesting observation is that StdSERK3A seemed to be easier to spot at the tonoplast. The biological relevance of the tonoplast localization remains to be explored but it will be interesting to see if it is recruited to the site of infection by *P. infestans* for the uptake of nutrients for example.

4.3.5. ELR1 signaling

How do RLPs transduce the signal after elicitor perception? Since RLPs lack a kinase cytoplasmic domain RLPs may need a partner protein, which has such a domain. One possibility would be to couple the RLP to a cytoplasmic protein kinase or another

adaptor molecule with a signaling motif, which could be recruited to the PM after elicitation. Another possibility would be to couple RLPs with an RLK. Such an example is CLV2 an RLP that forms a complex with the RLK CLV1 which is important to control stem cell proliferation and cell differentiation in the shoot apical meristem (Becraft, 2002). Moreover CLV2 is presumably required for CLV1 protein stability since *clv2* mutants do not accumulate CLV1 protein although its transcription is not affected (Jeong et al., 1999). Most likely CLV3 binds CLV1 but the CLV2 protein brings stability to the whole complex. An alternative would be that ELR1 functions in a similar manner as CLV2 in which case the INF1-binding receptor is still unknown and would most likely be an RLK like FLS2 or EFR. However, SERK3/BAK1 forms a complex with ELR1 that is enhanced after INF1 perception pointing to a model in which ELR1 is the ligand-binding receptor as so far BAK1 only binds the ligand-binding receptor to enhance signaling. Perhaps in RLP-mediated signal transduction SERK3/BAK1 role is more of a co-receptor than a regulator. SERK3/BAK1 has been reported as having different roles in RLK and RLP signaling: although both types of proteins require it, the mechanism seems to differ (Beck et al., 2012). Having steady state levels of heterodimers at the cell surface may facilitate the recruitment of other signaling components or set the stage for conformational changes that transduce the signal (Latz et al., 2007). There is a chance that as in TLR9, homodimers of ELR1 are important for signaling and these dimers in turn are associating with SERK3 (Latz et al., 2007). An alternative could be that after elicitor perception the heterodimers undergo endocytosis mediated by SERK3 and this would result in signal transduction.

4.4. Conclusion

This is perhaps the first example of a ligand-induced complex formation between an RLP and the PTI regulator SERK3. Further investigation on the molecular mechanism of INF1 perception by ELR1 should cast light on how oomycete PAMP signaling is initiated and regulated.

4.5. Perspectives

Future experiments should aim towards clarifying whether ELR1 is the INF1-binding receptor and whether SERK3A functions as a regulator or a co-receptor. For the latter *S. tuberosum* cv. Désirée plants carrying ELR1 should be silenced for SERK3 and then assessed if ELR1 is still capable of binding INF1 (provided it binds directly to INF1). It could also be plausible that SERK3 binds INF1 if it functions as a co-receptor. Another question to address is whether the localization of ELR at the ER is relevant for INF1 perception. Is it possible that INF1 is internalized and then gets recognized by the ER resident ELR1? But then what would be the biological relevance of the association with

PM and tonoplast resident SERK3? It may be the initial signaling step towards full signal transduction. BAK1 did not contribute as a positive regulator for EIX signaling, but instead it seemed to be required for LeEIX1 to down regulate LeEIX2 responses (Bar et al., 2010). What is then the real contribution of SERK3/BAK1 to RLP signaling? Is it a positive or negative regulator for RLP responses? To shed some light on this matter it would be interesting to test the possibility that SERK3 actually associates physically with other RLPs like Ve1 as previously proposed (Fradin et al., 2009). SERK3 has not been described so far to be required for Cf-9/Avr9 or Cf-4/Avr4 HR but it would be interesting to test whether these RLPs also associate with SERK3 because they required CMPG1 for signaling (Gonzalez-Lamothe et al., 2006) whereas Ve1-mediated resistance does not (Fradin et al., 2009). In a similar fashion LeEIX binds in Y2H to a SUMO protein (de Witt 2009). This all suggests that there are significant differences in requirements for signaling components among RLPs involved in plant immunity.

CHAPTER 5: AVR3a suppresses early defense responses in *Nicotiana benthamiana*

5.1 Introduction

Plants have evolved a multilayer defense response to keep pathogen attack at bay. The molecular events underlying the first layer of defense encompass membrane-bound receptors that are able to recognize microbe molecules so called pathogen associated molecular patterns (PAMPs) that initiate a signaling cascade that most of the time results in arrest of pathogen growth (Monaghan and Zipfel, 2012). Deployment of effector proteins is a common feature of plant pathogens to promote virulence. Bacterial pathogens use the type III secretion system to deliver effectors such as AvrPtoB to suppress immunity (Abramovitch et al., 2003). The AvrPtoB N-terminal domain is required for its ability to trigger Pto-mediated cell death (Abramovitch et al., 2003), whereas its C-terminal domain, that resembles E3 ubiquitin ligases (Janjusevic et al., 2006) is necessary for its ability to suppress non-specific cell death (Abramovitch et al., 2003). In addition, AvrPtoB shows global suppression of early defense responses (Hann and Rathjen, 2007). AvrPto is another effector from *P. syringae* that blocks PAMP responses like production of reactive oxygen species (ROS) and MAPK activation (He et al., 2006) by targeting the receptors at the plasma membrane (Xiang et al., 2008). Further examples of effector proteins are *P. syringae* effectors AvrB, AvrRPM1 and AvrRpt2, which target the same host protein to modulate plant immunity (Dodds and Rathjen, 2010).

P. infestans the causal agent of potato and tomato late blight, deploys effectors in the cytoplasm that re-program host processes to further its infection and colonization (Kamoun, 2006). The cytoplasmic effector AVR3a is one of the most well studied effector proteins. AVR3a is an RXLR effector with a conserved pattern of expression peaking at 2 days post infection, typical of other RXLR effectors (Haas et al., 2009). AVR3a has two allelic variants encoding the proteins AVR3a^{KI} and AVR3a^{EM}, which differ in only two amino acids and that show differential activities. Only AVR3a^{KI} induces R3a-mediated resistance and is also a better suppressor of the cell death induced by *P. infestans* elicitin INF1 compared to AVR3a^{EM} (Armstrong et al., 2005; Bos et al., 2006). Moreover, mutants of AVR3a that fail to suppress cell death such as AVR3a$^{KI\text{-}Y147del}$, but still activate R3a, suggest that distinct amino acids condition the effector activities (Bos et al., 2009). In addition AVR3a seems to be essential for virulence as silencing AVR3a in *P. infestans* diminishes its pathogenicity (Bos et al., 2010).

INF1 is a 10 kDa conserved secreted protein of oomycetes with features of PAMPs. To trigger cell death INF1 requires the co-regulator of membrane-bound receptors, BAK1 (Heese et al., 2007) and the U-box E3 ligase CMPG1 which has been shown to be an essential positive regulator of plant defense mediated by the membrane-bound receptors Cf-9 and Cf-4 (Gonzalez-Lamothe et al., 2006). In addition CMPG1 is targeted and stabilized by AVR3a to presumably suppress INF1-mediated cell death (Bos et al., 2010). Ubiquitination has been reported as an important component of plant defense responses (Goritschnig et al., 2007) and AvrPtoB seems to use the plant proteasome pathway to target FLS2 for degradation (Gohre et al., 2008).

One hypothesis is that AVR3a targets CMPG1 to prevent signal transduction initiated by membrane-bound receptors. One of these receptors could be a BAK1-dependent INF1 receptor. Therefore, the main objective of this study was to evaluate the extent and specificity to which AVR3a suppresses canonical outputs of PTI signaling activated by different PAMPs such as production of reactive oxygen species (ROS), activation of mitogen-activated protein kinases (MAPKs), and induction of defense gene expression in *N. benthamiana*. In addition the role of CMPG1 in early defense responses was partly evaluated. One of the main findings was that AVR3a variants differentially suppress early defense responses triggered by INF1 but that all variants of AVR3a (AVR3a^{KI}, AVR3a^{EM}, and AVR3a$^{KI\text{-}Y174del}$) suppress flg22-induced ROS and subsequent plant gene induction to a similar extent. This suppression of flg22-induced responses was not due to interference with the pattern recognition receptor FLS2 localization or accumulation or inhibition of the heterodimerization of FLS2 with the co-regulator SERK3/BAK1. Finally, the results suggest that CMPG1 might exert a negative regulatory effect on ROS production.

5.2. Results

5.2.1. AVR3a^{KI} overexpression specifically enhances susceptibility to *P. infestans* in *N. benthamiana*

Silencing AVR3a in *P. inf*estans leads to loss of virulence, which is complemented when AVR3a^{KI} or AVR3a^{EM} are transiently expressed in *N. benthamiana* (Bos et al., 2010). To investigate whether stable over expression of alleles of *Avr3a* would impact upon *P. infestans* infection of *N. benthamiana*, stable transgenic *N. benthamiana* plants were generated expressing FLAG-AVR3a^{KI}, FLAG-AVR3a^{EM}, FLAG-AVR3a$^{KI\text{-}Y147del}$) or the vector control (pBinplus-ΔGFP) under control of the 35S promoter. Transgenic plants did not show any obvious developmental phenotype and the overall expression of the effector in all lines were similar (data not shown). Next I challenged detached

leaves of these plants with *P. infestans* 88069. I found that only plants over expressing AVR3a^{KI} led to enhanced-susceptibility of *N. benthamiana* to *P. infestans* (Fig. 5.1.A). Moreover, infection proceeded faster and greater sporulation was observed at 4 DPI on plants expressing AVR3a^{KI} (Fig. 5.1.B). Strikingly, plants over expressing AVR3a^{EM} or AVR3a$^{KI\text{-}Y147del}$ did not have an effect on *P. infestans* virulence (Fig. 5.1.B). This result indicates that AVR3a^{KI} might exert stronger suppression of plant defense.

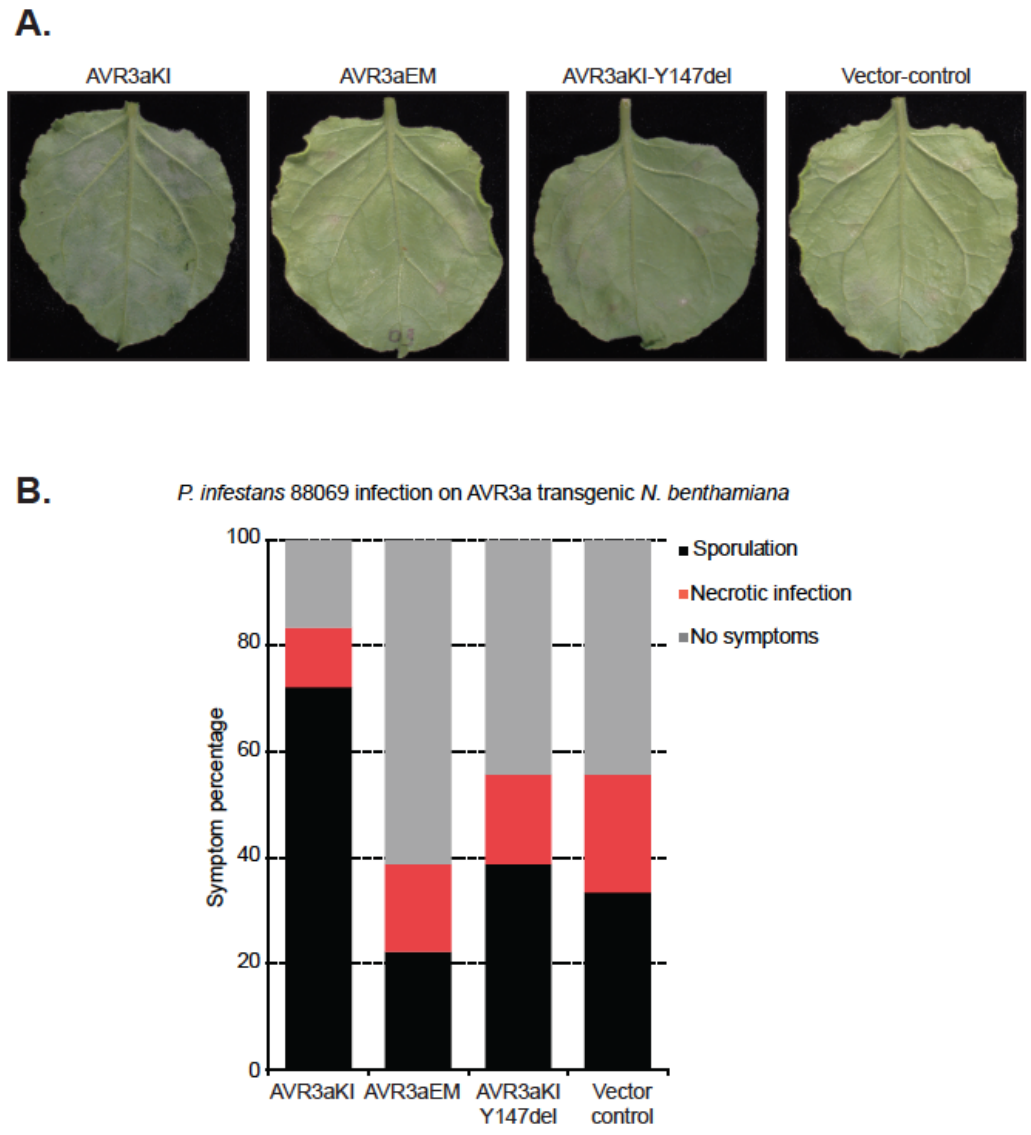

Fig. 5.2.1. AVR3a^{KI} but not other variants of AVR3a enhances *P. infestans* growth in *N. benthamiana*

N. benthamiana plants were stably transformed with pBinplus::AVR3a^{KI}, pBinplus::AVR3a^{EM}, pBinplus::AVR3a$^{KI\text{-}Y147del}$ or pBinplus::ΔGFP (vector-control) and taken to the third generation. Detached leaves of 4 to 5 week old plants were drop inoculated with a suspension of zoospores (100 zoospores/μl) of *P. infestans* 88069. Infection was followed starting at 2 DPI. (A) Representative pictures of the infection taken at 4 DPI. (B) Histogram depicting the range of

symptoms visualized at 4 DPI as a percentage based on the infection of at least 6 individual leaves per genotype. Two independent lines per genotype were used showing similar results.

5.2.2. AVR3a localizes to the cytoplasm in *N. benthamiana*

Study of the localization of translocated effector proteins in plant cells might point to their mechanism of action inside the host cell. The subcellular distribution of AVR3a was explored by Bos and colleagues (2010) only in the presence of CMPG1 and in the context of its stabilization. In order to gain some insights into AVR3a activities and to exclude that AVR3a localization was altered by CMPG1, I generated N-terminal GFP and RFP fusions of AVR3a. Transient expression in *N. benthamiana* of GFP-AVR3a showed that all variants of AVR3a localized to the cytoplasm and the plant cell nucleus (Fig. 5.2.A). Although the GFP tag was not cleaved (Fig. 5.2.C), AVR3a localization was similar to that of free GFP (Fig. 5.2.A). To ensure that addition of a GFP tag does not interfere with AVR3a functionality, I co-expressed GFP-AVR3a and the cognate potato resistance protein R3a and this led to HR for all variants of AVR3a except AVR3a^{EM} (Fig. 5.2.B). In the same fashion, INF1 cell death suppression activity was detectable in GFP-AVR3a^{KI} but not other variants of AVR3a (Fig. 5.2.B). Similar results were observed with the RFP fusion proteins (data not shown). Spatial distribution of GFP-AVR3a in the cell remained unchanged between 24-60 hours post infiltration. Thus GFP did not interfere with AVR3a activities probably pointing to an actual biological relevance of the observed subcellular distribution.

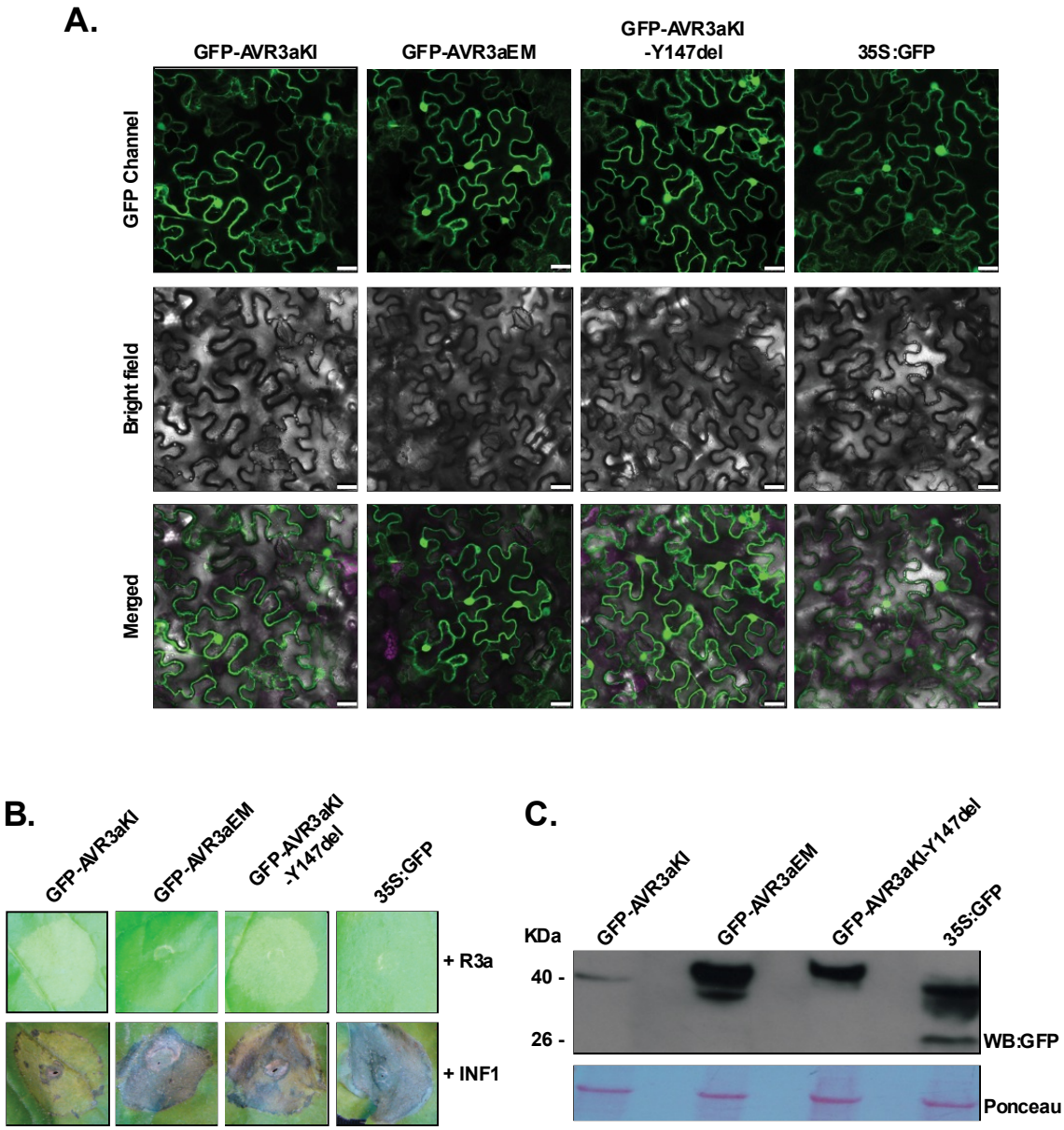

Fig. 5.2.2. AVR3a has cytoplasmic and nuclear localization in *N. benthamiana*

(A) GFP N-terminal fusions of AVR3a^{KI}, AVR3a^{EM}, AVR3a$^{KI\text{-}Y147del}$ or 35S:GFP were transiently expressed in *N. benthamiana* and subcellular distribution was imaged at 2.5 DPI. Bar = 25μm. Representative images are shown. (B) Functional characterization of the GFP-fusion proteins of AVR3a. Co-expression of the GFP fusion protein in a ratio 2:1 with R3a in *N. benthamiana* showed that the GFP tag did not affect recognition by R3a. In a similar manner, challenging with INF1 showed that the GFP did not alter INF1-cell death suppression. (C) Western blot of the fluorescent proteins in (A).

5.2.3. AVR3a variants show differential suppression of PTI-responses triggered by flg22 and INF1

Suppression of early defense responses is a common trait of effector proteins. To assess the extent and specificity to which AVR3a suppresses canonical outputs of early defense responses triggered by a bacterial and an oomycete elicitor, I tested the

oxidative burst production in *N. benthamiana* in the presence of the different variants of AVR3a upon flg22 or INF1 treatment. Variants of AVR3a (FLAG-AVR3a^{KI}, FLAG-AVR3a^{EM}, FLAG-AVR3a$^{KI\text{-}Y147del}$) or the vector control (pBinplus-ΔGFP) were transiently expressed in *N. benthamiana* and 2 DPI leaf-discs were collected and floated overnight in water. At 3 DPI leaf-discs were challenged with flg22 (100 nM) or INF1 (10 µg/ml) and the production of reactive oxygen species (ROS) was followed over time. I found that the ROS bust induced by flg22 was completely suppressed by all variants of AVR3a (Fig. 5.3.A) whereas AVR3a^{KI} better suppressed the ROS induced by INF1 (Fig. 5.3.B). INF1-triggered ROS (Fig. 5.3.B) production was different in amplitude and kinetics than flg22-ROS as previously shown (Chaparro-Garcia et al., 2011). Total ROS production expressed as a percentage of the total ROS produced in the control showed the same trend (Fig. A2.1A,B). Similar results were obtained when stably expressing AVR3a in *N. benthamiana* (Fig. A2.2A) and in *A. thaliana* for flg22 (Fig. A2.2B).

It has been established that inhibition of ROS does not automatically lead to suppression of MAPK activation or defense gene induction (Segonzac et al., 2011). Since transcriptional reprogramming is one of the more downstream defense responses related to PAMP recognition, I next tested whether AVR3a could also suppress defense gene induction. I checked two marker genes described by Segonzac et al. (2011) and Heese at al. (2007) *NbCYP71D20* and *NbACRE31* to assess if AVR3a suppression of PTI was sustained or was limited to very early activation of immunity. The transcription of these marker genes was monitored at the initial time and 180 minutes after elicitation instead of 60 minutes to allow proper induction by INF1. *NbCYP71D20* expression was induced 12-fold by flg22 (Fig. 5.3.C) and 80-fold by INF1 (Fig. 5.3.D) approximately in the control plants. All AVR3a variants significantly reduced the induction of *NbCYP71D20* by flg22 approximately 80% (Fig. 5.3.C) whereas reduction of INF1-induction of this same gene was only 40% for AVR3a^{KI} and AVR3a^{EM}. The variant AVR3a$^{KI\text{-}147del}$ did not show any reduction of this marker gene induction (Fig. 5.3D). In the same manner, the induction of *NbACRE31* by flg22 treatment decreased by 80% in the presence of any of the variants of AVR3a (Fig. A2.1C). Surprisingly, the induction of the gene *NbACRE31* by INF1 was not hindered by any of the AVR3a variants (Fig. A2.1D). Expression of the AVR3a proteins is shown in Fig. A2.1E,F. Notably, the expression of AVR3a in absence of PAMP elicitation already induces the transcription of the evaluated markers genes (Fig. 5.3.C,D time zero; Fig. A2.1.C,D time zero). Since the transcription of theses gene markers was followed in *N. benthamiana* stably expressing AVR3a, this probably indicates a general effect of AVR3a overexpression on transcription. However, the reduction after elicitation was robust and significant as evaluated by one-way ANOVA.

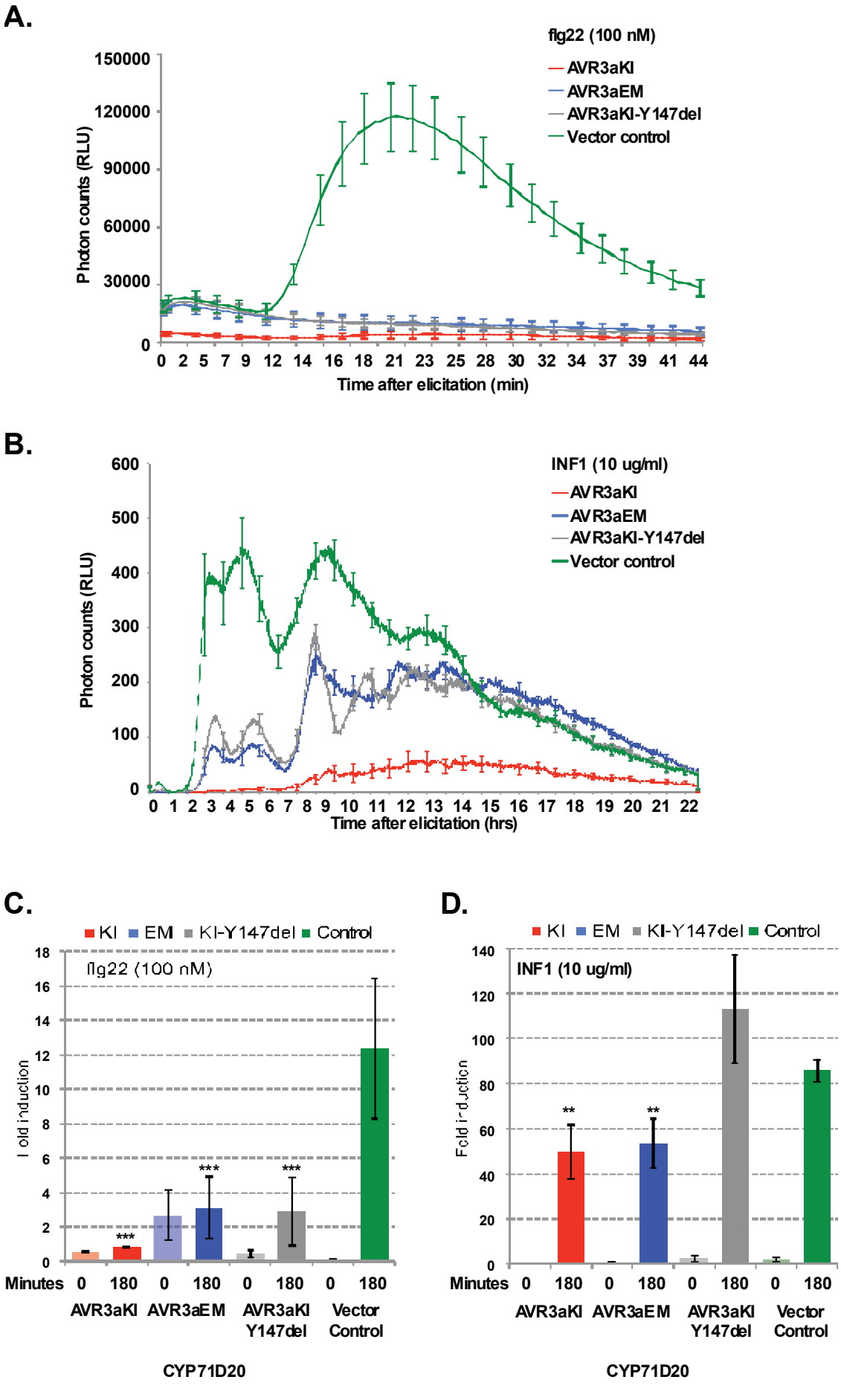
A.
flg22 (100 nM)
AVR3aKI
AVR3aEM
AVR3aKI-Y147del
Vector control
Photon counts (RLU)
150000
120000
90000
60000
30000
0
0 2 5 7 9 12 14 16 18 21 23 25 28 30 32 34 37 39 41 44
Time after elicitation (min)
B.
INF1 (10 ug/ml)
AVR3aKI
AVR3aEM
AVR3aKI-Y147del
Vector control
Photon counts (RLU)
600
500
400
300
200
100
0
0 1 2 3 4 5 6 7 8 9 10 11 12 13 14 15 16 17 18 19 20 21 22
Time after elicitation (hrs)
C.
KI EM KI-Y147del Control
flg22 (100 nM)
Fold induction
18
16
14
12
10
8
6
4
2
0
***
***
***
Minutes 0 180 0 180 0 180 0 180
AVR3aKI AVR3aEM AVR3aKI Y147del Vector Control
CYP71D20
D.
KI EM KI-Y147del Control
INF1 (10 ug/ml)
Fold induction
140
120
100
80
60
40
20
0
**
**
Minutes 0 180 0 180 0 180 0 180
AVR3aKI AVR3aEM AVR3aKI Y147del Vector Control
CYP71D20

Fig. 5.2.3. AVR3a suppresses elicitor-induced reactive oxygen species production (ROS) and gene induction

Oxidative burst triggered by 100 nM flg22 (A) or 10 µg/ml INF1 (B) in *N. benthamiana* agro infiltrated with pBinplus::AVR3a^{KI} (red), pBinplus::AVR3a^{EM} (blue), pBinplus::AVR3a$^{KI\text{-}Y147del}$ (grey) or pBinplus::ΔGFP control (green) or stably expressing AVR3a *N. benthamiana* for INF1. ROS production was measured in relative light units (RLU) over time. Induction of the marker gene NbCYP71 by 100 nM flg22 (C) or 10 µg/ml INF1 (D) in *N. benthamiana* under the same conditions described above. Expression was assessed by qRT-PCR at time zero and 180 minutes after elicitor treatment and normalized by NbEF1α gene expression. Statistical significance was evaluated in comparison to the control by one-way ANOVA followed by Tukey HSD test. *** $P < 0.001$, ** $P < 0.05$. Similar results were observed in at least four independent experiments and in transgenic *N. benthamiana* lines expressing the same constructs.

To test whether AVR3a interference with PAMP-triggered responses was a feature specific for SERK3/BAK1-dependent signaling pathways, I measured ROS production elicited by chitin, a fungal PAMP that is recognized by CERK1 (a non-eLRR membrane bound receptor) (Miya et al., 2007; Wan et al., 2008), in an SERK3/BAK1 independent fashion (Gimenez-Ibanez et al., 2009b). Chitin-induced ROS production was consistently not suppressed by any variant of AVR3a (Fig. 5.4C,D). Moreover, AVR3a variants did not affect CERK1 localization (Fig. 5.4.A) or its accumulation (Fig. 5.4.B), suggesting that AVR3a most likely suppresses defense responses pathways that required SERK3/BAK1.

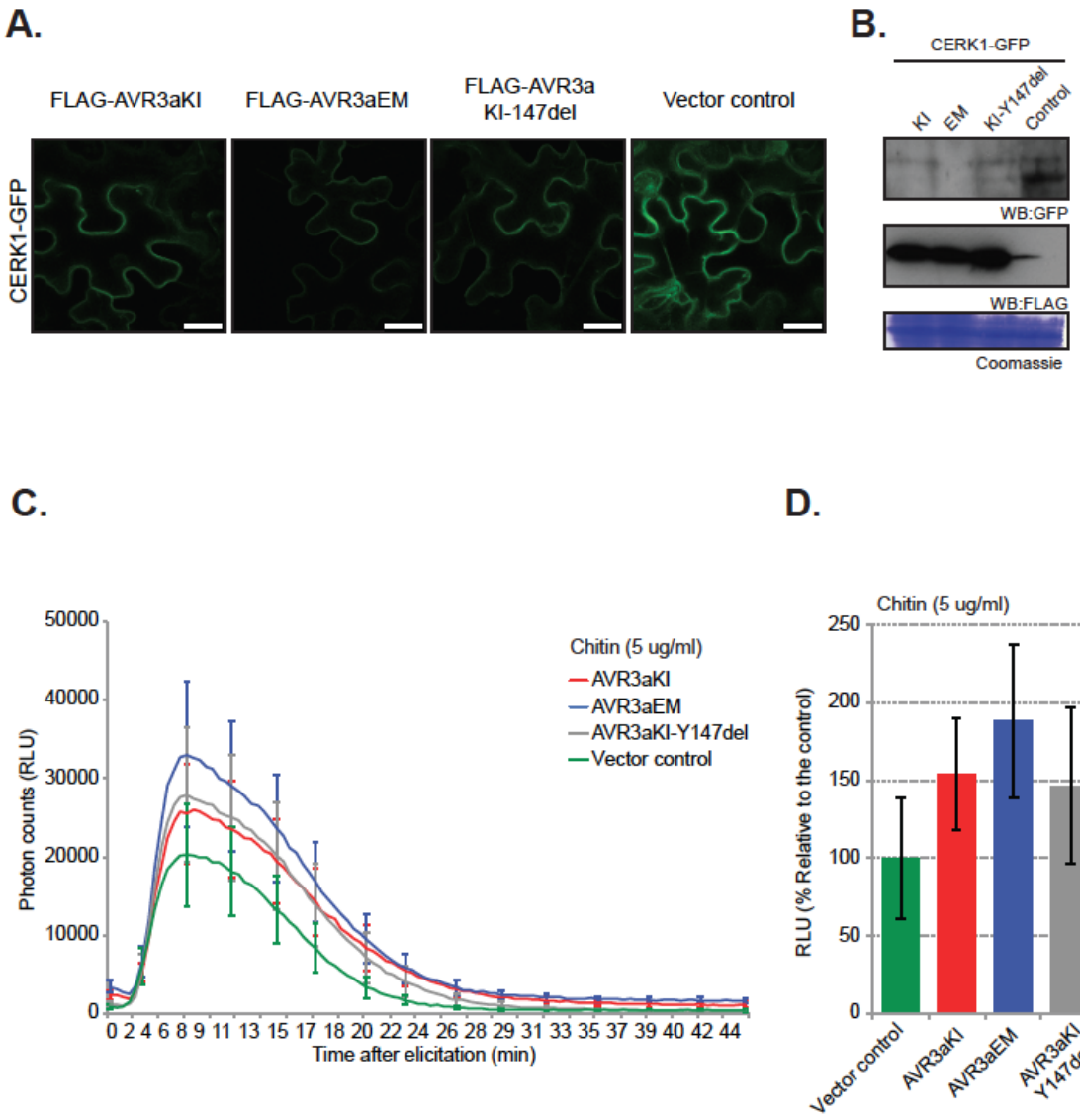

Fig. 5.2.4. AVR3a does not affect the localization or early signaling of the BAK1-independent receptor CERK1

Agrobacterium-mediated co-expression of pamMCSNut-35S:CERK1-GFP (Kindly provided by E. Petutschnig and V. Lipka, unpublished) with pBinplus-FLAG-AVR3a^{KI} or pBinplus-FLAG-AVR3a^{EM} or pBinplus-FLAG-AVR3a$^{KI-Y147del}$ or pBinplus:ΔGFP as indicated in *N. benthamiana*. (A) Plasma membrane localization of the BAK1-independent receptor CERK1 was not altered by the presence of variants of *P. infestans* effector AVR3a. (B) AVR3a effect on protein levels of CERK1 in (A). Total protein extracts were processed after confocal microscopy. Equal amounts of protein were analyzed (Coomassie lane) in all cases. Oxidative burst triggered by 5 µg/ml chitin (SIGMA) (B) in *N. benthamiana* agro infiltrated with pBinplus::AVR3a^{KI} (red), pBinplus::AVR3a^{EM} (blue), pBinplus::AVR3a$^{KI-Y147del}$ (grey) or pBinplus::ΔGFP control (green). Leaf discs were incubated in a chitin-containing solution and ROS was measured in relative light units (RLU) over time (C) or as total count percentage relative to the control over 45 minutes (D). Similar results were observed in at least three independent experiments.

5.2.4. AVR3a does not have general effects on PRR localization or steady state levels

It is known that some bacterial effectors target the membrane receptors FLS2 and BAK1 to suppress plant immunity (Shan et al., 2008; Xiang et al., 2008). To address whether the suppression activity of AVR3a of SERK3/BAK1-dependent signaling pathways was due to direct targeting of these receptors by AVR3a, I tested the effect of AVR3a on FLS2, BAK1, and EFR localization and protein accumulation rather than AVR3a-association with them as it was reported that association is not correlated with suppression activity (Shan et al., 2008). It is possible that mis-localization of the receptor would have a radical detrimental effect on their ability to transduce the signal. I transiently co-expressed FLS2-GFP, SERK3/BAK1-YFP, and EFR-YFP with FLAG-AVR3a variants in a 1:1 ratio and assessed the PRR localization by confocal microscopy at 2 and 3 DPI. I found that FLS2 and BAK1 were still at the PM as described (Li et al., 2002; Robatzek et al., 2006) suggesting that none of the variants of AVR3a had an effect on their native localization (Fig. 5.5.A). Surprisingly, I found that EFR localization was sometimes more abundant at the ER than at the PM when co-expressed with AVR3a, particularly AVR3a^{KI} in a certain number of cells (Fig. 5.5.A, bottom panel).

To investigate whether AVR3a^{KI} enhanced ER-localization of EFR was a broad phenomenon or an isolated event on some cells due to over expression, I treated plant tissue co-expressing EFR-GFP and FLAG-AVR3a^{KI} with the enzyme endoglycosidase H (EndoH). Proteins that are not fully mature and still containing ER-specific glycans are sensitive to cleavage by EndoH whereas mature proteins on their way to the PM should be resistant to treatment (Nekrasov et al., 2009). This revealed that AVR3a did not alter the ratio of EFR protein at the ER and PM relative to the control (Fig. 5.5.C). The reduced steady state levels of EFR retained at the ER in the sample with AVR3a$^{KI\text{-}Y147del}$ in this particular blot (Fig. 5.5.C) does not mean that this variant of AVR3a is affecting EFR localization, is only an overall effect of the lower total protein amounts in that sample. It seemed that the maturation process of FLS2 was faster than EFR as no cleavage of FLS2 was detected in any sample undergoing EndoH treatment (Fig. 5.5.C). From this experiment it was also evident that none of the variants of AVR3a had an effect on EFR or FLS2 steady state levels (Fig. 5.5.C, panel GFP-IP, WB:GFP, no EndoH treatment). This is contradictory to other experiments in which it seemed that AVR3a^{KI} and AVR3a^{EM} reduced EFR and FLS2 protein levels (Fig. 5.5.B). However, this is probably a technical problem, as independent experiments with only AVR3a^{KI} did not show such effect (Fig A2.3A). In addition, for the EndoH treatment the samples were concentrated using GFP-agarose beads and thus cannot be used for assessing

quantitative differences of protein levels. In conclusion AVR3a did not affect the subcellular distribution of EFR, FLS2, and BAK1 or their protein levels *in planta*.

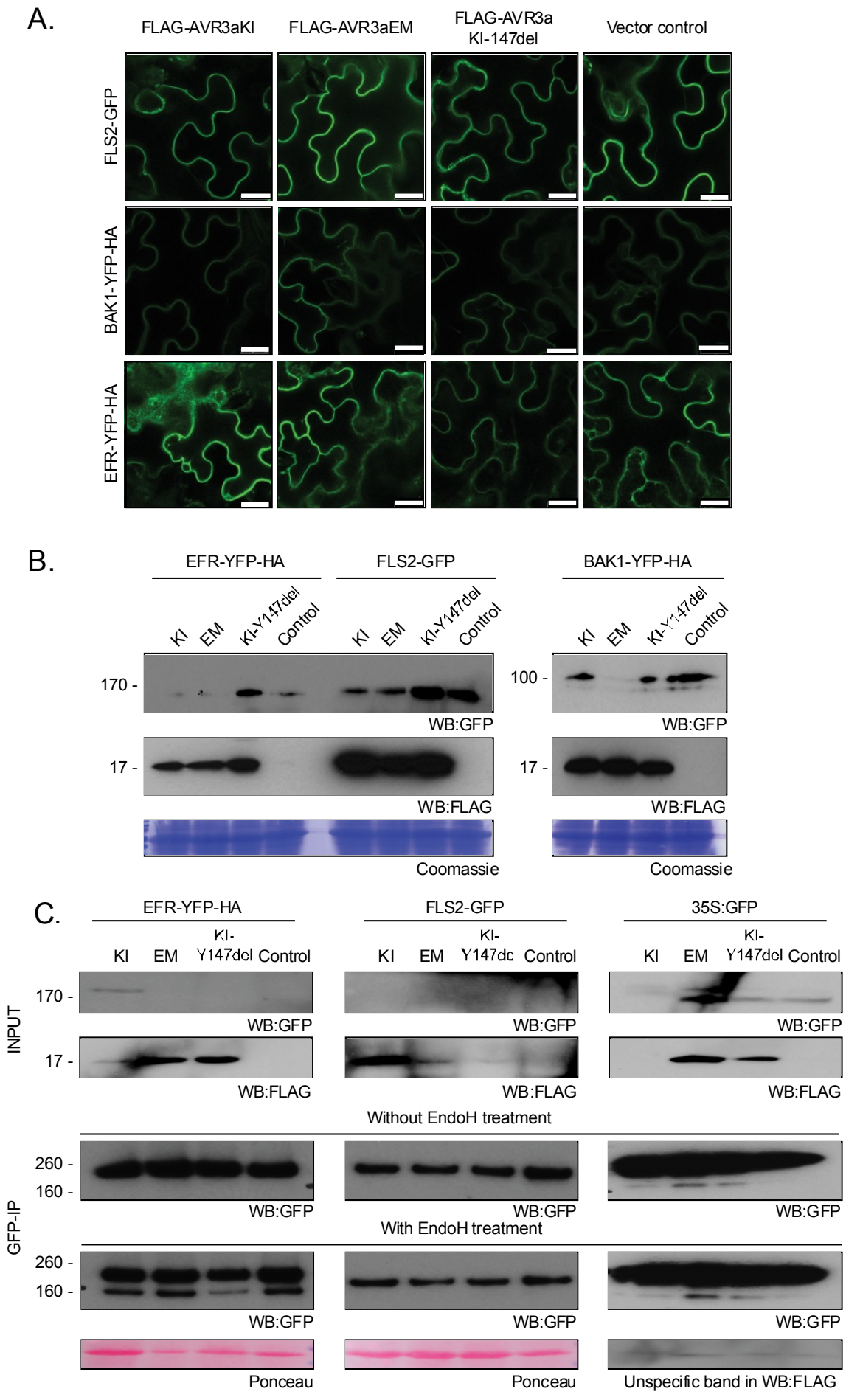
A.
FLAG-AVR3aKI
FLAG-AVR3aEM
FLAG-AVR3a KI-147del
Vector control
FLS2-GFP
BAK1-YFP-HA
EFR-YFP-HA
B.
EFR-YFP-HA
FLS2-GFP
BAK1-YFP-HA
KI
EM
KI-Y147del
Control
170 -
100 -
17 -
WB:GFP
WB:FLAG
Coomassie
C.
EFR-YFP-HA
FLS2-GFP
35S:GFP
KI
EM
KI-Y147del
Control
INPUT
170 -
17 -
WB:GFP
WB:FLAG
Without EndoH treatment
GFP-IP
260 -
160 -
With EndoH treatment
Ponceau
Unspecific band in WB:FLAG

Fig. 5.2.5. AVR3a does not affect the localization or turn over of the LRR-containing receptors FLS2, BAK1, and EFR

Transient co-expression in *N. benthamiana* of pK7FWG2-FLS2-GFP, pEarly103-BAK1-YFP-HA, and pEarly103-EFR-YFP-HA with pBinplus-FLAG-AVR3a^{KI} or pBinplus-FLAG-AVR3a^{EM} or pBinplus-FLAG-AVR3a$^{KI\text{-}Y147del}$ or pBinplus::ΔGFP (label in the figure as vector control) as indicated. (A) Plasma membrane localization of LRR-containing receptors FLS2, BAK1, and EFR was not altered by the presence of variants of *P. infestans* effector AVR3a. (B) AVR3a effect on protein levels of the receptors in (A). Total protein extracts were processed after confocal microscopy. Equal amounts of protein were analyzed (Coomassie lane) in all cases. (C) AVR3a^{KI} effect on EFR glycosylation state. EFR-YFP was co-expressed with FLAG-AVR3a^{KI} and total protein extracts were subjected to GFP-IP and incubated with EndoH for one hour at 37C. Accumulation of EFR at the ER was not affected or enhanced by AVR3a. FLS2 glycosylation was also assessed. 35S:GFP was used as control in the EndoH assay. Representative confocal images were taken at 2.5 DPI. Bar = 25 μm

5.2.5. AVR3a does not interfere with elicitor-induced association of FLS2 and SERK3/BAK1 *in planta*

One of the early events in PAMP recognition is the association of the co-regulator SERK3/BAK1 with the ligand-binding receptor (Chinchilla et al., 2007b; Heese et al., 2007; Roux et al., 2011). Therefore I tested whether AVR3a^{KI} was suppressing flg22-induced early defense by disrupting the FLS2/BAK1 complex. *N. benthamiana* leaves stably expressing AVR3a^{KI} or a vector control were used to transiently express 35S:FLS2-GFP and 35S:SERK3/BAK1-HA in a 1:1 ratio. Infiltrated sites were treated either with water or flg22 (100 nM) for 15 minutes. After immunoprecipitation of 35S:FLS2-GFP or 35S:GFP using GFP-trap beads (Chromotek), there was flg22-dependent recruitment of BAK1-HA only in samples containing FLS2 (Fig. 5.6), and this association was not affected or otherwise altered by the presence of AVR3a^{KI}. I repeatedly observed higher steady state levels of BAK1 but also GFP in samples where AVR3a^{KI} was co-expressed. For example, GFP expression is enhanced as seen in this experiment in the samples with 35S:GFP/BAK1-HA (Fig. 5.6 Marked with red asterisks, WB:GFP; also Input anti-HA for SERK3/BAK1). One reasonable explanation could be that AVR3a promotes enhanced transient expression or protein accumulation.

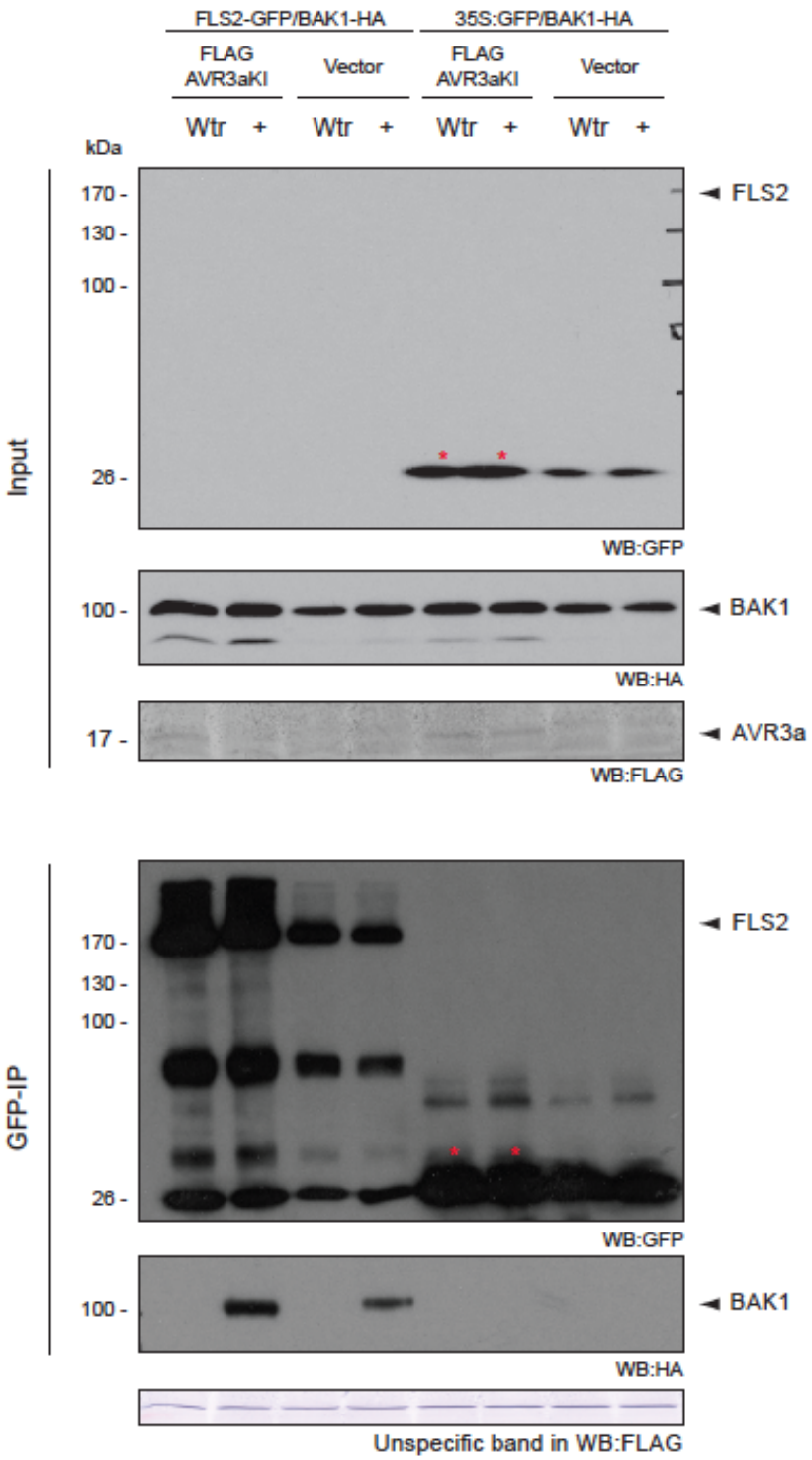

Fig. 5.2.6. AVR3a^{KI} does not affect FLS2 association with BAK1 *in planta*

Transgenic *N. benthamiana* expressing FLAG-AVR3a or the vector control 35S:ΔGFP transiently infiltrated with a mix (1:1) of FLS2-GFP/BAK1-HA and treated with flg22 (100 nM) (labeled in the figure with +) or water for 15 minutes (label in the figure as Wtr). Leaf-tissue was treated and collected 2.5 DPI and subjected to immunoprecipitation with anti GFP agarose beads (Cromotek). Purified complex formation dependent on flg22 was observed for FLS2-GFP and BAK1-HA by immunoblotting with the specified antibodies. 35S:GFP/BAK1-HA was used as control. Preliminary data of one experiment is shown.

5.2.6. Silencing CMPG1 enhances flg22-induced ROS

CMPG1 was identified as one of the genes whose expression rapidly changed after Avr9 elicitation (Durrant et al., 2000). CMPG1 is required for cell death following activation of the PRR Cf-9 by its ligand Avr9 and ICD (Gonzalez-Lamothe et al., 2006). $AVR3a^{KI}$ and $AVR3a^{EM}$ are able to suppress Cf-9 mediated cell death and stabilizes CMPG1 (Bos et al., 2010; Gilroy et al., 2011), thus it was interesting to check whether AVR3a's ability to suppress flg22 ROS burst was impaired upon altering CMPG1 levels or functionality. I used double-stranded RNA hairpin-mediated transient silencing of CMPG1 in *N. benthamiana* using the same construct used by Gonzalez-Lamothe (2006). Three days post silencing I incubated leaf discs on water and the next day I challenged the leaf-discs with a solution containing flg22 (100 nM). I found that the total photon count relative to the control was significantly enhanced by almost 50% (Fig. 5.7.C). This actually is in accordance with reports showing that silencing of E3 ligases can enhance the total amount of ROS produced by different PAMPs (Trujillo et al., 2008). To ensure that treatment with an RNAi construct was not interfering with ROS responses, wild type *N. benthamiana* leaves were included and showed similar levels of total ROS production as the RNAi-GFP control (Fig. 5.7.D).

Interestingly, over expression of one of the *N. benthamiana* homologs of CMPG1 (NbCMPG1A) did not have any effect on flg22-ROS production. Moreover, mutants of CMPG1, which are impaired in ubiquitination activity and act as dominant negative mutants (Gonzalez-Lamothe et al., 2006; Bos et al., 2010), NbCMPG1-C37A and NbCMPG1-W64A, did not show any effect on ROS (Fig. 5.7A). It is possible that the over expressed NbCMPG1 protein is non functional hence having no impact. The same could be true for the mutants tested. It is possible that these mutations (NbCMPG1-C37A and NbCMPG1-W64A) do not affect the ubiquitination activity in homologs of CMPG1 in *N. benthamiana*. Bos and colleagues (2010) showed that those mutations in the U-box self-stabilized CMPG1 suggesting that CMPG1 is unable to self-ubiquitinate and exert its normal function. Therefore it is more likely that the amount of mutated CMPG1 was not sufficient to exert a dominant negative effect over endogenous CMPG1 homologous proteins (Fig. 5.7.B). It is known that for these dominant negative mutants, their ability to diminish HR is directly correlated to their protein accumulation (Gonzalez-Lamothe et al., 2006). Given that the over expression of CMPG1 or the mutants tested did not show any effect on ROS it might be possible that CMPG1 serves as a negative regulator of ROS production after elicitor perception at the PM.

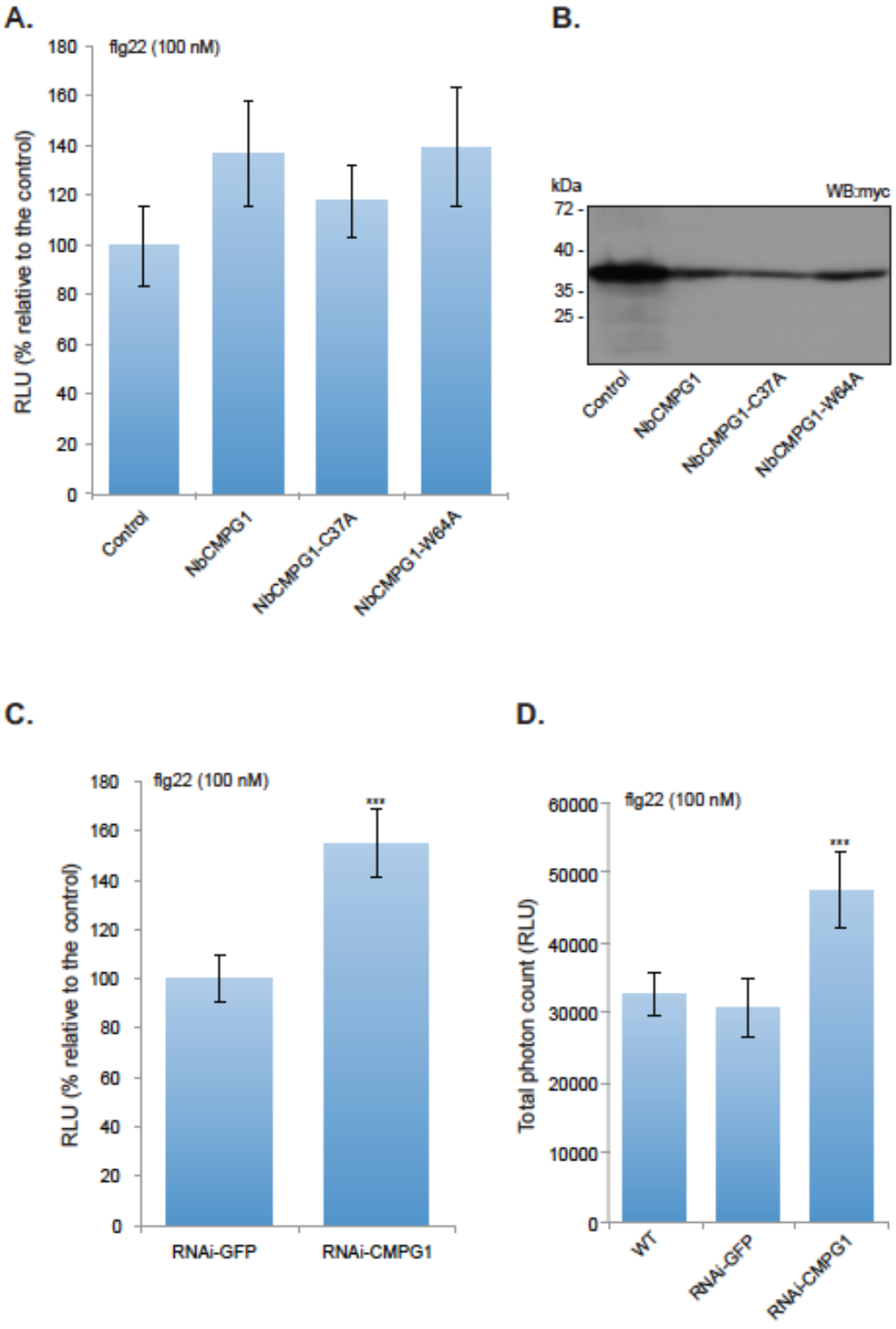

Fig. 5.2.7. Silencing CMPG1 enhances flg22-induced ROS

(A) Oxidative burst triggered by 100 nM flg22 in *N. benthamiana* agro infiltrated with 4xmyc-NbCMPG1, 4xmyc-NbCMPG1-C37A, 4xmyc-NbCMPG1-W64A or pGWB18-4xmyc-GFP (control). ROS production was measured in relative light units (RLU) over time. (B) Western blot showing the over expression of the constructs in (A). Leaves of *N. benthamiana* were silenced locally via RNAi-mediated silencing using the vector pHellsgate8 harboring the fragment used by Gonzalez-Lamothe et al., (2007) for silencing CMPG1 or a fragment targeting a region of GFP as a control. Three days post silencing, leaf-discs were incubated in water overnight. The

following day, leaf-discs were challenged with flg22 (100 nM) and ROS production was measured in a luminol-based assay. Histograms showing the total ROS production as percentage relative to the control over 45 minutes (C) or the total photon count (D). Values are average ± SE (n = 8). Asterisks represent statistical significance when compared to the control ($p \leq 4.947e-05$).

5.2.8. AVR3a stabilization of CMPG1 requires the C-terminal domain of CMPG1 containing the ARM repeats

E3 ligases such as CMPG1 are important enzymes in the process of ubiquitination and confer the specificity of the reaction by interacting with the target protein (Smalle and Vierstra, 2004). Gonzalez-Lamothe (2006) identified PUB20, an U-box and ARMADILLO (ARM) repeat containing protein from Arabidopsis to have the closest homology to the tobacco CMPG1. Previously it was observed that PUB20 steady state levels were sufficient to be detected by western blot analysis and that AVR3a did not have any effect on PUB20 protein stability (Jorunn Bos, personal communication). Although PUB20 and StCMPG1 amino acid sequence similarity is not very high (41%), their domain structure is conserved (Fig. 5.7A) and this allows the study of which domains of CMPG1 contribute to stabilization by AVR3a. Therefore, I designed a construct called Chimera I encoding the N-terminal U-box of PUB20 and the C-terminal ARM-domain of StCMPG1, and one other construct, Chimera II, encoding the N-terminal U-box domain of StCMPG1 and the C-terminal ARM-domain of PUB20 (Fig. 5.8.C). These chimeras were cloned into the Gateway compatible destination vector pGWB18 to generate 4X-myc tag N-terminal fusions as previously described (Bos et al., 2010). I transiently co-expressed the chimeras with all variants of AVR3a and tested for stabilization. Full-length StCMPG1 and PUB20 served as controls. As expected PUB20 protein levels were not affected by any of the AVR3a variants (Fig. 5.8.B) and only $AVR3a^{KI}$ and $AVR3a^{EM}$ stabilized StCMPG1, shown not only as an increase in protein accumulation but also by the presence of a double band above the expected size for StCMPG1 (Fig. 5.8.B). Interestingly, $AVR3a^{KI}$ and $AVR3a^{EM}$ stabilized Chimera I harboring the ARMADILLO (ARM) domain of CMPG1 indicating that AVR3a mediated CMPG1 stabilization requires this region (Fig. 5.8.B). The ARM domain of U-box proteins represents the protein-protein interaction domain and might be the binding domain that couples the E3 ligase to a protein targeted for ubiquitination (Mudgil et al., 2004). It remains to be studied whether AVR3a stabilization via the ARM repeats is achieved by preventing binding of unknown substrates to CMPG1. In addition, the double band that accompanies AVR3a stabilization of CMPG1 seemed to be specifically related to the U-box of CMPG1 as it was only visualized for Chimera II (Fig.

5.8.B). It is tempting to speculate that this double band is caused by an AVR3a induced modification of the CMPG1 U-box.

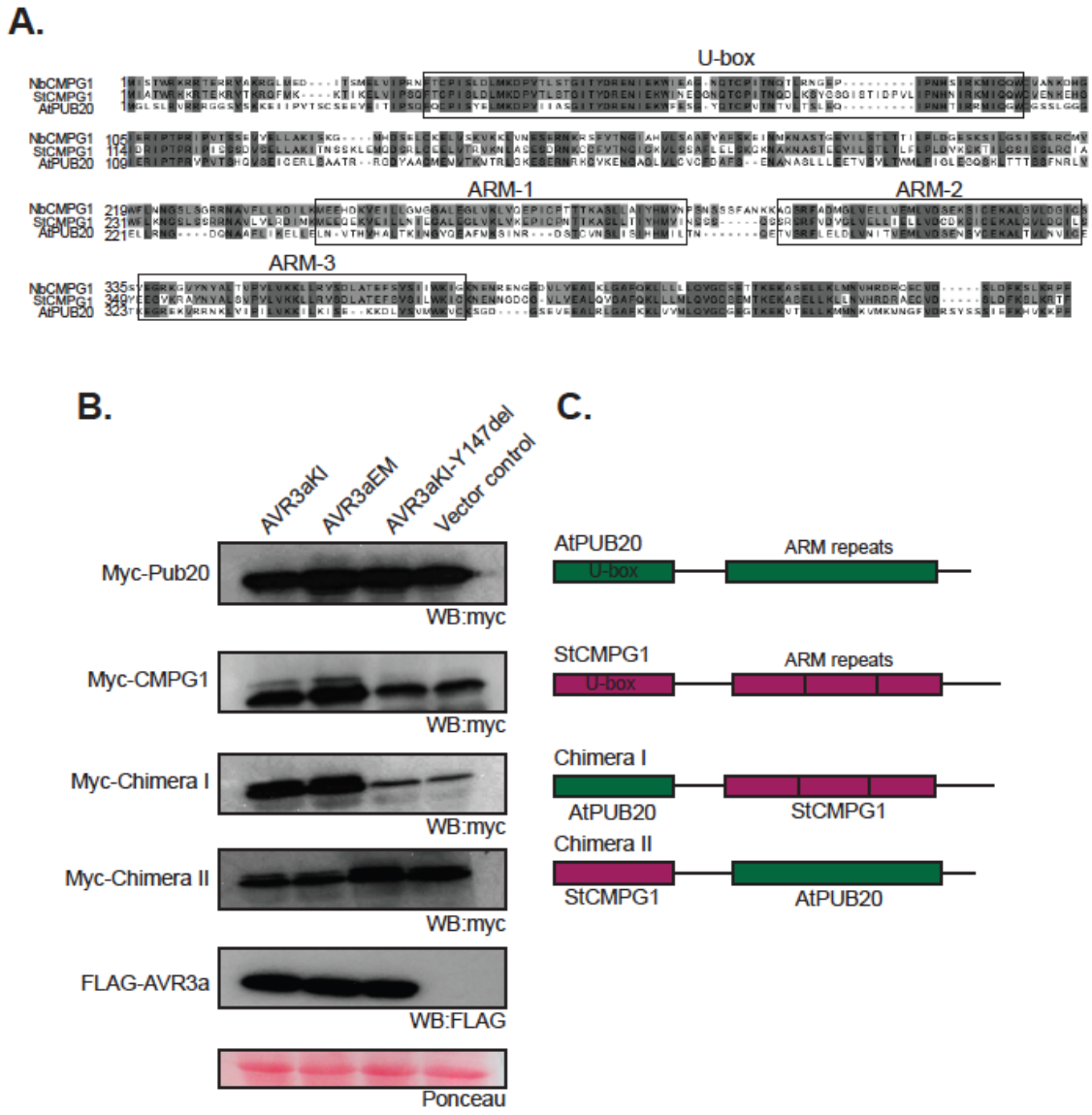

Fig. 5.2.8. CMPG1 stabilization requires its ARM-containing domain

(A) ClustalW alignment showing CMPG1 from *S. tuberosum*, *N. benthamiana* and their closest homolog in Arabidopsis PUB20. Amino acid residues are shaded dark grey if identical and a lighter shade of grey if similar. Sequences were viewed in Jalview. The U-box domain important for E3 ligase activity and the position of the ARMADILLO (ARM) repeats based on the StCMPG1 sequence is indicated. (B) Transient expression of 4x-myc-StCMPG1, or 4x-myc-Chimera I, or 4x-myc-Chimera II, or 4x-myc-PUB20 in the presence of FLAG- AVR3a^{KI}, or FLAG- AVR3a^{EM}, or FLAG- AVR3a$^{KI\text{-}147del}$, or vector control (pBinplus-ΔGFP). Immuno blots showing AVR3a stabilization and putative modification (seen as a double band) of StCMPG1 and Chimera I by AVR3a^{KI} and AVR3a^{EM} at 4 DPI. Protein loading control is shown by Ponceau

staining. (C) Schematic representation of the chimeric construct between StCMPG1 (magenta) and AtPUB20 (green).

5.2.9. ROS suppression by members of the *AVR3a* family

Variants of *P. infestans* AVR3a show differential activities as descried earlier. However, all variants of AVR3a suppressed early defense responses triggered by flg22. This overall suppression of PTI elicited by flg22 suggests that there could be uncharacterized PAMPs from *P. infestans* signaling through a pathway similar to FLS2/flg22. Given that AVR3a^{EM} shows the same level of suppression as AVR3a^{KI} for flg22-triggered responses, it is possible that suppression of such pathway is the more ancient activity of this effector, and it is therefore conserved among other members of the AVR3a family in other species of *Phytophthora*. To address this possibility, I transiently expressed 6 members of the *AVR3a* family from *P. infestans*, *P. sojae*, and *P. capsici* in *N. benthamiana*. Elicitation with flg22 (100 nM) was performed and the ROS burst was measured at 3 DPI. One homolog of AVR3a from *P. infestans* PEX147-3 and one from *P. sojae* AVR1b were able to suppress flg22-induced ROS. PEX147-3 suppressed ROS to the same extent as AVR3a^{KI} whereas AVR1b showed only 40% suppression activity (Fig. 5.9). Other members of the *AVR3a* family tested did not have any impact on the suppression of flg22-ROS although their subcellular localization is also cytoplasmic and nuclear as *P. infestans* AVR3a (Fig. A2.4). Given that the suppression activity seems widespread it is possible that this is indeed the more ancestral activity of AVR3a.

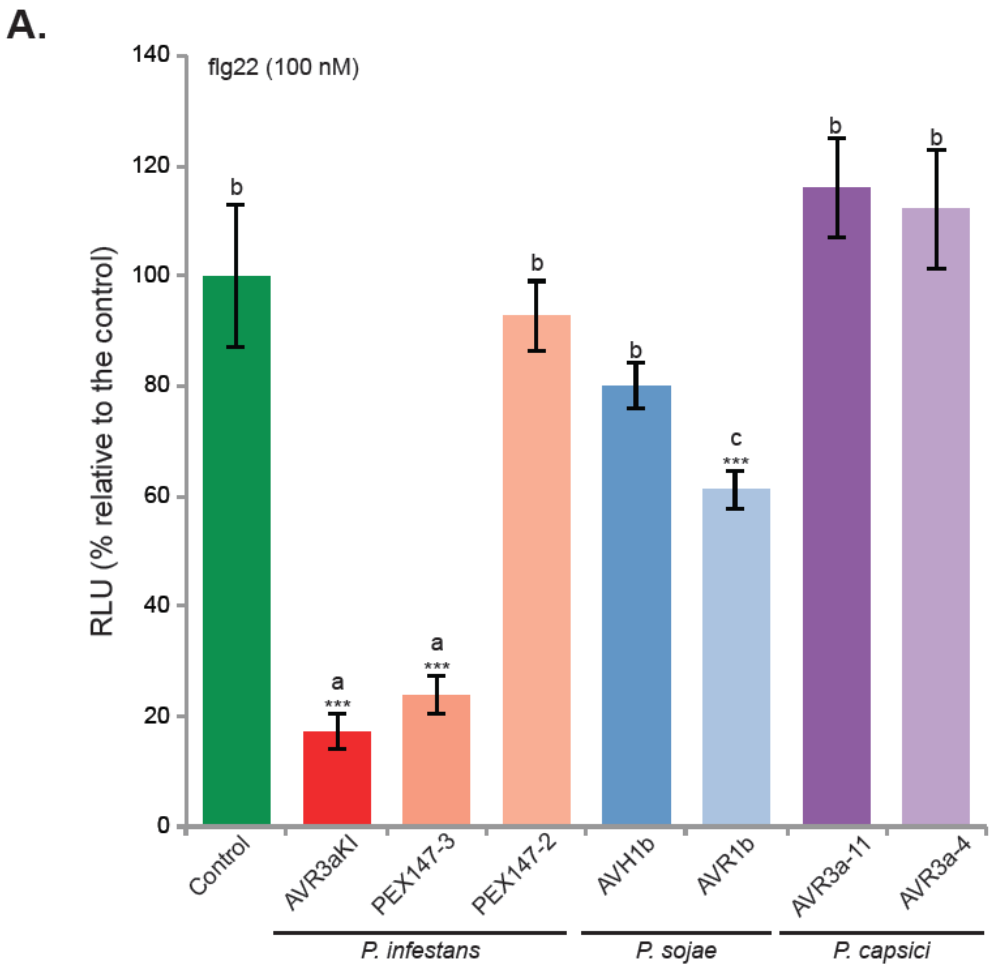

Fig. 5.2.9. Other members of the *Avr3a* family can suppress flg22-induced ROS

(A) Oxidative burst triggered by 100 nM flg22 in *N. benthamiana* agro infiltrated with members of the *Avr3a* family in the pTRBO vector. ROS production was measured in relative light units (RLU) over time and depicted as relative to the total ROS burst of the control. Values are average ± SE (n = 16). Statistical significance was evaluated in comparison to the control by one-way ANOVA followed by Tukey HSD test. *** P < 0.001. Experiment was repeated 4 times with similar results.

5.3. Discussion

Early recognition of pathogen molecular signatures by receptors at the plasma membrane is one of the hallmarks of plant defense and many pathogen effectors target these early events. In this chapter I showed that AVR3a inhibits basal plant immunity as evidenced by ROS suppression and transcriptional reprogramming induced by PAMP elicitors. Interestingly, AVR3a suppressed defense responses mediated by PRRs that require the co-regulator SERK3/BAK1 for signaling.

One key aspect toward understanding the molecular mechanism by which AVR3a suppresses immune responses is to assess where along the signaling cascade AVR3a

exerts its suppression activity. In recent years the molecular steps after PAMP recognition have been widely studied and it is possible to monitor the immune responses almost in real time. One mechanism by which bacterial effectors disrupt PTI is by targeting the receptors directly. For example, the bacterial effector AvrPtoB associates with FLS2 and through its U-box E3 ligase ubiquitin domain ubiquitinates the receptor to promote FLS2 degradation inactivating flg22-signaling (Gohre et al., 2008). Therefore, one possibility is that AVR3a might alter PTI at the receptor level. With this in mind, I was able to show that one of the earliest steps after PAMP perception, the complex formation between FLS2 and SERK3/BAK1, was not altered by AVR3a neither the steady state levels or localization of the receptors. Another possibility could be that AVR3a associates with the receptors themselves or interferes with their kinase activity. Multiple attempts to test AVR3a association with FLS2, EFR and SERK3/BAK1 failed suggesting no interaction or that the experimental approach required further optimization. Although there is no evidence favoring AVR3a action downstream of SERK3/BAK1, AVR3a does not have a membrane localization that would point to interference at the receptor level. For example, AvrPto localizes to the plasma membrane and it has been shown to interact with the kinase domain of FLS2, EFR and SERK3/BAK1 (Xiang et al., 2008). However, it cannot be ruled out that AVR3a might impact receptor auto phosphorylation or trans phosphorylation activities.

AVR3a also suppressed changes in gene expression after PAMP perception pointing to a broad and sustained effect of PTI suppression. Gilroy and colleagues (2011) showed that AVR3a and CMPG1 co-localize in the nucleus. Therefore, one possibility is that AVR3a targets CMPG1 to shuttle to the nucleus where it exerts its inhibition of gene expression perhaps through unknown transcriptional factors. The E3 ligase ARC1 is involved in the self-incompatibility pathway in the pistil downstream of the self-incompatibility S receptor kinase (SRK) and it was shown to shuttle between the cytosol and the nucleus requiring an intact U-box (Stone et al., 2003). Accordingly, the nuclear localization of AVR3a should be assessed for its biological relevance also in the context of its interaction with CMPG1. Another PTI canonical output is ROS production. In this work only ROS production was assessed in the context of CMPG1 over expression or silencing but my results point to a role of CMPG1 as a negative regulator of PTI responses. E3 ligases closely related to CMPG1 have been shown to act as negative regulators not only of ROS production but also MAPK activation and transcriptional induction (Trujillo et al., 2008). In line with a role of CMPG1 as a negative regulator of PTI responses, silencing CMPG1 leads to less *P. infestans* growth (Bos et al., 2010). Since stabilization is not the only visible effect on CMPG1 by AVR3a (the presence of a second band indicates some sort of modifications) the most probable explanation is that the modifications exerted by AVR3a on CMPG1 and not

shifts in CMPG1 protein pool, are the cause of alterations in the substrates that CMPG1 regulates.

Ubiquitination is the covalent addition of a small ubiquitin moiety to cellular proteins that results in the post-translational regulation of a variety of cellular process either by targeting them to the proteasome or changing the localization of the target protein (Smalle and Vierstra, 2004). Toll-like receptor activity is activated through ubiquitination after perception of PAMPs (Boyer and Lemichez, 2004) and FLS2 in plants is itself polyubiquitinated by E3 ligases for down regulation of signaling after flg22 perception by sending the receptor for degradation (Lu et al., 2011). Bacterial effector AvrPtoB targets FLS2 for degradation through its E3 ligase activity (Gohre et al., 2008). It is then possible that AVR3a modulates CMPG1 activity to fine tune defense responses in a less evident way than just promoting receptor degradation perhaps by changing polyubiquitination to monoubiquitination, which would instead promote a change of localization of the targeted protein or by altering ubiquitin-mediated endocytosis of the receptor. Since the receptors per se did not seem to be targeted by AVR3a, checking for receptor alteration by means of phosphorylation (Xiang et al., 2008; Xiang et al., 2011) did not seem relevant. However, it would be interesting to test whether CMPG1 has any effect on PRR stability or subcellular localization.

The *avr3a* allele encoding AVR3a^{EM} is the most prevalent one in *P. infestans* populations (Bos et al., 2006) pointing to a key function. However, its virulence function has not been clearly established. Since AVR3a^{EM} suppresses flg22-induced ROS, the suppression of basal defense responses might be the ancestral function of AVR3a. Supporting this hypothesis homologs of AVR3a from other *Phytophthora* species also showed the same suppression activity although to a different extent. This suggests that perhaps the host process that AVR3a and homologs across *Phytophthora* species target is a more general defense plant mechanism as opposed to the specific INF1-responses, which are only affected by AVR3a^{KI}. It was surprising that none of the homologs of AVR3a in *P. capsici* had an effect on early defense responses given the high degree of structural similarity (Boutemy et al., 2011; Yaeno et al., 2011). It is probable that the particular tested homologs fulfill other activities beneficial to *P. capsici* and since this family is highly divergent and has a large number of homologs, other effectors of this family might then suppress PTI (Bos, 2007). PEX147-3 is a paralog of AVR3a in *P. infestans* that is recognized by R3a but does not suppress INF1 cell death. Nevertheless, this paralog was able suppress flg22 ROS burst to the same extent as AVR3a. This gene is not expressed in *P. infestans* (Bos, 2007) but supports the fact that suppression of a flg22-like elicited pathway is a common virulence function of AVR3a and perhaps AVR3a^{KI} and AVR3a^{EM} additionally gained the ability to

suppress INF1-triggered responses. It is intriguing that the overexpression of AVR3a^{EM} did not enhance *P. infestans* pathogenicity in *N. benthamiana* probably reflecting that AVR3a^{KI} is in general a better suppressor of plant immunity. Of course, there is the cost of recognition should the plant carry the cognate *R* gene.

5.4. Conclusions

In this chapter I showed that AVR3a suppression of early defense responses is specific to PTI signaling pathways for which the co-regulator of PTI SERK3/BAK1 is required. Equal levels of suppression by variants of AVR3a after elicitation by the bacterial PAMP flg22, may indicate that AVR3a targets a common mechanism involved in the recognition of an unknown oomycete PAMP and flg22-induced PTI responses. Generally, flg22-response suppression is prevalent in AVR3a variants and homologs from other *Phytophthora* species and thus represents the most ancient activity of AVR3a. Future experiments aiming to identifying the precise molecular mechanism of AVR3a suppression of PTI should reveal novel plant components and thereby identify the conserved mechanism involved in regulating PTI responses to flg22 and to unknown oomycete PAMPs.

CHAPTER 6: *Phytophthora infestans* RXLR effector AVR3a targets a GTPase involved in plant immunity

6.1 Introduction

Plant-associated microorganisms secrete effector proteins to various sites in the host cell to alter host structure and processes to promote colonization and successful infection (Kamoun, 2006; Hogenhout et al., 2009). It is becoming evident that effectors target critical cellular plant processes beyond innate immunity to achieve virulence (Bhavsar et al., 2007; Canonne and Rivas, 2012). Several effectors from diverse families accumulate in the nucleus (Van den Ackerveken et al., 1996; Hotson et al., 2003; Bai et al., 2009; van Damme et al., 2012) and some others target the host cytoskeleton (Bhavsar et al., 2007; Lee et al., 2012). For example, the bacterial effector HopM1 localizes to the trans-Golgi network where it targets an important member of vesicle trafficking AtMIN7 for degradation to manipulate the outcome of defense responses (Nomura et al., 2006; Nomura et al., 2011).

P. infestans is a hemibiotroph which during its biotrophic phase of infection penetrates the epidermal cells forming an infection vesicle and a feeding structure known as haustoria, which expands from the penetration site towards neighboring cells (Kamoun et al., 1999; van Damme et al., 2009). Haustoria are digit-like structures that cause invagination of the host membrane and provide a specialized interface of interaction between *P. infestans* and its host. It is thought that at this interface *P. infestans* delivers effector proteins to re-program host processes to further infection and colonization. Interestingly, two *P. infestans* effectors AVR2 and AvrBlb2 re-localize from the plasma membrane to the site of infection around haustoria (Bozkurt et al., 2011; Saunders et al., 2012) highlighting how crucial and highly dynamic this stage of infection is. Recently Lu and colleagues (2012) reported that there are differences in the recruitment of host proteins to the extrahaustorial membrane (EHM) between the oomycete *H. arabidopsidis*, an obligate biotrophic pathogen, and *P. infestans*. For example FLS2 is actively recruited around the EHM in *H. arabidopsidis* (Hpa) but is completely absent from the EHM that surrounds *P. infestans* haustoria. Remarkably, stressing the dynamic nature of the interface between the plant cell and the oomycete haustorium, active endosomal trafficking occurs in infected cells with Hpa and most of the tested host proteins involved in endocytic trafficking accumulate around Hpa and Pi haustoria (Lu et al., 2012). Finally, rearrangement of cytoplasmic strands, endoplasmic reticulum (ER) and Golgi around the site of oomycete infection has also been reported for non-host, incompatible and compatible interactions (Takemoto et al., 2003).

The *P. infestans* RXLR effector AVR3a has two forms, AVR3a^{KI} and AVR3a^{EM}, which differentially suppress PTI responses triggered by INF1. However, both forms and the mutant AVR3a$^{KI\text{-}Y174del}$ suppress flg22-induced ROS and subsequent plant gene induction to a similar extent (Chapter 5). CMPG1 is one host protein that is involved in the differential suppression of INF1 responses by AVR3a variants. Both AVR3a^{KI} and AVR3a^{EM} interact with and stabilize CMPG1 but the AVR3a variant (AVR3a$^{KI\text{-}Y174del}$) that can no longer suppress INF1 cell death does not interact with or stabilize CMPG1 pointing to a key role of CMPG1 in INF1-elicited cell death. However, it was intriguing that all AVR3a variants equally suppress flg22-activated PTI, indicating that AVR3a also interferes with a CMPG1-independent pathway and, suggesting additional effector activities.

The pattern recognition receptor FLS2 is internalized upon flg22 elicitation into vesicles and this internalization is impaired by chemical inhibition of the endocytic pathway indicating that FLS2 does undergo endocytosis (Robatzek et al., 2006). Recent reports also indicate that FLS2 is constitutively recycled from the plasma membrane and co-localizes with the endosomal markers ARA7 and ARA6 confirming FLS2 distribution into endosomes (Beck et al., 2012). Given that endosomal trafficking is such an important regulator of protein homeostasis (Reyes et al., 2011) and that FLS2 is excluded from the EHM during *P. infestans* infection (Lu et al., 2012), it seems possible that AVR3a targets cellular trafficking pathways to suppress plant immunity. Therefore, in this chapter I first investigated the impact of AVR3a on FLS2 endocytosis upon ligand binding (Robatzek et al., 2006) and found that all variants of AVR3a inhibit this process. In order to get some insights into the mechanism by which AVR3a interferes with the host endocytic pathway to support *P. infestans* pathogenicity, additional plant targets of AVR3a were searched using plant protein complex purification. A homolog of the Arabidopsis dynamin-related proteins DRP2A/B was found. Dynamin is a GTPase protein involved during endocytosis in the scission of clathrin-coated vesicles (Robatzek, 2007; Ferguson and De Camilli, 2012). Additional results in this chapter also demonstrate that dynamin does associate with all variants AVR3a and that over expression of this dynamin *in planta* suppresses flg22-elicited ROS, and it is required by AVR3a to suppress INF1 cell death. Moreover, dynamin overexpression enhances *P. infestans* infection in *N. benthamiana* suggesting that dynamin might be a susceptibility factor in the *P. infestans/N. benthamiana* interaction.

6.2. Results

6.2.1. AVR3a inhibits FLS2 endocytosis

In chapter 5, I described that AVR3a^{KI} was overall a better suppressor of INF1-elicited responses compared to other variants of AVR3a probably through stabilization of CMPG1 as suggested by Bos and colleagues (2010) for INF1 cell death suppression activity. However, all variants of AVR3a suppressed defense responses triggered by flg22 to the same extent. Experiments aiming to identify a direct effect of AVR3a on FLS2 protein or immediate signaling mechanisms did not give positive evidence for direct involvement. An alternative possibility is that perhaps AVR3a might alter FLS2 internalization. It remains to be tested whether altered FLS2 localization in endosomes upon treatment with flg22 is part of the signaling cascade or a regulatory mechanism for attenuation of signaling (Geldner and Robatzek, 2008). Previous studies showed that chemical impairment of FLS2 internalization had an effect on flg22-triggered oxidative burst and gene expression (Serrano et al., 2007). Therefore, the internalization of the membrane-bound receptor FLS2 induced by flg22 (Robatzek et al., 2006) was followed in the presence of AVR3a. I used 4 to 5 week-old stably transformed *N. benthamiana* expressing different variants of AVR3a under a constitutive promoter and transiently expressed full length AtFLS2-GFP. After 2.5 DPI I treated half of the leaf with water and the other half with flg22 and checked for the occurrence of FLS2-GFP labeled endomembrane compartments at 60 min and 120 minutes. Using confocal microscopy I observed that after 60 minutes FLS2 localization was still at the periphery and visible vesicles were not observed irrespective of the treatment (data not shown). However, in the vector control plants, after 120 minutes of flg22 treatment, fluorescence of FLS2 was detected in small vesicles close to the PM whereas in the samples treated with water not such distribution was observed (Fig. 6.2.1.A). Surprisingly, in the presence of all AVR3a variants (AVR3a^{KI}, AVR3a^{EM}, and AVR3a$^{KI\text{-}Y147del}$), FLS2-GFP flg22-induced internalization was inhibited (Fig. 6.2.1.A). Similar results were obtained upon transient co-expression of both FLS2 and AVR3a (Fig. A3.7). This suggests that possibly AVR3a targets a host component required for FLS2 internalization to modulate early defense responses probably to dampen or interfere with membrane-bound receptor-endocytosis as this signaling step seems to be required to mount full resistance (Robatzek et al., 2006).

In Arabidopsis, the internalization process of FLS2 seems to progress faster and the fraction of FLS2 at the PM tends to disappear (Robatzek et al., 2006). In *N. benthamiana* the fraction of FLS2 at the PM was still abundant and occurrence of FLS2-GFP labeled endomembrane compartments took a longer time to visualize. Nevertheless, Beck and colleagues (2012) seemed to have similar results when using

tomato FLS2 indicating that there are some intrinsic differences in the endocytic process between plant species. It cannot be ruled out that there might be subtle differences between the receptors from Arabidopsis and *N. benthamiana* that require species-specific components to achieve a full response as I showed in chapter 4 for the RLP ELR1 (all experiments done in this thesis were conducted with the Arabidopsis FLS2 fused to GFP).

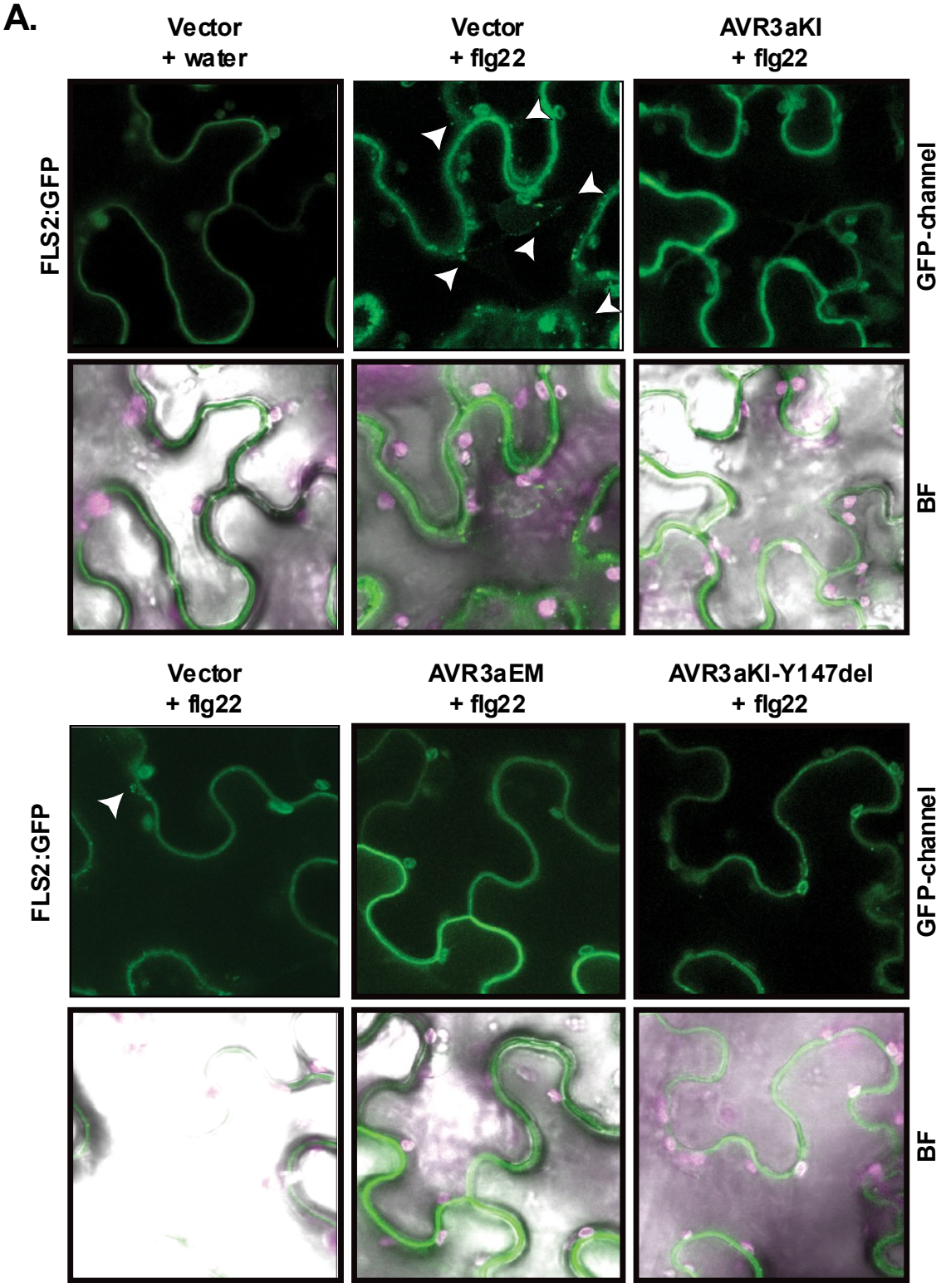

Fig. 6.2.1. AVR3a inhibits FLS2 endocytosis

(A) *N. benthamiana* plants stably expressing FLAG-AVR3a^{KI} or FLAG-AVR3a^{EM} or FLAG-AVR3a$^{KI\text{-}Y147del}$ or the vector control (pBinplus) were infiltrated with AtFLS2-GFP and at 2.5 DPI challenged with 10 μM flg22 or water as indicated for 120 minutes. Representative images showed a clear accumulation of FLS2 in vesicles after flg22 elicitation in the vector control plants (white arrows) whereas this distinct re-distribution of FLS2-GFP was inhibited by the presence of all variants of AVR3a. All images are a maximum projection of 20 slices taken at

10-μM step-size. Same confocal settings were used to acquire all images. Experiment repeated at least four times with similar results.

6.2.2. AVR3a associates with a plant protein involved in cellular trafficking

Given that all variants of AVR3a suppressed defense responses triggered by flg22 and inhibited flg22-elicited FLS2 internalization to the same extent, I reasoned that perhaps a virulence activity of AVR3a might be to interfere with basal defense responses triggered by a yet-to-be-identified *Phytophthora* PAMP that signal through a similar pathway as flg22. Since the suppression of flg22-responses was equal among the AVR3a variants, including AVR3a$^{KI\text{-}Y147del}$, which doesn't bind CMPG1, AVR3a must be interfering with a CMPG1 independent defense-signaling pathway. To further investigate this possibility, a search for additional plant targets of AVR3a was performed using complex purification with FLAG-AVR3a^{KI} in *N. benthamiana* followed by SDS-PAGE and in-gel trypsin digestion. Subsequent mass spectrometry analysis identified peptides matching the GTPase dynamin (gi|100255051|) specifically in the samples containing AVR3a in 3 out of 4 experiments performed (Table 6.2.1). Mascot searches were verified using Scaffold (Proteome Software). True indication of association was based on the following threshold in Scaffold: 95% confidence for protein match and a minimum of two unique peptide matches with 95% confidence. Additional plant proteins with a potential role in ribosome biogenesis and nucleo-cytoplasmic transport were also identified (Table 6.2.1; Experiment done in collaboration with Dr. Tolga Bozkurt).

Table 6.2.1. Plant proteins that associate specifically with AVR3a *in planta*

Identified protein	Description	Accession (GenBank)	Unique peptides			
			Exp. 1	Exp. 2	Exp. 3	Exp. 4
Dynamin	GTPase	gi|100255051	15	1	0	35
Nucleolin	Nuclear phosphoprotein	gi|21700195	8	0	0	33
Alpha-1-4-glucan-protein synthase (UDPforming)	Reversibly glycosylated polypeptide family protein (RGP)	gi|350537551	0	1	2	0

Dynamin is a GTPase presumably involved in endocytosis in the scission of clathrin-coated vesicles (Fujimoto et al., 2010; Chen et al., 2011). Recent evidence showed

that AVR3a has a phospholipid binding activity that is important for its ability to suppress INF1 cell death (Yaeno et al., 2011). Phosphoinositide-binding infers membrane association (Martin, 1998) and given that dynamin proteins also have the ability to bind phospholipids, it seemed possible that AVR3a and dynamin might indeed co-occur at endomembrane compartments. The latter explanation plus the putative role of dynamin in endocytosis were the selection criteria to further characterize the role of dynamin in AVR3a-related phenotypes.

From the mass spectrometry analysis the retrieved GTPase sequence corresponded to dynamin from *Vitis vinifera*. This sequence was used to search the available genome database of *N. benthamiana* and *N. tabacum* revealing partial sequences annotated as Dynamin-2A (DRP2A). Similar searches in early versions of the potato and tomato genome databases before the full genome sequence was released, yielded also incomplete sequence matches mainly covering the N-terminus and other regions along the *V. vinifera* sequence (data not shown). Partial sequences closer to the N-terminus and C-terminus along the *V. vinifera* sequence from *N. tabacum* and tomato were retrieved to generate several combinations of primers for cloning dynamin from *N. benthamiana* cDNA. All attempts to clone dynamin from *N. benthamiana* failed most likely because the region used for designing the primers is not conserved. However, in parallel I also used the same set of primers to clone dynamin from *N. tabacum* cDNA. I cloned two almost identical homologs (99% similarity, Fig. 6.2.2.A) from *N. tabacum*, which had their closest homologs in Arabidopsis (DRP2A and DRP2B, previously known as ADL6 and ADL3, respectively). NtDynamin A was 78% similar to DRP2A/B and had the closest genetic distance (Fig. 6.2.2.B). Homologs in Arabidopsis DRP2A and DRP2B are functionally redundant (Taylor, 2011) but it remains to be established whether this is the case for the paralogs in *N. tabacum*. Reciprocal tBlastn using the *N. tabacum* dynamin A or B sequence (herein NtDynA, NtDynB) as a query against the Arabidopsis genome confirmed the homology.

DRP2A and DRP2B are the only reported/characterized plant dynamin proteins that have all five dynamin-distinctive domains (Praefcke and McMahon, 2004). A search of databases for domain configuration revealed that NtDynA and NtDynB also follow the classical five-domain structure of known dynamin proteins (Fig. 6.2.2A; Fig. 6.2.3A): an N-terminal GTP binding domain (G domain); the middle domain; a Pleckstrin-homolgy domain (PH), which has the capacity to bind various phosphoinositides and it is possibly involved in association with membranes; the GTPase effector domain (GED), important for oligomerization; and the proline rich domain, which mediates interaction with proteins containing the SRC-homology-3 (SH3) domain, a protein module that interacts with proline-rich sequences and was first identified in the protein kinase Src,

hence the name (Lam et al., 2002; Praefcke and McMahon, 2004). Given the high degree of similarity of the *N. tabacum* dynamin proteins to each other, first I confirmed the association of AVR3a with NtDynA. Transient co-expression of GFP-NtDynA (in pK7WGF2) and FLAG-AVR3a^{KI} (in pTRBO) was carried out in 5 week-old *N. benthamiana* plants. Tissue was collected at 3 DPI and subjected to immunoprecipitation with GFP-trap beads (Chromotek). Complex formation was observed only between NtDynA and AVR3a^{KI} and not between NtDynA and other membrane associated *P. infestans* RXRL effector AVRBlb2 or GFP (Fig. 6.2.2.C). Moreover, the GFP tag was not cleaved but dynamin showed a double band in range of the expected size and a secondary protein-pool around 45 kDa (Fig. 6.2.2.C) suggesting that dynamin might undergo some modification and/or processing independent of the effector.

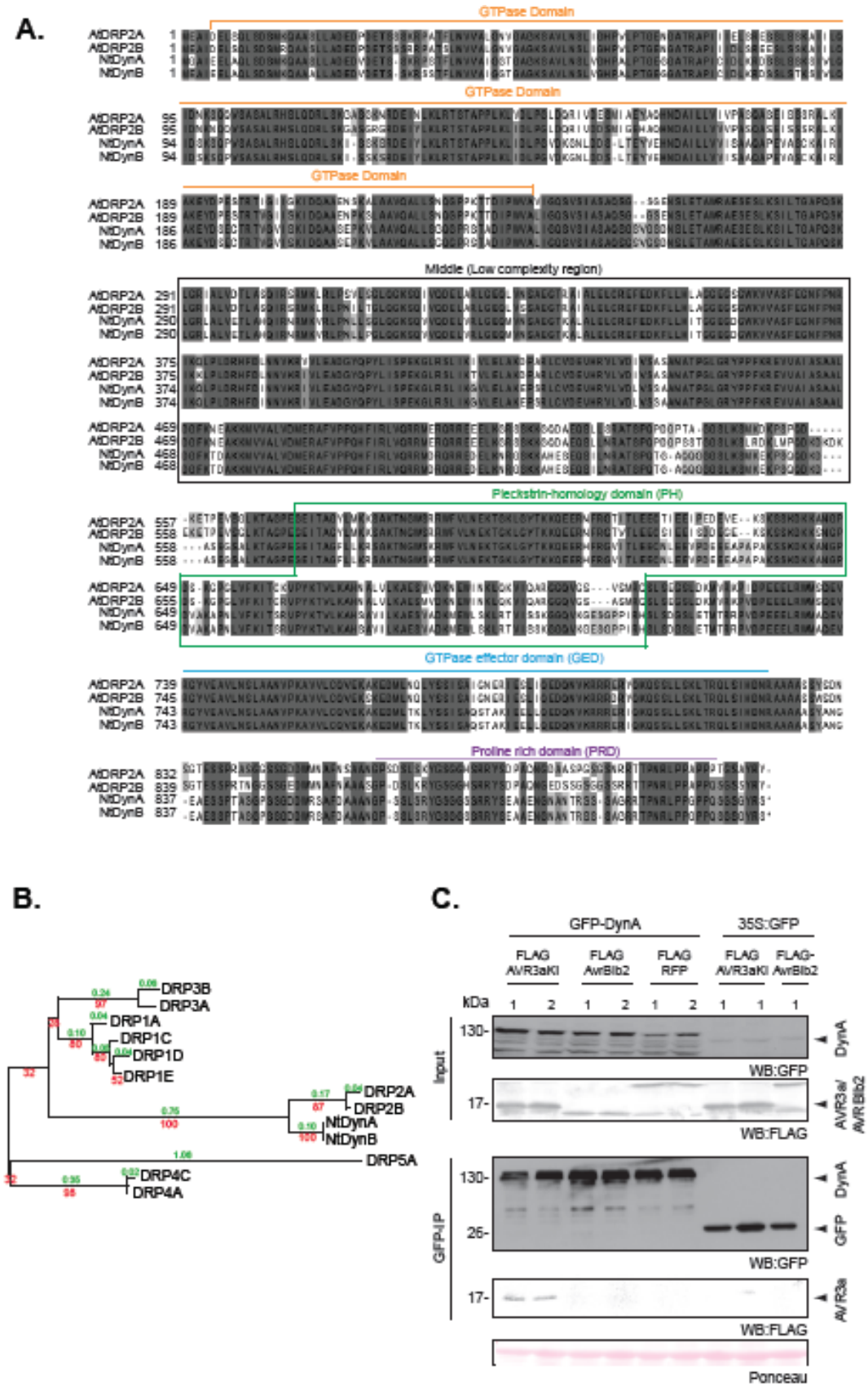

Fig. 6.2.2. AVR3a associates with NtDynaminA (NtDynA)

(A) ClustalW alignment showing homologs of AtDRP2/B in *N. tabacum*. Amino acid residues are shaded dark grey if identical and a lighter shade of grey if similar. Sequences were viewed in Jalview. Canonical domains are specified and color-coded according to the schematic in Fig. 6.2.3A. (B) Phylogenetic tree of Arabidopsis dynamin-related proteins (DRP) and *N. tabacum*

dynamin proteins A and B. The unrooted tree was constructed using maximum likelihood method (PhyML at Phylogeny.fr, Dereeper et al., 2008) with full-length amino acid sequences. Branch length (green values) represents the estimated genetic distance. Bootstrap (100) support values are in red. (C) DynA co-immunoprecipitated specifically with AVR3a in *N. benthamiana.* GFP-DynA was transiently co-expressed with FLAG-AVR3aKI or FLAG-AVRblb2 and immunoprecipitated with anti GFP-agarose beads. Immunoprecipitates and total extracts were immunoblotted with the appropriate antisera. Numbers on top of the blot correspond to two independent experiments. However, this experiment was repeated at least five times.

To evaluate whether NtDynA/B might have a similar biological role as DRP2A/B and their mammalian homolog (Lam et al., 2002), the subcellular localization of these proteins was studied by confocal microscopy. I generated N-terminal GFP fusions (Fig. 6.2.3.A) and transiently expressed them in *N. benthamiana*. Both NtDynA and NtDynB localized to the plasma membrane and the cytoplasm, probably suggesting that dynamin cycles between these two localizations according to its activity profile (Fig. 6.3.B; Additional images in Fig. A3.1A). Plasma membrane localization was retained upon plasmolysis (Fig. 6.2.3.C, far right panel). It is possible that PM accumulation is more favored after elicitation with an exogenous microbe elicitor, as membrane binding sites become available. *Drosophila* dynamin has been reported to also have PM localization (Damke et al., 1994). Interestingly, lower level expression of NtDynA or NtDynB in transient assays, achieved by reducing the initial infiltrated inoculum, revealed the presence of dynamin in a punctate distribution, previously masked by the high levels of expression, which might correspond to the trans-Golgi network (TGN). TGN distribution is usually seen enveloping the nucleus, which is more clearly seen in Fig. A3.1. It is also possible that the punctate distribution corresponds to coated pits hence co-localization studies with TGN and clathrin markers are necessary. However, reports have emerged linking the TGN to clathrin-mediated endocytosis and Arabidopsis DRP2A and DRP2B have also been localized to the TGN favoring the idea that the observed punctate localization might indeed correspond to the TGN (Lam et al., 2002).

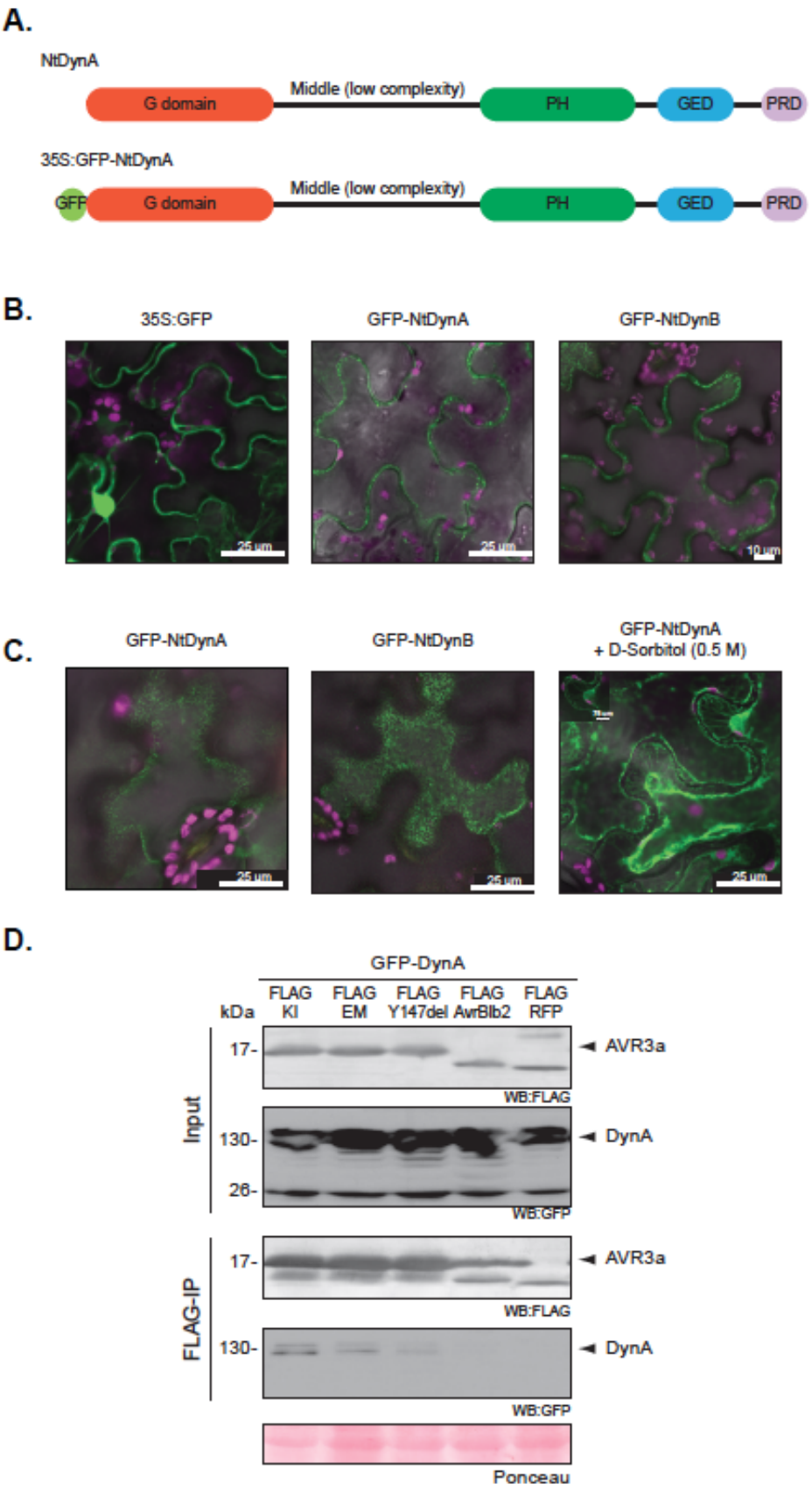

Fig. 6.2.3. Dynamin is a modular protein localized to the PM and cytosol that associates with all AVR3a variants *in planta*

(A) Schematic representation of *N. tabacum* dynamin (NtDynA) showing its domain organization. NtDynA has the canonical GTPase dynamin domains: GTPase domain (G domain), Pleckstrin homology domain (PH), GTPase effector domain (GED), and a proline-rich domain (PRD). (B)

and (C) *N. tabacum* Dynamin subcellular distribution. (B) Transient expression of GFP-DynA or GFP-DynB showed that both paralogs localized mainly to the plasma membrane (PM). PM localization was confirmed by plasmolysis (C), far right end. (C) Transient expression of NtDynA and NtDynB at a final OD_{600mm} of 0.05 - 0.1 showed a punctate or small vesicle-like distribution of dynamin. Scale bar values are shown in each picture. Representative confocal images were taken at 3 DPI. (D) All variants of AVR3a associated with NtDynA *in planta*. Co-expression in *N. benthamiana* of FLAG-AVR3a^{KI}, or FLAG-AVR3a^{EM}, or FLAG-AVR3a$^{KI\text{-}Y147del}$ with GFP-DynA was subjected to immunoprecipitation with anti-FLAG antiserum and blotted as shown. FLAG-AVRblb2 and FLAG-RFP were used as controls.

6.2.3. All variants of AVR3a associate with NtDynA *in planta*

If AVR3a mediates suppression of early defense responses triggered by flg22 and inhibit FLS2 endocytosis to the same extent by its interaction with dynamin, all variants of AVR3a should associate with dynamin. I did co-immunoprecipitation assays with anti-FLAG beads (SIGMA) following transient expression of GFP-NtDynA and FLAG-AVR3a^{KI} or FLAG-AVR3a^{EM} or FLAG-AVR3a$^{KI\text{-}Y147del}$ or FLAG-RFP in *N. benthamiana* in a 1:1 ratio (final OD_{600mm} 0.2). I found that all variants of AVR3a but not the control RFP, associated with dynamin to a similar extent (Fig. 6.2.3.D) indicating that this protein is part of a complex that is targeted by AVR3a.

6.2.4. NtDynA is involved in INF1 signaling but not in R3a-mediated HR

Next I studied the effect of increased dynamin levels on AVR3a activities. I transiently over expressed NtDynA in *N. benthamiana* and 1 DPI I challenged the leaves with INF1, NPP1 or a mix (2:1) of R3a/AVR3a^{KI}. I found that NtDynA over expression specifically enhanced INF1 cell death whereas NPP1 cell death was unaffected (Fig. 6.2.4.A) starting at 3 DPI. The difference was marked at the 3 DPI time point. At early days the development of the cell death was almost imperceptible, and starting at 4 DPI the infiltrated spots were completely necrotic (Fig. 6.2.4.A). In contrast, over expression of dynamin did not alter the progression of the hypersensitive response triggered by R3a and AVR3a^{KI} (Fig. 6.2.4.B). These results suggest that the cell death process as such is not enhanced by dynamin over expression and that the observed elevated INF1 response was rather specific.

I also determined whether NtDynA interferes with the ability of AVR3a^{KI} to suppress INF1 cell death. I observed that in NtDynA overexpressing leaf tissues AVR3a^{KI} was unable to suppress INF1-cell death to levels observed in wild type plants or the GFP control (Fig. A3.2A).

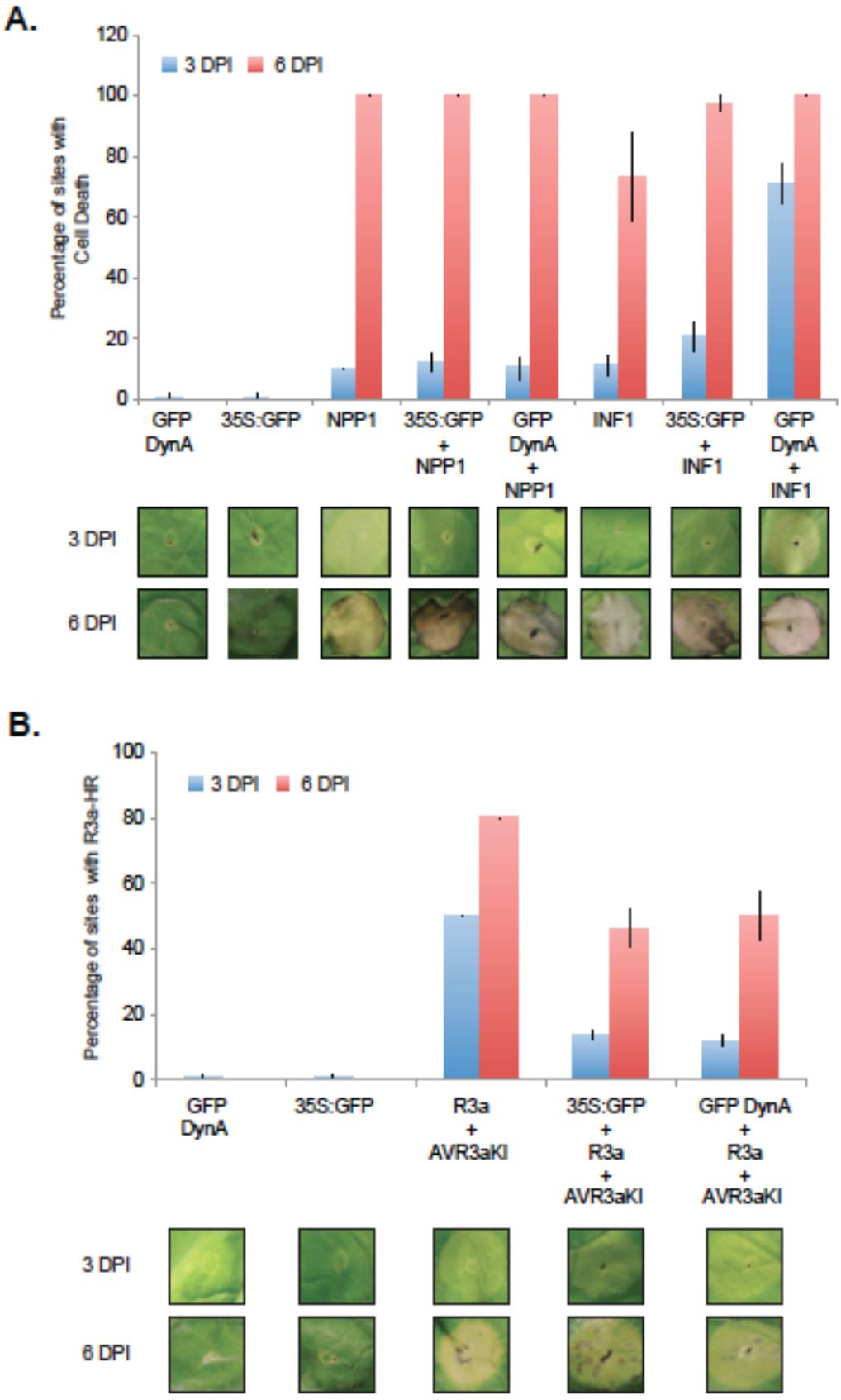

Fig. 6.2.4. NtDynaminA (NtDynA) overexpression enhances INF1-cell death but does not affect R3a-mediated hypersensitive response (HR)

(A) Leaves of *N. benthamiana* were infiltrated with either GFP-DynA or the control 35S:GFP and challenged one-day post infiltration with pGR106-INF1 or pGR106-NPP1. Percentages of

infiltration sites showing the cell death induced by INF1 or NPP1 are shown. Enhancement of the cell death triggered by INF1 started at 3 DPI whereas NPP1 cell death was not affected. At 6 DPI the effect was no longer visible. Similar results were obtained in at least three experiments and also when challenging with pTRBO-INF1 or pTRBO-NPP1. Values are average ± SE (n = 15). (B) Transient expression of GFP-DynA or 35S:GFP in *N. benthamiana* challenged one-day post infiltration with a mix of 35S:R3a and FLAG-AVR3a^{KI} (2:1). Percentages of infiltration sites with R3a-mediated HR scored at 3 and 6 DPI. Values are average ± SE (n = 18). Experiment was repeated at least three times with similar results.

To assess whether wild type dynamin levels are required by AVR3a to suppress INF1 cell death, silencing experiments were performed. Using virus-induced gene silencing (VIGS) aimed at both *NtDynA* and *NtDynB* I observed that attenuation of dynamin expression led to lethality (Fig. A3.3). The essential nature of dynamin has been observed before for DRP2A for *A. thaliana* development and cell cycle progression in gametophytes (Backues et al., 2010). To circumvent lethality, I generated a hairpin construct (in pHellsgate8) using the sequence of NtDynamin to knockdown *Dynamin* homologs in *N. benthamiana*, to be delivered by *A. tumefaciens* to transiently and locally silence dynamin. Knockdown of *NbDynamin* did not affect INF1 cell death or enhanced it but it impaired the ability of AVR3a to suppress INF1 cell death (Fig. 6.2.5.B,C). R3a-mediated hypersensitive response (HR) was not affected by silencing *dynamin* (Fig. A3.4). These results indicate that dynamin is involved in the activity of AVR3a to suppress INF1 cell death.

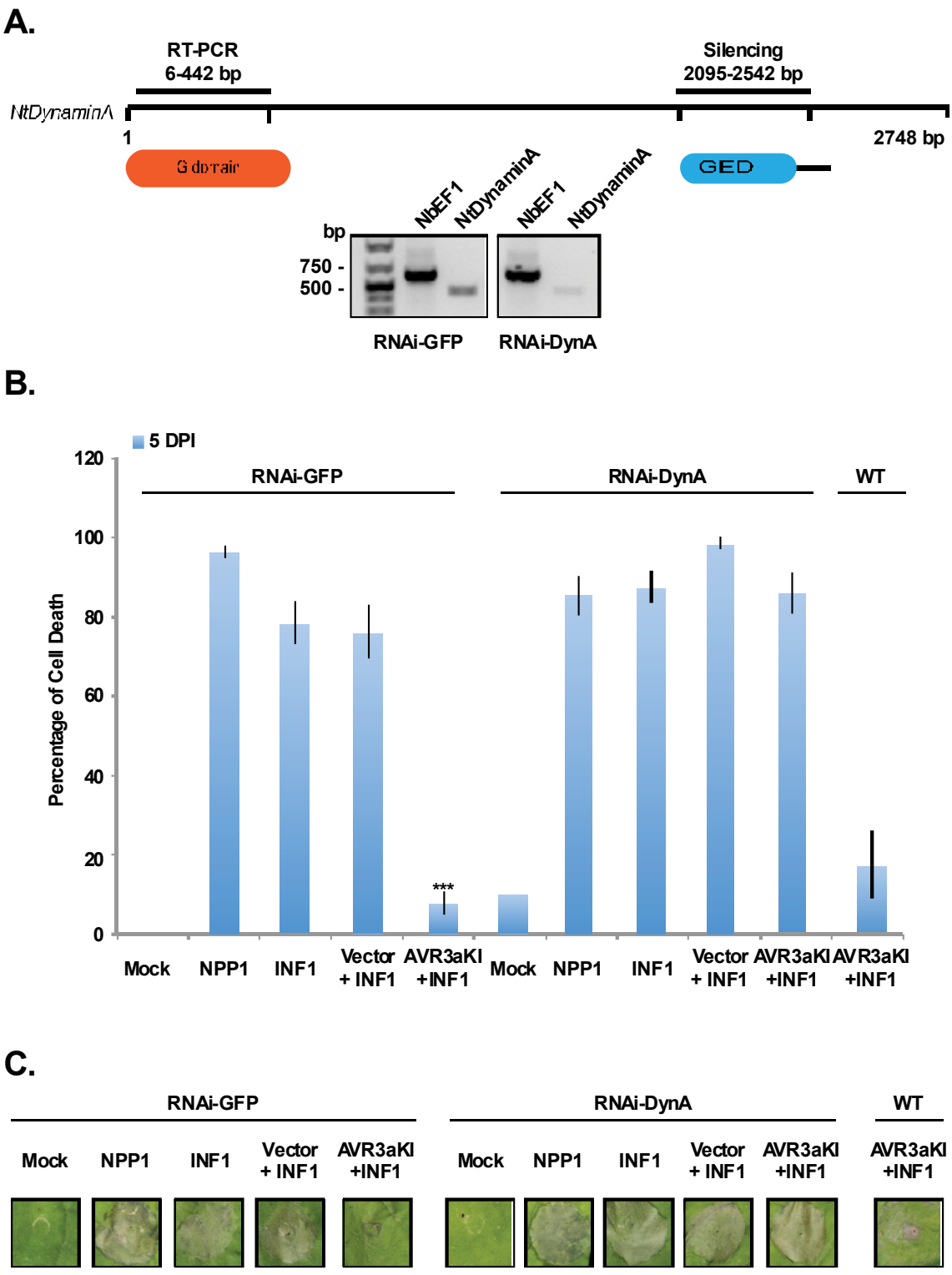

Fig. 6.2.5. *NbDynamin* is required by AVR3a to suppress INF1 cell death

Leaves of *N. benthamiana* were silenced locally via RNAi-mediated silencing using the vector pHellsgate8 harboring the fragment of dynamin depicted in (A) or a fragment targeting a region of GFP as a control. One and a half days post silencing, a mix (1:1) of FLAG-AVR3a^{KI} and pCB302:INF1 were infiltrated into leaves. RT-PCR was carried out on silenced leaf-discs using primers that amplify a region that does not overlap with the silencing target sequence (A). Validation of the silencing by RT-PCR (~150 ng cDNA) is shown in (A). Internal control *NbEF1α* has been described in Segonzac et al., 2011. (B) A histogram representing the percentages of cell death induced by INF1 in the presence or absence of AVR3aKI at 5 DPI. Values are

average ± SE (n = 15). Statistical significance was evaluated by one-way ANOVA followed by Tukey HSD test. *** P < 0.001. (C) Representative pictures of the cell-death phenotype scored at 5 DPI that was depicted in (B). Experiments were repeated at least three times.

6.2.5. NtDynA accumulates around *P. infestans* haustoria and enhances its growth

In animal systems, dynamin is an essential protein in the scission of vesicles including clathrin-coated vesicles that are a hallmark of the clathrin-mediated endocytic pathway (Praefcke and McMahon, 2004; Doherty and McMahon, 2009). To assess the effect of indirectly altering this process by manipulating dynamin concentrations in the cellular space on *P. infestans* pathogenicity, I transiently overexpressed NtDynA in *N. benthamiana* and at 1 DPI I inoculated detached leaves with a solution of *P. infestans* 88069 zoospores. *N. benthamiana* showed increase levels of infection and sporulation by *P. infestans* suggesting that dynamin might act as a negative regulator of defense responses towards *P. infestans* (Fig. 6.2.6.A). The moderate increase in growth was probably due to the low levels of overexpression of NtDynA (Fig. 6.2.6.D). Similar results were observed by expressing NtDynB (data not shown). However, depleting the levels of dynamin by transiently silencing dynamin did not have any impact on *P. infestans* growth measured as the total area of infection in mm^2 (Fig. A3.5A,B).

Next, I tested whether dynamin subcellular distribution was altered during infection. I inoculated *N. benthamiana* leaves transiently expressing GFP-NtDynA/B with a *P. infestans* strain expressing a red fluorescent marker tandem dimer RFP (*P. infestans* 88069td). GFP fluorescence was preferentially detected around haustoria in infected cells although PM localization was still seen (Fig. 6.2.6.C, Fig. A3.8). Accumulation of GFP-NtDynA around haustoria seemed to occur at the neck of the haustorium but also enveloping the whole surface of the haustoria (Fig. 6.2.6.C, Fig. A3.8). The same localization pattern was found for NtDynB (Fig. A3.6). This focal accumulation was seen at low expression (Fig. 6.2.6.B) and at higher expression levels, which seem to favor cytosolic distribution of NtDynA/B (data not shown). NtDynA/B show localization around haustoria, which represent newly, formed subcellular structures suggesting that dynamin localization might be influenced by cellular re-polarization.

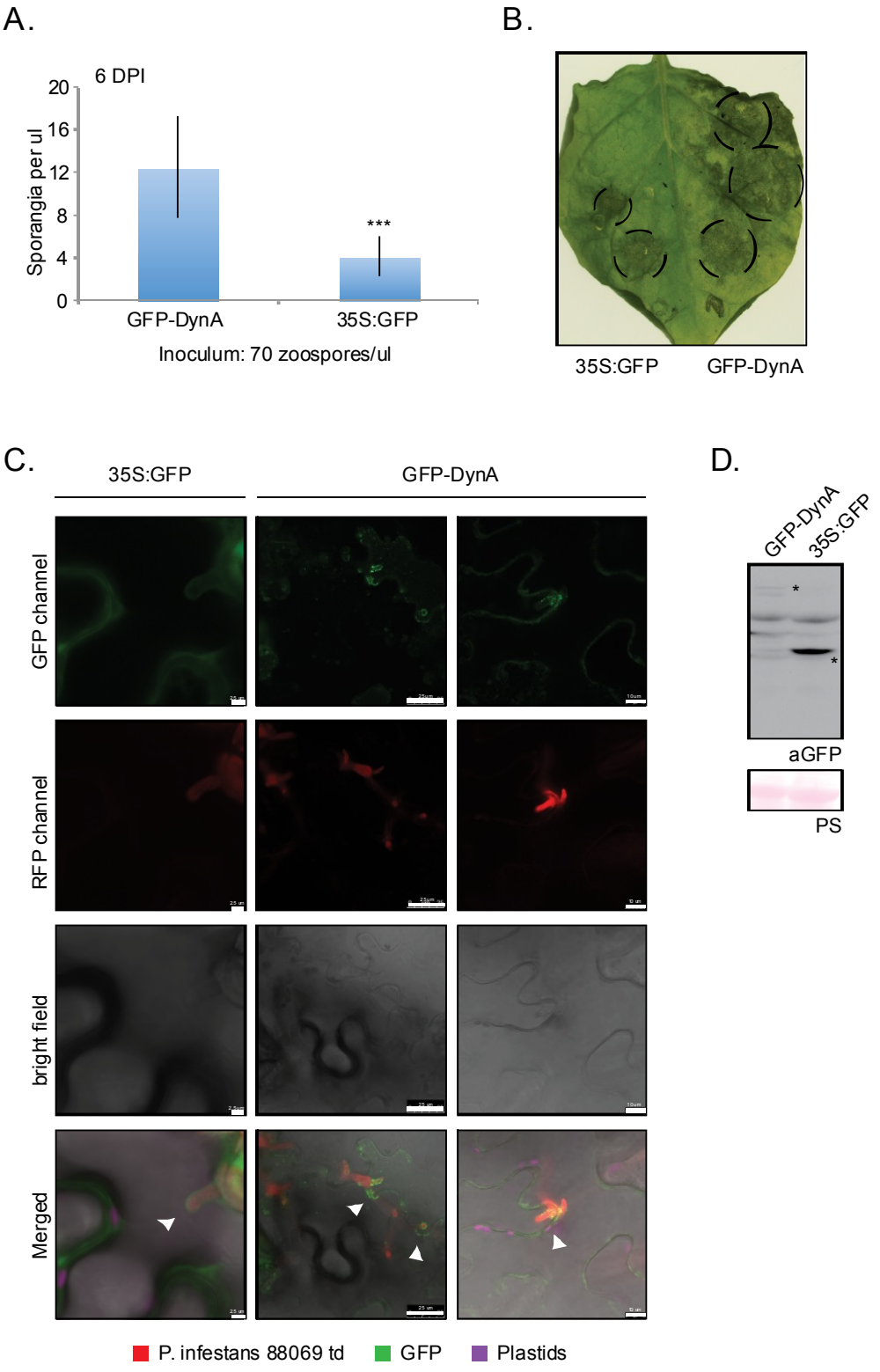

Fig. 6.2.6. NtDynaminA (NtDynA) accumulates around *P. infestans* haustoria and enhances *P. infestans* growth

Detached leaves of *N. benthamiana* (4.5 week-old) transiently expressing GFP-DynA or 35S:GFP were drop-inoculated at 1 DPI with *P. infestans* 88069. (A) Infection was scored by counting the sporangia at 6 DPI. GFP-DynA supported better and faster infection of *P. infestans* compared to the 35S:GFP control. Values are average ± SE (n = 15). Statistical significance was evaluated by T- test. *** P < 0.001. (B) Representative picture of the infection on (A). Experiment repeated three times with similar results. (C) Detached leaves of *N. benthamiana*

transiently expressing GFP-DynA or 35S:GFP were drop-inoculated at 1 DPI with *P. infestans* 88069-tdtom (100 zoospores/µl). Representative confocal images were taken at 3 days post infection. GFP-DynA accumulates around haustoria penetration sites (white arrows) and envelops the haustorium. For additional images see Fig. A.3.8.II (D) Immunoblot of the expressed constructs in (A). Asterisks indicate the protein expressed by the constructs used.

6.2.6. Overexpression of a dominant negative NtDynA variant attenuates *P. infestans* growth in *N. benthamiana*

To further examine the role of NtDynA in *P. infestans* pathogenicity, I introduced a mutation on the GTP-binding domain of NtDynA that has a reduced affinity for GTP favoring the inactive state of dynamin in its GDP-bound state (Damke et al., 1994; Damke et al., 2001). This mutant has one amino acid change at position 50 from where a conserved lysine is switched to glutamic acid (K50E) and has previously been characterized in homologs of dynamin as having a dominant negative effect (Taylor, 2011). Transient over expression of such mutant in *N. benthamiana* leaves did not show any detrimental effect in the agro infiltrated leaf patches. However, NtDynA-K50E overexpression did not support enhanced *P. infestans* growth as the wild type protein (Fig. 6.2.7.C). Instead, no alteration in growth behavior of *P. infestans* was detectable. Next, I assessed whether this could be due to mis-localization of the protein. Transient expression of GFP-DynA-K50E revealed that this mutant also had PM and cytosolic distribution and to a certain extent the dot-like pattern of the wild type protein (Fig. 6.2.7.A). In some cells I also observed some fluorescence at the nucleus but the expression levels were rather low and were not observable by total extract WB analysis (data not shown) and I could not address whether cleavage of the tag would explain this free GFP-like distribution. Given that impairment of GTP-binding (and possibly its hydrolysis) activity does not affect wild type subcellular distribution, I tested whether it might have an impact on the focal accumulation around *P. infestans* haustoria during infection. Following the same infection procedure as explained in section 6.2.5. I saw that GFP-DynA-K50E still localizes around *P. infestans* haustoria. This localization was seen for both *P. infestans* 88069td and *P. infestans* 88069 (Fig. 6.2.7.B,D). The functional basic unit for dynamin protein that is required for function is a dimer (Ferguson and De Camilli, 2012) and the previously described results suggest that a lack of GTP-binding activity probably does not affect the dimerization ability of dynamin, suggesting that dimerization might not be sufficient for downstream signaling.

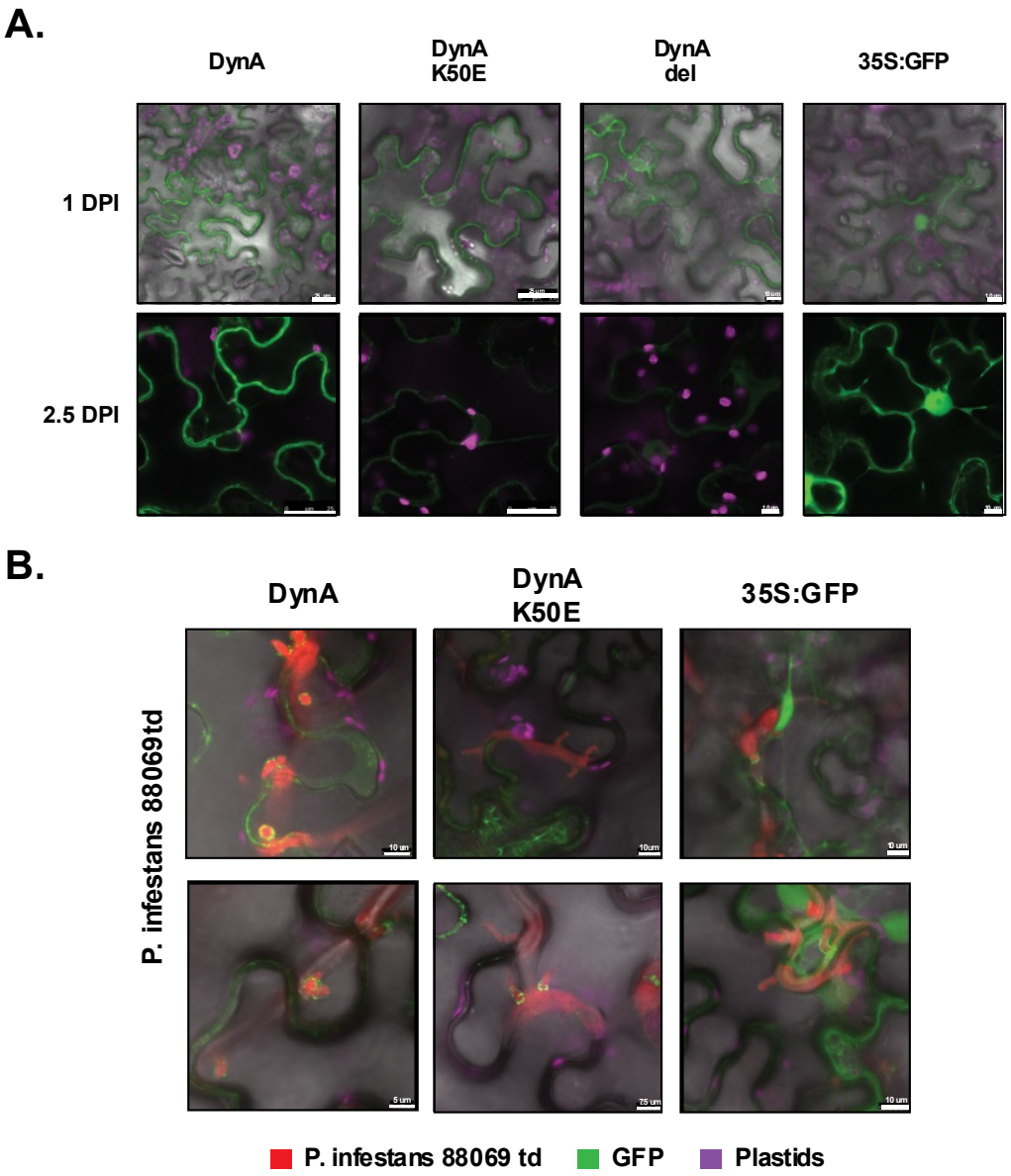
A.
DynA
DynA K50E
DynA del
35S:GFP
1 DPI
2.5 DPI
B.
DynA
DynA K50E
35S:GFP
P. infestans 88069td
P. infestans 88069 td
GFP
Plastids
C.
4 DPI
Infection area in square mm
30
25
20
15
10
5
0
***
DynA
DynA K50E
DynA del
35S:GFP
n=12
D.
P. infestans 88069
DynA
35S:GFP
DynA K50E
DynA del

Fig. 6.2.7. NtDynA accumulates around *P. infestans* haustoria and enhances *P. infestans* growth

(A) Transient expression in *N. benthamiana* of GFP-DynA or GFP-DynA-K50E or GFP-DynA-del or 35S:GFP (Final OD_{600mm} of 0.4) showing mainly plasma membrane (PM) localization for NtDynA as a result of overexpression. The GTPase mutant shows the same PM localization whereas the truncated version of dynamin resembles that of free GFP. However both mutants show low protein levels. Representative confocal images were taken at 3 DPI. Scale bar values are shown in each picture. (B) Detached leaves of *N. benthamiana* (4.5 week-old) transiently expressing GFP-DynA or GFP-DynA-K50E or 35S:GFP (Final OD_{600mm} of 0.3) were drop-inoculated at 1 DPI with *P. infestans* 88069-tdtom. Representative confocal images were taken at 3 days post infection. GFP-DynA and GFP-DynA-K50E accumulate around haustoria penetration sites. (C) Detached leaves transiently expressing GFP-DynA or GFP-DynA-K50E or GFP-DynA-del or 35S:GFP (Final OD_{600mm} of 0.3) were inoculated with *P. infestans* 88069 tdtom (100 zoospores/µl). Individual infection spots (6 per leaf, 12 leaves per construct) were followed with a Leica stereoscope and images were taken for each of them at 4 DPI. Images were processed as explained in the methods sections. Resulting values from the image analysis corresponds to area lesion size in mm^2. (D) Same experiment as in (B) except the infection was performed with *P. infestans* 88069. Representative confocal images were taken at 3 days post infection. GFP-DynA and GFP-DynA-K50E accumulate around haustoria penetration sites unlike GFP-DynA-del or 35S:GFP. Asterisks indicate haustoria.

6.2.7. Full-length dynamin is required for its localization around haustoria and enhancement of *P. infestans* growth

To further examine dynamin activity I generated a C-terminal truncated version of dynamin that lacks the last 344 amino acids comprising the PH, the GED and the PR domain (PRD) and that has been demonstrated to retain the GTPase activity of dynamin (Lam et al., 2002). It is thought that the ability to bind phosphoinositides resides in the PH domain and that this would target dynamin to the membrane or would be relevant for protein-protein interaction (Ferguson and De Camilli, 2012). Mutations aimed at the PH domain have a dominant negative effect on endocytosis (Ferguson and De Camilli, 2012) just as discrete deletions of the PRD (Damke et al., 1994). The PRD is important for interaction with SH3 containing proteins and this interaction recruits dynamin to the complex. Since both domains, PH and PRD, seem to be important for dynamin's proper recruitment and localization, testing a PH and PRD deletion mutant, called herein NtDynA-del, would allow the assessment of recruitment of dynamin (besides its proper localization to the PM) for its function. I found that DynA-del had mainly cytosolic distribution and a fraction of it accumulated at the nucleus (Fig. 6.2.7.A). As expected the focal accumulation of dynamin around haustoria requires active recruitment to it as lacking the PRD abolished this localization.

However, it could also imply that dynamin association to the haustoria requires its presence at the PM, which is achieved through its phospholipid-binding domain (Fig. 6.2.7.D). Constitutive expression of NtDynA-del did not provide the enhancement of *P. infestans* infection seen with the wild type protein (Fig. 6.2.7.C). These results indicate that this truncated protein cannot localize properly affecting NtDynA accumulation around haustoria, which by itself is not the only step needed towards influencing *P. infestans* infection output but dynamin's intrinsic activity most likely endocytosis.

6.2.8. Recruitment of dynamin around haustoria is not necessary for its association with AVR3a

To test whether the GTPase domain of dynamin is sufficient for association with AVR3a, I did co-immunoprecipitation experiments with FLAG-AVR3a^{KI} and GFP-DynA-del. Using GFP-trap beads (Chromotek), I pulled down dynamin proteins and checked for recovery of AVR3a^{KI}. Preliminary results showed that AVR3a^{KI} still associates with DynA-del (Fig. 6.2.8.A). Since DynA-del probably does not exert a dominant negative effect on the GTPase dynamin function and/or GTP hydrolysis it is possible that the G domain is actually the one mediating association with AVR3a. Interestingly, the dominant negative mutant of dynamin no longer associated with AVR3a^{KI} (Fig. 6.2.8.A). Given that the expression level of DynA-K50E is low, and even hard to visualize after Co-IP (Fig. 6.2.8.B), it is possible that lack of association with AVR3a is due to a technical limitation. However, it is tempting to speculate that the interaction of AVR3a with dynamin does indeed occur through the G domain and does not implicate dynamin's phospholipid-binding ability but only its GTPase activity.

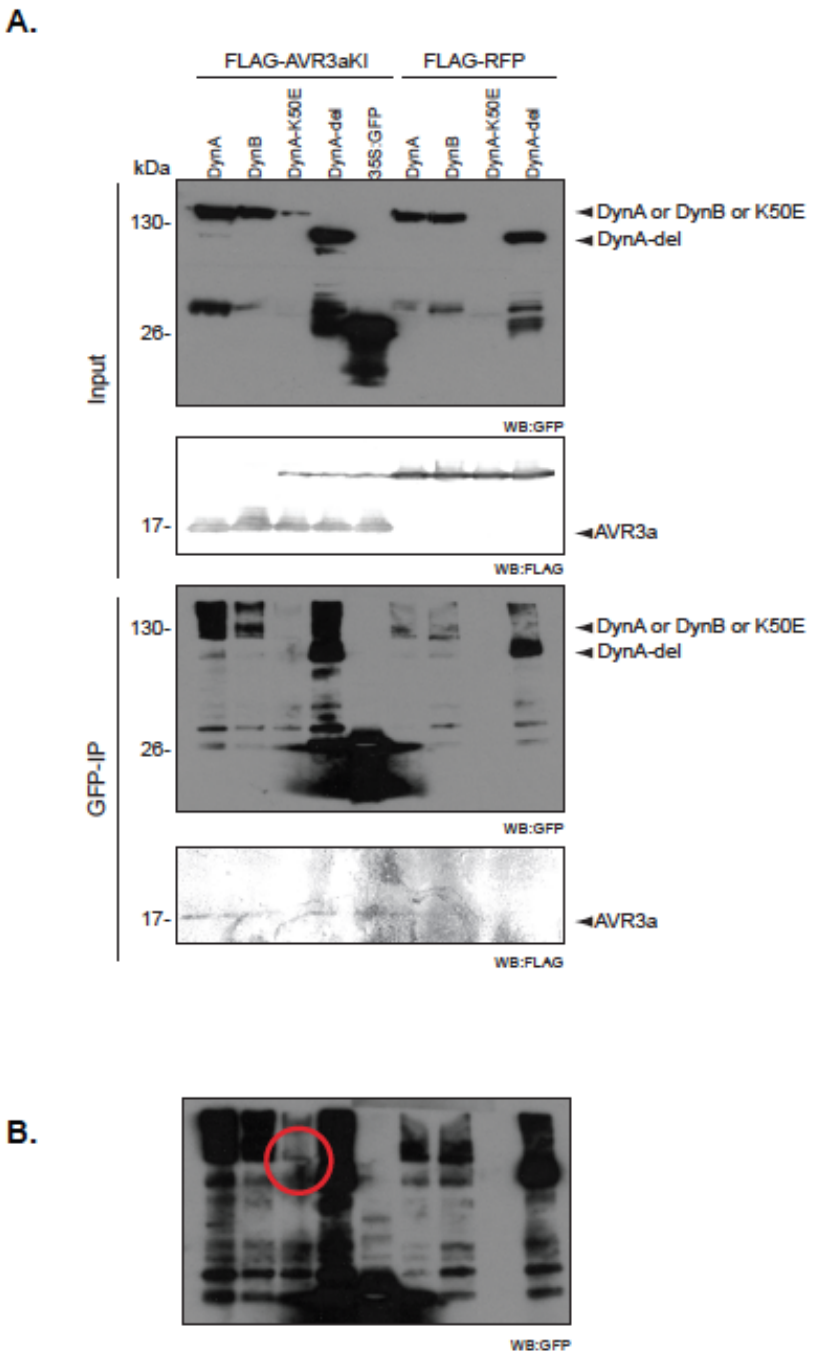

Fig. 6.2.8. NtDynA mutants show distinct association with AVR3a^{KI}

(A) DynA-del co-immunoprecipitated with AVR3a in *N. benthamiana*. FLAG-AVR3aKI or FLAG-RFP (in the TRBO vector) was transiently co-expressed with GFP-DynA or GFP-DynA-K50E or GFP-DynA-del or 35S:GFP (in the pK7FWG2 vector) and the dynamin protein were pulled down with anti GFP-agarose beads. Immunoprecipitates and total extracts were immunoblotted with the appropriate antisera. This is a preliminary result, done once. (B) Blot showing a longer exposure after immunoprecipitation and GFP WB. The red circle shows the very low amount of GFP-DynA-K50E protein recovered even after IP.

6.2.9. Altering dynamin cellular concentration affects the plant ability to produce ROS but does not affect PAMP gene induction

Given that AVR3a suppresses defense responses elicited by several elicitors (Chapter 5) and because of the association of AVR3a with dynamin the role of dynamin in early defense responses was investigated. I assessed the effect of overexpression NtDynA/B and NtDynA mutants in the production of reactive oxygen species (ROS). I used *Agrobacterium*-mediated expression of the GFP protein fusions for the different versions of dynamin in *N. benthamiana* and at 3 DPI challenged leaf-discs with flg22 (Fig. 6.2.9.A,B), chitin (Fig. 6.2.9.C), and INF1 (Fig. 6.2.9.D,E). Transient expression of dynamin reduces the amount of ROS that the plant can produce upon flg22, INF1 and chitin perception suggesting that dynamin probably acts downstream elicitor recognition at the PM (Fig. 6.2.9.A, C, D). The fact that chitin-elicited ROS production was also reduced might suggest that NtDynA mediated alteration of normal endocytosis also affects signaling of SERK3/BAK1 independent receptors. This suggests that probably DynA mediated endocytosis and traffic from the TGN might have a general role in plant defense. In addition, it was evident that dynamin required an intact GTPase activity as the dominant negative mutant slight impairment of ROS production was not statistically significant for flg22 elicitation, and was very modest for INF1 (Fig. 6.2.9.B, E). Intriguingly, the GTPase activity seems to be relevant to a certain extent for chitin ROS production (Fig. 6.2.9.C). Likewise, loss of most of the C-terminus region compromised the ability of NtDynA to suppress ROS (Fig. 6.2.9.B, C, E). Given that the truncated mutant also lacks the GED, it is possible that these observations were due to a lack of dynamin function, which seems to require dimerization that happens through the GED (Ferguson and De Camilli, 2012). Surprisingly, depleting dynamin also reduced the ROS elicited by flg22 (Fig. 6.2.10.A), INF1 (Fig. 6.2.10.C), and chitin (Fig. 6.2.10.B), suggesting that a disturbance of the process of endocytosis/endosomal trafficking leads to loss in fine-tuning of the defense response.

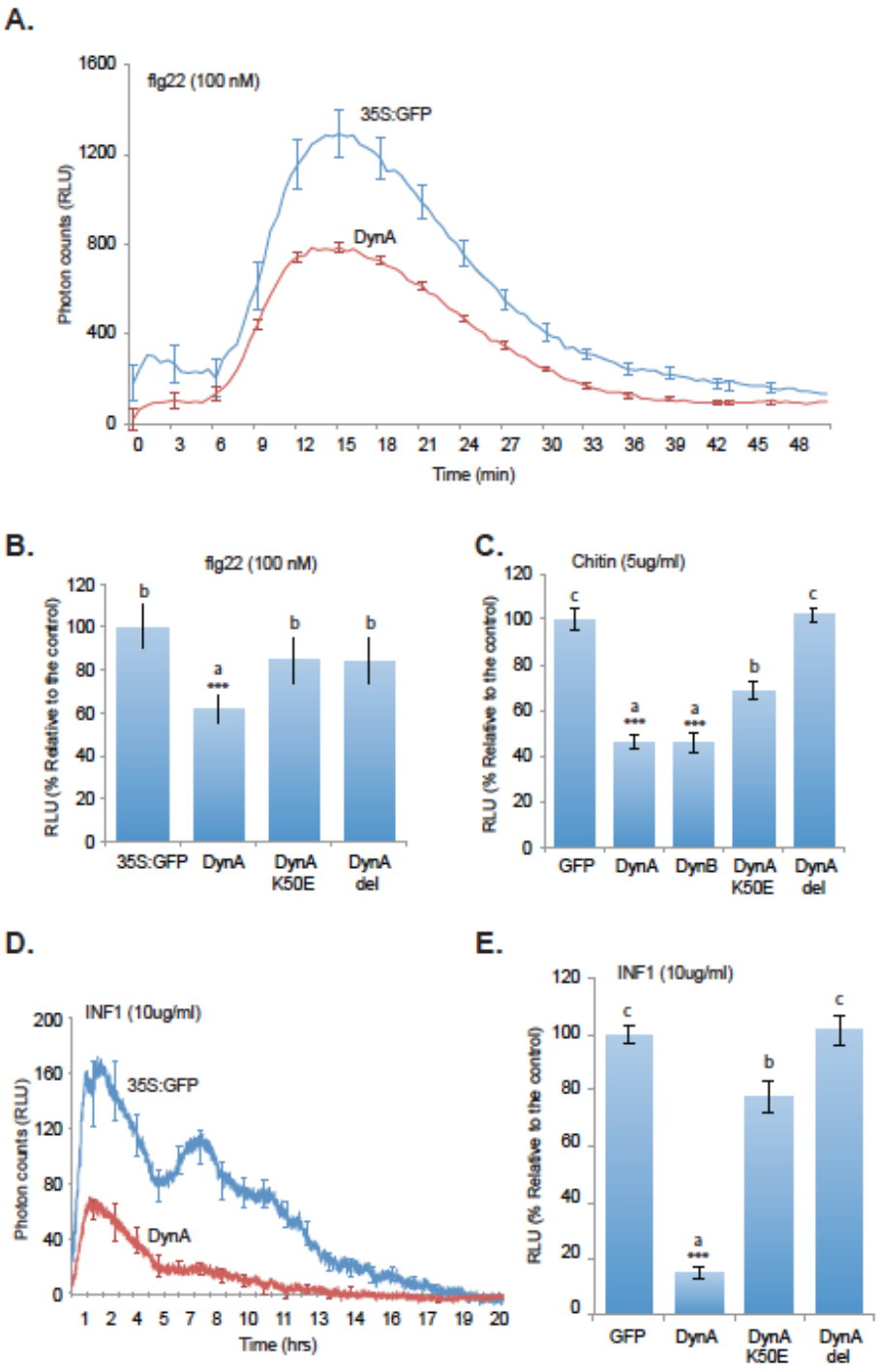

Fig. 6.2.9. Changes in dynamin cellular concentration impairs cellular ROS production

Oxidative burst triggered by 100 nM flg22 (A) or 10 µg/ml INF1 (D) in *N. benthamiana* agroinfiltrated with pK7FWG2-DynA or 35S:GFP. ROS production was measured in relative light units (RLU) over time. Transient expression of GFP-DynA or GFP-DynA-K50E or GFP-DynA-del or 35S:GFP (in the pK7FWG2 vector) in *N. benthamiana*. Total ROS production measured in relative light units (RLU) is expressed as percentage of the control treated with 100 nM flg22 over 45 minutes (B) or 5 µg/ml chitin over 45 minutes (C) or 10 µg/ml INF1 over 22 hours (E). Values are average ± SE (n = 24). Statistical significance was evaluated in comparison to the control by one-way ANOVA followed by Tukey HSD test. *** P < 0.001. Same

letter indicate statistical similarity. Similar results were observed in at least three independent experiments.

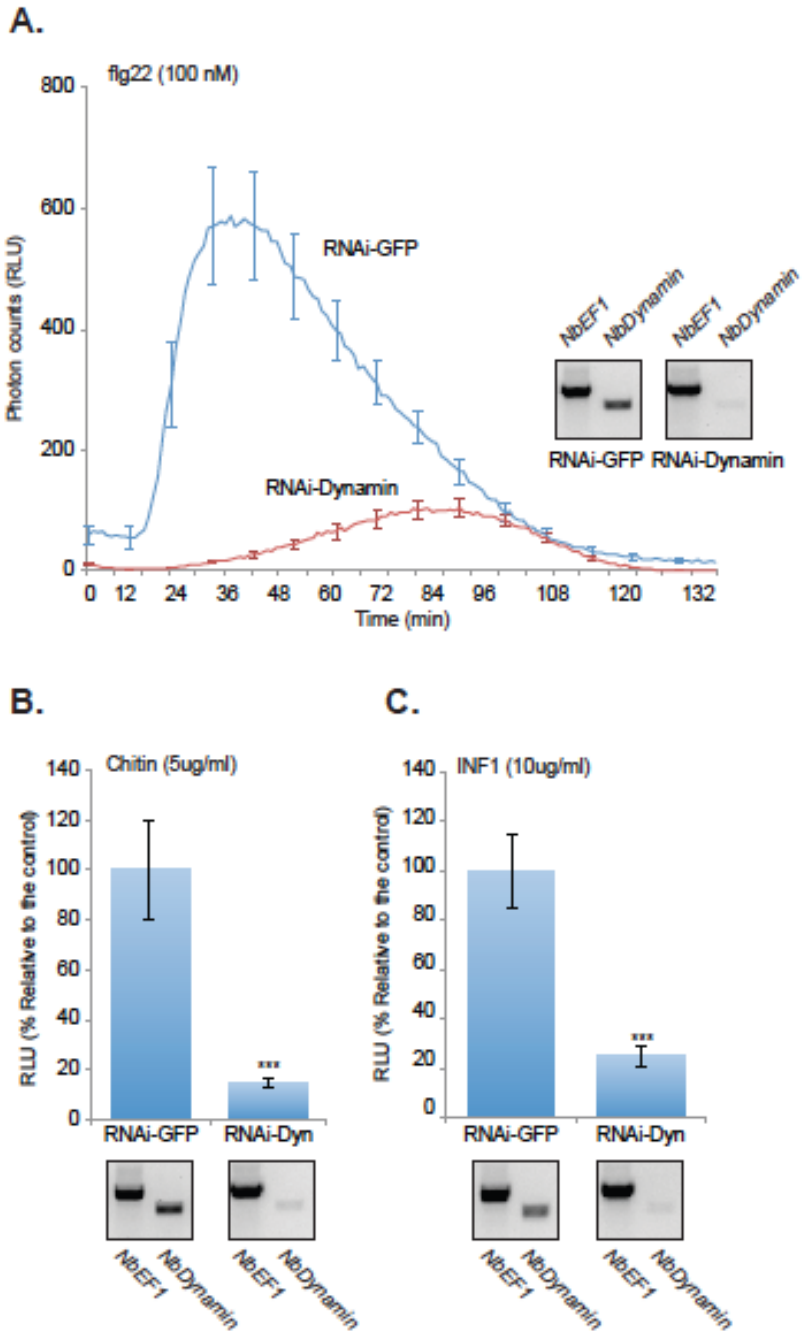

Fig. 6.2.10. Silencing dynamin inhibits ROS production

Leaves of *N. benthamiana* were silenced locally via RNAi-mediated silencing using the vector pHellsgate8 harboring a fragment of *NtDynamin* or a fragment targeting a region of GFP as a control. Three days post silencing, the oxidative burst triggered by 100 nM flg22 was measured (A). Histograms representing total ROS production measured in relative light units (RLU) as a percentage of the control treated with 5 µg/ml chitin over 45 minutes (B) or 10 µg/ml INF1 over 20 hours (C). Values are average ± SE (n = 24). Statistical significance was evaluated in comparison to the control by one-way ANOVA followed by Tukey HSD test. *** P < 0.001.

Validation of the silencing by RT-PCR (~150 ng cDNA) is shown in each panel. Internal control is *NbEF1α*.

One of the latest signaling steps after PAMP perception is the induction of a myriad of genes some of them directly implicated in defense response (Navarro et al., 2004; Zipfel et al., 2004). I then tested whether silencing dynamin in *N. benthamiana* would have an effect on the expression of PAMP-induced marker genes *NbCYP71D20* and *NbACRE31* (Segonzac et al., 2011). Preliminary results indicate that the expression of these genes was not altered after elicitation with several PAMPs (Fig. 6.2.11) independently of whether the signaling pathway requires SERK3/BAK1 or not. This is also in line with previous evidence showing that lack of ROS does not automatically lead to attenuation of defense gene induction after PAMP perception (Segonzac et al., 2011).

Overall these results suggest that dynamin might have a general impact on early defense responses independently of specific signaling components required by the ligand-binding receptors and that its role might be early on along the signaling pathway.

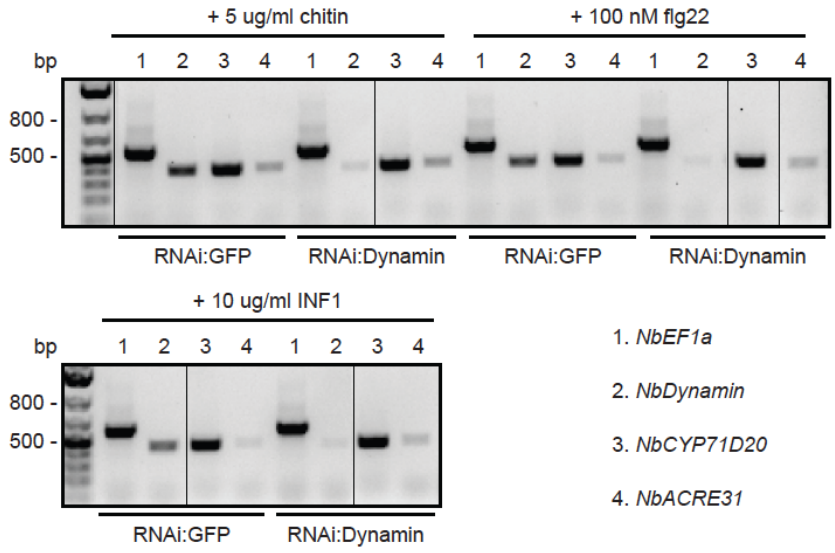

Fig. 6.2.11. Silencing dynamin has no impact on PAMP gene induction

Leaves of *N. benthamiana* were silenced locally via RNAi-mediated silencing as explained in Fig. 6.2.10. Three days post silencing, defense gene induction was monitored after elicitation with 100 nM flg22 or 5 µg/ml chitin or 10 µg/ml INF1 for 180 minutes. Gene expression was measured by RT-PCR using ~150 ng cDNA. *NbEF1α* was used as the reference gene.

6.3. Discussion

Deployment of effectors is a prevalent strategy of microorganisms towards colonization of their host. I showed here that the *P. infestans* RXLR effector AVR3a inhibits internalization of the membrane bound receptor FLS2 and targets an important component of clathrin mediated endocytosis, dynamin. Moreover, dynamin cellular concentration affects early defense responses and is required by AVR3a to suppress ICD. Finally, dynamin accumulates around *P. infestans* haustoria during infection placing it at an important site of the interaction.

Endocytosis is one of the most important physiological processes in any organism. Although controversial at first in plants (Holstein, 2002), it was later demonstrated that it allows the plant to internalize extracellular material probably to assess extracellular conditions and control cellular signaling in response to diverse stimuli and to take-up nutrients (Doherty and McMahon, 2009). Some pathogens like *Salmonella enterica* subsp. *enterica* serovar Typhimurium interact with the host endocytic pathway to control the integrity of the vacuole to replicate inside the host (Ham et al., 2011). It has been reported that clathrin-mediated endocytosis is triggered by cryptogein, an oomycete elicitin (Leborgne-Castel et al., 2008) and the fact that FLS2 undergoes endocytosis after elicitor treatment (Robatzek et al., 2006) points to an active role of endocytosis in signal transduction of molecules perceived at the periphery of the cell.

AVR3a suppress early defense responses in *N. benthamiana* elicited by SERK3/BAK1-dependent PAMPs (Chapter 5). One possibility is that AVR3a interferes with endocytosis to control membrane-bound receptor signaling. Indeed all variants of AVR3a prevent FLS2 endocytosis upon flg22 elicitation. Receptor endocytosis is one mechanism to down regulate intensity and duration of the signaling and it is usually clathrin-mediated (Polo and Di Fiore, 2006). The epidermal growth factor receptor (EGFR) undergoes two types of endocytosis depending on the available amount of elicitor initiating signaling; if it is low, clathrin mediated endocytosis is favored as the endocytosed receptor is still able to signal from the endosomes whereas clathrin-independent endocytosis usually sends the receptor for degradation (Polo and Di Fiore, 2006). Since AVR3a blocks FLS2 endocytosis it is possible to speculate that FLS2 undergoes clathrin-mediated endocytosis (CME) during signaling and preventing this type of endocytosis would diminish the signal that is transduced. Supporting the idea that AVR3a is interfering with CME, AVR3a associates with dynamin, a protein implicated in CME (Ferguson and De Camilli, 2012) although there is some evidence of its involvement in clathrin-independent pathways (Doherty and McMahon, 2009).

Interestingly, the cellular concentration of dynamin was found to be crucial for the production of reactive oxygen species, a hallmark of PTI. Data in this chapter showed

that either overexpression or depletion of dynamin consistently led to a loss of ROS. ROS production can have a direct antimicrobial effect or be a secondary signal to stimulate defense responses (Apel and Hirt, 2004). It is likely that the type of ROS produced upon elicitor perception is the membrane-permeable hydrogen peroxide (H_2O_2) which is implicated in cell signaling (Allan and Fluhr, 1997) rather than acting directly on the site of production. The fact that this ROS signaling is impaired in dynamin-deregulated plants positions dynamin as a component of early signaling upon PAMP perception. Moreover, dynamin mediated endocytosis might be an important component for ROS generation. Further experiments are required to address which molecular mechanisms leading to ROS production are impaired in dynamin-deregulated plants. One good candidate is ligand-induced receptor internalization. In contrast, reduced dynamin concentration did not impact defense gene induction supporting a role of dynamin limited to early signaling steps of PAMP recognition rather than further downstream responses. In addition, as demonstrated by Segonzac and colleagues (2011) impairment of ROS production had a negligible contribution towards pathogen growth. It is then possible that the suppression of ROS by AVR3a is a byproduct of its activity on other PTI signaling components, perhaps in altering the cytoskeleton through dynamin or by redirection of gene expression that results in suppression of ROS.

Given the results discussed in this chapter, it can be hypothesized that in the presence of AVR3a, signaling pathways elicited by SERK3/BAK1-dependent PAMP leading to oxidative burst production and finally gene induction are suppressed and this probably culminates in the observable enhanced growth phenotype of *P. infestans* in *N. benthamiana* (Fig. 6.2.12A). Knockdown of dynamin presumably has a detrimental effect on endocytosis or other dynamin processes like cytoskeleton organization and somehow this seems to interfere with the ability of the plant to produce ROS. However, the transcriptional induction after PAMP perception is not affected, nor the normal growth of *P. infestans* (Fig. 6.2.12B). These results suggest, first that AVR3a mediated suppression of PTI culminating in enhancement of *P. infestans* growth requires blocking PTI gene induction while ROS production and probably dynamin-mediated endocytosis are negligible. Second, since silencing dynamin does not seem to affect *P. infestans* growth it is possible that clathrin-mediated endocytosis is not involved in establishing a successful infection. It is therefore tempting to speculate that AVR3a targeting of dynamin is not aimed at dynamin's role in ROS production but other dynamin-mediated processes such as association with the cytoskeleton (Ferguson and De Camilli, 2012) and hence vesicle trafficking could be what AVR3a targets. It is known that inhibiting microtubule networks can promote pathogen growth and the bacterial effector HopZ1a destroys microtubule networks to achieve this (Lee et al.,

2012). Indeed components of vesicular trafficking (endomembrane compartments) are recruited to the haustoria of *P. infestans* (Lu et al., 2012) and I could demonstrate that dynamin also accumulates around haustoria. It is reasonable that the recruitment of endomembrane compartments to the site of infection facilitates biogenesis of nascent membranes to help accommodate the haustoria. Hence overexpression of dynamin would alter such process with an enhancing effect on *P. infestans* growth.

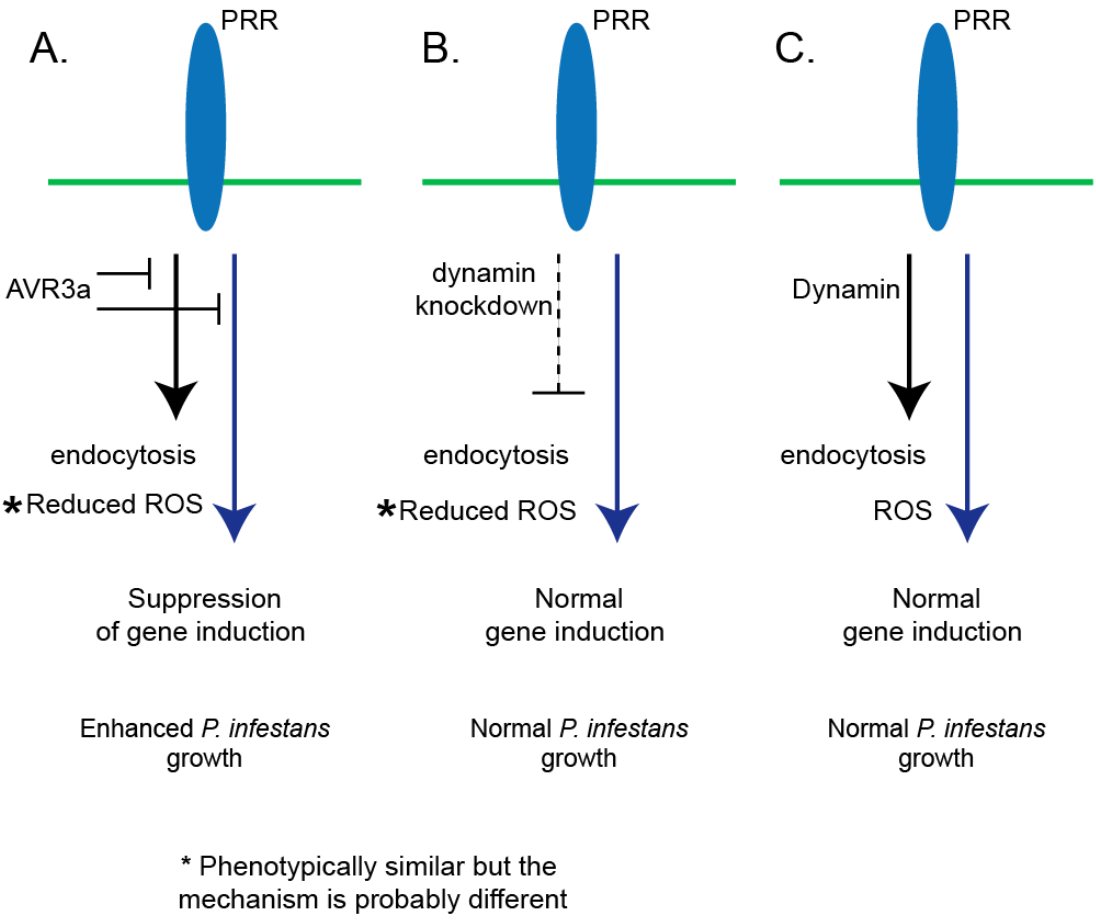

Fig. 6.2.12. Conceptualization of AVR3a/Dynamin role in immunity

(A) AVR3a suppression activity resulting in enhancement of *P. infestans* growth. (B) The result of decreasing dynamin cellular concentration. (C) Proposed signaling steps in normal dynamin conditions. The dashed line indicates unknown in the system used.

Alternatively, AVR3a interacts with dynamin to achieve additional functionality and proper subcellular positioning. In this case, dynamin acts as a helper protein for AVR3a mediated activities. Therefore, mutations in dynamin would not necessarily have an effect on AVR3a-mediated virulence as a whole but rather would only affect a subset of AVR3a virulence activities, namely those that rely on dynamin related processes. In

accordance with this notion, depleting dynamin impairs the ability of AVR3a to suppress INF1 cell death but does not affect gene induction or *P. infestans* growth. In line with this, suppression of PTI by AVR3a could be independent of dynamin and perhaps AVR3a association with dynamin might facilitate/promote more haustoria formation; therefore in dynamin's absence haustoria formation would not be blocked and just proceed at normal levels (Fig. 6.2.12C). Moreover, the enhancement of *P. infestans* growth stimulated by dynamin overexpression might be attributable to meeting *P. infestans* higher demands for endocytosis during infection, like haustorium formation or effector delivery, and could be unrelated to AVR3a.

It remains unclear whether AVR3a disturbs specific endocytic processes initiated by an exogenous stimulus recognized at the cell periphery or affects constitutive endocytosis. Perhaps internalization of FM4-64 can be followed in the presence of AVR3a with and without elicitation to determine the role of AVR3a in endocytosis. Alternatively, the effects of AVR3a on the constitutive endocytic recycling process of the brassinosteroid receptor (BRI1) could be tested as well. In addition, addressing the functionality of the NtDynamin in endocytosis and the impact of the dominant negative mutant in FLS2 endocytosis is necessary. It has been demonstrated that the expression of a dominant negative form of DRP2A/B compromises endocytosis (Taylor, 2011). Co-localization studies with clathrin light chain would give indirect evidence of the involvement of dynamin in endocytosis as reported previously (Ito et al., 2012).

CHAPTER 7: General Discussion and Outlook

Pathogens by definition are microorganisms that successfully conquer their hosts and cause disease. Pathogens deliver effector proteins to the host cell cytoplasm or to the apoplastic environment to suppress host immunity or induce processes benefiting their multiplication. The filamentous oomycete pathogen *P. infestans* secretes a vast array of effector molecules that contribute to its ability to infect and colonize its host. Examples of *P. infestans* apoplastic effectors include EPI1 and EPI10, which are serine proteases inhibitors of the pathogenesis-related protein P69B (Tian et al., 2004b; Tian et al., 2005). *P. infestans* also has a large class of cytoplasmic effector proteins represented by different classes. The best characterized is the RXLR class distinguished by this motif that is required for translocation of the effector by unknown mechanisims (Morgan and Kamoun, 2007). The best-studied RXLR effector to date is AVR3a (Armstrong et al., 2005; Bos et al., 2006; Bos et al., 2009; Bos et al., 2010; Gilroy et al., 2011; Yaeno et al., 2011). AVR3a was shown to activate immunity in plants carrying the cognate disease resistance gene *R3a* but more importantly, AVR3a also suppresses defense responses triggered by the conserved extracellular *P. infestans* protein INF1. The exact molecular mechanism of INF1 cell death suppression and the extent to which AVR3a exerts additional virulence activities was the focus of this work.

7.1. AVR3a suppression of basal immunity

Several lines of evidence, listed below, suggest that AVR3a is a strong suppressor of innate immunity. (1) AVR3a suppresses the accumulation of reactive oxygen species and affects the induction of defense genes involved specifically in elicitor-induced signaling pathways requiring the co-regulator of PTI SERK3/BAK1 (Chapter 5). Given that suppression of flg22-elicited responses was similar for all variants of AVR3a, it is likely that suppression of an FLS2-like pathway is the ancestral or an evolutionary older activity of AVR3a compared to INF1 cell death suppression. (2) AVR3a stabilizes PRRs signaling components such as CMPG1 (Bos et al., 2010). CMPG1 steady state levels are low (Bos et al., 2010) and represent a technical challenge to assess protein function. However silencing experiments suggested that CMPG1 might be acting as a negative regulator of PTI (Chapter 5). (3) AVR3a associates with the host protein dynamin (Chapter 6), an important component of endocytosis and potentially required for internalization of PRRs.

What is the precise molecular mechanism of AVR3a suppression of PTI? AVR3a could interfere with signaling elements like CMPG1. This E3 ligase is required by the membrane-bound receptor Cf-9 to mediate recognition of the fungal molecule Avr9 and also for responses triggered by INF1 that is most likely recognized at the membrane

(Gonzalez-Lamothe et al., 2006). Moreover, AVR3a is able to suppress the CMPG1-dependent cell death triggered by elicitors recognized by PM receptors (Gilroy et al., 2011). This strongly supports the fact that AVR3a is targeting signaling transduction cascades initiated at the PM.

Alternatively, AVR3a might be interfering with receptor internalization. This study showed that AVR3a associates with a component of endocytosis and following activation by an external signal some receptors at the PM undergo internalization probably through endocytosis (Murphy et al., 2005; Robatzek, 2007). Ubiquitination is also used as a signal for internalization and there are some examples of PRR receptors labeled by ubiquitination for internalization and subsequent degradation. FLS2 is ubiquitinated by the Arabidopsis E3 ligases PUB12 and PUB13 leading to FLS2 degradation for attenuating signaling (Lu et al., 2011). Hence, a possible scenario is that AVR3a tempers with the self-ubiquitination activity of CMPG1 and likely its substrates resulting in restrictions to PRRs internalization. In support of this hypothesis, I showed that AVR3a associates with dynamin and that it does inhibit the internalization of FLS2 (Chapter 6). It is still necessary to elucidate whether this interference is CMPG1-dependent and the role of dynamin in the process.

Consistent with AVR3a interference with receptor internalization, I showed that AVR3a associates with the plant protein dynamin, a protein that is implicated in endocytosis and cytokinesis (Ferguson and De Camilli, 2012; Mooren et al., 2012). Ligand-binding membrane receptors seem to be down regulated through their internalization (Murphy et al., 2005; Polo, 2012) but some membrane receptors also signal from endosomes (Wang et al., 2002; Murphy et al., 2009) which raises the possibility that AVR3a might be targeting the plant endocytic pathway, a process that is actively regulated by ubiquitination (Polo, 2012). Dynamin could be a target at sites where abolishment of PRR endocytosis is required. In line with that, it has been reported that FLS2 is absent from the extrahaustorial matrix (EHM) enveloping haustoria (Lu et al., 2012) and in this work it was shown that dynamin accumulates at the EHM, supporting a role for endocytosis (and interference of endocytosis by AVR3a) at the haustoria. It would be interesting to determine if the recruitment of dynamin promotes the exchange of cellular components at the EHM or if the involvement of dynamin is unidirectional: internalization of PAMPs and/or PRRs or carrying cellular proteins to the periphery of the cell necessary for the biogenesis of the haustoria. One way to explore this would be to test whether FLS2 and dynamin associate *in vivo*, and whether FLS2 and BAK1 association is disrupted by changing the cellular concentrations of dynamin, provided that BAK1 undergoes internalization along with FLS2 as it is the case for BRI1-BAK1 (Russinova et al., 2004). In addition the results presented in Chapter 6 showed that

altering the concentration of dynamin interfered with the cell ability to produce ROS but did not affect the transcriptional re-programming triggered by exogenous elicitors confirming that dynamin role in immunity occurs early in the signaling pathway after elicitor perception. Assessing the impact of dynamin on MAPK activation and calcium influx might help narrow the exact input of dynamin in PTI if any.

Internalization of the RLP LeEix2 upon perception of xylanase occurs (Bar and Avni, 2009) suggesting that endocytosis could be a common regulatory system for membrane-bound receptors. In my experiments, the candidate INF1 receptor ELR1 was primarily localized at the ER making it difficult to evaluate whether or not it undergoes internalization. However, this could be addressed indirectly by assessing ELR1 ability to mediate ICD in INF1 non-responsive potato plants treated with an inhibitor of endocytosis like wortmannin (Emans et al., 2002) or Tyrphostin A23 (Leborgne-Castel et al., 2008) or by co-expressing ELR1 with AtEHD2, a protein exerting an inhibitory effect in LeEix2 endocytosis (Bar and Avni, 2009). In the event that tampering with the endocytic pathway inhibited ICD, it could perhaps indicate that the INF1 receptor undergoes internalization. It has not been demonstrated that SERK3/BAK1 is also internalized upon flg22 elicitation but it is necessary for FLS2-mediated signaling. I showed in Chapter 4 that ELR1 associates with SERK3/BAK1 and that this association is enhanced by elicitation with INF1. It is tempting to speculate that because FLS2 and ELR1 share some signaling components and since AVR3a affects their signaling outcome, these receptors might also share some molecular processes like internalization. However, to get a clear picture of INF1 signaling a more detailed dissection of the putative receptor ELR1 is needed. It would be interesting to assess the phosphorylation status of StdSERK3 with and without INF1, whether INF1 directly binds to ELR1 and to look for additional plant proteins interacting with ELR1. In addition, to assess whether constitutive association of StdSERK3 with ELR1 reflects a general distinction between RLKs and RLPs, it would be necessary to test if other RLPs like Cf-4 or Cf-9 interact with StdSERK3. In the possible scenario in which there is no association, this could indicate that constitutive association is only a requirement for SERK3/BAK1 dependent receptors like LeEIX1/2 and Ve1 for which there is evidence that SERK3/BAK1 is necessary for signaling (Fradin et al., 2009; Bar et al., 2010).

Evidence presented in this thesis along with other findings discussed above suggests that AVR3a has evolved strategies to interfere with membrane-bound receptor signaling. Some Type III bacterial effectors target PM components to suppress innate immunity. AvrPto interacts with the kinase domain of FLS2 and EFR (Zong et al., 2008) and suppresses PTI by inhibiting kinase activity (Xiang et al., 2008). Remarkably,

AvrPto also interacts with the membrane bound kinase Pto that is probably "guarded" by the R protein Prf to activate ETI (Deslandes and Rivas, 2012). It has been hypothesized that the real target of AvrPto are PRRs like FLS2 and that Pto evolved as a decoy (Block and Alfano, 2011). AVR3a did not affect the heterodimerization of FLS2 and SERK3/BAK1 but it is still important to determine whether AVR3a associates with the receptors themselves and whether this association is altered by elicitation with the corresponding PAMP and to test if AVR3a affects the phosphorylation status of the PRRs. Interestingly, AvrPtoB interacts with the kinase domain of FLS2 by tampering with the ubiquitination status of the receptor and mediating its degradation (Gohre et al., 2008). It was shown that expression of AvrPtoB resulted in decreased FLS2 levels as a result of promoting its degradation (Gohre et al., 2008). In addition AvrPtoB targets CERK1 for ubiquitination and subsequent degradation to achieve PTI suppression revealing shared signaling components that are not affected by having SERK3/BAK1 as a signaling regulator (Gimenez-Ibanez et al., 2009b). However, AVR3a did not affect the levels of the studied PRRs (Chapter 5) indicating that the modification on CMPG1 is actually not promoting degradation of the PRRs and there must be additional roles for CMPG1 besides targeting proteins to the ubiquitin-26S proteasome.

7.2. Effectors require additional plant protein as helpers

Elucidating AVR3a functional mechanisms requires that we discriminate between interacting proteins that are crucial targets of AVR3a to prevent PTI and interactors that are required by it to exert its suppression activity and should rather be considered helper proteins (Win et al., 2012). The fact that some of the AVR3a-related activities like INF1 cell death suppression were affected by dynamin depletion whereas others such as enhanced *in planta* growth of *P. infestans* were not affected, raises the possibility that effector proteins not only rely on plant targets to achieve functionality but also associate with other plant proteins that help the effector to fully function (Win et al., 2012). Consequently, effector helper proteins are host molecules required by the effector but not necessarily directly implicated in the cellular process that the effector is targeting. From the results described in Chapter 6, I propose that dynamin could act as a host helper protein because silencing dynamin and the loss of function mutants did not have any effect on *P. infestans* growth whereas dynamin was still required for AVR3a ICD suppression activity. In addition, it is expected that perturbations on effector targets show the same phenotype that is induced by the effector. However, INF1 *per se* does not require dynamin to trigger cell death (in clear contrast with CMPG1), and defense gene transcription after INF1 elicitation was not suppressed by altering dynamin cellular levels. These results support dynamin as an important but not essential element for AVR3a to enable full activity towards *P. infestans* pathogenicity.

Several examples of host helpers of effectors have been described. Cyclophilin, a peptidyl-prolyl *cis/trans* isomerase (PPIase) is required by the bacterial effector AvrRpt2 for activation upon delivery inside the host cell (Coaker et al., 2005). Cytosolic PPIases are chaperones that catalyze and accelerate protein folding (Chou and Gasser, 1997). The model is that the Arabidopsis cyclophilin ROC1 activates self-processing of the cysteine protease AvrRpt2 inside the host cytosol and this in turn leads to the direct cleavage of RIN4 (Coaker et al., 2006). The cleavage product is thought to be a more effective negative regulator of defense responses (Afzal et al., 2011). AvrRpt2 mutants in cyclophilin binding sites lack protease activity and are unable to induce RPS2 resistance confirming ROC1 role in defense responses (Coaker et al., 2006). Similar to the effector AvrRpt2, the *P. syringae* effector HopZ1a is activated inside the host cell by phytic acid to become a functional acetyltransferase that acetylates the plant target of HopZ1a, tubulin (Lee et al., 2012). Acetylation of tubulin seems to dramatically compromise normal disposition of microtubule networks promoting *P. syringae* growth (Lee et al., 2012).

Bacterial pathogens of mammalian cells also target additional host components that are not necessarily target proteins but that are important cofactors for effector activity. The *Yersinia* effector YopT is a cysteine protease translocated to the plasma membrane that binds and cleaves the C-terminal cysteine of Rho GTPases leading to their release from the membrane (Shao et al., 2002). The direct binding and modification of RhoA favors the accumulation of RhoA in the cytosol resulting in disruption of actin fibers (Aepfelbacher et al., 2003). Interestingly, YopT cannot cleave RhoA in the absence of phosphatidylinositolbiphosphate (PIP2) suggesting that PIP2 might be an essential factor for YopT activity. However, direct binding of YopT to PIP2 was not shown (Aepfelbacher et al., 2003). In a similar fashion, AVR3a binds phosphatidylinositol monophosphates (PIPs) and this association seems to be essential for the effector virulence activity of suppressing INF1 cell death (Yaeno et al., 2011). AVR3a accumulation is affected by activating the phosphorylation of PIP3P and PIP4P and this in turn blocks the ability of AVR3a to suppress INF1 cell death. Yaeno and colleagues (2011) hypothesized that binding to phosphatidylinositol monophosphates would make AVR3a “immune” to an intrinsic mechanism of degradation thereby allowing the effector and its target CMPG1 to migrate to the nucleus where CMPG1 stabilization occurs leading to INF1 cell death suppression. Hence PIPs are not the effector target of AVR3a *per se* but being essential for achieving its virulence activity PIPs are effector helpers. It is tempting to speculate that AVR3a has multiple effector helpers depending on the activity it is performing. Alternatively, AVR3a could require phosphatidylinositol monophosphates for manipulating the amount of proteins at the PM. Phospholipids are known to be

important signaling molecules that contribute to the regulation of the protein complexes at membrane domains within the cell and at the interface with the cytosol (Martin, 1998; Doherty and McMahon, 2009) and for the recruitment of adaptor proteins in endocytosis (Chen et al., 2011). If this last hypothesis were correct, the association of AVR3a with phosphatidylinositol and dynamin would probably affect the same cellular process (endocytosis of PM localized receptors for example).

There are still many open questions regarding AVR3a activities despite the identification of multiple new cellular elements and interference points along the signaling cascade leading to innate immunity. Future experiments should aim to resolve (i) whether known PRRs and AVR3a interact, (ii) whether there is a common pathway element required for multiple PRRs, (iii) the subcellular localization at which AVR3a acts (this is probably better explored by biochemical methods as microscopy experiments were inconclusive) and (iv) whether AVR3a affects PRRs at the PM or at any other point along their way to the PM.

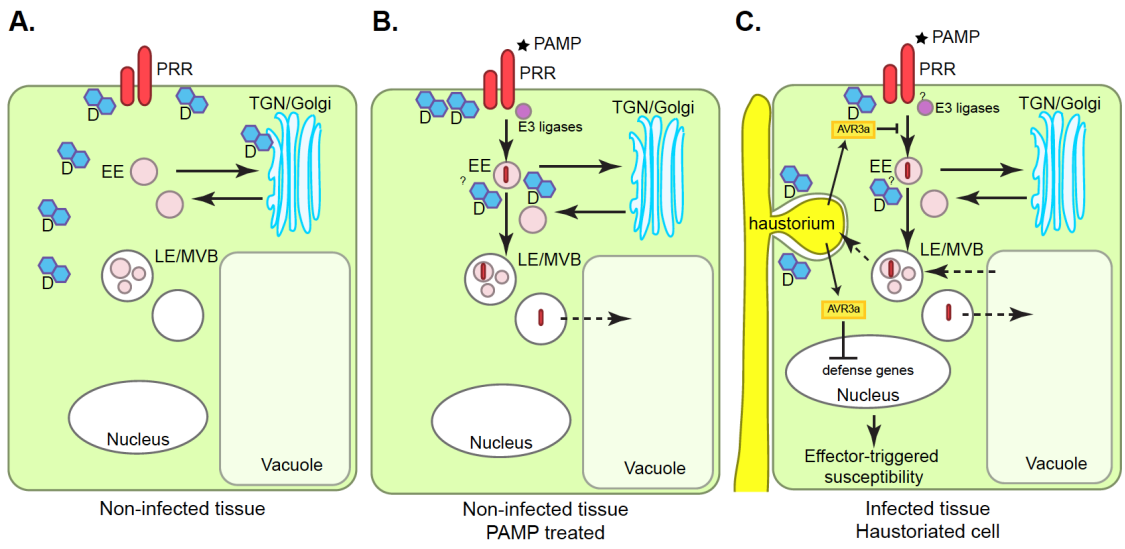

Fig. 7.1. During a compatible interaction AVR3a suppresses immunity to promote *P. infestans* infection.

(A) The AVR3a helper protein dynamin (D) localizes to the Trans-Golgi Network (TGN), plasma membrane and cytoplasm and it is thought to be involved in endocytosis. (B) Upon PAMP perception, dynamin gets internalized into vesicles probably the early endosomes (EE). Receptor internalization also occurs and E3 ligases like PUB12 and PUB13 ubiquitinate the receptors to probably send them for degradation. It is unknown whether the internalized receptors signal from within the endosomes. (C) During *P. infestans* infection, in haustoriated cells, dynamin accumulates around haustoria as well as other cellular compartments such as

the vacuole and late endosomes (LE). AVR3a is translocated inside the host cytoplasm and associates with dynamin presumably to inhibit membrane-bound receptor internalization.

MVB: multivesicular bodies, PRR: pattern recognition receptors, PAMP: pathogen-associated molecular pattern. Dashed lines and (?) indicates unknown pathways or associations. Adapted from a figure made by Dr. Sebastian Schornack.

Appendix 1

Supplementary figures for chapter 4: Characterization of a receptor-like protein (RLP) from *Solanum microdontum* that mediates the response *to P. infestans* elicitin INF1

Table A1.1. Specificity of the cell death induced by INF1 elicitin in different *Nicotiana* species

	Response to INF1[a] (in percentage of INF1 cell death)		
Species/accessions	Strong cell death	Weak cell death	No response
Nicotiana simulans			
TW122-4	100	0	0
TW122-1	0	0	100
N. sylvestris			
TW136	70	30	0
TW137	0	100	0
TW138[b]	0	0	100
N. stocktonii			
TW86	100	0	0
TW87	100	0	0
TW126[c]	100	0	0

[a.] Transient *Agrobacterium*-mediated expression of 35S:INF1

[b.] Yellowing seeds

[c.] Massive and fast cell death

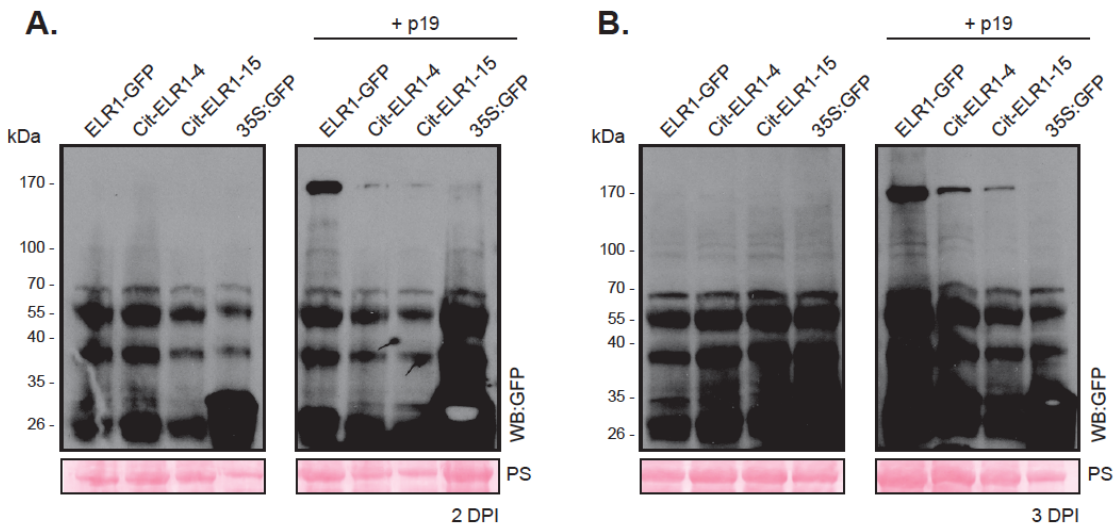

Fig. A1.1. ELR1-GFP and Citrine-ELR1 protein accumulates only upon overexpression
Immuno blots showing the stability of the fusion proteins ELR1-GFP and Cit-ELR1 in *planta* at two and three days post infiltration. This figure is the complete image of the blot showed in Figure 4.3 panel D that corresponds to the localization assays in panel (A) and (B) in the same figure. *Agrobacterium*-mediated expression was used to infiltrate ELR1-GFP, Cit-ELR1 or 35S:GFP with and without p19. Leaf samples were taken for confocal microscopy (Fig. 4.3) at the shown days. After microscopy, leaf discs were collected and the protein was extracted in SDS-PAGE buffer and subjected to western blot analysis.

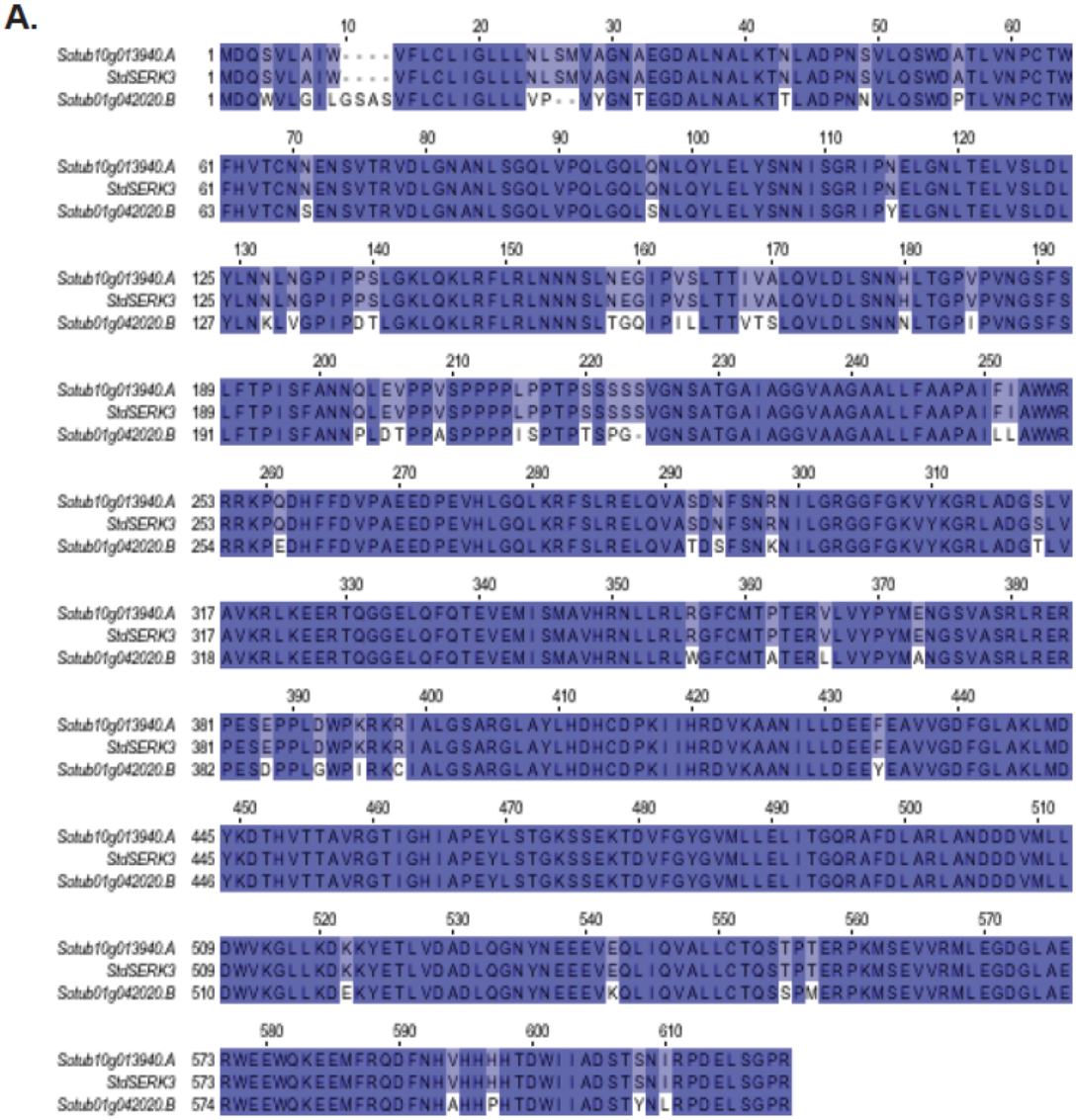

Fig. A1.2. Alignment of StdSERK3 with the potato sequences closest to AtBAK1

ClustalW alignment of the amino acid sequence of the cloned protein StdSERK3 with the two protein sequences retrieved after tblastn using BAK1 as query from the latest version of the potato genome. StdSERK3 corresponds to the protein Sotub10g013940, which is annotated as SERK3A. The other protein Sotub01g042020 is annotated as SERK3B and shares 83% similarity with BAK1. Amino acid residues are shaded dark blue if identical and a lighter shade of blue if similar.

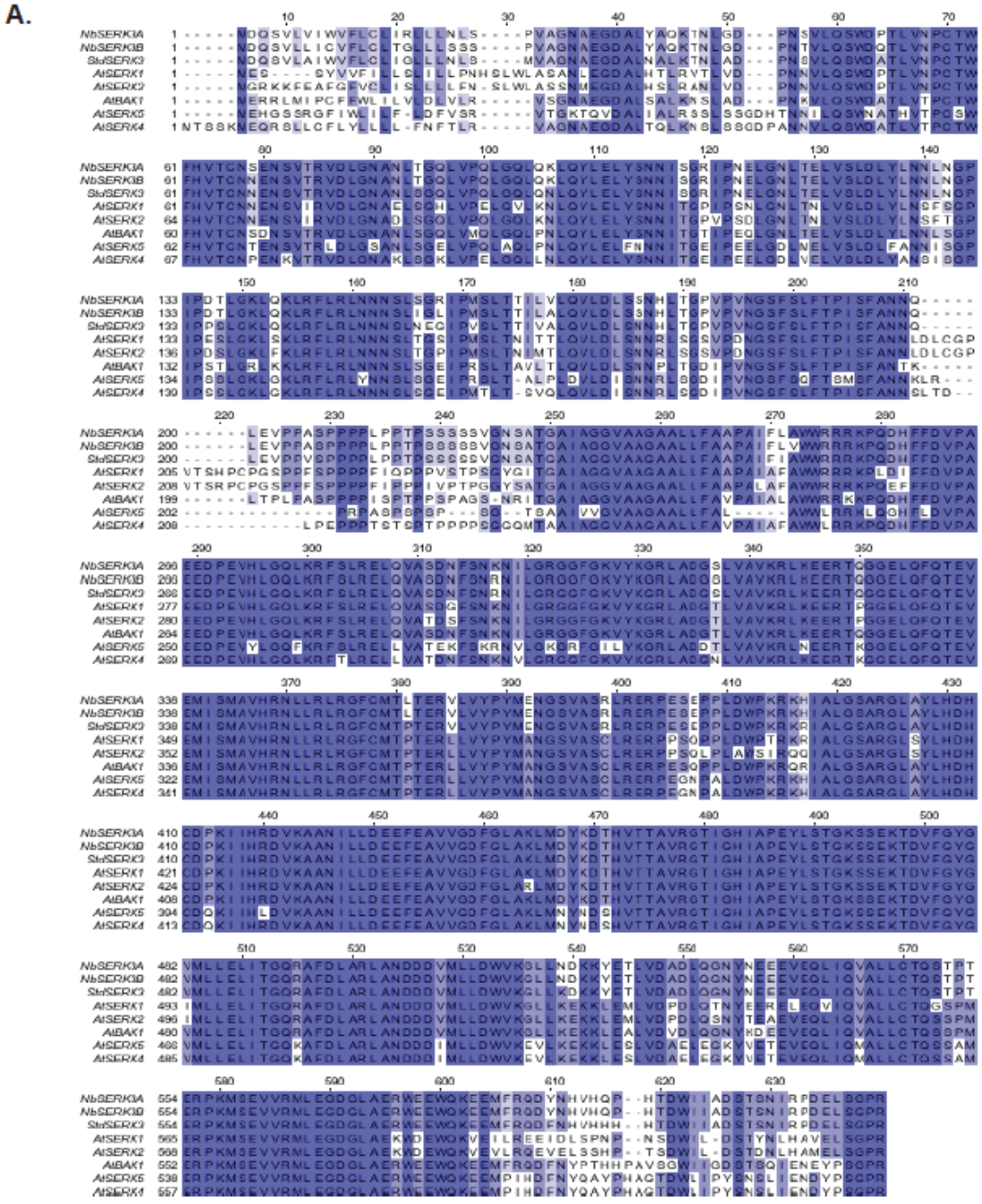

Fig. A1.3. StdSERK3A is more similar to SERK3/BAK1 than to other members of the SERK family

Multiple alignment showing homologs of AtBAK1 in *N. benthamiana* and one of the homologs in *S. tuberosum* cv. Désirée StdSERK3A and all the other members of the somatic embryogenesis receptor kinases (SERK) from Arabidopsis. Identical residues are shaded in dark blue and similar amino acids are shaded in light blue. Sequences were aligned in ClustalW and viewed in Jalview.

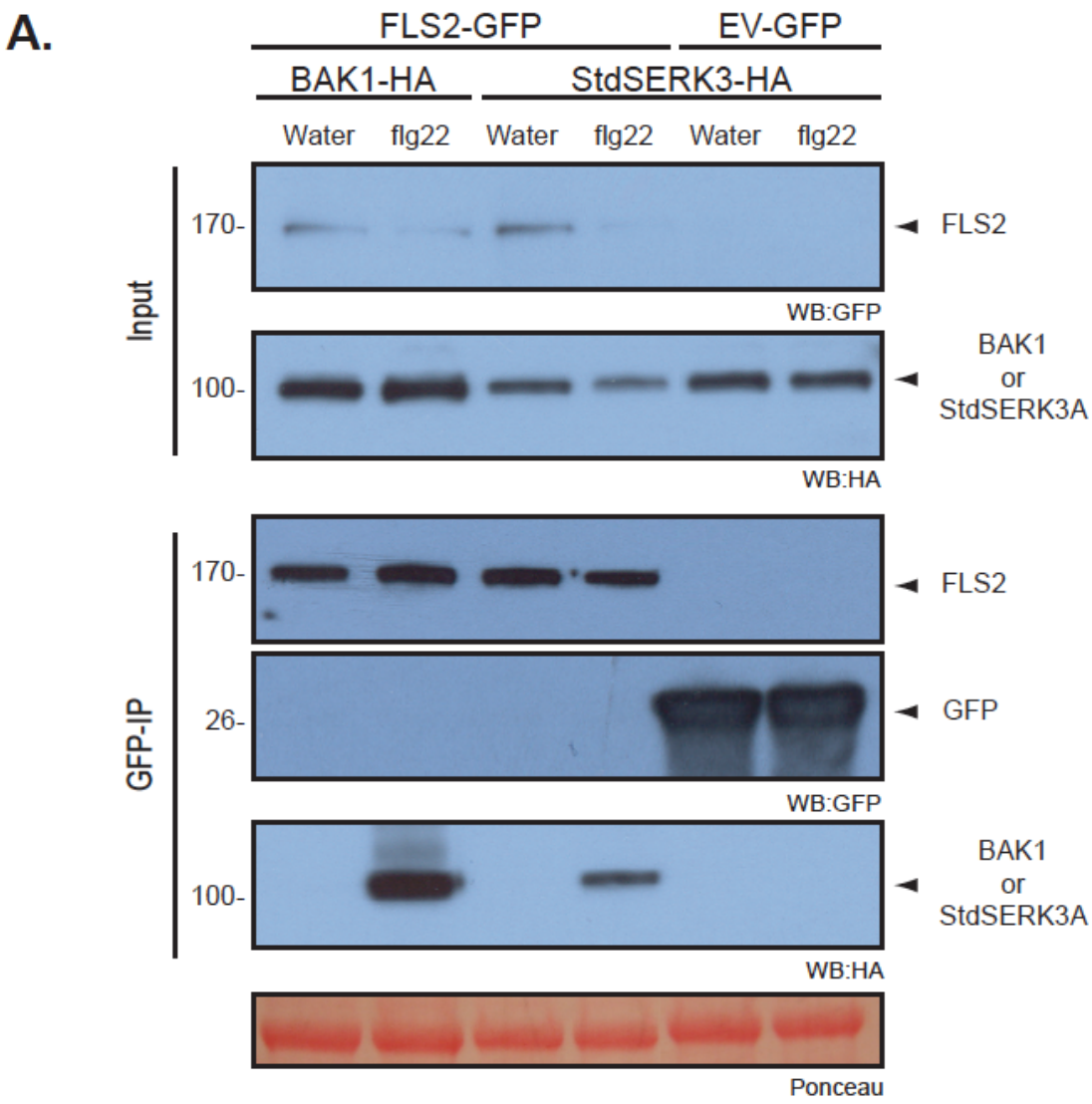

Fig. A1.4. AtFLS2 forms a ligand-induced complex with StdSERK3A *in planta*

AtFLS2 heterodimerizes with AtBAK1 and its potato homolog StdSERK3A. FLS2-GFP was transiently co-expressed with AtBAK1-HA or StdSERK3A-HA in the absence of p19 and challenged with flg22 (100nM) or water for 15 minutes. Immunoprecipitation (IP) was carried out with GFP beads and total protein extracts and IP were blotted with the appropriate antisera as indicated. As negative control AtBAK1-HA was also co-expressed with 35S:GFP and subjected to the same treatment as described above. Ponceau staining of the total protein extracts blot indicates protein-loading control (bottom).

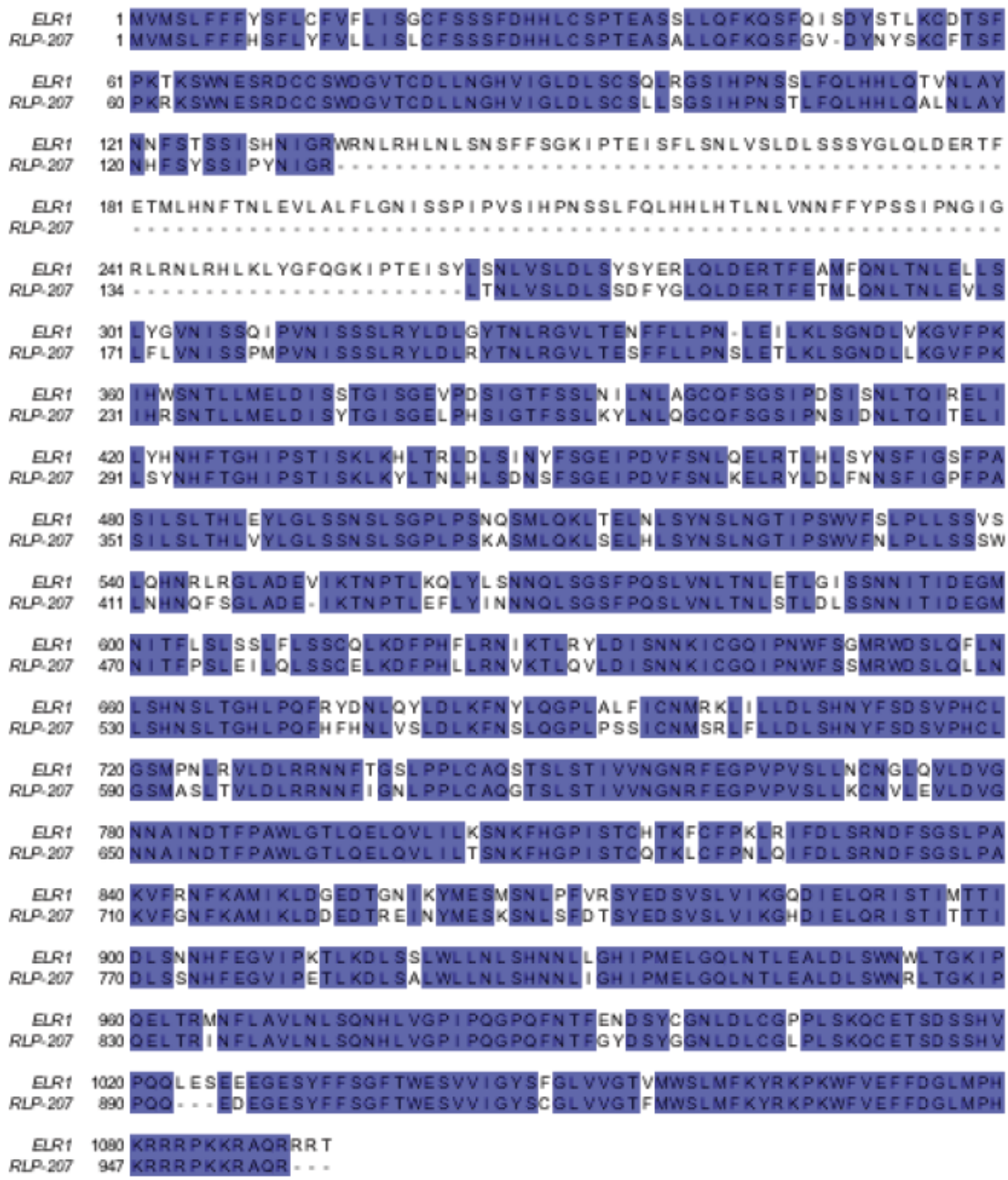

Fig. A1.5. ELR1 and a close paralog from *S. microdontum* RLP-207

Protein sequence alignment of ELR1and the paralog RLP-207. ELR1 and RLP-207 belong to a large cluster of RLPs in *S. microdontum*. RLP-207 was one of the two candidate genes identified in the physical mapping of the gene involved in INF1 cell death response (Verzaux, 2010). Amino acid residues are shaded dark blue if identical and a lighter shade of blue if similar.

Appendix 2

Supplementary figures for Chapter 5: AVR3a suppresses early defense responses in *Nicotiana benthamiana*

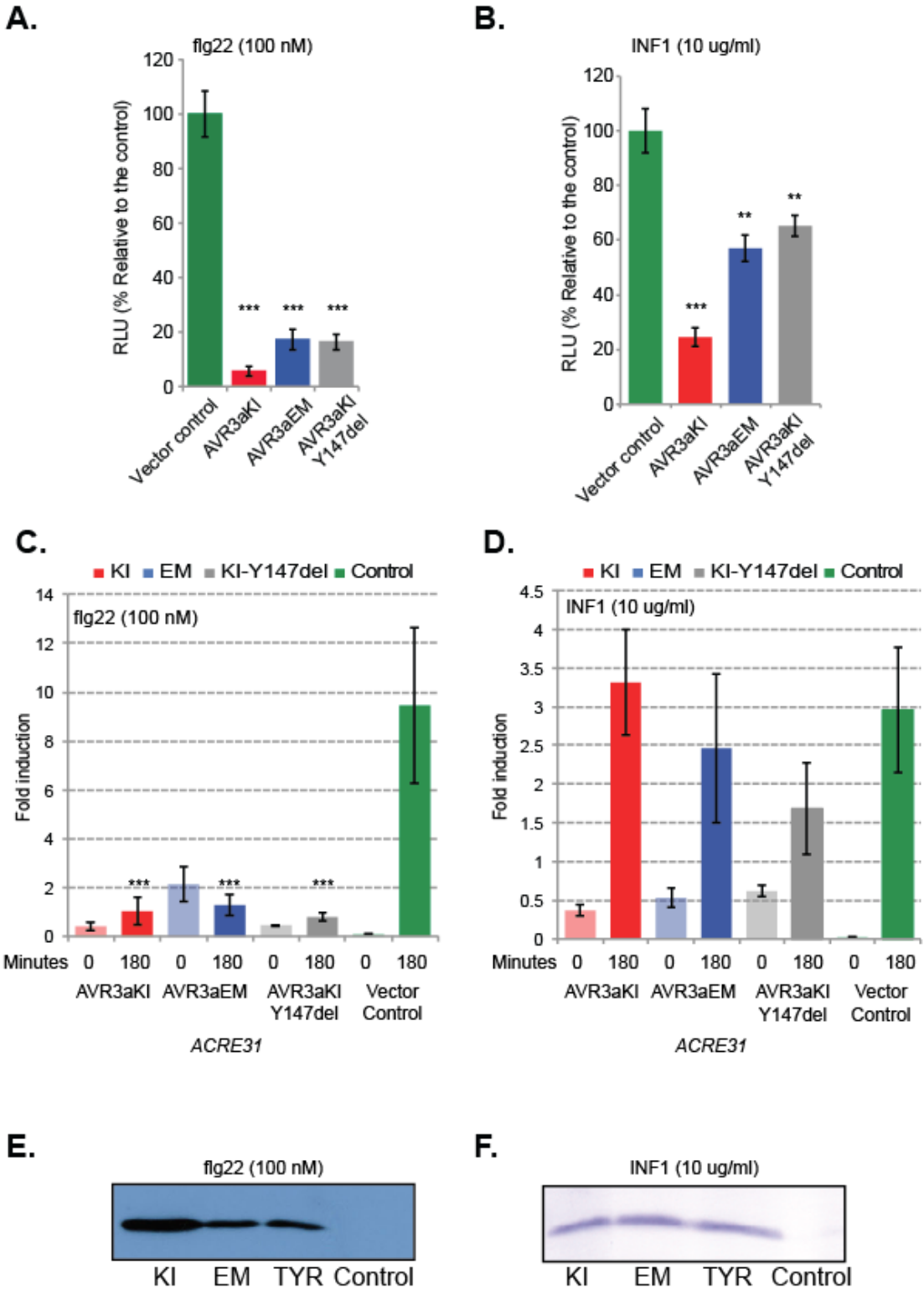

Fig. A2.1. All variants of AVR3a suppress the oxidative burst upon elicitor treatment *in N. benthamiana* but show differential suppression of the marker gene *NbACRE31*

Total ROS production measured in relative light units (RLU) is expressed as percentage of the control treated with 100 nM flg22 over 45 minutes (A) or 10 µg/ml INF1 over 22 hours (B). Values are average ± SE (n = 24). Statistical significance was evaluated in comparison to the control by one-way ANOVA followed by Tukey HSD test. *** P < 0.001, ** P< 0.05. Gene-induction of the marker gene *NbACRE31* in response to 100 nM flg22 (C) or 10 µg/ml INF1 (D). Gene expression was measured by qRT-PCR at time zero and 180 minutes after elicitor treatment and normalized by NbEF1α gene expression. Results are average ± SE (n = 2). AVR3a variants were transiently expressed in *N. benthamiana* using the following constructs: pBinplus::AVR3a^{KI} (red), pBinplus::AVR3a^{EM} (blue), pBinplus::AVR3a$^{KI\text{-}Y147del}$ (grey) or pBinplus::ΔGFP control (green). Statistical significance was evaluated in comparison to the control by one-way ANOVA followed by Tukey HSD test. *** P < 0.001, ** P< 0.05. Anti-FLAG antibodies after flg22 (E) or INF1 (F) treatment detected total protein expression of AVR3a variants.

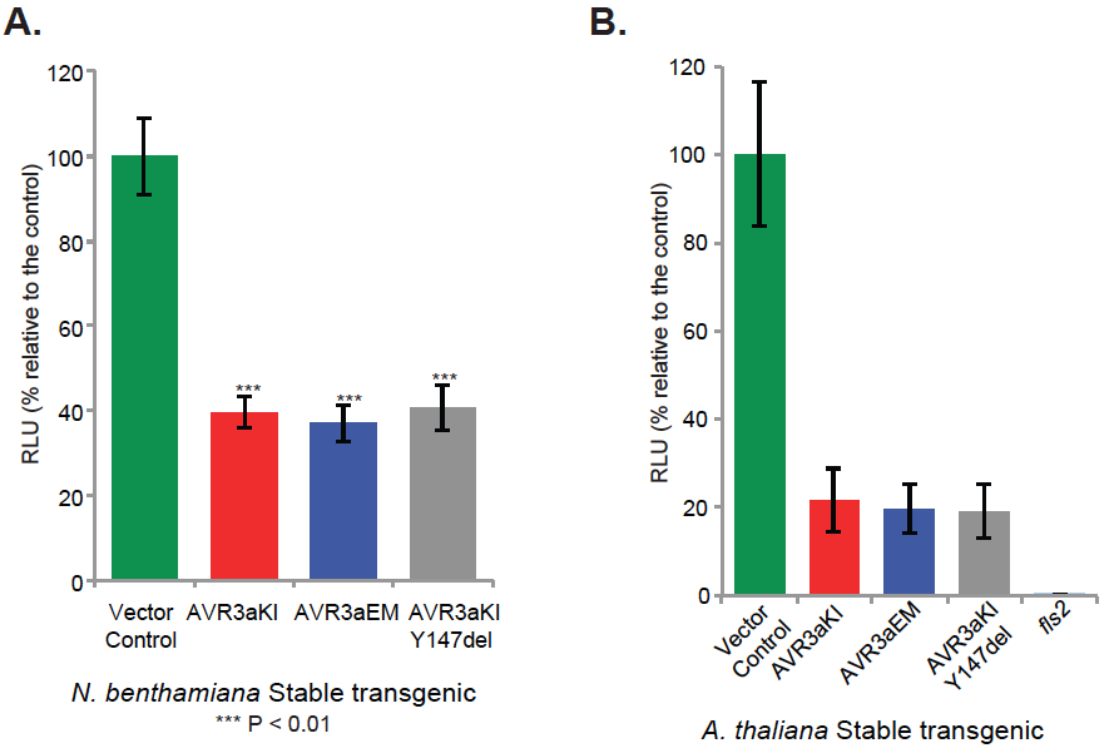

Fig. A2.2. All variants of AVR3a suppress the oxidative burst upon elicitor treatment *in N. benthamiana* and *A. thaliana*

Total ROS production measured in relative light units (RLU) is expressed as percentage of the control treated with 100 nM flg22 over 45 minutes in transgenic plants of *N. benthamiana* (A) or *A. thaliana* (B). Plants were stably transformed with the following constructs: pBinplus::AVR3a^{KI} (red), pBinplus::AVR3a^{EM} (blue), pBinplus::AVR3a$^{KI\text{-}Y147del}$ (grey) or pBinplus::ΔGFP control (green). Values are average ± SE (n = 24). Statistical significance was evaluated in comparison to the control by one-way ANOVA followed by Tukey HSD test. *** P < 0.001.

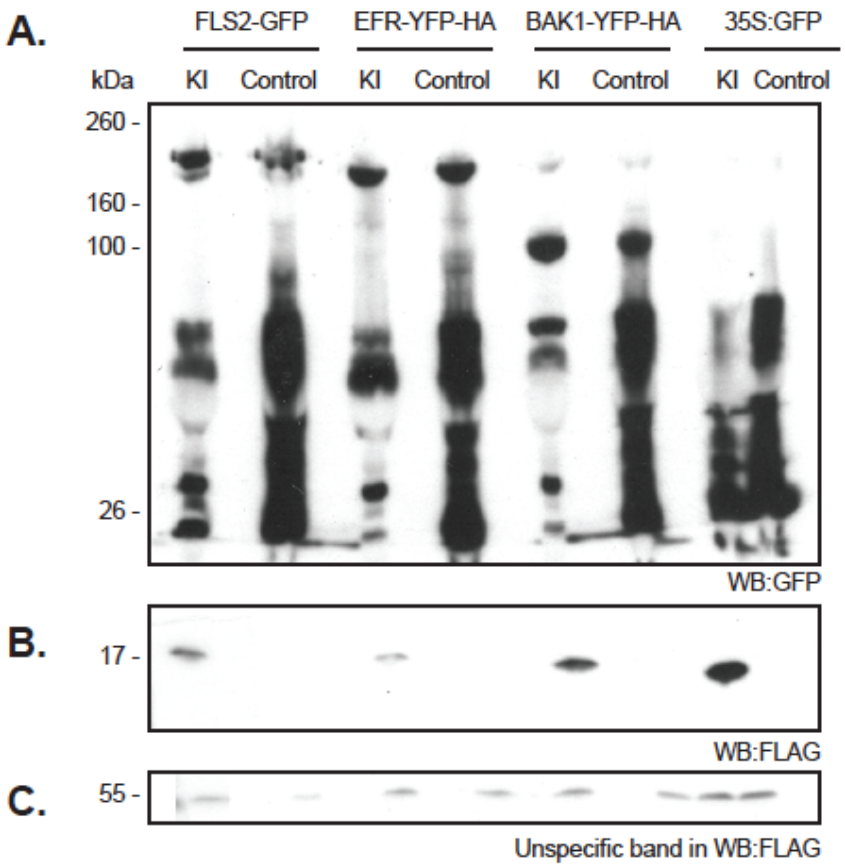

Fig. A2.3. AVR3a^{KI} effect on protein accumulation and degradation of LRR-containing receptors

Transient co-expression of FLAG-AVR3a^{KI} and FLS2-GFP, EFR-YFP or BAK1-YFP in *N. benthamiana* at 3 DPI. (A) AVR3a^{KI} does not affect the protein levels of the receptors *per se* but it seems to have an effect on their processing status. Protein total extracts were immunoprecipitated with anti-GFP agarose beads (Chromotek) to enrich for the fluorescent proteins and detected using anti-GFP antibody (sc-9996 Santa Cruz). 35S:GFP was used as a control. (B) Total protein extracts were blotted with anti-FLAG antibody (sc-807 Santa Cruz). (C) Unspecific band in the anti-FLAG blot is shown to account for protein loading.

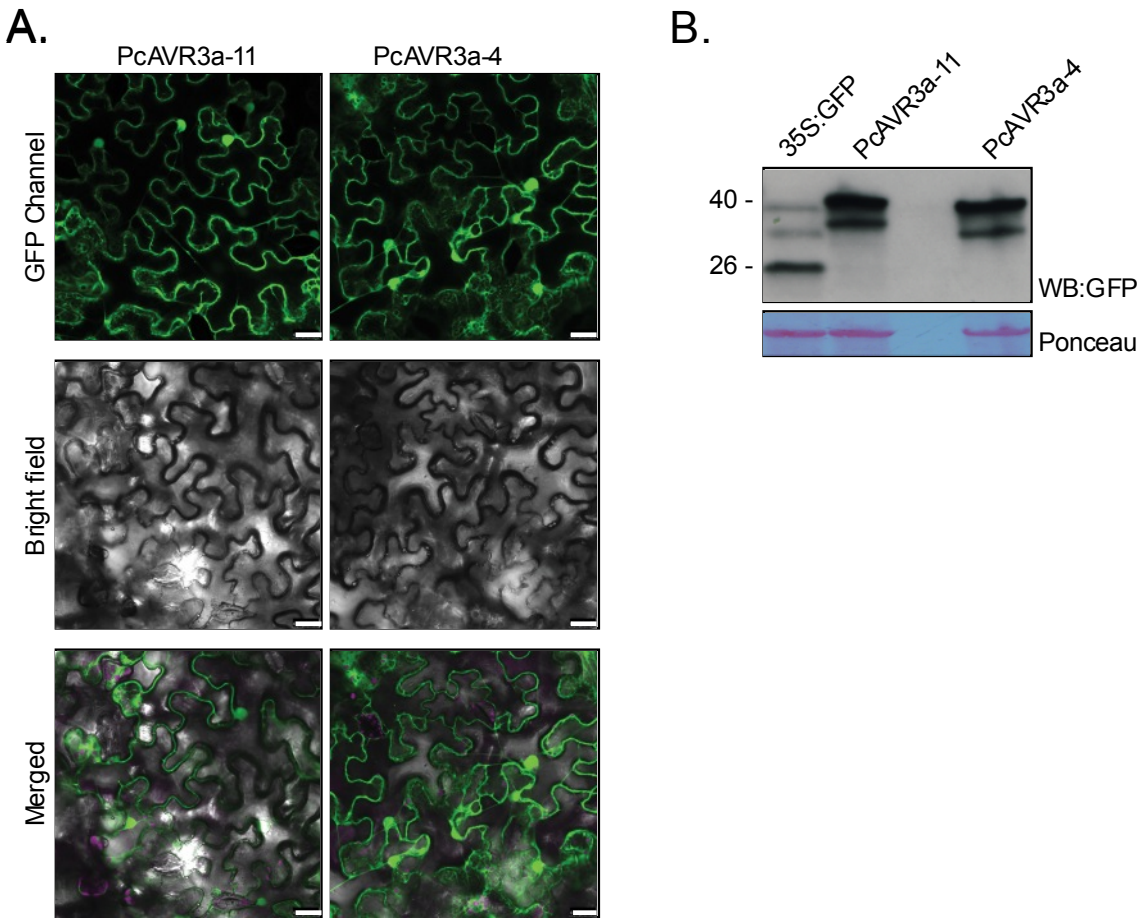

Fig. A2.4. *P. capsici* homologs of AVR3a PcAVR3a-11 and PcAVR3a-4 also have cytoplasmic and nuclear localization in *N. benthamiana*

(A) GFP N-terminal fusions of PcAVR3a-11, PcAVR3a-4 or 35S:GFP were transiently expressed in *N. benthamiana* and subcellular distribution was imaged at 2.5 DPI. Bar = 25μm. Representative images are shown. (B) Western blot of the fluorescent proteins expressed in (A).

Appendix 3

Supplementary figures for Chapter 6: *Phytophthora infestans* RXLR effector AVR3a targets a GTPase involved in plant immunity.

A.

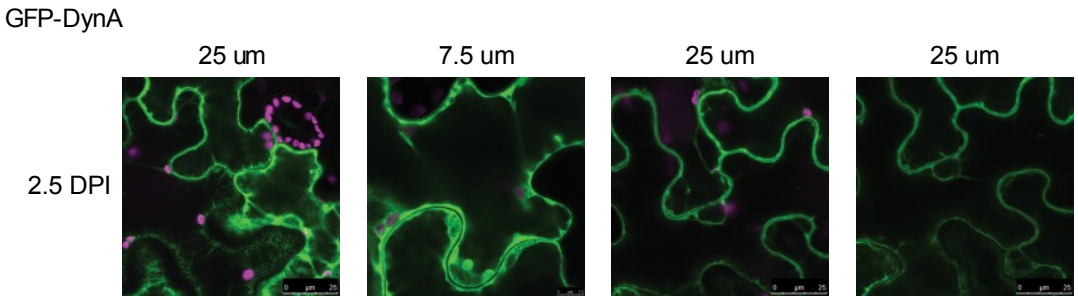

Fig. A3.1. NtDynA localization

(A) Transient expression of GFP-DynA (final OD_{600mm} of 0.3) localizes mainly to the plasma membrane (PM). Scale bar values are shown in each picture. Representative confocal images were taken at 2.5 DPI.

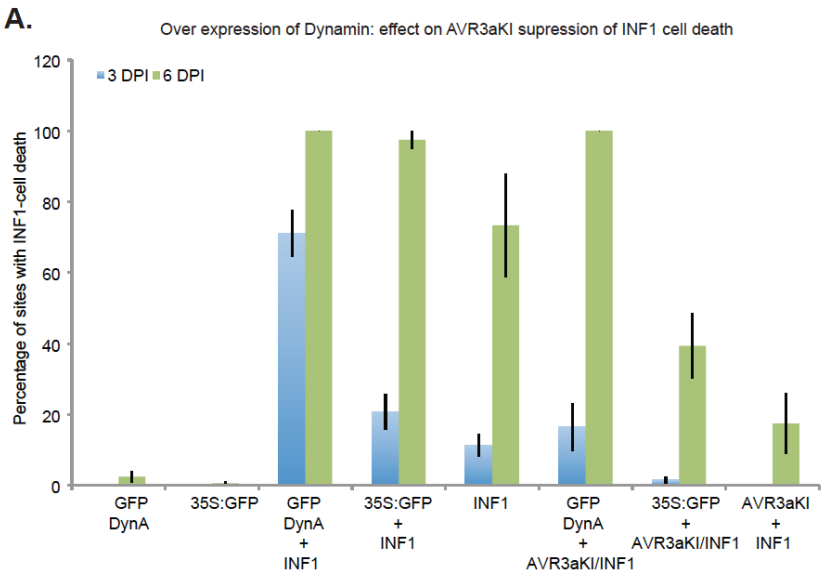

Fig. A3.2. NtDynA overexpression effect on AVR3a^{KI} suppression of INF1 cell death

(A) Leaves of *N. benthamiana* were infiltrated with a mix (1:1) of FLAG-AVR3a^{KI} and GFP-DynA or FLAG-AVR3a^{KI} and 35S:GFP and challenged one-day post infiltration with pCB302:INF1 Percentages of infiltration sites showing the cell death induced by INF1 are shown. Enhancement of the cell death triggered by INF1 started at 3 DPI and still AVR3a was able to suppress INF1 cell death (ICD). At 6 DPI AVr3a could no longer suppress ICD. Values are average ± SE (n = 15). Experiment was repeated at least three times with similar results.

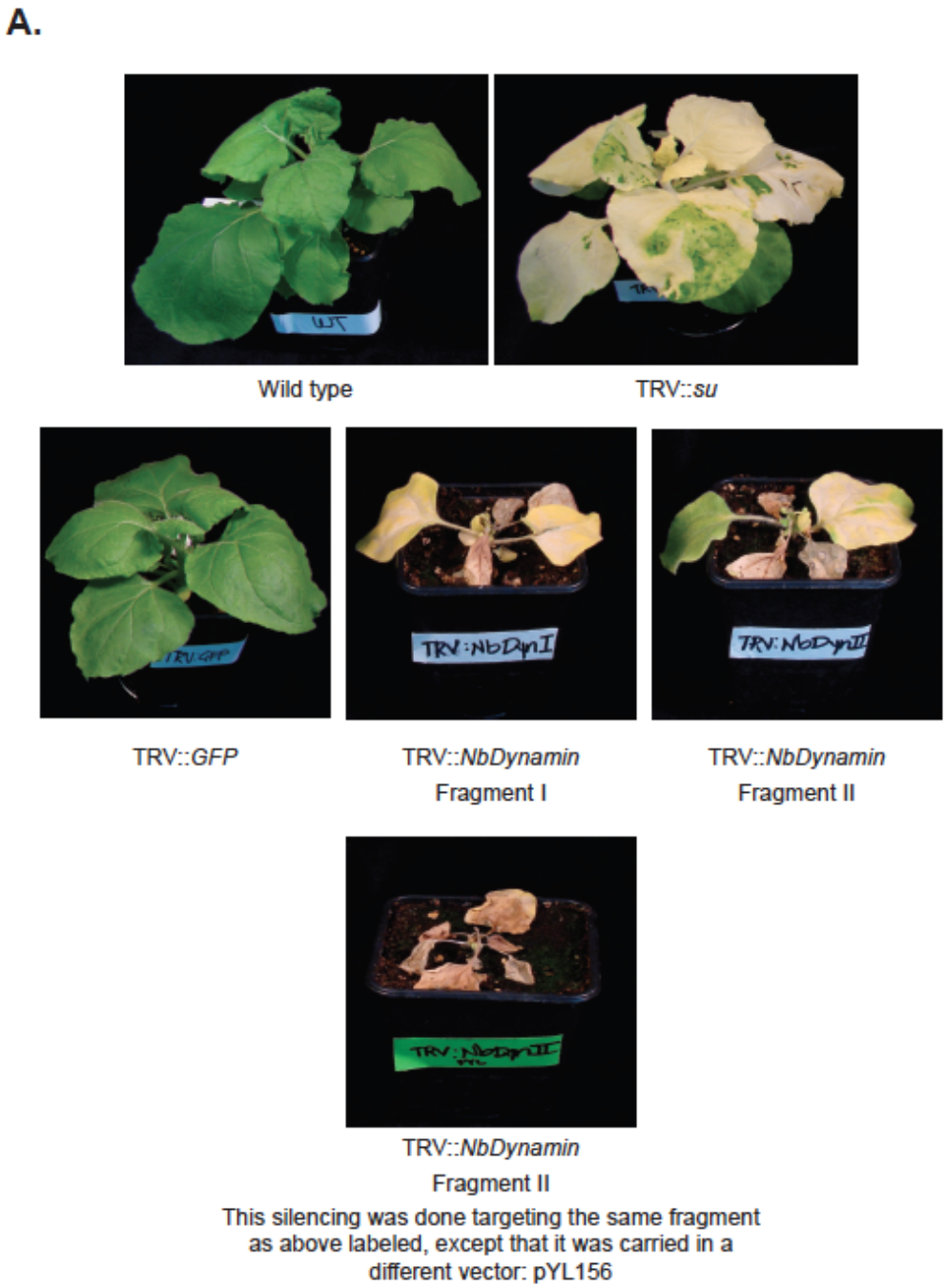

Fig. A3.3. Impact of systemic silencing of dynamin in *N. benthamiana* using VIGS

(A) *N. benthamiana* plants were silenced using tobacco rattle virus vectors harboring a partial sequence of *NtDynamin* (TRV::*NbDynamin* Fragment I or TRV::*NbDynamin* Fragment II) or an empty cloning site (TRV::*GFP*). Pictures were taken 2.5 weeks after the initial infiltration with the silencing constructs.

A.

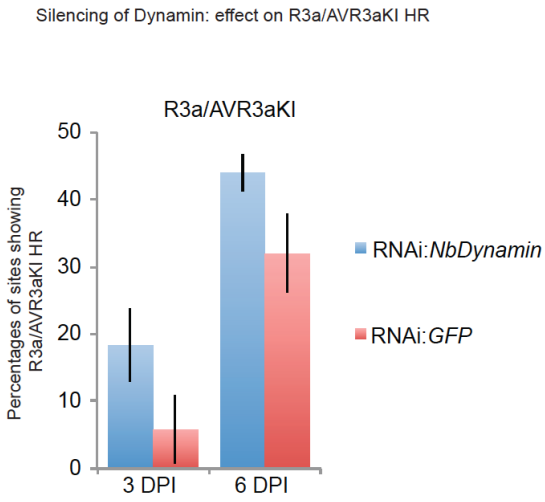

Fig. A3.4. Transient silencing of *NbDynamin* does not affect R3a-HR induce by AVR3a

Leaves of *N. benthamiana* were silenced locally via RNAi-mediated silencing using the vector pHellsgate8 harboring a fragment of dynamin or a fragment targeting a region of GFP as a control. One and a half days post silencing, a mix (1:2) of pBINPLUS-FLAG-AVR3a^{KI} and pCB302:R3a was infiltrated on those leaves. Validation of the silencing by RT-PCR (~150 ng cDNA) is shown in Fig. 6.5.A. (A) Histogram representing the percentages of HR at 3 and 6 DPI is shown. Values are average ± SE (n = 12). Experiment was repeated at least three times.

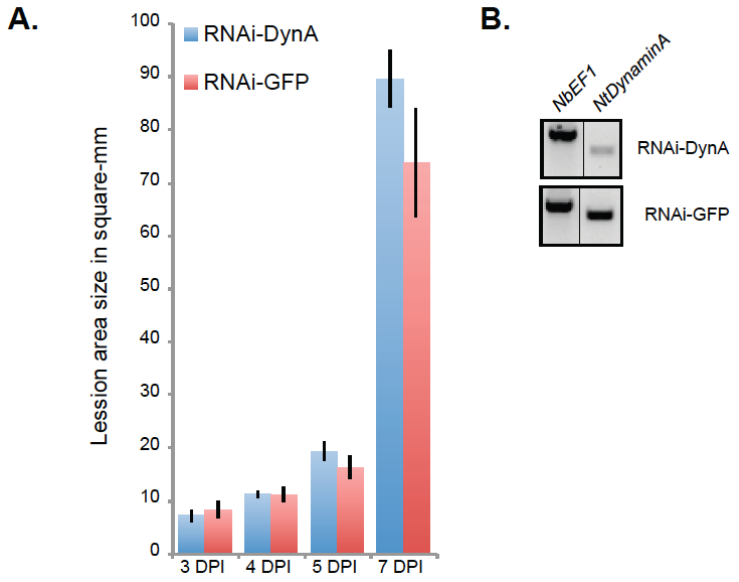

Fig. A3.5. Silencing of *NbDynamin* does not have an effect on *P. infestans* pathogenicity in *N. benthamiana*

One and half days post transiently silencing *NbDynamin* in *N. benthamiana*, detached leaves were inoculated with *P. infestans* 88069 tdtom (100 zoospores/µl) and the infection was followed at the indicated days. (A) Individual infection spots (6 per leaf) were followed with a Leica stereoscope and images were taken for each of them at 3, 4, 5, and 7 DPI. Images were processed as explained in the methods sections. Resulting values from the image analysis corresponds to area lesion size in mm^2. Values in the histogram represent the average value of the lesion sizes for each day and silencing treatment. For 3 and 7 DPI (n=12); for 4 and 5 DPI (n=38). No statistical significance was found by T-test comparison within each day. Experiment was repeated at least three times. (B) Confirmation of silencing by RT-PCR was done as explained in Fig. 6.2.5.

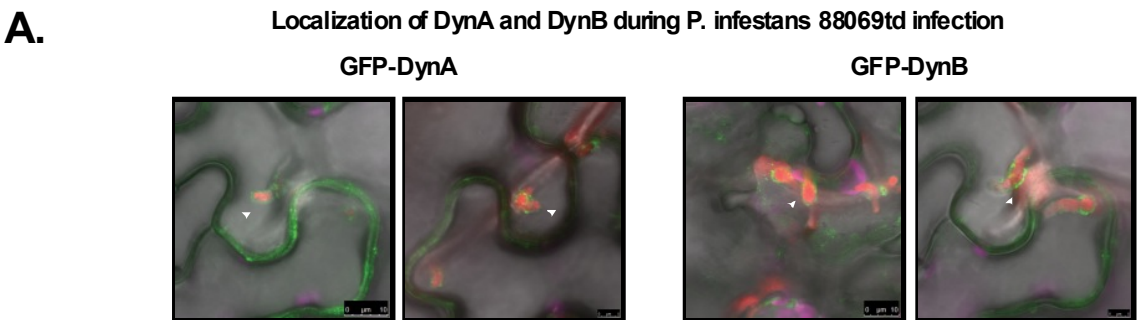

Fig. A3.6. NtDynaminB (NtDynB) also accumulates around *P. infestans* haustoria

Detached leaves of *N. benthamiana* (4.5 week-old) transiently expressing GFP-DynA or GFP-DynB were drop-inoculated at 1 DPI with *P. infestans* 88069-tdtom (100 zoospores/µl). Representative confocal images were taken at 3 days post infection. GFP-DynB accumulates around haustoria penetration sites (white arrows) and envelops the haustorium.

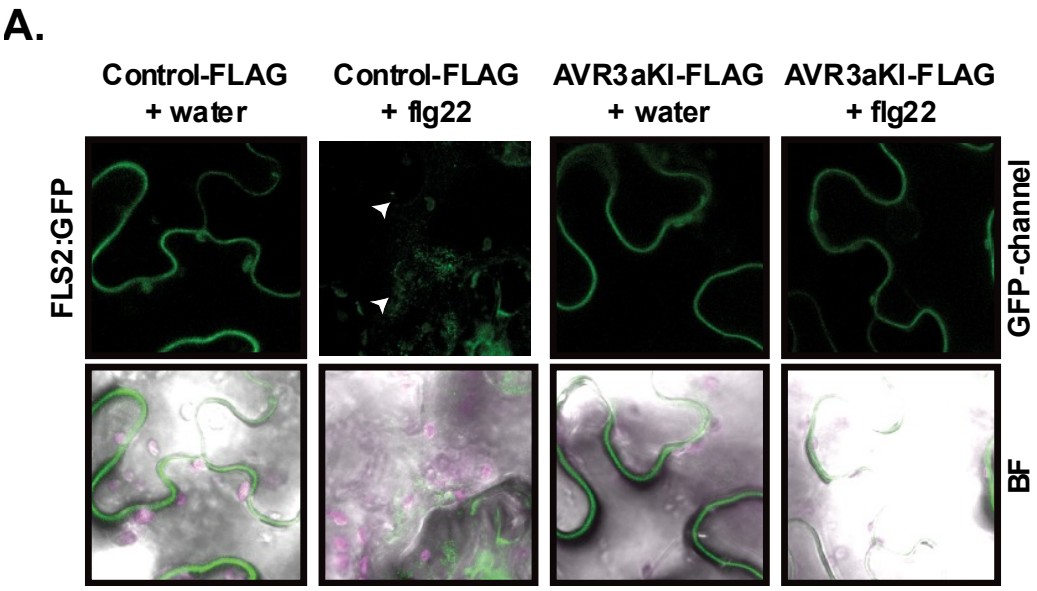

Fig. A3.7. AVR3a inhibits FLS2 endocytosis

(A) Transient expression of FLAG-AVR3a^{KI} or FLAG-AVR3a^{EM} or FLAG-AVR3a$^{KI\text{-}Y147del}$ or the vector control (pBinplus) in *N. benthamiana* co-expressing AtFLS2-GFP and 2.5 DPI challenged with 10 μM flg22 or water as indicated for 120 minutes. Representative images showed accumulation of FLS2 in vesicles after flg22 elicitation in the control leaves (white arrows) whereas this distinct re-distribution of FLS2-GFP was inhibited by the presence of all variants of AVR3a. All images are a maximum projection of 20 slices taken at 10-μM step-size. Same confocal settings were used to acquire all images. Experiment done twice.

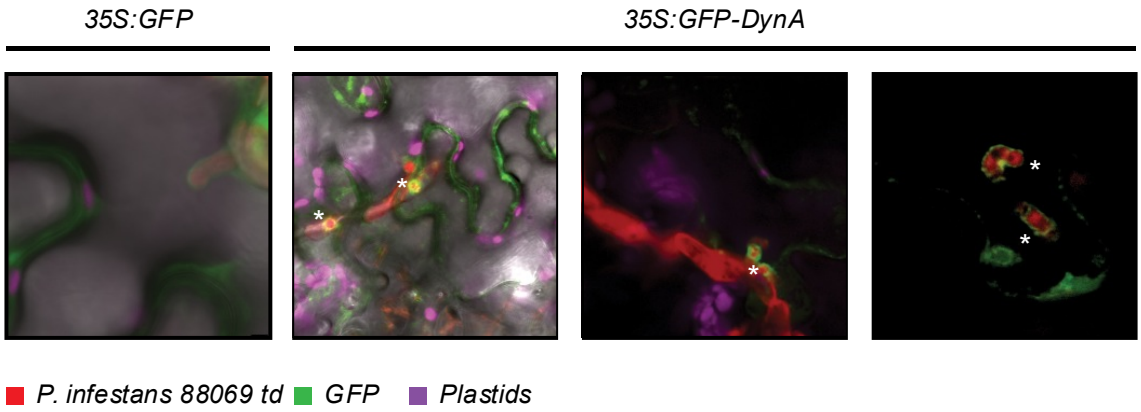

Fig. A3.8. NtDynaminA (NtDynA) accumulates around *P. infestans* haustoria and enhances *P. infestans* growth

Detached leaves of *N. benthamiana* transiently expressing GFP-DynA or 35S:GFP were drop-inoculated at 1 DPI with *P. infestans* 88069-tdtom (100 zoospores/μl). Representative confocal images were taken at 3 days post infection. GFP-DynA accumulates around haustoria penetration sites and envelops the haustorium (white asterisks).

References

Abramovitch, R.B., Kim, Y.J., Chen, S., Dickman, M.B., and Martin, G.B. (2003). Pseudomonas type III effector AvrPtoB induces plant disease susceptibility by inhibition of host programmed cell death. The EMBO journal **22,** 60-69.

Aepfelbacher, M., Trasak, C., Wilharm, G., Wiedemann, A., Trulzsch, K., Krauss, K., Gierschik, P., and Heesemann, J. (2003). Characterization of YopT effects on Rho GTPases in Yersinia enterocolitica-infected cells. J Biol Chem **278,** 33217-33223.

Afzal, A.J., da Cunha, L., and Mackey, D. (2011). Separable fragments and membrane tethering of Arabidopsis RIN4 regulate its suppression of PAMP-triggered immunity. Plant Cell **23,** 3798-3811.

Ahmad-Nejad, P., Hacker, H., Rutz, M., Bauer, S., Vabulas, R.M., and Wagner, H. (2002). Bacterial CpG-DNA and lipopolysaccharides activate Toll-like receptors at distinct cellular compartments. European journal of immunology **32,** 1958-1968.

Albert, M., Jehle, A.K., Mueller, K., Eisele, C., Lipschis, M., and Felix, G. (2010). Arabidopsis thaliana Pattern Recognition Receptors for Bacterial Elongation Factor Tu and Flagellin Can Be Combined to Form Functional Chimeric Receptors. J Biol Chem **285,** 19035-19042.

Alfano, J.R., and Collmer, A. (2004). Type III secretion system effector proteins: double agents in bacterial disease and plant defense. Annual review of phytopathology **42,** 385-414.

Allan, A.C., and Fluhr, R. (1997). Two Distinct Sources of Elicited Reactive Oxygen Species in Tobacco Epidermal Cells. Plant Cell **9,** 1559-1572.

Allen, R.L., Bittner-Eddy, P.D., Grenville-Briggs, L.J., Meitz, J.C., Rehmany, A.P., Rose, L.E., and Beynon, J.L. (2004). Host-parasite coevolutionary conflict between Arabidopsis and downy mildew. Science **306,** 1957-1960.

Angot, A., Vergunst, A., Genin, S., and Peeters, N. (2007). Exploitation of eukaryotic ubiquitin signaling pathways by effectors translocated by bacterial type III and type IV secretion systems. PLoS pathogens **3,** e3.

Antolin-Llovera, M., Ried, M.K., Binder, A., and Parniske, M. (2012). Receptor kinase signaling pathways in plant-microbe interactions. Annual review of phytopathology **50,** 451-473.

Apel, K., and Hirt, H. (2004). Reactive oxygen species: metabolism, oxidative stress, and signal transduction. Annu Rev Plant Biol **55,** 373-399.

Armstrong, M.R., Whisson, S.C., Pritchard, L., Bos, J.I., Venter, E., Avrova, A.O., Rehmany, A.P., Bohme, U., Brooks, K., Cherevach, I., Hamlin, N., White, B., Fraser, A., Lord, A., Quail, M.A., Churcher, C., Hall, N., Berriman, M., Huang, S., Kamoun, S., Beynon, J.L., and Birch, P.R. (2005). An ancestral oomycete locus contains late blight avirulence gene Avr3a, encoding a protein that is recognized in the host cytoplasm. Proc Natl Acad Sci U S A **102,** 7766-7771.

Asai, S., Ohta, K., and Yoshioka, H. (2008). MAPK signaling regulates nitric oxide and NADPH oxidase-dependent oxidative bursts in Nicotiana benthamiana. Plant Cell **20,** 1390-1406.

Austin, M.J., Muskett, P., Kahn, K., Feys, B.J., Jones, J.D., and Parker, J.E. (2002). Regulatory role of SGT1 in early R gene-mediated plant defenses. Science **295,** 2077-2080.

Axtell, M.J., and Staskawicz, B.J. (2003). Initiation of RPS2-specified disease resistance in Arabidopsis is coupled to the AvrRpt2-directed elimination of RIN4. Cell **112,** 369-377.

Azevedo, C., Sadanandom, A., Kitagawa, K., Freialdenhoven, A., Shirasu, K., and Schulze-Lefert, P. (2002). The RAR1 interactor SGT1, an essential component of R gene-triggered disease resistance. Science **295,** 2073-2076.

Azevedo, C., Betsuyaku, S., Peart, J., Takahashi, A., Noel, L., Sadanandom, A., Casais, C., Parker, J., and Shirasu, K. (2006). Role of SGT1 in resistance protein accumulation in plant immunity. The EMBO journal **25,** 2007-2016.

Backues, S.K., Korasick, D.A., Heese, A., and Bednarek, S.Y. (2010). The Arabidopsis dynamin-related protein2 family is essential for gametophyte development. Plant Cell **22,** 3218-3231.

Bai, X., Correa, V.R., Toruno, T.Y., Ammar el, D., Kamoun, S., and Hogenhout, S.A. (2009). AY-WB phytoplasma secretes a protein that targets plant cell nuclei. Molecular plant-microbe interactions : MPMI **22,** 18-30.

Bar, M., and Avni, A. (2009). EHD2 inhibits signaling of leucine rich repeat receptor-like proteins. Plant signaling & behavior **4,** 682-684.

Bar, M., Sharfman, M., Ron, M., and Avni, A. (2010). BAK1 is required for the attenuation of ethylene-inducing xylanase (Eix)-induced defense responses by the decoy receptor LeEix1. Plant J **63,** 791-800.

Beck, M., Heard, W., Mbengue, M., and Robatzek, S. (2012). The INs and OUTs of pattern recognition receptors at the cell surface. Curr Opin Plant Biol **15,** 367-374.

Becktell, M.C., Smart, C.A., Haney, C.H., and Fry, W.E. (2006). Host-pathogen interactions between Phytophthora infestans and the Solanaceous hosts Calibrachoa x Hybridus, Petunia x hybrida, and Nicotiana benthamiana. Plant Dis **90,** 24-32.

Becraft, P.W. (2002). Receptor kinase signaling in plant development. Annual review of cell and developmental biology **18,** 163-192.

Bergmann, D.C., and Sack, F.D. (2007). Stomatal development. Annu Rev Plant Biol **58,** 163-181.

Bhattacharjee, S., Hiller, N.L., Liolios, K., Win, J., Kanneganti, T.D., Young, C., Kamoun, S., and Haldar, K. (2006). The malarial host-targeting signal is conserved in the Irish potato famine pathogen. PLoS pathogens **2,** e50.

Bhavsar, A.P., Guttman, J.A., and Finlay, B.B. (2007). Manipulation of host-cell pathways by bacterial pathogens. Nature **449,** 827-834.

Bhoj, V.G., and Chen, Z.J. (2009). Ubiquitylation in innate and adaptive immunity. Nature **458,** 430-437.

Block, A., and Alfano, J.R. (2011). Plant targets for Pseudomonas syringae type III effectors: virulence targets or guarded decoys? Current opinion in microbiology **14,** 39-46.

Block, A., Li, G., Fu, Z.Q., and Alfano, J.R. (2008). Phytopathogen type III effector weaponry and their plant targets. Curr Opin Plant Biol **11,** 396-403.

Boller, T., and Felix, G. (2009). A renaissance of elicitors: perception of microbe-associated molecular patterns and danger signals by pattern-recognition receptors. Annu Rev Plant Biol **60,** 379-406.

Bos, J.I. (2007). FUNCTION, STRUCTURE AND EVOLUTION OF THE RXLR EFFECTOR AVR3a OF *PHYTOPHTHORA INFESTANS*. In PhD Thesis (Ohio State University).

Bos, J.I., Kanneganti, T.D., Young, C., Cakir, C., Huitema, E., Win, J., Armstrong, M.R., Birch, P.R., and Kamoun, S. (2006). The C-terminal half of Phytophthora infestans RXLR effector AVR3a is sufficient to trigger R3a-mediated hypersensitivity and suppress INF1-induced cell death in Nicotiana benthamiana. Plant J **48,** 165-176.

Bos, J.I., Armstrong, M.R., Gilroy, E.M., Boevink, P.C., Hein, I., Taylor, R.M., Zhendong, T., Engelhardt, S., Vetukuri, R.R., Harrower, B., Dixelius, C., Bryan, G., Sadanandom, A., Whisson, S.C., Kamoun, S., and Birch, P.R. (2010). Phytophthora infestans effector AVR3a is essential for virulence and manipulates plant immunity by stabilizing host E3 ligase CMPG1. Proc Natl Acad Sci U S A **107,** 9909-9914.

Bos, J.I.B., Chaparro-Garcia, A., Quesada-Ocampo, L.M., Gardener, B.B.M., and Kamoun, S. (2009). Distinct Amino Acids of the Phytophthora infestans Effector AVR3a Condition Activation of R3a Hypersensitivity and Suppression of Cell Death. Mol Plant Microbe In **22,** 269-281.

Boutemy, L.S., King, S.R., Win, J., Hughes, R.K., Clarke, T.A., Blumenschein, T.M., Kamoun, S., and Banfield, M.J. (2011). Structures of Phytophthora RXLR effector proteins: a conserved but adaptable fold underpins functional diversity. J Biol Chem **286,** 35834-35842.

Boyer, L., and Lemichez, E. (2004). Targeting of host-cell ubiquitin and ubiquitin-like pathways by bacterial factors. Nature reviews. Microbiology **2,** 779-788.

Bozkurt, T.O., Schornack, S., Banfield, M.J., and Kamoun, S. (2012). Oomycetes, effectors, and all that jazz. Curr Opin Plant Biol **15,** 483-492.

Bozkurt, T.O., Schornack, S., Win, J., Shindo, T., Ilyas, M., Oliva, R., Cano, L.M., Jones, A.M., Huitema, E., van der Hoorn, R.A., and Kamoun, S. (2011). Phytophthora infestans effector AVRblb2 prevents secretion of a plant immune protease at the haustorial interface. Proc Natl Acad Sci U S A **108,** 20832-20837.

Brinkmann, M.M., Spooner, E., Hoebe, K., Beutler, B., Ploegh, H.L., and Kim, Y.M. (2007). The interaction between the ER membrane protein UNC93B and TLR3, 7, and 9 is crucial for TLR signaling. The Journal of cell biology **177,** 265-275.

Brutus, A., Sicilia, F., Macone, A., Cervone, F., and De Lorenzo, G. (2010). A domain swap approach reveals a role of the plant wall-associated kinase 1 (WAK1) as a receptor of oligogalacturonides. P Natl Acad Sci USA **107,** 9452-9457.

Canonne, J., and Rivas, S. (2012). Bacterial effectors target the plant cell nucleus to subvert host transcription. Plant signaling & behavior **7,** 217-221.

Chaparro-Garcia, A., Wilkinson, R.C., Gimenez-Ibanez, S., Findlay, K., Coffey, M.D., Zipfel, C., Rathjen, J.P., Kamoun, S., and Schornack, S. (2011). The Receptor-Like Kinase SERK3/BAK1 Is Required for Basal Resistance against the Late Blight Pathogen Phytophthora infestans in Nicotiana benthamiana. Plos One **6**.

Chen, X., Irani, N.G., and Friml, J. (2011). Clathrin-mediated endocytosis: the gateway into plant cells. Curr Opin Plant Biol **14,** 674-682.

Chinchilla, D., Boller, T., and Robatzek, S. (2007a). Flagellin signalling in plant immunity. Advances in experimental medicine and biology **598,** 358-371.

Chinchilla, D., Bauer, Z., Regenass, M., Boller, T., and Felix, G. (2006). The Arabidopsis receptor kinase FLS2 binds flg22 and determines the specificity of flagellin perception. Plant Cell **18,** 465-476.

Chinchilla, D., Shan, L., He, P., De Vries, S., and Kemmerling, B. (2009). One for all: the receptor-associated kinase BAK1. Trends Plant Sci **14,** 535-541.

Chinchilla, D., Zipfel, C., Robatzek, S., Kemmerling, B., Nurnberger, T., Jones, J.D., Felix, G., and Boller, T. (2007b). A flagellin-induced complex of the receptor FLS2 and BAK1 initiates plant defence. Nature **448,** 497-500.

Chisholm, S.T., Coaker, G., Day, B., and Staskawicz, B.J. (2006). Host-microbe interactions: Shaping the evolution of the plant immune response. Cell **124,** 803-814.

Chou, I.T., and Gasser, C.S. (1997). Characterization of the cyclophilin gene family of Arabidopsis thaliana and phylogenetic analysis of known cyclophilin proteins. Plant molecular biology **35,** 873-892.

Clough, S.J., and Bent, A.F. (1998). Floral dip: a simplified method for Agrobacterium-mediated transformation of Arabidopsis thaliana. Plant J **16,** 735-743.

Coaker, G., Falick, A., and Staskawicz, B. (2005). Activation of a phytopathogenic bacterial effector protein by a eukaryotic cyclophilin. Science **308,** 548-550.

Coaker, G., Zhu, G., Ding, Z., Van Doren, S.R., and Staskawicz, B. (2006). Eukaryotic cyclophilin as a molecular switch for effector activation. Molecular microbiology **61,** 1485-1496.

Coppinger, P., Repetti, P.P., Day, B., Dahlbeck, D., Mehlert, A., and Staskawicz, B.J. (2004). Overexpression of the plasma membrane-localized NDR1 protein results in enhanced bacterial disease resistance in Arabidopsis thaliana. Plant J **40,** 225-237.

Couve, A., Filippov, A.K., Connolly, C.N., Bettler, B., Brown, D.A., and Moss, S.J. (1998). Intracellular retention of recombinant GABAB receptors. J Biol Chem **273,** 26361-26367.

Damke, H., Baba, T., Warnock, D.E., and Schmid, S.L. (1994). Induction of mutant dynamin specifically blocks endocytic coated vesicle formation. The Journal of cell biology **127,** 915-934.

Damke, H., Binns, D.D., Ueda, H., Schmid, S.L., and Baba, T. (2001). Dynamin GTPase domain mutants block endocytic vesicle formation at morphologically distinct stages. Molecular biology of the cell **12,** 2578-2589.

Dangl, J.L., and Jones, J.D. (2001). Plant pathogens and integrated defence responses to infection. Nature **411,** 826-833.

de Jonge, R., van Esse, H.P., Maruthachalam, K., Bolton, M.D., Santhanam, P., Saber, M.K., Zhang, Z., Usami, T., Lievens, B., Subbarao, K.V., and Thomma, B.P. (2012). Tomato immune receptor Ve1 recognizes effector of multiple fungal pathogens uncovered by genome and RNA sequencing. Proc Natl Acad Sci U S A **109,** 5110-5115.

Deslandes, L., and Rivas, S. (2012). Catch me if you can: bacterial effectors and plant targets. Trends Plant Sci.

Dodds, P.N., and Rathjen, J.P. (2010). Plant immunity: towards an integrated view of plant-pathogen interactions. Nat Rev Genet **11,** 539-548.

Doherty, G.J., and McMahon, H.T. (2009). Mechanisms of endocytosis. Annual review of biochemistry **78,** 857-902.

Dong, S., Yin, W., Kong, G., Yang, X., Qutob, D., Chen, Q., Kale, S.D., Sui, Y., Zhang, Z., Dou, D., Zheng, X., Gijzen, M., Tyler, B.M., and Wang, Y. (2011). Phytophthora sojae avirulence effector Avr3b is a secreted NADH and ADP-

ribose pyrophosphorylase that modulates plant immunity. PLoS pathogens **7,** e1002353.

Dou, D.L., Kale, S.D., Wang, X.L., Chen, Y.B., Wang, Q.Q., Wang, X., Jiang, R.H.Y., Arredondo, F.D., Anderson, R.G., Thakur, P.B., McDowell, J.M., Wang, Y.C., and Tyler, B.M. (2008). Conserved C-terminal motifs required for avirulence and suppression of cell death by Phytophthora sojae effector Avr1b. Plant Cell **20,** 1118-1133.

Durrant, W.E., Rowland, O., Piedras, P., Hammond-Kosack, K.E., and Jones, J.D. (2000). cDNA-AFLP reveals a striking overlap in race-specific resistance and wound response gene expression profiles. Plant Cell **12,** 963-977.

Emans, N., Zimmermann, S., and Fischer, R. (2002). Uptake of a fluorescent marker in plant cells is sensitive to brefeldin A and wortmannin. Plant Cell **14,** 71-86.

Espinosa, A., and Alfano, J.R. (2004). Disabling surveillance: bacterial type III secretion system effectors that suppress innate immunity. Cell Microbiol **6,** 1027-1040.

Felix, G., and Boller, T. (2003). Molecular sensing of bacteria in plants. The highly conserved RNA-binding motif RNP-1 of bacterial cold shock proteins is recognized as an elicitor signal in tobacco. J Biol Chem **278,** 6201-6208.

Ferguson, S.M., and De Camilli, P. (2012). Dynamin, a membrane-remodelling GTPase. Nature reviews. Molecular cell biology **13,** 75-88.

Feys, B.J., Wiermer, M., Bhat, R.A., Moisan, L.J., Medina-Escobar, N., Neu, C., Cabral, A., and Parker, J.E. (2005). Arabidopsis SENESCENCE-ASSOCIATED GENE101 stabilizes and signals within an ENHANCED DISEASE SUSCEPTIBILITY1 complex in plant innate immunity. Plant Cell **17,** 2601-2613.

Flor, A.H. (1955). Host-parasite interactions in flax rust-its genetics and other implications. Phytopathology **45,** 680-685.

Fradin, E.F., Abd-El-Haliem, A., Masini, L., van den Berg, G.C., Joosten, M.H., and Thomma, B.P. (2011). Interfamily transfer of tomato Ve1 mediates Verticillium resistance in Arabidopsis. Plant Physiol **156,** 2255-2265.

Fradin, E.F., Zhang, Z., Ayala, J.C.J., Castroverde, C.D.M., Nazar, R.N., Robb, J., Liu, C.M., and Thomma, B.P.H.J. (2009). Genetic Dissection of Verticillium Wilt Resistance Mediated by Tomato Ve1. Plant Physiol **150,** 320-332.

Fujimoto, M., Arimura, S., Ueda, T., Takanashi, H., Hayashi, Y., Nakano, A., and Tsutsumi, N. (2010). Arabidopsis dynamin-related proteins DRP2B and DRP1A participate together in clathrin-coated vesicle formation during endocytosis. P Natl Acad Sci USA **107,** 6094-6099.

Gassmann, M., Haller, C., Stoll, Y., Abdel Aziz, S., Biermann, B., Mosbacher, J., Kaupmann, K., and Bettler, B. (2005). The RXR-type endoplasmic reticulum-retention/retrieval signal of GABAB1 requires distant spacing from the membrane to function. Molecular pharmacology **68,** 137-144.

Geldner, N., and Robatzek, S. (2008). Plant receptors go endosomal: a moving view on signal transduction. Plant Physiol **147,** 1565-1574.

Gilroy, E.M., Taylor, R.M., Hein, I., Boevink, P., Sadanandom, A., and Birch, P.R. (2011). CMPG1-dependent cell death follows perception of diverse pathogen elicitors at the host plasma membrane and is suppressed by Phytophthora infestans RXLR effector AVR3a. The New phytologist **190,** 653-666.

Gimenez-Ibanez, S., Ntoukakis, V., and Rathjen, J.P. (2009a). The LysM receptor kinase CERK1 mediates bacterial perception in Arabidopsis. Plant signaling & behavior **4,** 539-541.

Gimenez-Ibanez, S., Hann, D.R., Ntoukakis, V., Petutschnig, E., Lipka, V., and Rathjen, J.P. (2009b). AvrPtoB targets the LysM receptor kinase CERK1 to promote bacterial virulence on plants. Curr Biol **19,** 423-429.

Gohre, V., Spallek, T., Haweker, H., Mersmann, S., Mentzel, T., Boller, T., de Torres, M., Mansfield, J.W., and Robatzek, S. (2008). Plant pattern-recognition receptor FLS2 is directed for degradation by the bacterial ubiquitin ligase AvrPtoB. Curr Biol **18,** 1824-1832.

Gomez-Gomez, L., and Boller, T. (2000). FLS2: an LRR receptor-like kinase involved in the perception of the bacterial elicitor flagellin in Arabidopsis. Molecular cell **5,** 1003-1011.

Gonzalez-Lamothe, R., Tsitsigiannis, D.I., Ludwig, A.A., Panicot, M., Shirasu, K., and Jones, J.D.G. (2006). The U-Box protein CMPG1 is required for efficient activation of defense mechanisms triggered by multiple resistance genes in tobacco and tomato. Plant Cell **18,** 1067-1083.

Goodin, M.M., Zaitlin, D., Naidu, R.A., and Lommel, S.A. (2008). Nicotiana benthamiana: Its history and future as a model for plant-pathogen interactions. Mol Plant Microbe In **21,** 1015-1026.

Goritschnig, S., Zhang, Y., and Li, X. (2007). The ubiquitin pathway is required for innate immunity in Arabidopsis. Plant J **49,** 540-551.

Griesbeck, O., Baird, G.S., Campbell, R.E., Zacharias, D.A., and Tsien, R.Y. (2001). Reducing the environmental sensitivity of yellow fluorescent protein. Mechanism and applications. J Biol Chem **276,** 29188-29194.

Haas, B.J., Kamoun, S., Zody, M.C., Jiang, R.H., Handsaker, R.E., Cano, L.M., Grabherr, M., Kodira, C.D., Raffaele, S., Torto-Alalibo, T., Bozkurt, T.O., Ah-Fong, A.M., Alvarado, L., Anderson, V.L., Armstrong, M.R., Avrova, A., Baxter, L., Beynon, J., Boevink, P.C., Bollmann, S.R., Bos, J.I., Bulone, V., Cai, G., Cakir, C., Carrington, J.C., Chawner, M., Conti, L., Costanzo, S., Ewan, R., Fahlgren, N., Fischbach, M.A., Fugelstad, J., Gilroy, E.M., Gnerre, S., Green, P.J., Grenville-Briggs, L.J., Griffith, J., Grunwald, N.J., Horn, K., Horner, N.R., Hu, C.H., Huitema, E., Jeong, D.H., Jones, A.M., Jones, J.D., Jones, R.W., Karlsson, E.K., Kunjeti, S.G., Lamour, K., Liu, Z., Ma, L., Maclean, D., Chibucos, M.C., McDonald, H., McWalters, J., Meijer, H.J., Morgan, W., Morris, P.F., Munro, C.A., O'Neill, K., Ospina-Giraldo, M., Pinzon, A., Pritchard, L., Ramsahoye, B., Ren, Q., Restrepo, S., Roy, S., Sadanandom, A., Savidor, A., Schornack, S., Schwartz, D.C., Schumann, U.D., Schwessinger, B., Seyer, L., Sharpe, T., Silvar, C., Song, J., Studholme, D.J., Sykes, S., Thines, M., van de Vondervoort, P.J., Phuntumart, V., Wawra, S., Weide, R., Win, J., Young, C., Zhou, S., Fry, W., Meyers, B.C., van West, P., Ristaino, J., Govers, F., Birch, P.R., Whisson, S.C., Judelson, H.S., and Nusbaum, C. (2009). Genome sequence and analysis of the Irish potato famine pathogen Phytophthora infestans. Nature **461,** 393-398.

Ham, H., Sreelatha, A., and Orth, K. (2011). Manipulation of host membranes by bacterial effectors. Nature reviews. Microbiology **9,** 635-646.

Han, J. (2006). MyD88 beyond Toll. Nature immunology **7,** 370-371.

Hann, D.R., and Rathjen, J.P. (2007). Early events in the pathogenicity of Pseudomonas syringae on Nicotiana benthamiana. Plant J **49,** 607-618.

Haweker, H., Rips, S., Koiwa, H., Salomon, S., Saijo, Y., Chinchilla, D., Robatzek, S., and von Schaewen, A. (2010). Pattern recognition receptors require N-glycosylation to mediate plant immunity. J Biol Chem **285,** 4629-4636.

He, P., Shan, L., Lin, N.C., Martin, G.B., Kemmerling, B., Nurnberger, T., and Sheen, J. (2006). Specific bacterial suppressors of MAMP signaling upstream of MAPKKK in Arabidopsis innate immunity. Cell **125,** 563-575.

He, Z.H., Wang, Z.Y., Li, J.M., Zhu, Q., Lamb, C., Ronald, P., and Chory, J. (2000). Perception of brassinosteroids by the extracellular domain of the receptor kinase BRI1. Science **288,** 2360-2363.

Hecht, V., Vielle-Calzada, J.P., Hartog, M.V., Schmidt, E.D.L., Boutilier, K., Grossniklaus, U., and de Vries, S.C. (2001). The Arabidopsis SOMATIC EMBRYOGENESIS RECEPTOR KINASE 1 gene is expressed in developing ovules and embryos and enhances embryogenic competence in culture. Plant Physiol **127,** 803-816.

Heese, A., Hann, D.R., Gimenez-Ibanez, S., Jones, A.M.E., He, K., Li, J., Schroeder, J.I., Peck, S.C., and Rathjen, J.P. (2007). The receptor-like kinase SERK3/BAK1 is a central regulator of innate immunity in plants. P Natl Acad Sci USA **104,** 12217-12222.

Helliwell, C., and Waterhouse, P. (2003). Constructs and methods for high-throughput gene silencing in plants. Methods **30,** 289-295.

Hilbi, H., and Haas, A. (2012). Secretive bacterial pathogens and the secretory pathway. Traffic **13,** 1187-1197.

Hogenhout, S.A., Van der Hoorn, R.A., Terauchi, R., and Kamoun, S. (2009). Emerging concepts in effector biology of plant-associated organisms. Molecular plant-microbe interactions : MPMI **22,** 115-122.

Holstein, S.E. (2002). Clathrin and plant endocytosis. Traffic **3,** 614-620.

Hotson, A., Chosed, R., Shu, H., Orth, K., and Mudgett, M.B. (2003). Xanthomonas type III effector XopD targets SUMO-conjugated proteins in planta. Molecular microbiology **50,** 377-389.

Huang, S., van der Vossen, E.A., Kuang, H., Vleeshouwers, V.G., Zhang, N., Borm, T.J., van Eck, H.J., Baker, B., Jacobsen, E., and Visser, R.G. (2005). Comparative genomics enabled the isolation of the R3a late blight resistance gene in potato. Plant J **42,** 251-261.

Huffaker, A., Pearce, G., and Ryan, C.A. (2006). An endogenous peptide signal in Arabidopsis activates components of the innate immune response. Proc Natl Acad Sci U S A **103,** 10098-10103.

Ito, E., Fujimoto, M., Ebine, K., Uemura, T., Ueda, T., and Nakano, A. (2012). Dynamic behavior of clathrin in Arabidopsis thaliana unveiled by live imaging. Plant J **69,** 204-216.

Jaillais, Y., Belkhadir, Y., Balsemao-Pires, E., Dangl, J.L., and Chory, J. (2011). Extracellular leucine-rich repeats as a platform for receptor/coreceptor complex formation. P Natl Acad Sci USA **108,** 8503-8507.

Janjusevic, R., Abramovitch, R.B., Martin, G.B., and Stebbins, C.E. (2006). A bacterial inhibitor of host programmed cell death defenses is an E3 ubiquitin ligase. Science **311,** 222-226.

Jeong, S., Trotochaud, A.E., and Clark, S.E. (1999). The Arabidopsis CLAVATA2 gene encodes a receptor-like protein required for the stability of the CLAVATA1 receptor-like kinase. Plant Cell **11,** 1925-1934.

Jones, D.A., and Jones, J.D.G. (1997). The Role of Leucine-Rich Repeat Proteins in Plant Defences. Advances in Botanical Research **24,** 90-167.

Jones, D.A., Thomas, C.M., Hammond-Kosack, K.E., Balint-Kurti, P.J., and Jones, J.D. (1994). Isolation of the tomato Cf-9 gene for resistance to Cladosporium fulvum by transposon tagging. Science **266,** 789-793.

Jones, J.D.G., and Dangl, J.L. (2006). The plant immune system. Nature **444,** 323-329.

Kadota, Y., Shirasu, K., and Guerois, R. (2010). NLR sensors meet at the SGT1-HSP90 crossroad. Trends in biochemical sciences **35,** 199-207.

Kamoun, S. (2001). Nonhost resistance to Phytophthora: novel prospects for a classical problem. Curr Opin Plant Biol **4,** 295-300.

Kamoun, S. (2006). A catalogue of the effector secretome of plant pathogenic oomycetes. Annual review of phytopathology **44,** 41-60.

Kamoun, S. (2007). Groovy times: filamentous pathogen effectors revealed. Curr Opin Plant Biol **10,** 358-365.

Kamoun, S., and Smart, C.A. (2005). Late Blight of Potato and Tomato in the Genomics Era. Plant Dis **89**.

Kamoun, S., and Goodwin, S.B. (2007). Fungal and oomycete genes galore. The New phytologist **174,** 713-717.

Kamoun, S., Lindqvist, H., and Govers, F. (1997a). A novel class of elicitin-like genes from Phytophthora infestans. Mol Plant Microbe In **10,** 1028-1030.

Kamoun, S., Huitema, E., and Vleeshouwers, V.G. (1999). Resistance to oomycetes: a general role for the hypersensitive response? Trends Plant Sci **4,** 196-200.

Kamoun, S., Klucher, K.M., Coffey, M.D., and Tyler, B.M. (1993). A Gene Encoding a Host-Specific Elicitor Protein of Phytophthora-Parasitica. Mol Plant Microbe In **6,** 573-581.

Kamoun, S., Young, M., Forster, H., Coffey, M.D., and Tyler, B.M. (1994). Potential Role of Elicitins in the Interaction between Phytophthora Species and Tobacco. Applied and environmental microbiology **60,** 1593-1598.

Kamoun, S., van West, P., Vleeshouwers, V.G., de Groot, K.E., and Govers, F. (1998a). Resistance of nicotiana benthamiana to phytophthora infestans is mediated by the recognition of the elicitor protein INF1. Plant Cell **10,** 1413-1426.

Kamoun, S., van der Lee, T., van den Berg-Velthuis, G., de Groot, K.E., and Govers, F. (1998b). Loss of Production of the Elicitor Protein INF1 in the Clonal Lineage US-1 of Phytophthora infestans. Phytopathology **88,** 1315-1323.

Kamoun, S., vanWest, P., deJong, A.J., deGroot, K.E., Vleeshouwers, V.G.A.A., and Govers, F. (1997b). A gene encoding a protein elicitor of Phytophthora infestans is down-regulated during infection of potato. Mol Plant Microbe In **10,** 13-20.

Kamoun, S., van West, P., de Jong, A.J., de Groot, K.E., Vleeshouwers, V.G., and Govers, F. (1997c). A gene encoding a protein elicitor of Phytophthora infestans is down-regulated during infection of potato. Molecular plant-microbe interactions : MPMI **10,** 13-20.

Kanzaki, H., Saitoh, H., Takahashi, Y., Berberich, T., Ito, A., Kamoun, S., and Terauchi, R. (2008). NbLRK1, a lectin-like receptor kinase protein of Nicotiana benthamiana, interacts with Phytophthora infestans INF1 elicitin and mediates INF1-induced cell death. Planta **228,** 977-987.

Kanzaki, H., Saitoh, H., Ito, A., Fujisawa, S., Kamoun, S., Katou, S., Yoshioka, H., and Terauchi, R. (2003). Cytosolic HSP90 and HSP70 are essential components of INF1-mediated hypersensitive response and non-host

resistance to Pseudomonas cichorii in Nicotiana benthamiana. Mol Plant Pathol **4,** 383-391.

Karimi, M., Inze, D., and Depicker, A. (2002). GATEWAY vectors for Agrobacterium-mediated plant transformation. Trends Plant Sci **7,** 193-195.

Kawchuk, L.M., Hachey, J., Lynch, D.R., Kulcsar, F., van Rooijen, G., Waterer, D.R., Robertson, A., Kokko, E., Byers, R., Howard, R.J., Fischer, R., and Prufer, D. (2001). Tomato Ve disease resistance genes encode cell surface-like receptors. Proc Natl Acad Sci U S A **98,** 6511-6515.

Kay, S., Hahn, S., Marois, E., Hause, G., and Bonas, U. (2007). A bacterial effector acts as a plant transcription factor and induces a cell size regulator. Science **318,** 648-651.

Kay, S., Hahn, S., Marois, E., Wieduwild, R., and Bonas, U. (2009). Detailed analysis of the DNA recognition motifs of the Xanthomonas type III effectors AvrBs3 and AvrBs3Deltarep16. Plant J **59,** 859-871.

Kim, T.W., and Wang, Z.Y. (2010). Brassinosteroid Signal Transduction from Receptor Kinases to Transcription Factors. Annu Rev Plant Biol **61,** 681-704.

Kunze, G., Zipfel, C., Robatzek, S., Niehaus, K., Boller, T., and Felix, G. (2004). The N terminus of bacterial elongation factor Tu elicits innate immunity in Arabidopsis plants. Plant Cell **16,** 3496-3507.

Lacombe, S., Rougon-Cardoso, A., Sherwood, E., Peeters, N., Dahlbeck, D., van Esse, H.P., Smoker, M., Rallapalli, G., Thomma, B.P., Staskawicz, B., Jones, J.D., and Zipfel, C. (2010). Interfamily transfer of a plant pattern-recognition receptor confers broad-spectrum bacterial resistance. Nature biotechnology **28,** 365-369.

Lam, B.C., Sage, T.L., Bianchi, F., and Blumwald, E. (2002). Regulation of ADL6 activity by its associated molecular network. Plant J **31,** 565-576.

Latz, E., Verma, A., Visintin, A., Gong, M., Sirois, C.M., Klein, D.C., Monks, B.G., McKnight, C.J., Lamphier, M.S., Duprex, W.P., Espevik, T., and Golenbock, D.T. (2007). Ligand-induced conformational changes allosterically activate Toll-like receptor 9. Nature immunology **8,** 772-779.

Leborgne-Castel, N., Adam, T., and Bouhidel, K. (2010). Endocytosis in plant-microbe interactions. Protoplasma **247,** 177-193.

Leborgne-Castel, N., Lherminier, J., Der, C., Fromentin, J., Houot, V., and Simon-Plas, F. (2008). The plant defense elicitor cryptogein stimulates clathrin-mediated endocytosis correlated with reactive oxygen species production in bright yellow-2 tobacco cells. Plant Physiol **146,** 1255-1266.

Lee, A.H., Hurley, B., Felsensteiner, C., Yea, C., Ckurshumova, W., Bartetzko, V., Wang, P.W., Quach, V., Lewis, J.D., Liu, Y.C., Bornke, F., Angers, S., Wilde, A., Guttman, D.S., and Desveaux, D. (2012). A bacterial acetyltransferase destroys plant microtubule networks and blocks secretion. PLoS pathogens **8,** e1002523.

Leifer, C.A., Kennedy, M.N., Mazzoni, A., Lee, C., Kruhlak, M.J., and Segal, D.M. (2004). TLR9 is localized in the endoplasmic reticulum prior to stimulation. J Immunol **173,** 1179-1183.

Li, J., Wen, J., Lease, K.A., Doke, J.T., Tax, F.E., and Walker, J.C. (2002). BAK1, an Arabidopsis LRR receptor-like protein kinase, interacts with BRI1 and modulates brassinosteroid signaling. Cell **110,** 213-222.

Li, Y., Berke, I.C., and Modis, Y. (2012). DNA binding to proteolytically activated TLR9 is sequence-independent and enhanced by DNA curvature. The EMBO journal **31,** 919-931.

Lipka, V., Dittgen, J., Bednarek, P., Bhat, R., Wiermer, M., Stein, M., Landtag, J., Brandt, W., Rosahl, S., Scheel, D., Llorente, F., Molina, A., Parker, J., Somerville, S., and Schulze-Lefert, P. (2005). Pre- and postinvasion defenses both contribute to nonhost resistance in Arabidopsis. Science **310,** 1180-1183.

Liu, Y., Burch-Smith, T., Schiff, M., Feng, S., and Dinesh-Kumar, S.P. (2004). Molecular chaperone Hsp90 associates with resistance protein N and its signaling proteins SGT1 and Rar1 to modulate an innate immune response in plants. J Biol Chem **279,** 2101-2108.

Lu, D., Wu, S., Gao, X., Zhang, Y., Shan, L., and He, P. (2010). A receptor-like cytoplasmic kinase, BIK1, associates with a flagellin receptor complex to initiate plant innate immunity. Proc Natl Acad Sci U S A **107,** 496-501.

Lu, D., Lin, W., Gao, X., Wu, S., Cheng, C., Avila, J., Heese, A., Devarenne, T.P., He, P., and Shan, L. (2011). Direct ubiquitination of pattern recognition receptor FLS2 attenuates plant innate immunity. Science **332,** 1439-1442.

Lu, Y.J., Schornack, S., Spallek, T., Geldner, N., Chory, J., Schellmann, S., Schumacher, K., Kamoun, S., and Robatzek, S. (2012). Patterns of plant subcellular responses to successful oomycete infections reveal differences in host cell reprogramming and endocytic trafficking. Cell Microbiol **14,** 682-697.

Lukasik, E., and Takken, F.L. (2009). STANDing strong, resistance proteins instigators of plant defence. Curr Opin Plant Biol **12,** 427-436.

Mackey, D., Holt, B.F., 3rd, Wiig, A., and Dangl, J.L. (2002). RIN4 interacts with Pseudomonas syringae type III effector molecules and is required for RPM1-mediated resistance in Arabidopsis. Cell **108,** 743-754.

Marino, D., Peeters, N., and Rivas, S. (2012). Ubiquitination during Plant Immune Signaling. Plant Physiol **160,** 15-27.

Marois, E., Van den Ackerveken, G., and Bonas, U. (2002). The xanthomonas type III effector protein AvrBs3 modulates plant gene expression and induces cell hypertrophy in the susceptible host. Molecular plant-microbe interactions : MPMI **15,** 637-646.

Martin, G.B., Bogdanove, A.J., and Sessa, G. (2003). Understanding the functions of plant disease resistance proteins. Annu Rev Plant Biol **54,** 23-61.

Martin, T.F. (1998). Phosphoinositide lipids as signaling molecules: common themes for signal transduction, cytoskeletal regulation, and membrane trafficking. Annual review of cell and developmental biology **14,** 231-264.

Medzhitov, R., and Janeway, C.A. (1997). Innate immunity: The virtues of a nonclonal system of recognition. Cell **91,** 295-298.

Miya, A., Albert, P., Shinya, T., Desaki, Y., Ichimura, K., Shirasu, K., Narusaka, Y., Kawakami, N., Kaku, H., and Shibuya, N. (2007). CERK1, a LysM receptor kinase, is essential for chitin elicitor signaling in Arabidopsis. Proc Natl Acad Sci U S A **104,** 19613-19618.

Monaghan, J., and Zipfel, C. (2012). Plant pattern recognition receptor complexes at the plasma membrane. Curr Opin Plant Biol **15,** 349-357.

Mooren, O.L., Galletta, B.J., and Cooper, J.A. (2012). Roles for actin assembly in endocytosis. Annual review of biochemistry **81,** 661-686.

Morgan, W., and Kamoun, S. (2007). RXLR effectors of plant pathogenic oomycetes. Current opinion in microbiology **10,** 332-338.

Mudgil, Y., Shiu, S.H., Stone, S.L., Salt, J.N., and Goring, D.R. (2004). A large complement of the predicted Arabidopsis ARM repeat proteins are members of the U-box E3 ubiquitin ligase family. Plant Physiol **134,** 59-66.

Mueller, K., Bittel, P., Chinchilla, D., Jehle, A.K., Albert, M., Boller, T., and Felix, G. (2012). Chimeric FLS2 Receptors Reveal the Basis for Differential Flagellin Perception in Arabidopsis and Tomato. Plant Cell **24,** 2213-2224.

Murphy, A.S., Bandyopadhyay, A., Holstein, S.E., and Peer, W.A. (2005). Endocytotic cycling of PM proteins. Annu Rev Plant Biol **56,** 221-251.

Murphy, J.E., Padilla, B.E., Hasdemir, B., Cottrell, G.S., and Bunnett, N.W. (2009). Endosomes: a legitimate platform for the signaling train. Proc Natl Acad Sci U S A **106,** 17615-17622.

Nakagawa, T., Kurose, T., Hino, T., Tanaka, K., Kawamukai, M., Niwa, Y., Toyooka, K., Matsuoka, K., Jinbo, T., and Kimura, T. (2007). Development of series of gateway binary vectors, pGWBs, for realizing efficient construction of fusion genes for plant transformation. Journal of bioscience and bioengineering **104,** 34-41.

Nam, K.H., and Li, J. (2002). BRI1/BAK1, a receptor kinase pair mediating brassinosteroid signaling. Cell **110,** 203-212.

Navarro, L., Zipfel, C., Rowland, O., Keller, I., Robatzek, S., Boller, T., and Jones, J.D. (2004). The transcriptional innate immune response to flg22. Interplay and overlap with Avr gene-dependent defense responses and bacterial pathogenesis. Plant Physiol **135,** 1113-1128.

Nekrasov, V., Li, J., Batoux, M., Roux, M., Chu, Z.H., Lacombe, S., Rougon, A., Bittel, P., Kiss-Papp, M., Chinchilla, D., van Esse, H.P., Jorda, L., Schwessinger, B., Nicaise, V., Thomma, B.P., Molina, A., Jones, J.D., and Zipfel, C. (2009). Control of the pattern-recognition receptor EFR by an ER protein complex in plant immunity. The EMBO journal **28,** 3428-3438.

Nishiya, T., Kajita, E., Miwa, S., and Defranco, A.L. (2005). TLR3 and TLR7 are targeted to the same intracellular compartments by distinct regulatory elements. J Biol Chem **280,** 37107-37117.

Nomura, K., Debroy, S., Lee, Y.H., Pumplin, N., Jones, J., and He, S.Y. (2006). A bacterial virulence protein suppresses host innate immunity to cause plant disease. Science **313,** 220-223.

Nomura, K., Mecey, C., Lee, Y.N., Imboden, L.A., Chang, J.H., and He, S.Y. (2011). Effector-triggered immunity blocks pathogen degradation of an immunity-associated vesicle traffic regulator in Arabidopsis. Proc Natl Acad Sci U S A **108,** 10774-10779.

Ntoukakis, V., Schwessinger, B., Segonzac, C., and Zipfel, C. (2011). Cautionary notes on the use of C-terminal BAK1 fusion proteins for functional studies. Plant Cell **23,** 3871-3878.

Oh, S.K., Young, C., Lee, M., Oliva, R., Bozkurt, T.O., Cano, L.M., Win, J., Bos, J.I., Liu, H.Y., van Damme, M., Morgan, W., Choi, D., Van der Vossen, E.A., Vleeshouwers, V.G., and Kamoun, S. (2009). In planta expression screens of Phytophthora infestans RXLR effectors reveal diverse phenotypes, including activation of the Solanum bulbocastanum disease resistance protein Rpi-blb2. Plant Cell **21,** 2928-2947.

Park, C.J., Bart, R., Chern, M., Canlas, P.E., Bai, W., and Ronald, P.C. (2010). Overexpression of the endoplasmic reticulum chaperone BiP3 regulates XA21-mediated innate immunity in rice. Plos One **5,** e9262.

Peart, J.R., Cook, G., Feys, B.J., Parker, J.E., and Baulcombe, D.C. (2002). An EDS1 orthologue is required for N-mediated resistance against tobacco mosaic virus. Plant J **29,** 569-579.

Pel, M.A. (2010). Mapping, isolation and characterization of genes responsible for late blight resistance in potato. (Wageningen Univ.), pp. 210.

Piedras, P., Rivas, S., Droge, S., Hillmer, S., and Jones, J.D. (2000). Functional, c-myc-tagged Cf-9 resistance gene products are plasma-membrane localized and glycosylated. Plant J **21,** 529-536.

Pillitteri, L.J., and Torii, K.U. (2012). Mechanisms of stomatal development. Annu Rev Plant Biol **63,** 591-614.

Polo, S. (2012). Signaling-mediated control of ubiquitin ligases in endocytosis. BMC biology **10,** 25.

Polo, S., and Di Fiore, P.P. (2006). Endocytosis conducts the cell signaling orchestra. Cell **124,** 897-900.

Postel, S., and Kemmerling, B. (2009). Plant systems for recognition of pathogen-associated molecular patterns. Semin Cell Dev Biol **20,** 1025-1031.

Praefcke, G.J., and McMahon, H.T. (2004). The dynamin superfamily: universal membrane tubulation and fission molecules? Nature reviews. Molecular cell biology **5,** 133-147.

Rafiqi, M., Gan, P.H., Ravensdale, M., Lawrence, G.J., Ellis, J.G., Jones, D.A., Hardham, A.R., and Dodds, P.N. (2010). Internalization of flax rust avirulence proteins into flax and tobacco cells can occur in the absence of the pathogen. Plant Cell **22,** 2017-2032.

Rehmany, A.P., Gordon, A., Rose, L.E., Allen, R.L., Armstrong, M.R., Whisson, S.C., Kamoun, S., Tyler, B.M., Birch, P.R., and Beynon, J.L. (2005). Differential recognition of highly divergent downy mildew avirulence gene alleles by RPP1 resistance genes from two Arabidopsis lines. Plant Cell **17,** 1839-1850.

Reyes, F.C., Buono, R., and Otegui, M.S. (2011). Plant endosomal trafficking pathways. Curr Opin Plant Biol **14,** 666-673.

Rivas, S., and Thomas, C.M. (2005). Molecular interactions between tomato and the leaf mold pathogen Cladosporium fulvum. Annual review of phytopathology **43,** 395-436.

Rivas, S., Romeis, T., and Jones, J.D. (2002a). The Cf-9 disease resistance protein is present in an approximately 420-kilodalton heteromultimeric membrane-associated complex at one molecule per complex. Plant Cell **14,** 689-702.

Rivas, S., Mucyn, T., van den Burg, H.A., Vervoort, J., and Jones, J.D. (2002b). An approximately 400 kDa membrane-associated complex that contains one molecule of the resistance protein Cf-4. Plant J **29,** 783-796.

Robatzek, S. (2007). Vesicle trafficking in plant immune responses. Cell Microbiol **9,** 1-8.

Robatzek, S., Chinchilla, D., and Boller, T. (2006). Ligand-induced endocytosis of the pattern recognition receptor FLS2 in Arabidopsis. Genes & development **20,** 537-542.

Robatzek, S., Bittel, P., Chinchilla, D., Kochner, P., Felix, G., Shiu, S.H., and Boller, T. (2007). Molecular identification and characterization of the tomato flagellin receptor LeFLS2, an orthologue of Arabidopsis FLS2 exhibiting characteristically different perception specificities. Plant molecular biology **64,** 539-547.

Ron, M., and Avni, A. (2004). The receptor for the fungal elicitor ethylene-inducing xylanase is a member of a resistance-like gene family in tomato. Plant Cell **16,** 1604-1615.

Rooney, H.C., Van't Klooster, J.W., van der Hoorn, R.A., Joosten, M.H., Jones, J.D., and de Wit, P.J. (2005). Cladosporium Avr2 inhibits tomato Rcr3

protease required for Cf-2-dependent disease resistance. Science **308,** 1783-1786.

Rosebrock, T.R., Zeng, L., Brady, J.J., Abramovitch, R.B., Xiao, F., and Martin, G.B. (2007). A bacterial E3 ubiquitin ligase targets a host protein kinase to disrupt plant immunity. Nature **448,** 370-374.

Roux, M., Schwessinger, B., Albrecht, C., Chinchilla, D., Jones, A., Holton, N., Malinovsky, F.G., Tor, M., de Vries, S., and Zipfel, C. (2011). The Arabidopsis leucine-rich repeat receptor-like kinases BAK1/SERK3 and BKK1/SERK4 are required for innate immunity to hemibiotrophic and biotrophic pathogens. Plant Cell **23,** 2440-2455.

Royle, S.J., Qureshi, O.S., Bobanovic, L.K., Evans, P.R., Owen, D.J., and Murrell-Lagnado, R.D. (2005). Non-canonical YXXGPhi endocytic motifs: recognition by AP2 and preferential utilization in P2X4 receptors. Journal of cell science **118,** 3073-3080.

Russinova, E., Borst, J.W., Kwaaitaal, M., Cano-Delgado, A., Yin, Y., Chory, J., and de Vries, S.C. (2004). Heterodimerization and endocytosis of Arabidopsis brassinosteroid receptors BRI1 and AtSERK3 (BAK1). Plant Cell **16,** 3216-3229.

Rytkonen, A., and Holden, D.W. (2007). Bacterial interference of ubiquitination and deubiquitination. Cell Host Microbe **1,** 13-22.

Saunders, D.G., Breen, S., Win, J., Schornack, S., Hein, I., Bozkurt, T.O., Champouret, N., Vleeshouwers, V.G., Birch, P.R., Gilroy, E.M., and Kamoun, S. (2012). Host Protein BSL1 Associates with Phytophthora infestans RXLR Effector AVR2 and the Solanum demissum Immune Receptor R2 to Mediate Disease Resistance. Plant Cell.

Schornack, S., Fuchs, R., Huitema, E., Rothbauer, U., Lipka, V., and Kamoun, S. (2009a). Protein mislocalization in plant cells using a GFP-binding chromobody. Plant J **60,** 744-754.

Schornack, S., van Damme, M., Bozkurt, T.O., Cano, L.M., Smoker, M., Thines, M., Gaulin, E., Kamoun, S., and Huitema, E. (2010). Ancient class of translocated oomycete effectors targets the host nucleus. P Natl Acad Sci USA **107,** 17421-17426.

Schornack, S., Huitema, E., Cano, L.M., Bozkurt, T.O., Oliva, R., van Damme, M., Schwizer, S., Raffaele, S., Chaparro-Garcia, A., Farrer, R., Segretin, M.E., Bos, J., Haas, B.J., Zody, M.C., Nusbaum, C., Win, J., Thines, M., and Kamoun, S. (2009b). Ten things to know about oomycete effectors. Mol Plant Pathol **10,** 795-803.

Schulze, B., Mentzel, T., Jehle, A.K., Mueller, K., Beeler, S., Boller, T., Felix, G., and Chinchilla, D. (2010). Rapid heteromerization and phosphorylation of ligand-activated plant transmembrane receptors and their associated kinase BAK1. J Biol Chem **285,** 9444-9451.

Schwessinger, B., and Zipfel, C. (2008). News from the frontline: recent insights into PAMP-triggered immunity in plants. Curr Opin Plant Biol **11,** 389-395.

Schwessinger, B., and Ronald, P.C. (2012). Plant innate immunity: perception of conserved microbial signatures. Annu Rev Plant Biol **63,** 451-482.

Schwessinger, B., Roux, M., Kadota, Y., Ntoukakis, V., Sklenar, J., Jones, A., and Zipfel, C. (2011). Phosphorylation-dependent differential regulation of plant growth, cell death, and innate immunity by the regulatory receptor-like kinase BAK1. PLoS genetics **7,** e1002046.

Segonzac, C., Feike, D., Gimenez-Ibanez, S., Hann, D.R., Zipfel, C., and Rathjen, J.P. (2011). Hierarchy and roles of pathogen-associated molecular pattern-induced responses in Nicotiana benthamiana. Plant Physiol **156,** 687-699.

Serrano, M., Robatzek, S., Torres, M., Kombrink, E., Somssich, I.E., Robinson, M., and Schulze-Lefert, P. (2007). Chemical interference of pathogen-associated molecular pattern-triggered immune responses in Arabidopsis reveals a potential role for fatty-acid synthase type II complex-derived lipid signals. J Biol Chem **282,** 6803-6811.

Shan, L., Thara, V.K., Martin, G.B., Zhou, J.M., and Tang, X. (2000). The pseudomonas AvrPto protein is differentially recognized by tomato and tobacco and is localized to the plant plasma membrane. Plant Cell **12,** 2323-2338.

Shan, L., He, P., Li, J., Heese, A., Peck, S.C., Nurnberger, T., Martin, G.B., and Sheen, J. (2008). Bacterial effectors target the common signaling partner BAK1 to disrupt multiple MAMP receptor-signaling complexes and impede plant immunity. Cell Host Microbe **4,** 17-27.

Shao, F., Merritt, P.M., Bao, Z., Innes, R.W., and Dixon, J.E. (2002). A Yersinia effector and a Pseudomonas avirulence protein define a family of cysteine proteases functioning in bacterial pathogenesis. Cell **109,** 575-588.

Shao, F., Golstein, C., Ade, J., Stoutemyer, M., Dixon, J.E., and Innes, R.W. (2003). Cleavage of Arabidopsis PBS1 by a bacterial type III effector. Science **301,** 1230-1233.

Shibata, Y., Kawakita, K., and Takemoto, D. (2010). Age-Related Resistance of Nicotiana benthamiana Against Hemibiotrophic Pathogen Phytophthora infestans Requires Both Ethylene- and Salicylic Acid-Mediated Signaling Pathways. Mol Plant Microbe In **23,** 1130-1142.

Shirasu, K. (2009). The HSP90-SGT1 chaperone complex for NLR immune sensors. Annu Rev Plant Biol **60,** 139-164.

Shiu, S.H., and Bleecker, A.B. (2001). Receptor-like kinases from Arabidopsis form a monophyletic gene family related to animal receptor kinases. Proc Natl Acad Sci U S A **98,** 10763-10768.

Shiu, S.H., Karlowski, W.M., Pan, R., Tzeng, Y.H., Mayer, K.F., and Li, W.H. (2004). Comparative analysis of the receptor-like kinase family in Arabidopsis and rice. Plant Cell **16,** 1220-1234.

Smalle, J., and Vierstra, R.D. (2004). The ubiquitin 26S proteasome proteolytic pathway. Annu Rev Plant Biol **55,** 555-590.

Sohn, K.H., Lei, R., Nemri, A., and Jones, J.D. (2007). The downy mildew effector proteins ATR1 and ATR13 promote disease susceptibility in Arabidopsis thaliana. Plant Cell **19,** 4077-4090.

Song, W.Y., Wang, G.L., Chen, L.L., Kim, H.S., Pi, L.Y., Holsten, T., Gardner, J., Wang, B., Zhai, W.X., Zhu, L.H., Fauquet, C., and Ronald, P. (1995). A receptor kinase-like protein encoded by the rice disease resistance gene, Xa21. Science **270,** 1804-1806.

Stahl, E.A., and Bishop, J.G. (2000). Plant-pathogen arms races at the molecular level. Curr Opin Plant Biol **3,** 299-304.

Stergiopoulos, I., and de Wit, P.J. (2009). Fungal effector proteins. Annual review of phytopathology **47,** 233-263.

Stone, S.L., Anderson, E.M., Mullen, R.T., and Goring, D.R. (2003). ARC1 is an E3 ubiquitin ligase and promotes the ubiquitination of proteins during the rejection of self-incompatible Brassica pollen. Plant Cell **15,** 885-898.

Sullivan, J.A., Shirasu, K., and Deng, X.W. (2003). The diverse roles of ubiquitin and the 26S proteasome in the life of plants. Nat Rev Genet **4,** 948-958.

Szurek, B., Marois, E., Bonas, U., and Van den Ackerveken, G. (2001). Eukaryotic features of the Xanthomonas type III effector AvrBs3: protein domains involved in transcriptional activation and the interaction with nuclear import receptors from pepper. Plant J **26,** 523-534.

Takahashi, A., Casais, C., Ichimura, K., and Shirasu, K. (2003). HSP90 interacts with RAR1 and SGT1 and is essential for RPS2-mediated disease resistance in Arabidopsis. Proc Natl Acad Sci U S A **100,** 11777-11782.

Takemoto, D., Jones, D.A., and Hardham, A.R. (2003). GFP-tagging of cell components reveals the dynamics of subcellular re-organization in response to infection of Arabidopsis by oomycete pathogens. Plant J **33,** 775-792.

Tanaka, S., Ishihama, N., Yoshioka, H., Huser, A., O'Connell, R., Tsuji, G., Tsuge, S., and Kubo, Y. (2009). The Colletotrichum orbiculare ssd1 Mutant Enhances Nicotiana benthamiana Basal Resistance by Activating a Mitogen-Activated Protein Kinase Pathway. Plant Cell **21,** 2517-2526.

Taylor, N.G. (2011). A role for Arabidopsis dynamin related proteins DRP2A/B in endocytosis; DRP2 function is essential for plant growth. Plant molecular biology **76,** 117-129.

Thuerig, B., Felix, G., Binder, A., Boller, T., and Tamm, T. (2006). An extract of Penicillium chrysogenum elicits early defense-related responses and induces resistance in Arabidopsis thaliana independently of known signalling pathways. Physiological and Molecular Plant Pathology **67** 180–193.

Tian, G.W., Mohanty, A., Chary, S.N., Li, S., Paap, B., Drakakaki, G., Kopec, C.D., Li, J., Ehrhardt, D., Jackson, D., Rhee, S.Y., Raikhel, N.V., and Citovsky, V. (2004a). High-throughput fluorescent tagging of full-length Arabidopsis gene products in planta. Plant Physiol **135,** 25-38.

Tian, M., Benedetti, B., and Kamoun, S. (2005). A Second Kazal-like protease inhibitor from Phytophthora infestans inhibits and interacts with the apoplastic pathogenesis-related protease P69B of tomato. Plant Physiol **138,** 1785-1793.

Tian, M., Huitema, E., Da Cunha, L., Torto-Alalibo, T., and Kamoun, S. (2004b). A Kazal-like extracellular serine protease inhibitor from Phytophthora infestans targets the tomato pathogenesis-related protease P69B. J Biol Chem **279,** 26370-26377.

Torto, T.A., Li, S., Styer, A., Huitema, E., Testa, A., Gow, N.A., van West, P., and Kamoun, S. (2003). EST mining and functional expression assays identify extracellular effector proteins from the plant pathogen Phytophthora. Genome research **13,** 1675-1685.

Trujillo, M., Ichimura, K., Casais, C., and Shirasu, K. (2008). Negative regulation of PAMP-triggered immunity by an E3 ubiquitin ligase triplet in Arabidopsis. Curr Biol **18,** 1396-1401.

Tyler, B.M. (2009). Entering and breaking: virulence effector proteins of oomycete plant pathogens. Cell Microbiol **11,** 13-20.

Ubersax, J.A., and Ferrell, J.E. (2007). Mechanisms of specificity in protein phosphorylation. Nat Rev Mol Cell Bio **8,** 530-541.

van Damme, M., Schornack, S., Cano, L., Huitema, E., and Kamoun, S. (2009). Interactions between Phytophthora infestans and Solanum. (John Wiley & Sons, Inc.).

van Damme, M., Bozkurt, T.O., Cakir, C., Schornack, S., Sklenar, J., Jones, A.M., and Kamoun, S. (2012). The Irish Potato Famine Pathogen Phytophthora infestans Translocates the CRN8 Kinase into Host Plant Cells. PLoS pathogens **8,** e1002875.

Van den Ackerveken, G., Marois, E., and Bonas, U. (1996). Recognition of the bacterial avirulence protein AvrBs3 occurs inside the host plant cell. Cell **87,** 1307-1316.

van der Hoorn, R.A., and Kamoun, S. (2008). From Guard to Decoy: a new model for perception of plant pathogen effectors. Plant Cell **20,** 2009-2017.

van der Hoorn, R.A., Ven der Ploeg, A., de Wit, P.J., and Joosten, M.H. (2001). The C-terminal dilysine motif for targeting to the endoplasmic reticulum is not required for Cf-9 function. Molecular plant-microbe interactions : MPMI **14,** 412-415.

Van Der Hoorn, R.A., Rivas, S., Wulff, B.B., Jones, J.D., and Joosten, M.H. (2003). Rapid migration in gel filtration of the Cf-4 and Cf-9 resistance proteins is an intrinsic property of Cf proteins and not because of their association with high-molecular-weight proteins. Plant J **35,** 305-315.

van der Hoorn, R.A., Wulff, B.B., Rivas, S., Durrant, M.C., van der Ploeg, A., de Wit, P.J., and Jones, J.D. (2005). Structure-function analysis of cf-9, a receptor-like protein with extracytoplasmic leucine-rich repeats. Plant Cell **17,** 1000-1015.

Veronese, P., Nakagami, H., Bluhm, B., Abuqamar, S., Chen, X., Salmeron, J., Dietrich, R.A., Hirt, H., and Mengiste, T. (2006). The membrane-anchored BOTRYTIS-INDUCED KINASE1 plays distinct roles in Arabidopsis resistance to necrotrophic and biotrophic pathogens. Plant Cell **18,** 257-273.

Verzaux, E. (2010). Resistance and susceptibility to late blight in Solanum: gene mapping, cloning and stacking (Wageningen Univ.), pp. 144.

Vleeshouwers, V.G., Driesprong, J.D., Kamphuis, L.G., Torto-Alalibo, T., Van't Slot, K.A., Govers, F., Visser, R.G., Jacobsen, E., and Kamoun, S. (2006). Agroinfection-based high-throughput screening reveals specific recognition of INF elicitins in Solanum. Mol Plant Pathol **7,** 499-510.

Voinnet, O., Rivas, S., Mestre, P., and Baulcombe, D. (2003). An enhanced transient expression system in plants based on suppression of gene silencing by the p19 protein of tomato bushy stunt virus. Plant J **33,** 949-956.

von Heijne, G. (2006). Membrane-protein topology. Nature reviews. Molecular cell biology **7,** 909-918.

Wan, J., Zhang, X.C., Neece, D., Ramonell, K.M., Clough, S., Kim, S.Y., Stacey, M.G., and Stacey, G. (2008). A LysM receptor-like kinase plays a critical role in chitin signaling and fungal resistance in Arabidopsis. Plant Cell **20,** 471-481.

Wang, G., Fiers, M., Ellendorff, U., Wang, Z., de Wit, P.J., Angenent, G., and Thomma, B. (2010). The Diverse Roles of Extracellular Leucine-rich Repeat-containing Receptor-like Proteins in Plants. Critical Reviews in Plant Science **29,** 285–299.

Wang, G., Ellendorff, U., Kemp, B., Mansfield, J.W., Forsyth, A., Mitchell, K., Bastas, K., Liu, C.M., Woods-Tor, A., Zipfel, C., de Wit, P.J., Jones, J.D., Tor, M., and Thomma, B.P. (2008). A genome-wide functional investigation into the roles of receptor-like proteins in Arabidopsis. Plant Physiol **147,** 503-517.

Wang, Y., Pennock, S., Chen, X., and Wang, Z. (2002). Internalization of inactive EGF receptor into endosomes and the subsequent activation of endosome-

associated EGF receptors. Epidermal growth factor. Science's STKE : signal transduction knowledge environment **2002,** pl17.

Wei, C.F., Kvitko, B.H., Shimizu, R., Crabill, E., Alfano, J.R., Lin, N.C., Martin, G.B., Huang, H.C., and Collmer, A. (2007). A Pseudomonas syringae pv. tomato DC3000 mutant lacking the type III effector HopQ1-1 is able to cause disease in the model plant Nicotiana benthamiana. Plant J **51,** 32-46.

Wei, P., Wong, W.W., Park, J.S., Corcoran, E.E., Peisajovich, S.G., Onuffer, J.J., Weiss, A., and Lim, W.A. (2012). Bacterial virulence proteins as tools to rewire kinase pathways in yeast and immune cells. Nature **488,** 384-388.

Wendehenne, D., Binet, M.N., Blein, J.P., Ricci, P., and Pugin, A. (1995). Evidence for specific, high-affinity binding sites for a proteinaceous elicitor in tobacco plasma membrane. FEBS letters **374,** 203-207.

Win, J., Chaparro-Garcia, A., Belhaj, K., Saunders, D.G., Yoshida, K., Dong, S., Schornack, S., Zipfel, C., Robatzek, S., Hogenhout, S.A., and Kamoun, S. (2012). Effector Biology of Plant-Associated Organisms: Concepts and Perspectives. Cold Spring Harbor symposia on quantitative biology.

Xiang, T., Zong, N., Zhang, J., Chen, J., Chen, M., and Zhou, J.M. (2011). BAK1 is not a target of the Pseudomonas syringae effector AvrPto. Molecular plant-microbe interactions : MPMI **24,** 100-107.

Xiang, T., Zong, N., Zou, Y., Wu, Y., Zhang, J., Xing, W., Li, Y., Tang, X., Zhu, L., Chai, J., and Zhou, J.M. (2008). Pseudomonas syringae effector AvrPto blocks innate immunity by targeting receptor kinases. Curr Biol **18,** 74-80.

Xiao, F., He, P., Abramovitch, R.B., Dawson, J.E., Nicholson, L.K., Sheen, J., and Martin, G.B. (2007). The N-terminal region of Pseudomonas type III effector AvrPtoB elicits Pto-dependent immunity and has two distinct virulence determinants. Plant J **52,** 595-614.

Yaeno, T., Li, H., Chaparro-Garcia, A., Schornack, S., Koshiba, S., Watanabe, S., Kigawa, T., Kamoun, S., and Shirasu, K. (2011). Phosphatidylinositol monophosphate-binding interface in the oomycete RXLR effector AVR3a is required for its stability in host cells to modulate plant immunity. Proc Natl Acad Sci U S A **108,** 14682-14687.

Yamaguchi, Y., Pearce, G., and Ryan, C.A. (2006). The cell surface leucine-rich repeat receptor for AtPep1, an endogenous peptide elicitor in Arabidopsis, is functional in transgenic tobacco cells. Proc Natl Acad Sci U S A **103,** 10104-10109.

Yun, H.S., Bae, Y.H., Lee, Y.J., Chang, S.C., Kim, S.K., Li, J.M., and Nam, K.H. (2009). Analysis of phosphorylation of the BRI1/BAK1 complex in arabidopsis reveals amino acid residues critical for receptor formation and activation of BR signaling. Mol Cells **27,** 183-190.

Zhang, J., Li, W., Xiang, T., Liu, Z., Laluk, K., Ding, X., Zou, Y., Gao, M., Zhang, X., Chen, S., Mengiste, T., Zhang, Y., and Zhou, J.M. (2010). Receptor-like cytoplasmic kinases integrate signaling from multiple plant immune receptors and are targeted by a Pseudomonas syringae effector. Cell Host Microbe **7,** 290-301.

Zhang, X.S., Choi, J.H., Heinz, J., and Chetty, C.S. (2006). Domain-specific positive selection contributes to the evolution of Arabidopsis leucine-rich repeat receptor-like kinase (LRR RLK) genes. Journal of molecular evolution **63,** 612-621.

Zipfel, C. (2008). Pattern-recognition receptors in plant innate immunity. Curr Opin Immunol **20,** 10-16.

Zipfel, C., Robatzek, S., Navarro, L., Oakeley, E.J., Jones, J.D., Felix, G., and Boller, T. (2004). Bacterial disease resistance in Arabidopsis through flagellin perception. Nature **428,** 764-767.

Zipfel, C., Kunze, G., Chinchilla, D., Caniard, A., Jones, J.D., Boller, T., and Felix, G. (2006). Perception of the bacterial PAMP EF-Tu by the receptor EFR restricts Agrobacterium-mediated transformation. Cell **125,** 749-760.

Zong, N., Xiang, T., Zou, Y., Chai, J., and Zhou, J.M. (2008). Blocking and triggering of plant immunity by Pseudomonas syringae effector AvrPto. Plant signaling & behavior **3,** 583-585.